AD-A033 607 TEXAS UNIV PORT ARANSAS MARINE SCIENCE INST F/G 8/3
HYDRAULICS AND DYNAMICS OF NEW CORPUS CHRISTI PASS, TEXAS: A CA--ETC(U)
SEP 76 R L WATSON, E W BEHRENS DACW72-74-C-0017
UNCLASSIFIED WES-MITI-9 NL

1 OF 2
AD
A033607

Hydraulics and Dynamics of New Corpus Christi Pass, Texas: A Case History, 1973-75

by

Richard L. Watson and E. William Behrens

GITI REPORT 9

September 1976

Prepared for
U.S. Army Coastal Engineering Research Center
under
Contract DACW72-74-C-0017
by
University of Texas Marine Science Institute
Port Aransas, Texas 78373

GENERAL INVESTIGATION OF TIDAL INLETS

A Program of Research Conducted Jointly by
U.S. Army Coastal Engineering Research Center, Fort Belvoir, Virginia
U.S. Army Engineer Waterways Experiment Station, Vicksburg, Mississippi

Department of the Army
Corps of Engineers

Cover Photo: Corpus Christi Water Exchange Pass, Texas, July 1973

UNCLASSIFIED

SECURITY CLASSIFICATION OF THIS PAGE (When Data Entered)

REPORT DOCUMENTATION PAGE

READ INSTRUCTIONS BEFORE COMPLETING FORM

1. REPORT NUMBER: GITI Report 9

2. GOVT ACCESSION NO.

3. RECIPIENT'S CATALOG NUMBER

4. TITLE (and Subtitle): HYDRAULICS AND DYNAMICS OF NEW CORPUS CHRISTI PASS, TEXAS: A CASE HISTORY, 1973-75

5. TYPE OF REPORT & PERIOD COVERED: Final Report

6. PERFORMING ORG. REPORT NUMBER

7. AUTHOR(s): Richard L. Watson, E. William Behrens

8. CONTRACT OR GRANT NUMBER(s): DACW72-72-C-0027, DACW72-74-C-0017

9. PERFORMING ORGANIZATION NAME AND ADDRESS: University of Texas, Marine Science Institute, Port Aransas, Texas 78373

10. PROGRAM ELEMENT, PROJECT, TASK AREA & WORK UNIT NUMBERS: F31019

11. CONTROLLING OFFICE NAME AND ADDRESS: Department of the Army, Coastal Engineering Research Center (CERRE-SP), Kingman Building, Fort Belvoir, Virginia 22060

12. REPORT DATE: September 1976

13. NUMBER OF PAGES: 175 (2) 171p.

14. MONITORING AGENCY NAME & ADDRESS (if different from Controlling Office)

15. SECURITY CLASS. (of this report): UNCLASSIFIED

15a. DECLASSIFICATION/DOWNGRADING SCHEDULE

16. DISTRIBUTION STATEMENT (of this Report)

Approved for public release; distribution unlimited

(18) WES

(19) GITI-9

17. DISTRIBUTION STATEMENT (of the abstract entered in Block 20, if different from Report)

18. SUPPLEMENTARY NOTES

19. KEY WORDS (Continue on reverse side if necessary and identify by block number)

Corpus Christi Pass, Texas
Inlet hydraulics
Longshore sediment transport
Tidal discharge
Tidal inlets

20. ABSTRACT (Continue on reverse side if necessary and identify by block number)

A case history of the hydraulics and sedimentation of the Corpus Christi Water Exchange Pass, Texas, primarily from 1973 to 1975 is presented. This pass, and the larger Aransas Pass, connect Corpus Christi Bay with the Gulf of Mexico. Quantitative data on longshore sediment transport, tidal differentials across the pass, flood and ebb tidal discharge, wind waves, and local winds explain most of the bathymetric changes which have occurred in the flood tidal delta, baymouth shoreline, channel, gulf mouth, bar bypassing system, and the

Next page

DD FORM 1 JAN 73 1473 EDITION OF 1 NOV 65 IS OBSOLETE

UNCLASSIFIED

SECURITY CLASSIFICATION OF THIS PAGE (When Data Entered)

409 973

20. Abstract. (Continued)

adjacent Gulf of Mexico beaches. Dominant onshore winds produce gulf setup and bay setdown such that, with the exception of the duration of anticyclonic events with north winds, the pass is highly flood-dominated. Heavy surf in the pass mouth and the longshore bars sweeping around the short jetties provide the gulf mouth with a large sediment supply which must be flushed by tidal discharge if the pass is to remain open. Flood dominance combined with a long channel require that most of the littoral drift entering the channel be carried through its entire length to be deposited on the flood tidal delta rather than be returned seaward by ebb flow. Continued shoaling of the channel supports stability concepts of O'Brien (1931), Bruun and Gerritsen (1960), Escoffier (1940), and others which suggest that the pass is of marginal stability with a tendency toward closure. The stability diagram conceived by Escoffier and developed by O'Brien and Dean (1972) using Keulegan's inlet hydraulics shows the most promise for interpreting future behavior of the pass. Shoaling to a minimum cross-sectional area of less than 500 square feet (146 square meters) over a channel length of 500 to 1,000 feet (150 to 300 meters) will probably lead to rapid closure.

FOREWARD

This report results from work done under Contract Nos. DACW72-72-C-0027 and DACW72-74-C-0017 between the Coastal Engineering Research Center (CERC) and the University of Texas, Marine Science Institute, Port Aransas, Texas. It is one in a series of reports from the Corps of Engineers' General Investigation of Tidal Inlets (GITI), which is under the technical surveillance of CERC and is conducted by CERC, the U.S. Army Engineer Waterways Experiment Station (WES), other Government agencies, and by private organizations. Support for a part of the work in this report was also received from the Texas Parks and Wildlife Department.

The report was prepared by R.L. Watson and E.W. Behrens, the contract principal investigator. Assistance in data collection and analysis was provided by P.D. Carangelo, H.S. Finkelstein, and W.H. Sohl. CERC contract technical monitor was C. Mason.

Technical Directors of CERC and WES were T. Saville, Jr., and F.R. Brown, respectively.

Comments on this publication are invited.

Approved for publication in accordance with Public Law 166, 79th Congress, approved 31 July 1945, as supplemented by Public Law 172, 88th Congress, approved 7 November 1963.

JOHN L. CANNON
Colonel, Corps of Engineers
Commander and Director
Waterways Experiment Station

JOHN H. COUSINS
Colonel, Corps of Engineers
Commander and Director
Coastal Engineering Research Center

PREFACE

1. The Corps of Engineers, through its Civil Works program, has sponsored, over the past 23 years, research into the behavior and characteristics of tidal inlets. The Corps' interest in tidal inlet research stems from its responsibilities for navigation, beach erosion prevention and control, and flood control. Tasked with the creation and maintenance of navigable U.S. waterways, the Corps routinely dredges millions of cubic yards of material each year from tidal inlets that connect the ocean with bays, estuaries, and lagoons. Design and construction of navigation improvements to existing tidal inlets are an important part of the work of many Corps' offices. In some cases, design and construction of new inlets are required. Development of information concerning the hydraulic characteristics of inlets is important not only for navigation and inlet stability, but also because inlets play an important role in the flushing of bays and lagoons.

2. A research program, the General Investigation of Tidal Inlets program, was developed to provide quantitative data for use in design of inlets and inlet improvements. It is designed to meet the following objectives:

> To determine the effects of wave action, tidal flow, and related phenomena on inlet stability and on the hydraulic, geometric, and sedimentary characteristics of tidal inlets; to develop the knowledge necessary to design effective navigation improvements, new inlets, and sand transfer systems at existing tidal inlets; to evaluate the water transfer and flushing capability of tidal inlets; and to define the processes controlling inlet stability.

3. The GITI is divided into three major study areas: (a) inlet classification, (b) inlet hydraulics, and (c) inlet dynamics.

a. *Inlet Classification.* The objectives of the inlet classification study are to classify inlets according to their geometry, hydraulics, and stability, and to determine the relationships that exist among the geometric and dynamic characteristics and the environmental factors that control these characteristics. The classification study keeps the general investigation closely related to real inlets and produces an important inlet data base useful in documenting the characteristics of inlets.

b. *Inlet Hydraulics.* The objectives of the inlet hydraulics study are to define the tide-generated flow regime and water level fluctuations in the vicinity of coastal inlets and to develop techniques for predicting these phenomena. The inlet hydraulics study is divided into three areas: (1) idealized inlet model study, (2) evaluation of state-of-the-art physical and numerical models, and (c) prototype inlet hydraulics.

(1) The Idealized Inlet Model. The objectives of this model study are to determine the effect of inlet configurations and structures

on discharge, head loss and velocity distribution for a number of realistic inlet shapes and tide conditions. An initial set of tests in a trapezoidal inlet was conducted between 1966 and 1970. However, in order that subsequent inlet models are more representative of real inlets, a number of "idealized" models representing various inlet morphological classes are being developed and tested. The effects of jetties and wave action on the hydraulics are included in the study.

(2) Evaluation of State-of-the-Art Modeling Techniques. The objectives of this portion of the inlet hydraulics study are to determine the usefulness and reliability of existing physical and numerical modeling techniques in predicting the hydraulic characteristics of inlet/bay systems, and to determine whether simple tests, performed rapidly and economically, are useful in the evaluation of proposed inlet improvements. Masonboro Inlet, North Carolina, was selected as the prototype inlet which would be used with hydraulic and numerical models in the evaluation of existing techniques. In September 1969 a complete set of hydraulic and bathymetric data was collected at Masonboro Inlet. Construction of the fixed-bed physical model was initiated in 1969, and extensive tests have been performed since then. In addition, three existing numerical models were collected at Masonboro Inlet in August 1974 for use in evaluating the capabilities of the physical and numerical models.

(3) Prototype Inlet Hydraulics. Field studies at a number of inlets are providing information on prototype inlet/bay tidal hydraulic relationships and the effects of friction, waves, tides, and inlet morphology on these relationships.

c. *Inlet Dynamics.* The basic objective of the inlet dynamics study is to investigate the interactions of tidal flow, inlet configuration, and wave action at tidal inlets as a guide to improvement of inlet channels and nearby shore protection works. The study is subdivided into four specific areas: (1) model materials evaluation, (2) movable-bed modeling evaluation, (3) reanalysis of a previous inlet model study, and (4) prototype inlet studies.

(1) Model Materials Evaluation. This evaluation was initiated in 1969 to provide data on the response of movable-bed model materials to waves and flow to allow selection of the optimum bed materials for inlet models.

(2) Movable-Bed Model Evaluation. The objective of this study is to evaluate the state-of-the-art of modeling techniques, in this case movable-bed inlet modeling. Since, in many cases, movable-bed modeling is the only tool available for predicting the response of an inlet to improvements, the capabilities and limitations of these models must be established.

(3) Reanalysis of an Earlier Inlet Model Study. In 1957, a report entitled "Preliminary Report: Laboratory Study of the Effect of an Uncontrolled Inlet on the Adjacent Beaches" was published by the Beach

Erosion Board (now CERC). A reanalysis of the original data is being performed to aid in planning of additional GITI efforts.

(4) Prototype Dynamics. Field and office studies of a number of inlets are providing information on the effects of physical forces and artificial improvements on inlet morphology. Of particular importance are studies to define the mechanisms of natural sand bypassing at inlets, the response of inlet navigation channels to dredging and natural forces, and the effects of inlets on adjacent beaches.

4. This report is concerned primarily with presentation and analysis of data collected during a field study of Corpus Christi Water Exchange Pass, Texas, during 1973-75. However, selected results for the first year of study at the pass (1972-73) (reported previously by Behrens, Watson, and Mason; in preparation, 1976), are also presented. The data collected provide information on both the long- and short-term stability of the pass and on the processes affecting the dynamics of the pass and adjacent beaches.

CONTENTS

		Page
	CONVERSION FACTORS, U.S. CUSTOMARY TO METRIC (SI)	11
I	INTRODUCTION	13
II	TIDAL DYNAMICS	15
	1. Introduction	15
	2. Predicted Tides	15
	3. Observed Tides	17
	4. Diurnal Discharge Measurements	24
	5. Time History	34
III	SEDIMENTATION AND EROSION	47
	1. Introduction	47
	2. Gulf Beach Sedimentation	48
	3. Gulf Mouth Deposition	62
	4. Baymouth and Flood Tidal Delta	63
	5. Channel	71
IV	INLET STABILITY CONSIDERATIONS	83
	1. Introduction	83
	2. Tidal Prism-Cross-Sectional Area Relationships	83
	3. Comparisons with Other Empirical Relationships	83
	4. Escoffier Diagram Analysis	86
	5. Future Inlet Stability	89
V	CONCLUSIONS	91
	LITERATURE CITED	93
APPENDIX		
A	DIURNAL DISCHARGE STUDIES RESULTS	95
B	COMPUTED TIDAL DISCHARGE	108
C	BEACH PROFILES	119
D	GULF MOUTH BATHYMETRIC MAPS	153
E	BAYMOUTH BATHYMETRIC MAPS	161
F	CHANNEL AREAS AND HYDRAULIC RADII	168

CONTENTS

TABLES

		Page
1	Differences between observed and predicted tides compared with climatological factors	22
2	Summary of diurnal discharge studies	27
3	Tidal discharges for different periods of a norther	39
4	Summary of visual wave observations	50
5	Longshore transport rate, Mustang Island, Texas	51
6	Gulf beach deposition	59
7	Cumulative gulf beach deposition	60
8	Gulf mouth erosion-deposition	64
9	Baymouth erosion-deposition	66
10	Baymouth shoreline erosion	70
11	Tidal prism - inlet cross-sectional area relationships	84

FIGURES

1	Location map of study area	14
2	Tidal predictions and onshore winds	16
3	Tide gage data comparisons	19
4	Horace Caldwell Pier tide gage correction factors	20
5	Observed minus predicted monthly tide levels	20
6	Differences between predicted and observed high tides ($CCWEP_G$)	23
7	Comparisons of average monthly tide levels and ranges	25
8	Variations in cross-sectional areas	28
9	Manning's n versus velocity, 24 and 25 October 1974	31
10	Manning's n versus velocity, 28 and 29 December 1974	32

CONTENTS

FIGURES — Continued

		Page
11	Manning's n versus velocity, 25 and 26 April 1975	33
12	Tidal differential, velocity, and Manning's n through a diurnal period, 19 and 20 June 1974	35
13	Tidal differential, velocity, and Manning's n through a diurnal period, 25 and 26 June 1974	36
14	Tidal differential, velocity, and Manning's n through a diurnal period, 7 and 8 August 1974	37
15	Tidal differential, velocity, and Manning's n through a diurnal period, 15 and 16 October 1974	38
16	Tidal differential, velocity, and Manning's n through a diurnal period, 24 and 25 October 1974	39
17	Tidal differential, velocity, and Manning's n through a diurnal period, 28 and 29 December 1974	40
18	Tidal differential, velocity, and Manning's n through a diurnal period, 3 and 4 January 1975	41
19	Tidal differential, velocity, and Manning's n through a diurnal period, 11 and 12 February 1975	42
20	Tidal differential, velocity, and Manning's n through a diurnal period, 8 and 9 April 1975	43
21	Tidal differential, velocity, and Manning's n through a diurnal period, 25 and 26 April 1975	44
22	Tidal discharge by week and month	45
23	Weekly net tidal discharge and onshore wind	46
24	Corpus Christi Water Exchange Pass channel zones	49
25	Gulf beach accretion, preconstruction to June 1973	52
26	Gulf beach accretion, preconstruction to June 1974	53
27	Gulf beach accretion, June 1973 to June 1974	54
28	Gulf beach accretion, June 1974 to March 1975	55

CONTENTS

FIGURES—Continued

		Page
29	Gulf beach accretion, October 1972 to March 1975	56
30	Gulf beach accretion, preconstruction to March 1975	57
31	Gulf mouth sedimentation	65
32	Baymouth sedimentation	67
33	Bay shoreline erosion	69
34	Channel zones 1, 2, and 3	72
35	Channel zones 4, 5, and 6	73
36	Bend to jetties thalwegs	75
37	Entire channel sedimentation compared with gulf waves and tidal ranges	76
38	Total channel cumulative sedimentation	78
39	Annual rainfall and gross longshore current compared to total channel sedimentation	79
40	Environmental conditions for short-term channel studies	80
41	Deposition and erosion of channel for short-term study periods	82
42	Illustration of Escoffier's stability concept	87
43	Escoffier stability diagram	90

CONVERSION FACTORS, U. S. CUSTOMARY TO METRIC (SI) UNITS OF MEASUREMENT

U.S. customary units of measurement used in this report can be converted to metric (SI) units as follows:

Multiply	by	To obtain
inches	25.4	millimeters
	2.54	centimeters
square inches	6.452	square centimeters
cubic inches	16.39	cubic centimeters
feet	30.48	centimeters
	0.3048	meters
square feet	0.0929	square meters
cubic feet	0.0283	cubic meters
yards	0.9144	meters
square yards	0.836	square meters
cubic yards	0.7646	cubic meters
miles	1.6093	kilometers
square miles	259.0	hectares
acres	0.4047	hectares
foot-pounds	1.3558	newton meters
ounces	28.35	grams
pounds	453.6	grams
	0.4536	kilograms
ton, long	1.0160	metric tons
ton, short	0.9072	metric tons
degrees (angle)	0.1745	radians
Fahrenheit degrees	5/9	Celsius degrees or Kelvins[1]

[1]To obtain Celsius (C) temperature readings from Fahrenheit (F) readings, use formula: $C = (5/9)(F - 32)$. To obtain Kelvin (K) readings, use forumla: $K = (5/9)(F - 32) + 273.15$.

HYDRAULICS AND DYNAMICS OF NEW CORPUS CHRISTI PASS, TEXAS: A CASE HISTORY, 1973-75

by

Richard L. Watson and E. William Behrens

I. INTRODUCTION

The Corpus Christi Water Exchange Pass (Fig. 1) extends from Corpus Christi Bay to the Gulf of Mexico through Mustang Island, Texas. The pass was dredged by the Texas Parks and Wildlife Department to promote water exchange and fish migration between the two water bodies. Studies of sedimentation in and around the pass and its tidal hydraulics and stability began with its initial opening in August 1972, and continued intermittently for 3 years to August 1975.

The design, construction, environmental setting, and behavior of the inlet during its first year of existence were reported by Behrens, Watson, and Mason (in preparation, 1976). The objectives in continuing this inlet study were to:

(a) Document bathymetric changes at the gulf mouth of the inlet, especially in relation to bar-trough topography in the adjacent surf zone;

(b) record bathymetric changes of the inlet channel in response to increasing and decreasing tidal discharges which accompany seasonal climatic changes;

(c) record bathymetric changes at the bay mouth of the inlet and thus to continue to trace the development of the flood tidal delta in this area;

(d) obtain tidal current time histories by applying Manning's equation to continuously recorded tidal differential data between the gulf and bay;

(e) verify discharge and velocity computations by direct measurement in the channel over a maximum range of meteorological conditions and through any changes in channel morphology, and to try to define causes producing variations in instantaneous discharge-tidal differential correlations; and

(f) apply hydrographic, longshore sediment transport, and tidal discharge data to existing theories on inlet stability, and to evaluate these theories.

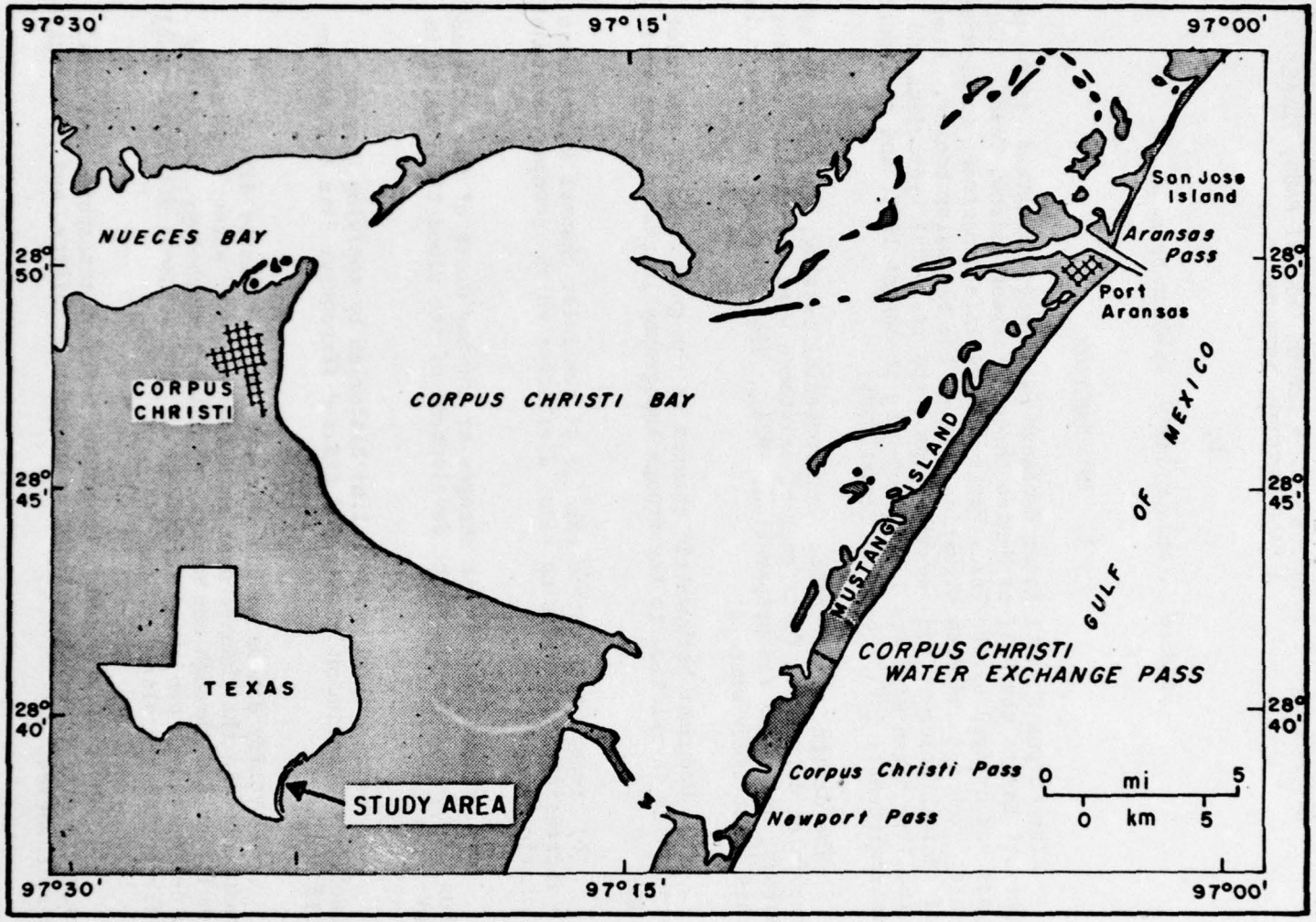

Figure 1. Location map of study area.

II. TIDAL DYNAMICS

1. Introduction.

One of the most important natural agents affecting an inlet is the tidal flow, because of its predominant influence on the sediment transport patterns which determine the size and morphology of the inlet. The tides in the Gulf of Mexico are a complex mixture of diurnal, mixed, and semidiurnal. The ranges and heights are controlled by daily and seasonal meteorological conditions as well as by monthly, annual, and longer astronomical cycles.

Predicted tides reveal the astronomical effects and the major seasonal and 2-week cycles which sedimentological changes might be expected to reflect. Comparison of observed with predicted tides reveals effects of small differences between the study site and the reference station tides and larger and more significant effects of local winds on the tide levels and flows. Short-period tidal current velocity measurements were made to determine a friction factor necessary to calculate longer term flow characteristics from tide gage data. The flow patterns and discharges should also be reflected in the sediment transport distribution patterns. The velocity measurements also suggest some sedimentological and hydraulic factors affecting significant channel friction variations through the tidal cycle.

2. Predicted Tides.

a. Source. The predicted tides were used for the study site (National Oceanic and Atmospheric Administration, 1972-75) at Aransas Pass.

b. Types. At the latitude of the study site, diurnal tides occur when the moon is at its maximum northern and southern declinations, and semidiurnal tides occur when it crosses the equator each 2-week period. Either tide may coincide with any lunar phase, e.g., diurnal tides occur with new and full moons at the solstices but with quadratures at the equinoxes.

c. Ranges. Although syzygy and quadrature affect the tidal ranges through the 2-week cycle, the declinational effect is greater so that diurnal tides always have larger ranges (1.8 to 2.8 feet or 55 to 85 centimeters) than semidurnal tides (0.8 to 1.4 feet or 24 to 43 centimeters). Seasonally, ranges are largest when syzygies coincide with maximum declinations at the equinoxes (Fig. 2) and smallest when syzygy and declination effects are opposed at the solstices. Similar tides occurring 2 weeks apart may have ranges which differ by 1 foot (30 centimeters) depending on whether one tide coincides with perigee and the other tide with apogee. Long-term astronomical cycles cause this inequality to shift from diurnal to semidiurnal phases over a period of about 1.5 years. An effect of this shift was a decrease in

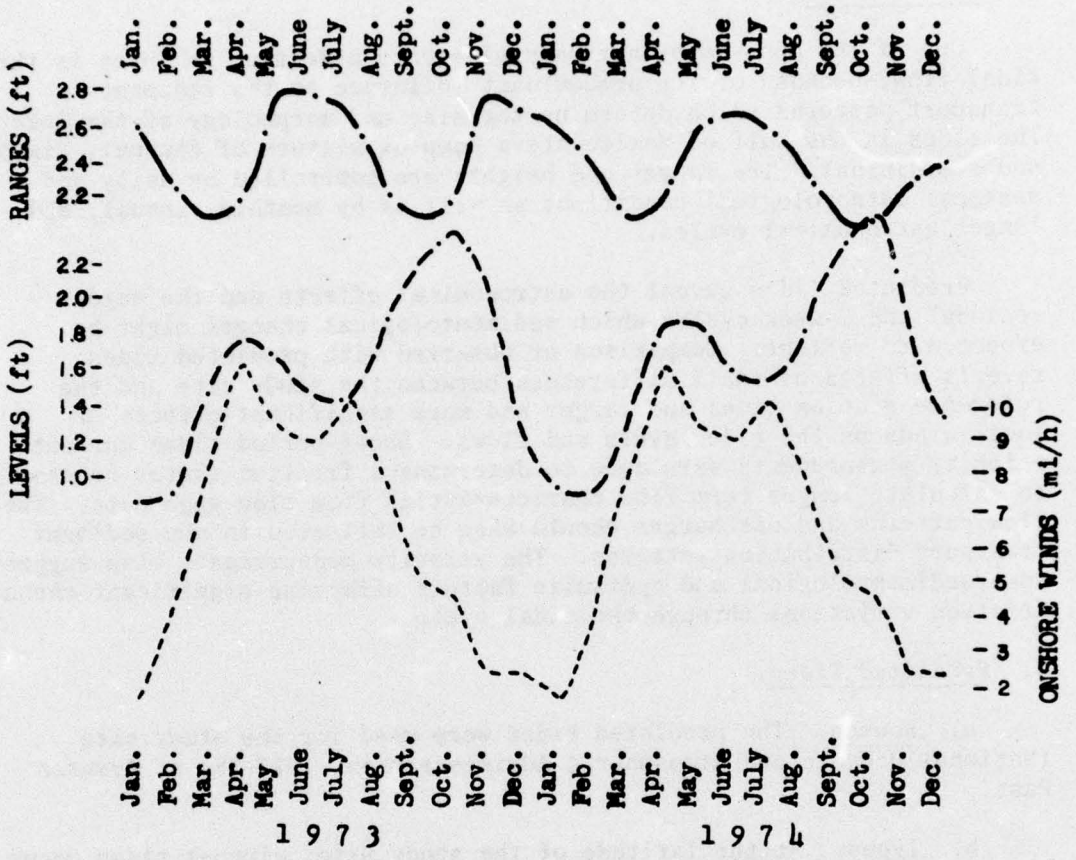

Figure 2. Tidal predictions and onshore winds. Ranges are monthly, maximum tidal ranges; levels are averages of monthly highest high, lowest high, highest low, and lowest low; and winds are the average, monthly, resultant windspeeds times the sine of the angle between the shoreline and the resultant direction (data from National Oceanic and Atmospheric Administration, 1972-75).

maximum, spring, and diurnal tidal ranges through the study period (Fig. 2).

d. Levels. Like tidal ranges, mean water levels have an annual cycle of two highs and two lows. However, the levels are not in phase with the ranges (Fig. 2). Highest water levels occur in October when gulf-wide steric expansion is greatest, and lowest water levels are in January and February when steric contraction is greatest (Whitaker, 1971). A second high occurs in April and May and a second low in July. These secondary fluctuations have no correlations with seasonal barometric pressure or steric effects but do correlate qualitatively with winds. The monthly onshore component of wind (calculated as the product of the monthly resultant windspeed and the sine of the angle between the shoreline and the wind direction) is small due to strong winter storms with predominantly offshore winds from September to March, has an annual maximum in April, and remains fairly large from June to September (Fig. 2). Thus, the high April water levels appear to be due to gulf wind setup.

Winds measured at the onshore weather station may have a similarly high onshore component during the summer low water level period, but may produce less setup because of shorter fetch. The spring winds are probably more a part of the prevailing trade wind system with an effective fetch of the whole Gulf of Mexico than are the summer winds which have a large component of daily sea breezes with effective fetches of only a few tens of miles.

3. Observed Tides.

a. Procedures. Tide data were gathered continuously with two Bristol nitrogen bubbler water level gages. One gage (identified as $CCWEP_G$) was installed on the north jetty with the orifice in the channel at a depth of about -1.6 feet (0.48 meter) mean low water (MLW) and about 500 feet (150 meters) from the gulf end. The other gage ($CCWEP_B$) was located on the north bank with the orifice in the channel about 500 feet (150 meters) inside the bay mouth. The bay gage had a 0- to 5-foot (0 to 1.5 meters) diaphram and began operation on 11 June 1974; the gulf gage had a 0- to 10-foot (0 to 3 meters) diaphram and began operation on 12 July 1974.

Two adjustments were made to these installations. Periodic sedimentation around the bay gage orifice during strong northers from December to March necessitated relocating the gage farther toward the center of the channel on 26 February 1975. On 4 November 1974, a damping reservoir was installed in the gulf gage to produce a more precise record by removing the effects of short-period wave action.

Orifice elevations were surveyed upon installation and three times subsequently when the records showed sharp displacements suggesting movements of the orifices. The tide records were read at 1-hour intervals, and orifice elevation corrections were made by a computer

which also determined hourly gulf-bay differences and water surface slopes.

Daily highs and lows and differences from predicted highs, lows, and times thereof were determined from these data; monthly averages were calculated by hand.

b. Observed Tide Levels and Ranges. To assess gage accuracy, the observations were compared with two National Ocean Survey (NOS) gages located near Port Aransas, Texas. The Horace Caldwell Pier (HCP) gage is located on a fishing pier spanning the surf zone about one-half mile southwest of the Aransas Pass jetty, and the Aransas Pass Channel (APC) gage is located inside the jetties about 6,000 feet (1,800 meters) from the gulf end (Fig. 1).

From July 1974 to February 1975, $CCWEP_G$ levels were higher than both those of APC (by 0.75 foot or 23 centimeters) and HCP (by 0.31 foot or 9 centimeters) (Fig. 3). However, the differences were quite consistent, especially between HCP and $CCWEP_G$ where they varied by no more than 0.04 foot (1 centimeter) for 8 months. The average differences between $CCWEP_G$ and both NOS gages changed significantly (>99.5-percent confidence level) after February 1975 with $CCWEP_G$>APC becoming 0.375 foot (11 centimeters) and $CCWEP_G$<HCP becoming 0.26 foot (8 centimeters). Although this suggests a calibration change of roughly one-half foot (15 centimeters) from the $CCWEP_G$ gage, no alteration of the data has been made because of two other considerations: (a) Correction of the $CCWEP_G$ data in the suggested direction would also require a simultaneous, arbitrary change in the CCWEP bay gage data by the same amount, or else calculated flow based on the water surface slopes between the two gages would have only 53 hours of ebbtide over a subsequent period of over 46 days (i.e., a flood:ebb ratio of 20:1 or only 1 hour of ebbtide per day on the average); and (b) both NOS gages show data discrepancies at the time of change. The APC gage was out for February 1975. Differences between observed and predicted tide levels for a 9-month period before it went out averaged over 0.2 foot (8 centimeters) greater than differences for an equivalent 9-month period after its operation was resumed (T-test difference confidence level >95 percent). Additionally, the HCP gage was discontinued in May 1975 due to malfunctioning 2 months after its relations to $CCWEP_G$ changed sharply. A plot of the correction factor applied to the HCP observations (Fig. 4) shows a sharply anomalous trend beginning when the relationship first changed (March 1975) and ending when the malfunction caused gage readings to be discontinued (May 1975). However, monthly differences between observed and predicted tide levels at the $CCWEP_G$ gage averaged 0.37 foot (11 centimeters) before and 0.33 foot (10 centimeters) after the apparent change (Fig. 5). No statistical significance can be assigned to this difference.

Tide levels and tide ranges observed at $CCWEP_G$, HCP, and APC follow the predicted seasonal trends quite well (Fig. 3). Deviations from

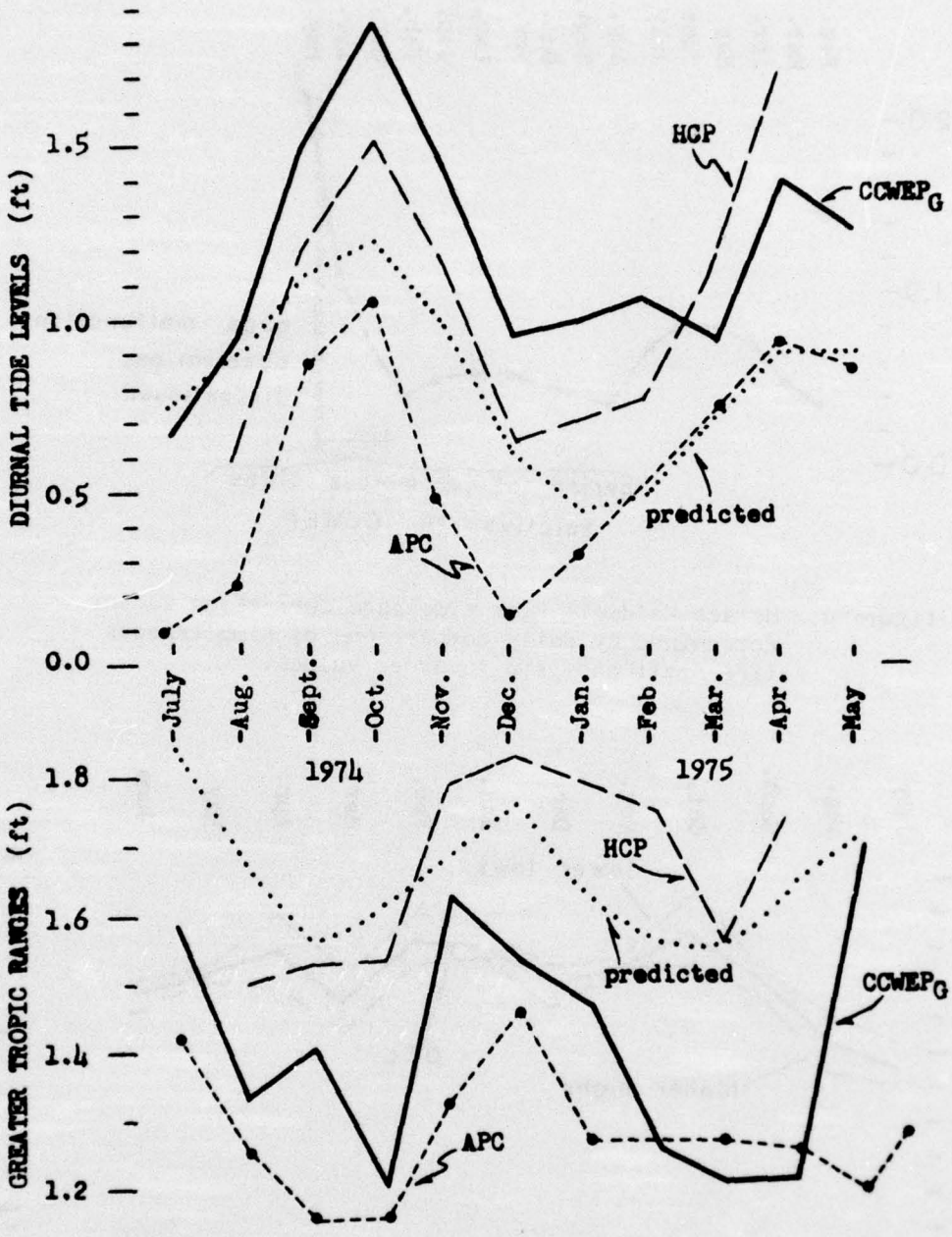

Figure 3. Corpus Christi Water Exchange Pass gulf gage ($CCWEP_G$) data compared with Aransas Pass Channel (APC) and Horace Caldwell Pier (HCP) data (National Oceanic and Atmospheric Administration, unpublished tidal data, 1975).

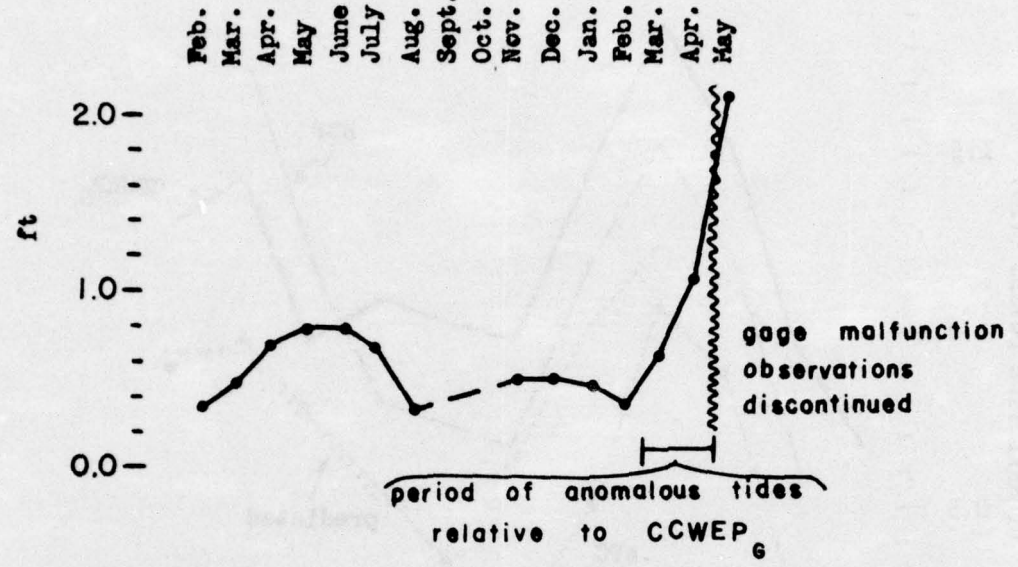

Figure 4. Horace Caldwell Pier tide gage correction factor determined by daily comparisons of simultaneous tide staff and gage recorder values.

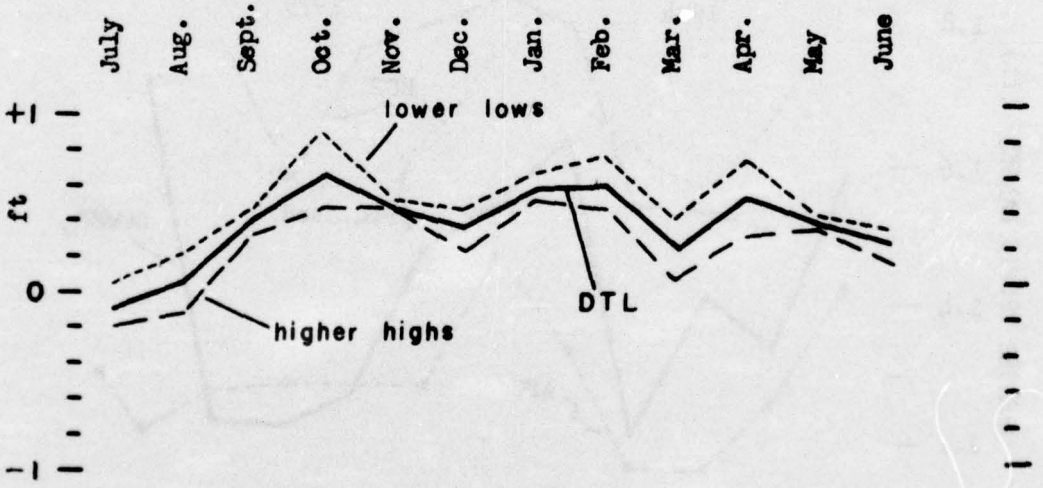

Figure 5. Observed minus predicted monthly tide levels at the Corpus Christi Water Exchange Pass gulf gage ($CCWEP_G$). DTL is monthly average of daily higher highs and lower lows.

predicted values show a very weak trend of higher than predicted tides mostly during September to March (Fig. 5). This weak trend as well as the average differences between predicted and observed tides may be due to differences between long-term averages of steric, barometric, and wind effects and the actual conditions during the study period. Therefore, Corpus Christi climatological data were compared with differences between predicted and observed tides (Table 1).

Steric effects are difficult to analyze, but since air temperatures (herein assumed to be an indirect measure of water density) for November 1974 to February 1975 were below normal (i.e., density above normal) when tides were higher than predicted, this was not the cause. Below average barometric pressures which occurred in September 1974 and from December 1974 to April 1975 may have been a contributing factor to the high tides during this period. However, sharply higher than average pressures for October 1974 did not correlate with the positive differences between actual and predicted tides which occurred then. Similarly, winds which might cause gulf setup and positive differences between actual and predicted tides if their onshore component were above average, actually had an onshore component about 1 mile per hour less than average for the September 1974 to May 1975 period of high tides.

While these climatological factors do not seem to account for the monthly or seasonal differences between observed and predicted tides, local winds are often strikingly correlated with daily and weekly tidal variations. Figure 6 shows the best example of such correlations. The effect seems to be that the channel acts like a part of Corpus Christi Bay especially during early fall, midwinter, and spring northers, i.e., the offshore winds associated with strong northers create setup in the southeastern part of the bay and raise water levels in the entire channel. Likewise, strong onshore winds pile up water in the northwestern part of the bay and tide levels in the southeastern part and in the channel are reduced. Wind effects on tidal discharges are discussed below.

c. Predicted Versus Observed Times. Observed times of high tides occurred an average of 14 minutes earlier than the times predicted; observed low tides occurred an average of 42.5 minutes later than the times predicted. The observed time differences would produce shorter floods and longer ebbs than predicted. However, other evidence supports a flood dominance in tidal discharges.

d. Bay Observed Tides. The average of all hourly tide level observations shows that at the pass, the mean bay water level is 0.25 foot (7.6 centimeters) below the mean gulf water level. This is about half the difference between the NOS gages at Port Aransas (0.46 foot or 14 centimeters), where the mean levels (DTL) were taken as the average of the daily higher highs and lower lows.

Table 1. Differences between observed and predicted tides compared to differences between average and actual climatological factors.

Month	Tide[1] (ft)	Temperature[2] (°F)	Barometric pressure[3] (in)	Onshore wind[4] (mi/h)
1974				
July	-0.08	+4.1	-0.02	-0.5
Aug.	+0.06	+0.1	0.0	+3.6
Sept.	+0.40	+0.6	+0.07	-2.9
Oct.	+0.65	+1.9	-0.12	+0.1
Nov.	+0.47	-2.0	-0.02	-2.0
Dec.	+0.34	0.0	+0.02	-2.8
1975				
Jan.	+0.55	-0.7	+0.04	+0.5
Feb.	+0.58	-1.0	+0.05	-2.0
Mar.	+0.21	+3.2	+0.09	-0.3
Apr.	+0.50	+1.0	+0.02	+0.4

1. $CCWEP_G$ minus predicted value.
2. Observed minus average monthly mean air temperature.
3. Observed minus average monthly mean barometric pressure.
4. Observed minus average onshore component of resultant wind.

Note: Comparisons were made so that all (+) values correlate with water levels above the predicted value and all (-) values correlate with water levels below predicted values.

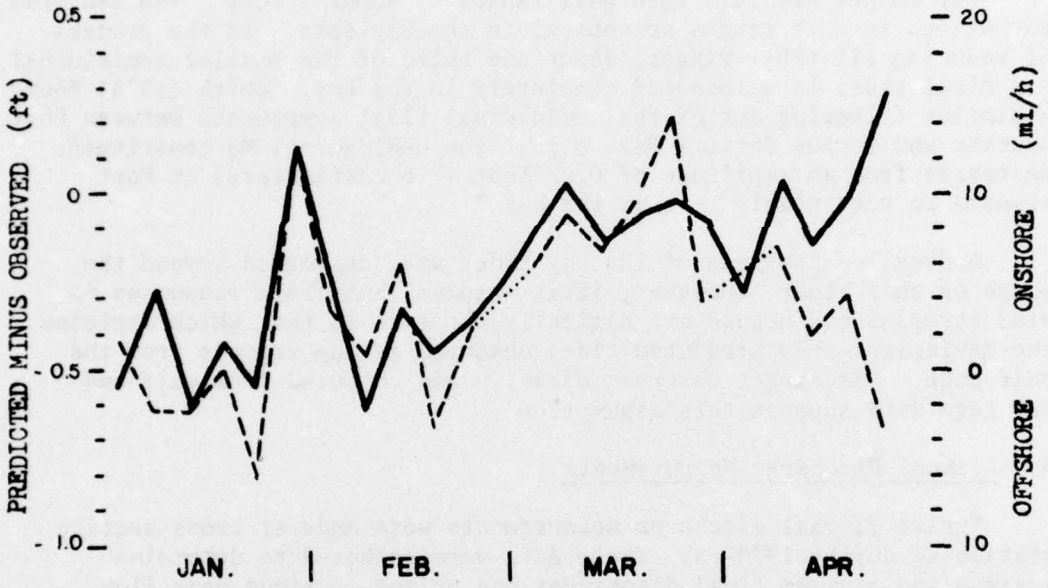

Figure 6. Differences between predicted and observed high tides ($CCWEP_G$) shown by dashline (dotted line where interpolated), compared to onshore component of resultant wind (solid line). Data are for 5-day averages.

The annual cycle of bay tide levels shows clearly the seasonal trend of fall and spring highs and winter and summer lows. The gulf levels exceed the bay levels most during low and rising seasonal tides, and least or are actually reversed during high or especially during falling seasonal levels (Fig. 7). This pattern suggests that there is a slight lag in bay response to the seasonal cycle similar to the lag in a daily tidal cycle.

Bay ranges are less than gulf ranges by about 1 foot. The seasonal variations in gulf ranges are absent in the bay data. In the process of reducing all tidal ranges, about one-third of the smaller semidiurnal and mixed tides is eliminated completely in the bay. Smith (1974) found a similar filtering out of the semidiurnal tidal components between Port Aransas and Corpus Christi Bay, e.g., "the semidiurnal M_2 constituent decreases from an amplitude of 0.25 foot (7.6 centimeters) at Port Aransas to very nearly zero in the bay."

A detailed analysis of the bay tides was considered beyond the scope of this study. However, it is assumed that their responses to wind stresses and setups are basically the same as that which explains the deviations from predicted tides observed in the records from the gulf gage. Discharges observed directly and computed from gulf and bay gage data support this assumption.

4. Diurnal Discharge Measurements.

Twelve diurnal discharge measurements were made at cross-section station X7 during 1974-75. These data were gathered to determine maximum and minimum tidal discharges and prisms, maximum mean flow velocities, and Manning's n for two sections of the channel.

a. Procedures. Water level data for each discharge measurement were gathered by the water level recorders previously described. For the eight studies from June 1974 to February 1975, the following procedure was followed. A 3/4-inch nylon line was stretched between two anchors across the pass. At intervals of 1 hour for a period of 25 hours, a boat was positioned at seven premarked stations along the taut rope. Current velocity was measured at each station with a Gurley-Price current meter at depths of 0.2, 0.6, and 0.8 foot of the total depth. Current velocity was measured at 1-foot intervals at the channel center. The total water depth was recorded hourly at each station. Measurements at each station took approximately 3 minutes.

The above data and water levels recorded at each of the three water level recorders were used to determine (a) the mean velocity for each profile; (b) the mean velocity, hydraulic radius, wetted perimeter, and area of the channel cross-section; and (c) Manning's n values for the entire channel and for the two reaches from bay to bend and from bend to gulf.

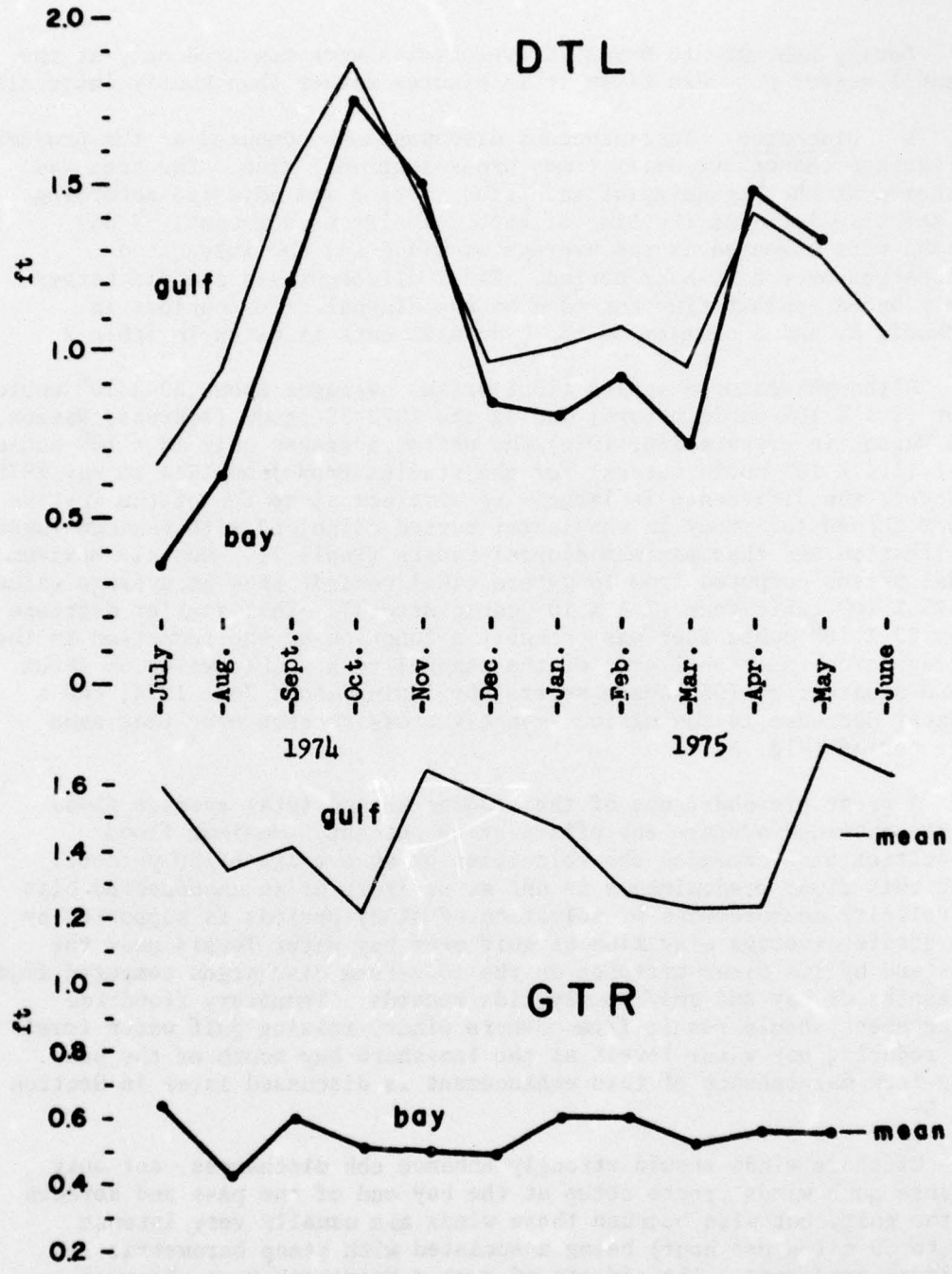

Figure 7. Comparison of average monthly tide levels (DTL) and ranges (GTR) for the Corpus Christi Water Exchange Pass bay and gulf gages.

During February to May 1975, velocities were measured only at the channel center but were taken at 15 minutes rather than hourly intervals.

b. Discharge. Instantaneous discharge was computed as the product of average channel velocity times cross-sectional area. The area was measured at the beginning of each study period and adjusted according to the tide level at the time of each velocity measurement. Tidal prisms were computed as the average of flood and ebb integrated discharges over a 25-hour period. Tidal differentials and discharges are plotted against time for each of the diurnal study periods in Appendix A, and a summary of the hydraulic data is given in Table 2.

Although measured spring tidal prisms averaged about 82 X 10^6 cubic feet (2.3 X 10^6 cubic meters) during the 1972-73 study (Behrens, Watson, and Mason, in preparation, 1976) the prisms averaged only 48 X 10^6 cubic feet (1.4 X 10^6 cubic meters) for the studies from June 1974 to May 1975. However, the difference is largely an artifact since few of the spring-tides chosen for study in the latter period coincided with maximum lunar declination and thus maximum diurnal ranges (Table 2). Monthly maximum tidal prisms computed from long-term tidal records show an average value of 75 X 10^6 cubic feet (2.1 X 10^6 cubic meters). This smaller decrease from 82 X 10^6 cubic feet was probably a function of the reduction in the average cross-sectional area of the channel to a stable value of about 1,000 square feet (93 square meters) beginning about June 1974, and a greater decrease in the minimum monthly cross section over that same time period (Fig. 8).

A great preponderance of the studies showed total average flood prisms exceeded average ebb prisms by 60 percent. Maximum flood velocities also exceeded ebb velocities by an average of 30 percent. That this flood predominance is not an artifact of an unsuspected bias in velocity measurements or selection of study periods is supported by the greater average elevation of gulf over bay water levels near the pass and by its clear presence in the long-term discharges computed from 10 months of bay and gulf hourly tide records. Temporary floodtide enhancement should result from onshore winds, raising gulf water levels and reducing bay water levels at the lee-shore bay mouth of the pass. Long-term maintenance of this enhancement is discussed later in Section II, 5.

Offshore winds should strongly enhance ebb discharges, not only because such winds create setup at the bay end of the pass and setdown in the gulf, but also because these winds are usually very intense (20 to 50 miles per hour) being associated with steep barometric pressure gradients. The effects of such a "norther" were observed on 12, 13, and 14 March 1975. A current meter observation was made every 15 minutes beginning at 1330 hours on 12 March. Strong onshore winds of 14 to 19 knots blew until 2330 hours. A calm lasted for almost 2 hours until about 0100 hours on 13 March when 34 hours of northerly winds began. Wind gusts up to 35 knots were common, and resultant winds

Table 2. Summary of diurnal discharge studies

Date started	Tide[1]	Apogee[2] perigee[2]	Lunar phases	Predicted tidal range (ft)			Hydraulic radius (ft)				Total discharge ($ft^3/10^6$)			Max. vel. (ft/s)		Manning's n for $\bar{V}$ > 0.5 ft/s		
				study days	monthly min.	monthly max.	X7	entire	bay bend	gulf bend	flood	ebb	total	flood	ebb	bay bend	jetty bend	entire channel
1974																		
19 June	D	P	new	2.4	0.6	2.4	5.6		5.0		72	38	110	1.9	1.2	0.024		
25 June	S	I	first qtr.	0.9	0.6	2.4	5.7		5.0		27	17	44	1.0	0.8	0.025		
7 Aug.	S	I	third qtr.	0.7	0.7	2.1	5.6		5.1		40	13	53	1.3	0.6	0.029		
16 Aug.	M	P	new	1.9	0.9	2.1	5.6	5.2	5.9	4.8	57	23	80	1.3	1.0		0.029	0.033
15 Oct.	M	I	new	1.8	0.7	1.8	5.1	5.0	4.9	4.8	27	54[3]	81	1.2	1.5	0.029	0.035	0.031
24 Oct.	S	A	first qtr.	0.9	0.7	1.8	5.7	4.6	5.0	4.4	52	5	57	1.6	0.5			0.021
28 Dec.	D	P	full	1.9	0.5	2.0	4.7	4.9	4.9	4.7	56	33	89	1.9	1.3	0.028	0.044	0.035
1975																		
3 Jan.	S	I	third qtr.	0.9	0.5	2.1	5.3	4.9	4.9	4.7	28	24	52	0.9	0.9	0.026	0.032	0.024
12 Feb.	S	A	new	1.1	0.7	1.8	5.4	4.7	4.9	4.4	13	35[3]	48	0.9	1.2	0.023	0.030	0.026
13 Mar.	S	A	new	0.9	0.8	1.7	5.0	4.5	4.6	4.4	49	53[3]	102	1.5	2.2			
8 Apr.	S	A	new	0.7	0.7	2.0	4.8	4.6	4.6	4.6	51	22	73	1.4	1.0	0.024	0.033	0.028
25 Apr.	M	P	full	2.2	1.0	2.2	5.7	4.5	4.5	4.4	92	26	118	2.5	1.2	0.021	0.030	0.023
									MEANS		47	29	76	1.4	1.1	0.025	0.033	0.028

1. D = diurnal
   S = semidiurnal
   M = mixed
2. P = perigee
   I = intermediate
   A = apogee
3. Ebb-dominated (norther)

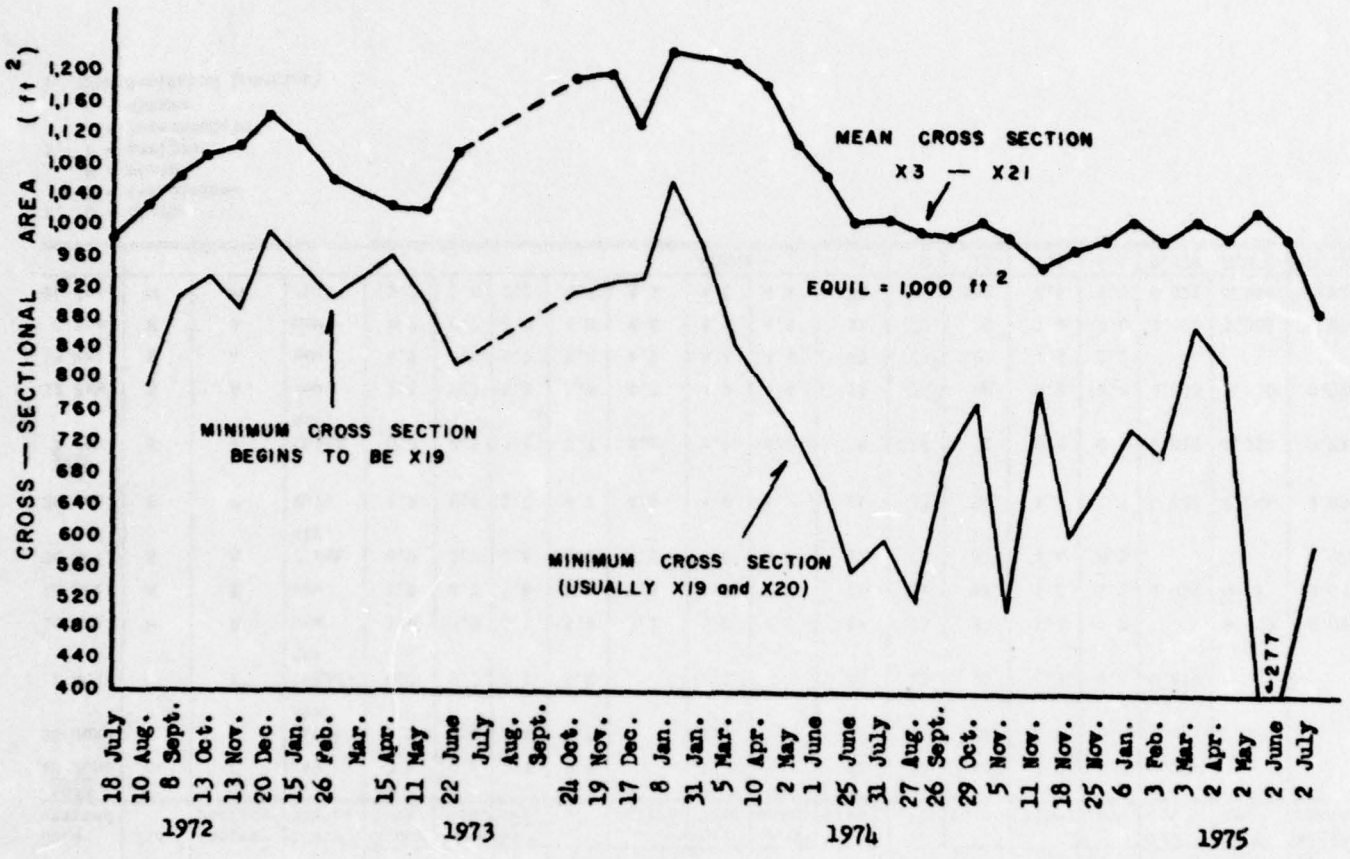

Figure 8. Variations in cross-sectional area of the Corpus Christi Water Exchange Pass.

of 20 knots or more persisted for 10 hours.

The effects of this norther may be seen by comparing tidal currents during three 25-hour periods: (a) 1400 hours on 12 March to 1445 hours on 13 March; (b) 0200 hours on 13 March to 0400 hours on 14 March; and (c) 1200 hours on 13 March to 1300 hours on 14 March. The first period included about 10 hours of strong onshore winds, 2 hours of near calm, and 13 hours of strong offshore winds. Flood and ebb currents coincided almost exactly with onshore and offshore winds, respectively.

The second period began about 2 hours after the norther began and included only offshore winds and almost no flood currents. Throughout the third period, winds were offshore but blew at only 7 to 17 knots.

The discharges for these time intervals (Table 3) show that the onshore winds preceding a norther may have as much effect enhancing the floodtide as the norther does the ebbtides. Ebbtides clearly predominate during the norther, but this condition diminishes as quickly as the northerly wind abates. The maximum flood velocity during the onshore wind was 1.6 feet per second (0.5 meter per second); the maximum ebb velocity during the offshore wind was 2.2 feet per second (0.7 meter per second).

Table 3. Tidal discharges for three 25-hour periods covering different parts of the norther of 13 March 1975.

Date	Time (h)	Flood discharge[2]	Ebb discharge[2]
12 and 13 Mar.	1400 to 1445	41	38[1]
13 and 14 Mar.	0300 to 0400	6	47[1]
13 and 14 Mar.	1200 to 1300	12	23

1. Minimal figure; operation of the current meter was impossible during heavy squalls at the beginning of the norther, and proper functioning of the meter during the next 6 hours of rough boating conditions was uncertain.

2. Millions of cubic feet.

A norther also occurred during a 25-hour diurnal study in February. The wind began to blow from the north after about 6 hours of current observation and continued through the rest of the study. Although the norther was quite mild with maximum sustained winds only 17 miles per hour, a net ebb discharge resulted: flood = 13 X 10^6 cubic feet (0.4 X 10^6 cubic meters); ebb = 35.5 X 10^6 cubic feet (1 X 10^6 cubic meters).

Maximum velocities were only 0.9 and 1.2 feet per second (0.3 and 0.4 meter per second) for flood and ebb flows, respectively.

c. Channel Friction. The Manning's n friction coefficient was computed for all diurnal discharge studies to allow calculation of long-term velocity and discharge time histories. The following empirical relationship relates the mean flow velocity to channel geometry, water surface slope, and Manning's n:

$$V = \frac{1.49\ R^{2/3} S^{1/2}}{n}\ , \qquad (1)$$

where V is the mean flow velocity in the channel, R is the hydraulic radius of the channel, and S may be taken as the water surface slope. Although this relationship is for steady open-channel flow, the acceleration of tidal currents is considered sufficiently small that the flow can be considered to be steady for short-time periods.

Manning's n values were computed each hour for the 1972-73 and June 1974 to February 1975 discharge measurements, and each quarter-hour for the February to May 1975 measurements. The 1972-73 studies were based on water level recorders placed in the bay near the channel mouth and at the bridge. The mean Manning's n for those studies increased from 0.019 in December 1972 to 0.030 in June 1973 (Behrens, Watson, and Mason, in preparation, 1976). The increase in channel friction is probably due to channel shoaling and the development of major dune-type bed forms in many reaches of the channel. Tide gages were relocated for the 1974-75 study so that friction factors could be estimated for the entire channel, the simple, straight reach from the bay to the bend, and the more complex section including the bend, bridge, and most of the jetties. The n values for the 1973 study are comparable with those of the bay to bend reach of the channel for 1974-75 shown in Table 2. Along with stabilization of the mean cross section at near 1,000 square feet (300 meters) since June 1974, the mean n for the entire channel has stabilized at about 0.028. The mean n for the reach from the bay to the bend is lower, averaging about 0.025; the bend and the reach from the bridge to the jetties averages 0.033. If the bay to bend n and the bend to gulf n are averaged with weighting for their respective channel lengths of 5,100 and 3,300 feet (1,554 and 1,006 meters), then the mean n computed for the entire channel is 0.028. This close agreement implies that the vertical control of the water level recorders is excellent. The mean Manning's n values presented in Table 2 are for flow velocities greater than 0.5 foot per second (15 centimeters per second). For flow velocities less 0.5 foot per second (15 centimeters per second), the Manning's n values are erratic due to much greater relative error in measurement of tidal differential and flow velocities, as well as inertial effects.

To determine if n values vary systematically with the mean flow velocity, they are compared for selected diurnals (Figs. 9, 10, and 11).

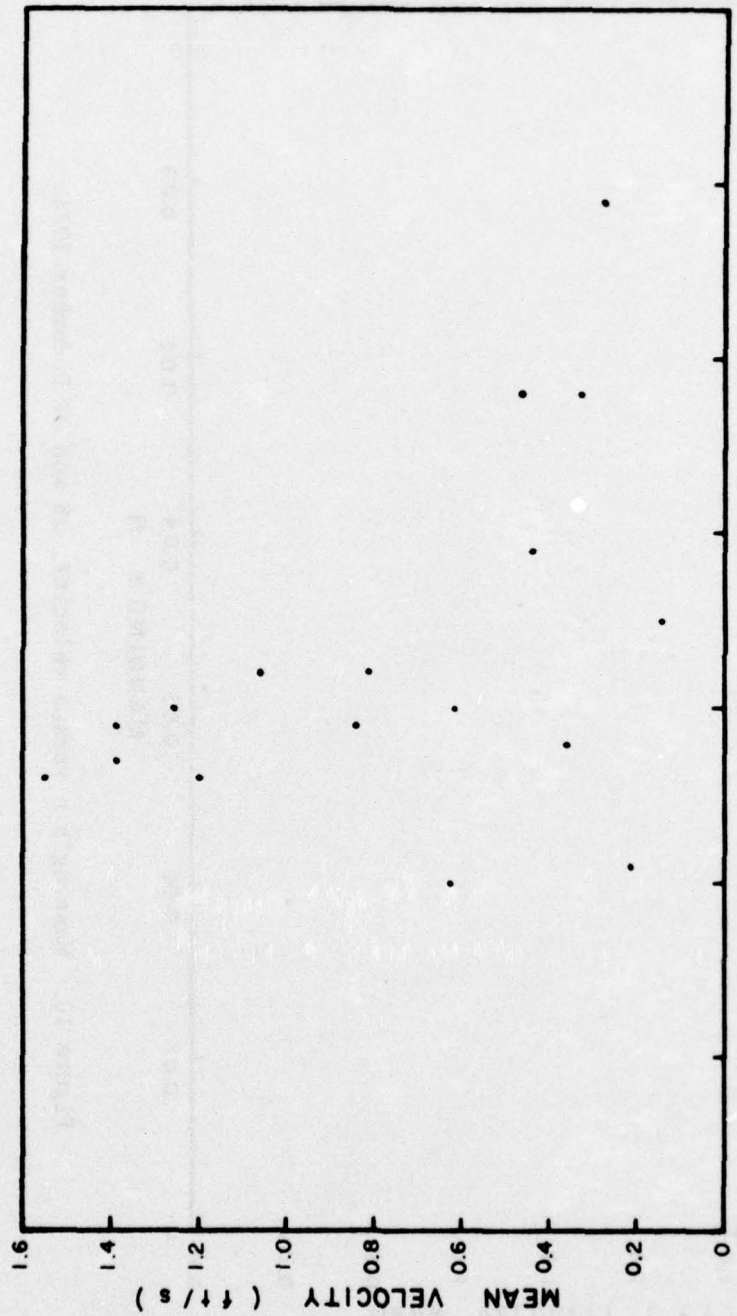

Figure 9. Manning's n versus velocity, 24 and 25 October 1974.

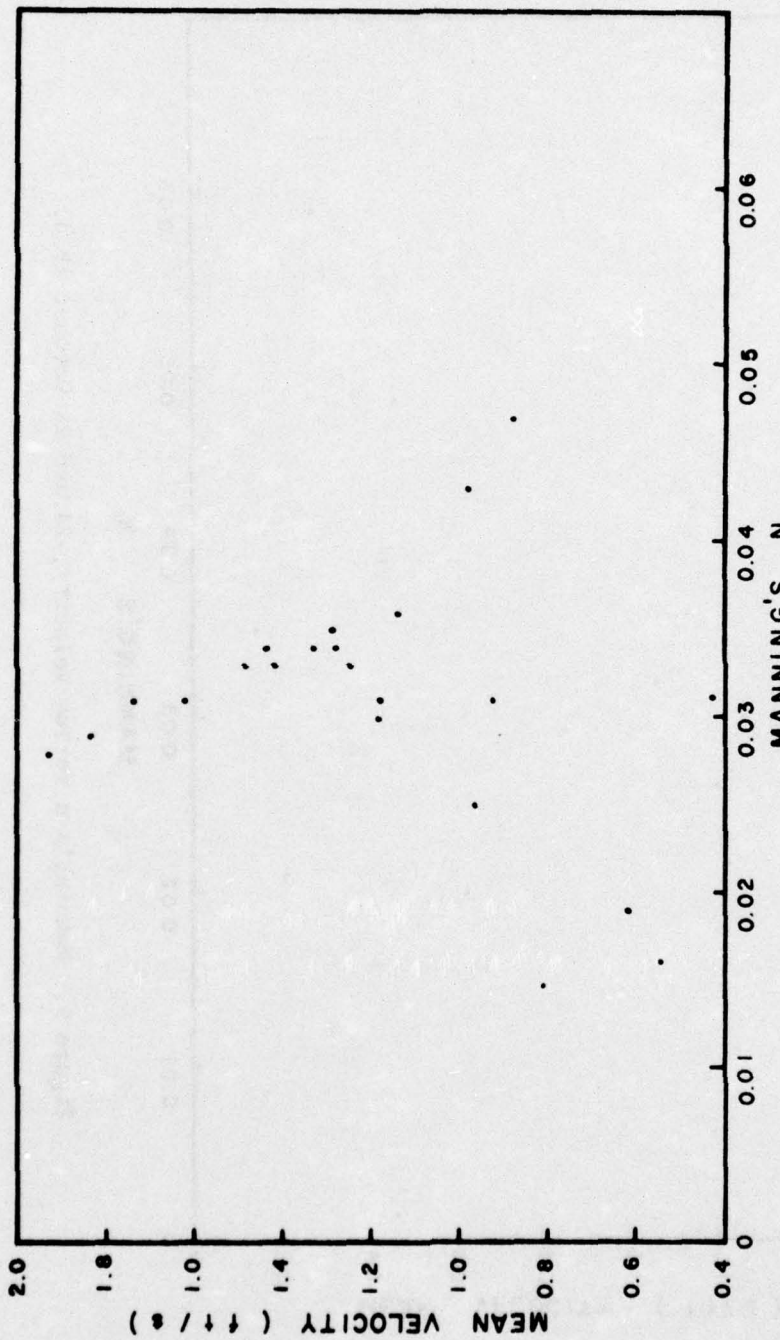

Figure 10. Manning's n versus velocity, 28 and 29 December 1974.

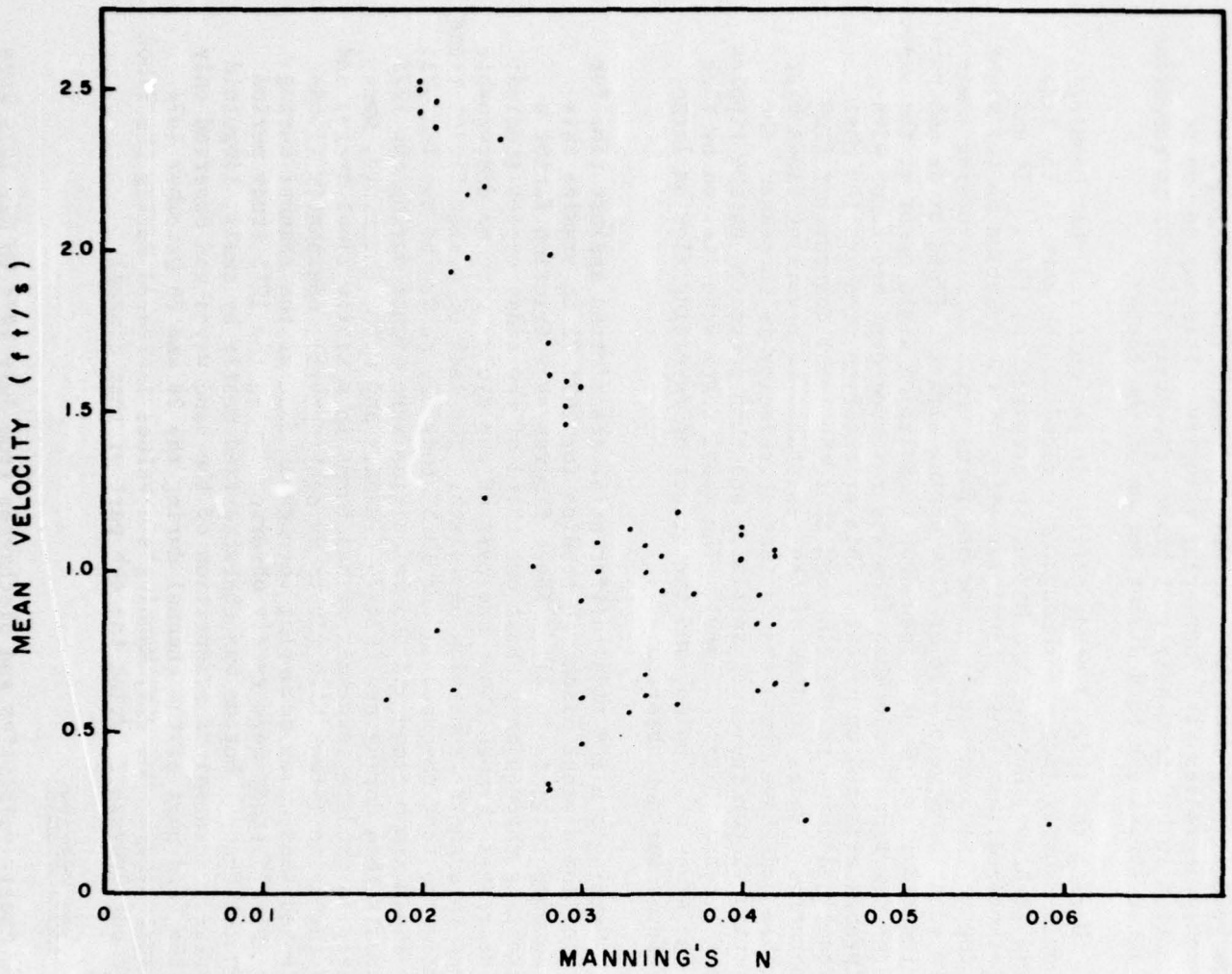

Figure 11. Manning's n versus velocity, 25 and 26 April 1975.

For flow velocities less than 1 foot per second (30 centimeters per second), there is no correlation between n and flow velocity, but for flow velocities greater than 1 foot per second that Manning's n commonly decreases with increasing velocity. This may be due to reduction in bed form height at higher flow velocities or to reduction in shear stress due to sediment motion on the bottom.

During the 1972-73 study period, it was observed that Manning's n would usually increase throughout a flood or ebb part of the tidal cycle (Behrens, Watson, and Mason, in preparation, 1976). It was hypothesized that this unusual variation of the friction factor might be due to the presence of major bed forms which were reversing their form with the development of flow during either a flood or an ebb part of the tidal cycle. A sudden drop in friction would occur at the onset of the new tidal cycle when flow was reversed over bed forms with slipfaces oriented upcurrent. This orientation produces the most streamlined shape to the flow and thus the least downcurrent flow separation. Model studies of the resistance to reversing flows over movable beds have demonstrated that as velocity is increased, the friction factor increases initially and then decreases as the ripples are flattened (Bayazit, 1969). The model tests were limited by size to the study of ripples, and the effect of reversing flow on larger bed forms was not observed.

Manning's n and tidal differential are plotted against time for each of the diurnal discharge studies for 1974-75 to examine this phenomenon (Figs. 12 to 21). These figures show friction factor n increasing through only about one-third of the tidal cycles studied; it decreases through about one-half of the cycles with no discernable trend through the remaining one-sixth. The lack of a significant trend similar to that observed in the 1973 study may be due to two factors: (a) The maximum flood and ebb velocities were higher during the 1973 diurnals than during the 1974-75 diurnals and were, therefore, more likely to produce reversals of bed forms in a single tidal cycle; and (b) the 1- to 3-foot high (30 to 90 centimeters), dominantly flood-oriented sand waves occurring throughout most of the channel during the 1974-75 study were rarely observed during the 1973 study period when the channel bottom was characterized mostly by small, linguloid ripples. Reversal of orientation of the sand waves was observed only in the bend part of the channel during the 28 and 29 December 1974 diurnal study. However, Manning's n values increased during the flood part but decreased during the ebb part of that diurnal.

5. Time History.

Hourly velocities and discharges from July 1974 to May 1975 were calculated using equation (1) and measured water surface slopes, average hydraulic radii, and friction coefficients. The results of these computations are given in Figures 22 and 23 and Appendix B.

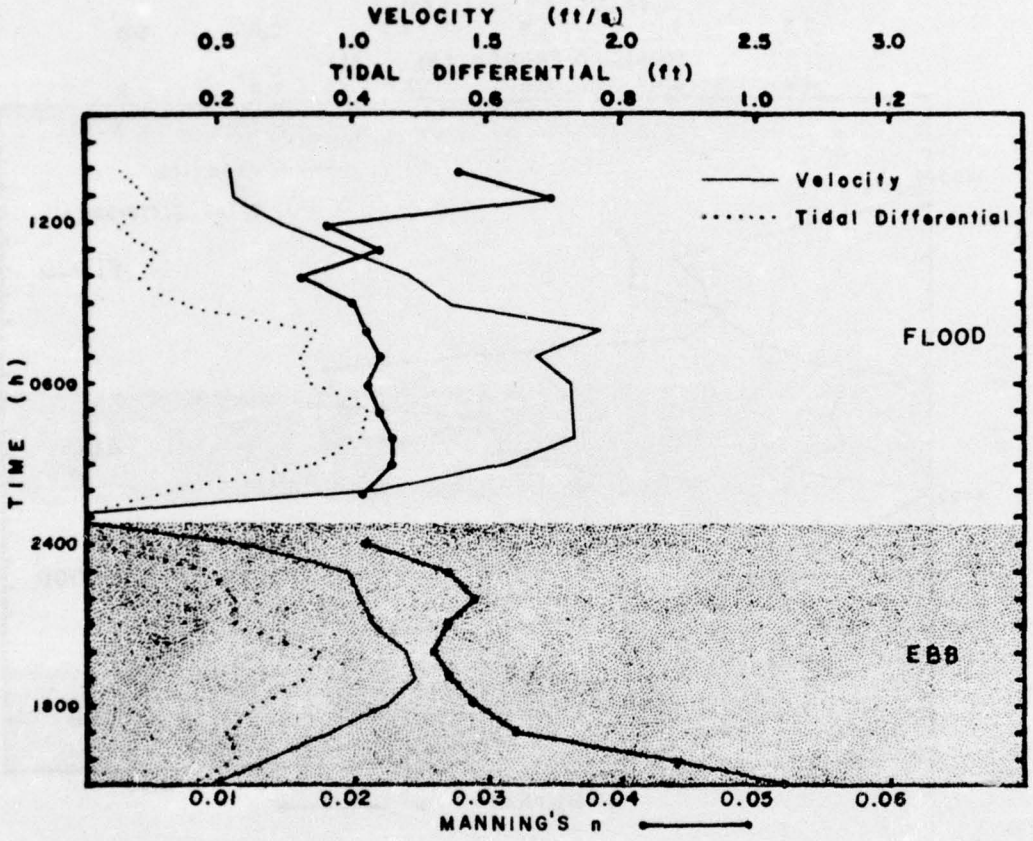

Figure 12. Tidal differential, velocity, and Manning's n through a diurnal period, 19 and 20 June 1974. Ebbtide period is shaded.

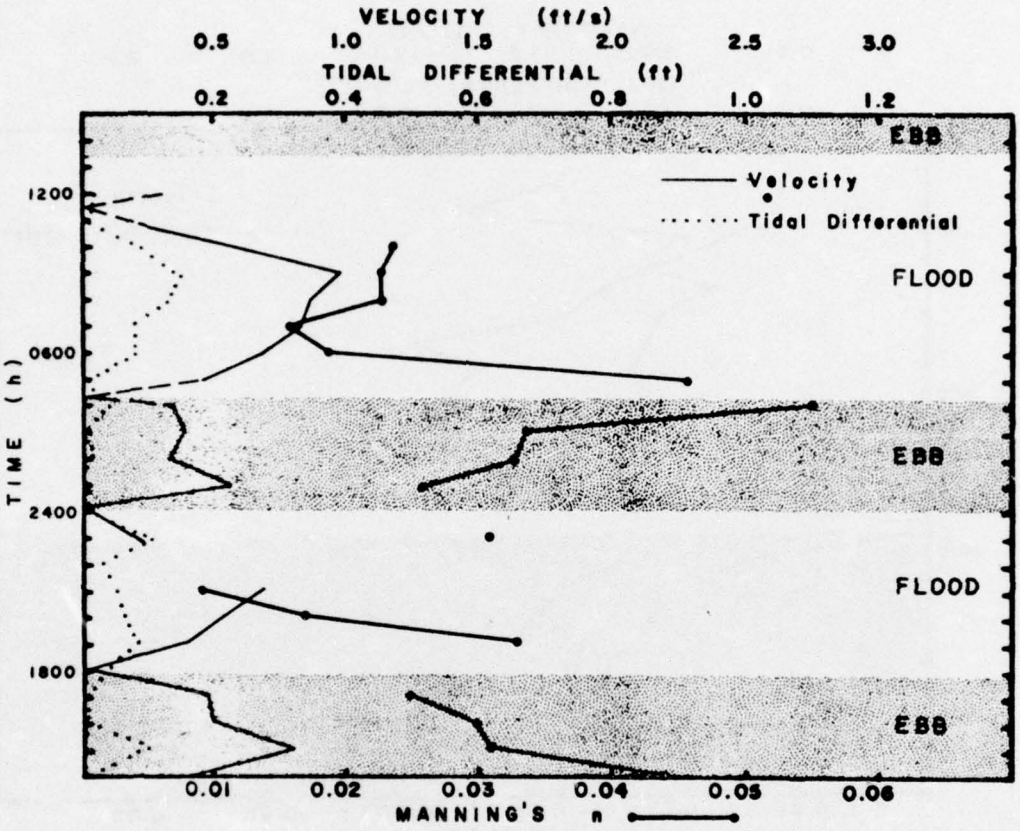

Figure 13. Tidal differential, velocity, and Manning's n through a diurnal period, 25 and 26 June 1974. Ebbtide periods are shaded.

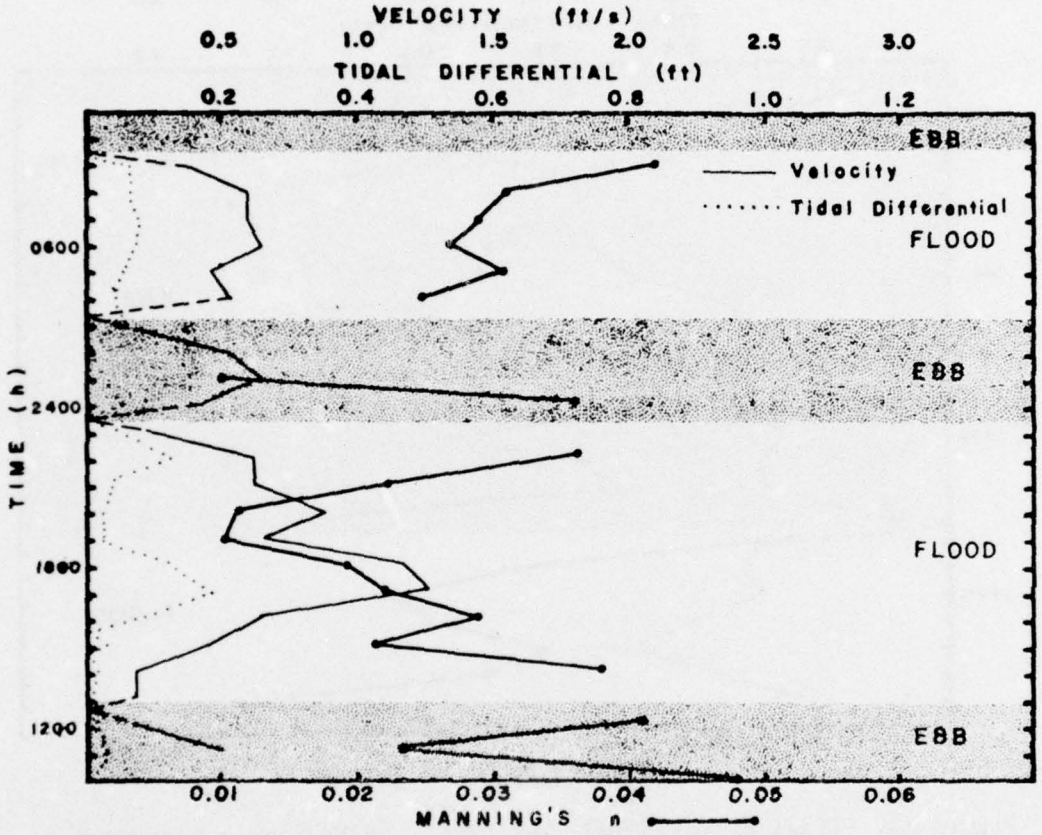

Figure 14. Tidal differential, velocity, and Manning's n through a diurnal period, 7 and 8 August 1974. Ebbtide periods are shaded.

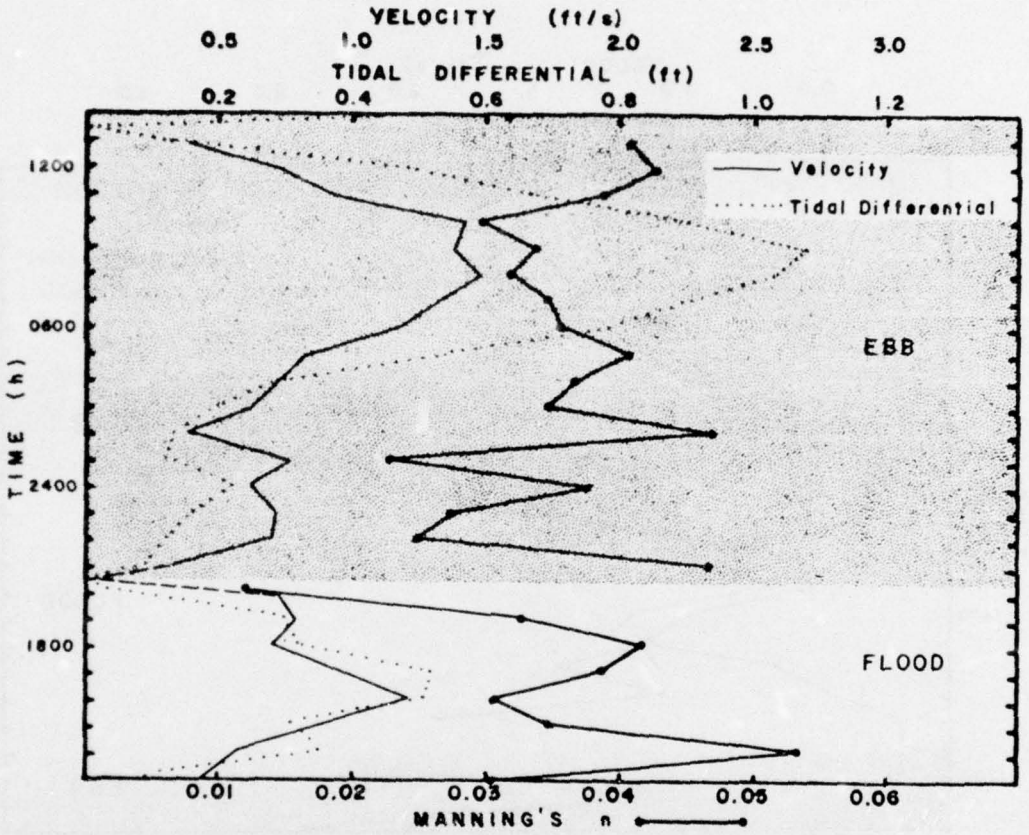

Figure 15. Tidal differential, velocity, and Manning's n through a diurnal period, 15 and 16 October 1974. Ebbtide period is shaded.

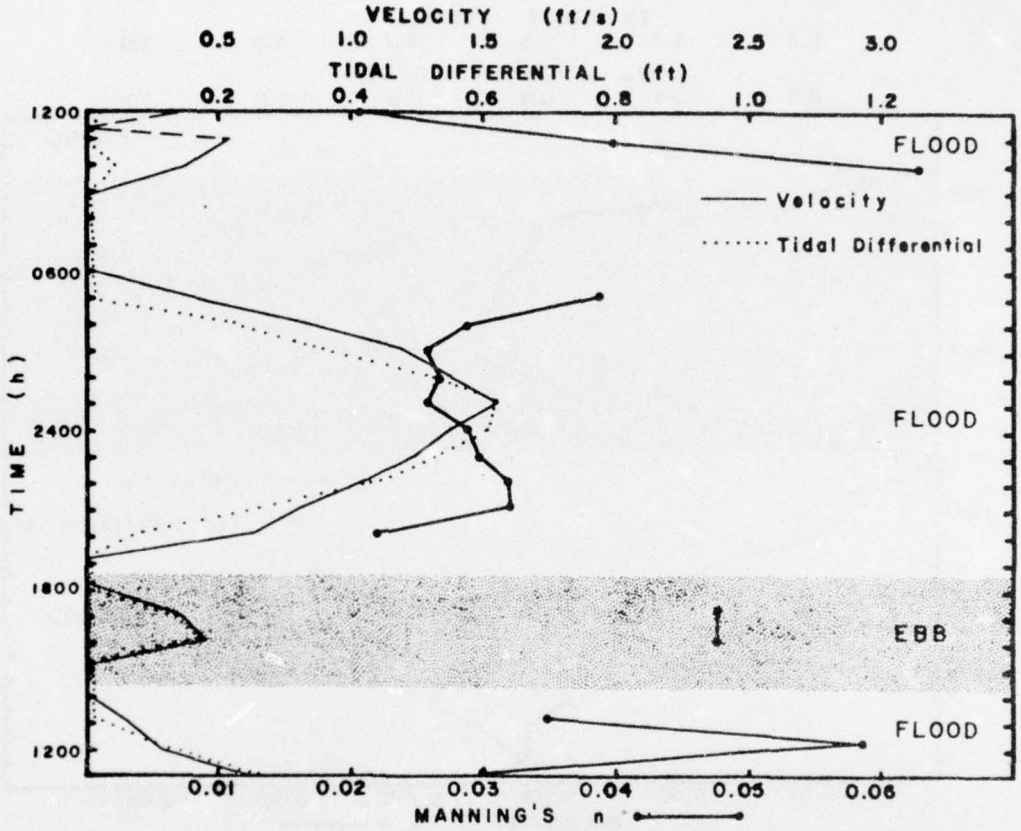

Figure 16. Tidal differential, velocity, and Manning's n through a diurnal period, 24 and 25 October 1974. Ebbtide period is shaded.

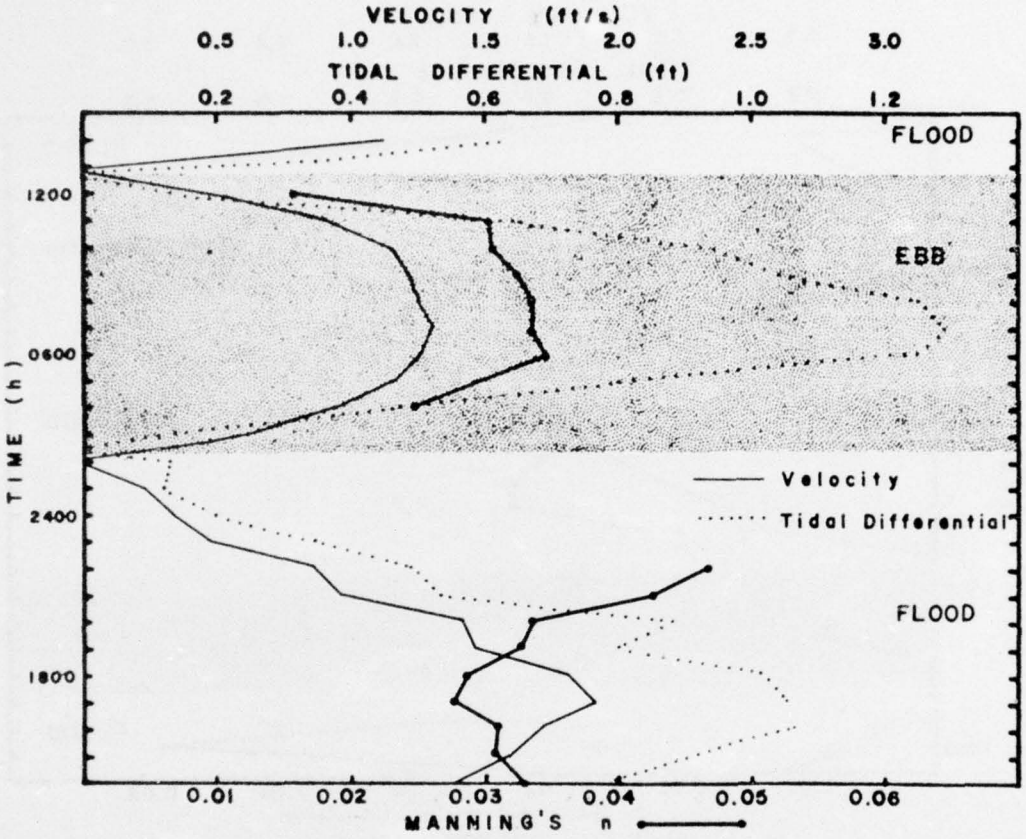

Figure 17. Tidal differential, velocity, and Manning's n through a diurnal period, 28 and 29 December 1974. Ebbtide period is shaded.

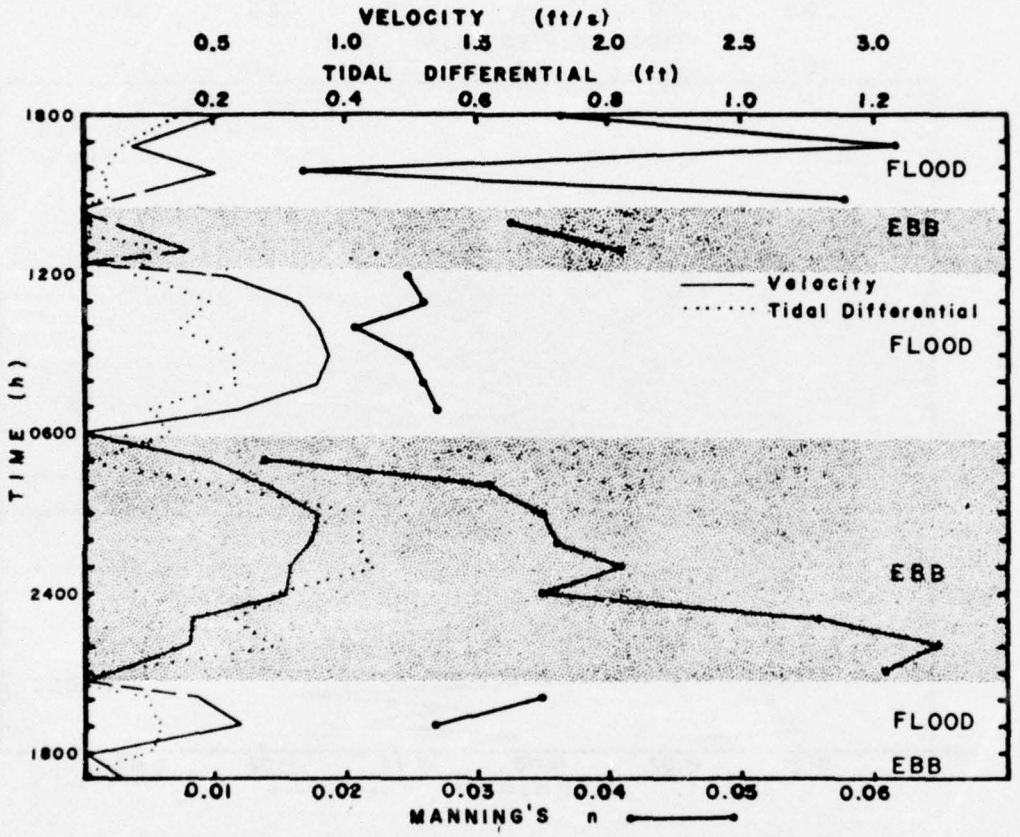

Figure 18. Tidal differential, velocity, and Manning's n through a diurnal period, 3 and 4 January 1975. Ebbtide periods are shaded.

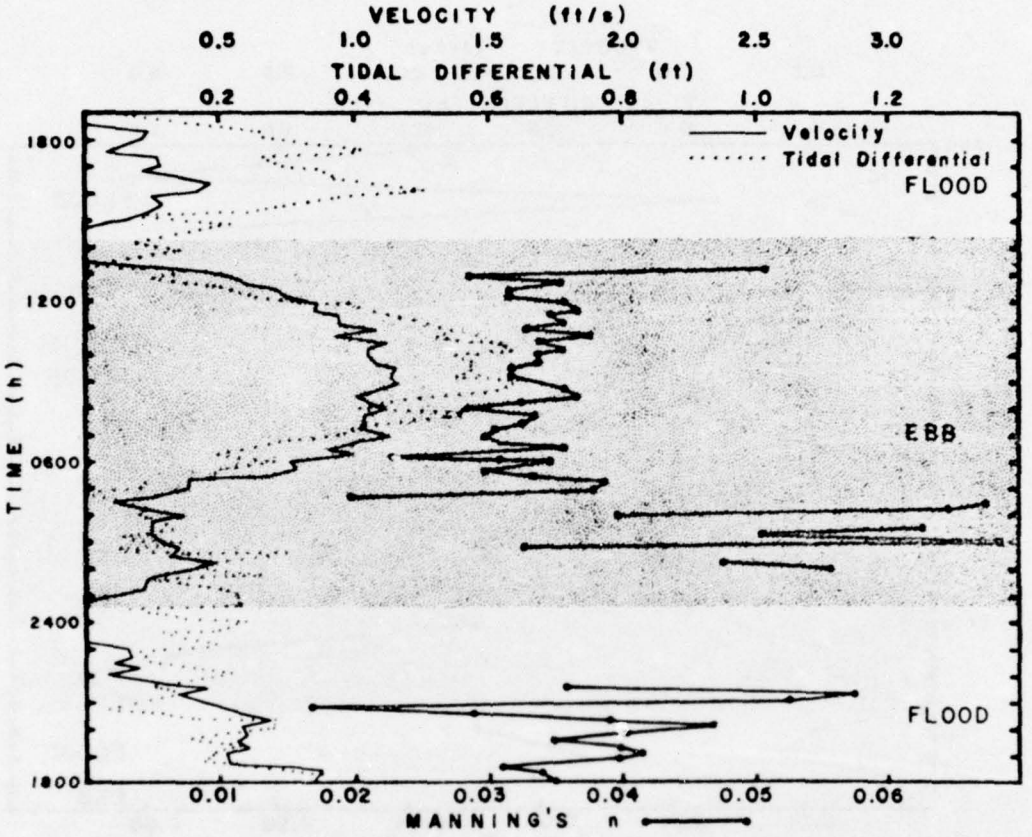

Figure 19. Tidal differential, velocity, and Manning's n through a diurnal period, 11 and 12 February 1975. Ebbtide period is shaded.

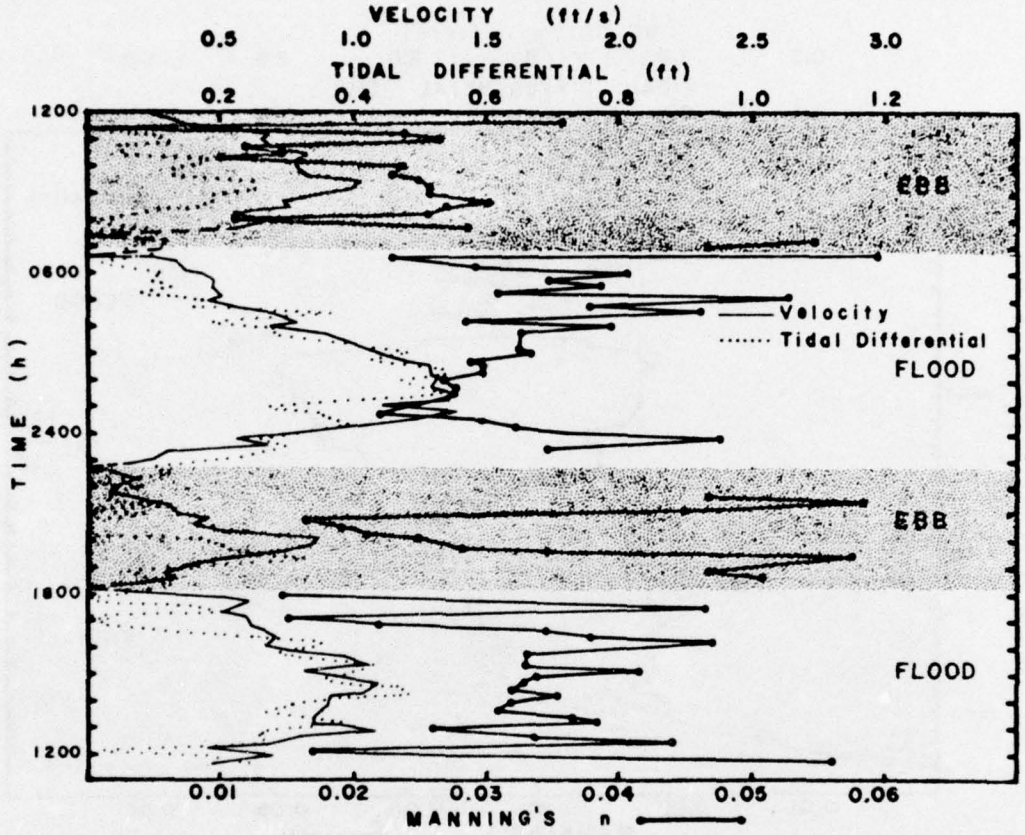

Figure 20. Tidal differential, velocity, and Manning's n through a diurnal period, 8 and 9 April. Ebbtide periods are shaded.

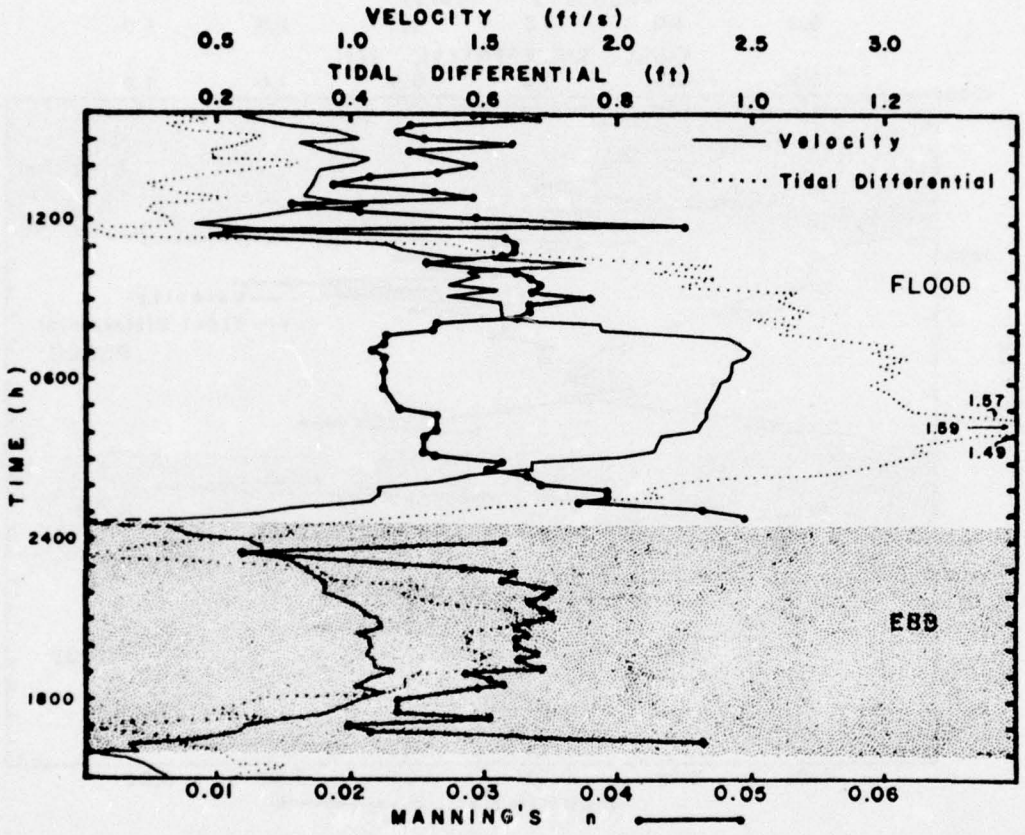

Figure 21. Tidal differential, velocity, and Manning's n through a diurnal period, 25 and 26 April 1975. Ebbtide period is shaded.

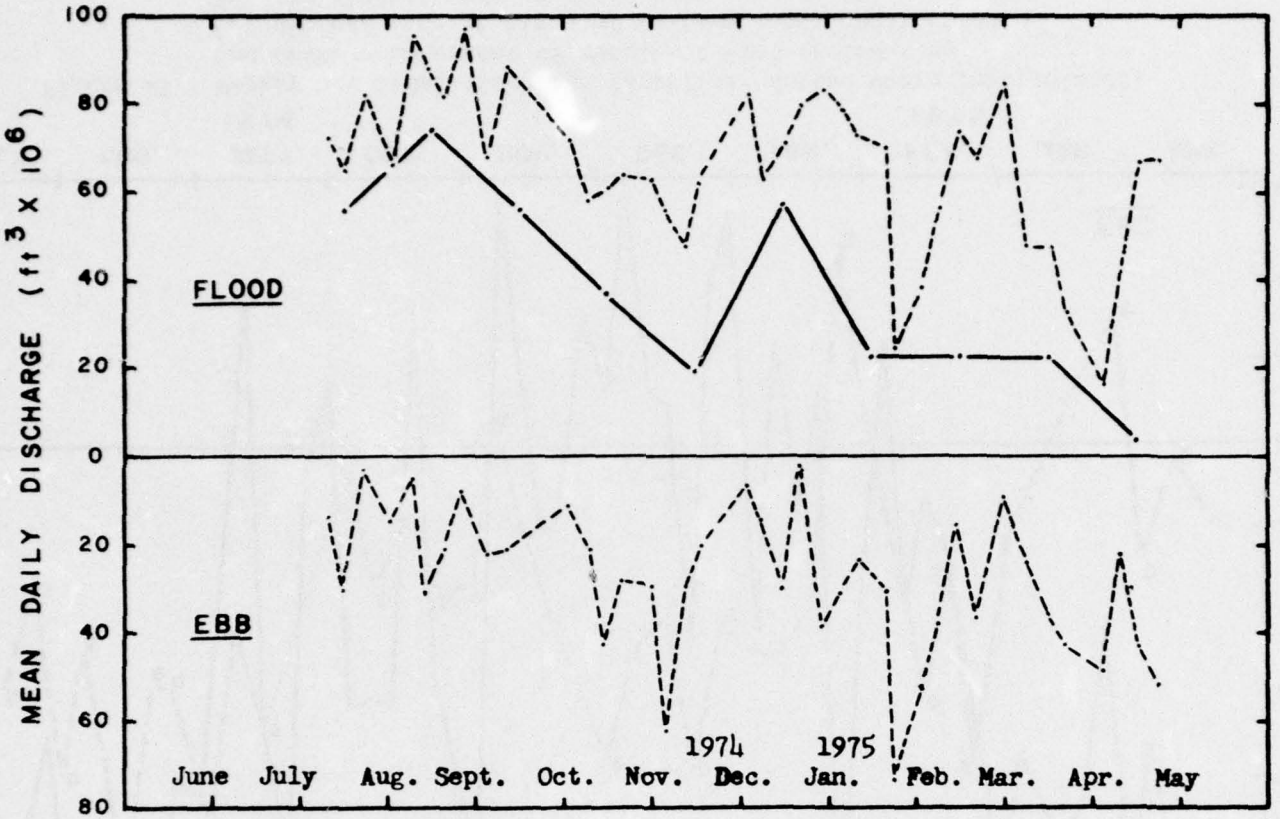

Figure 22. Tidal discharge by week and month. Discharges are mean daily values to reduce the effect of several short periods of incomplete data. Gross flood and ebb values are averages for approximately 7-day intervals beginning and ending with equatorial or positions of maximum declination of the moon. Net discharge is plotted for monthly averages. The high net flood value for December may be an artifact of partial data (about 50 percent of the month).

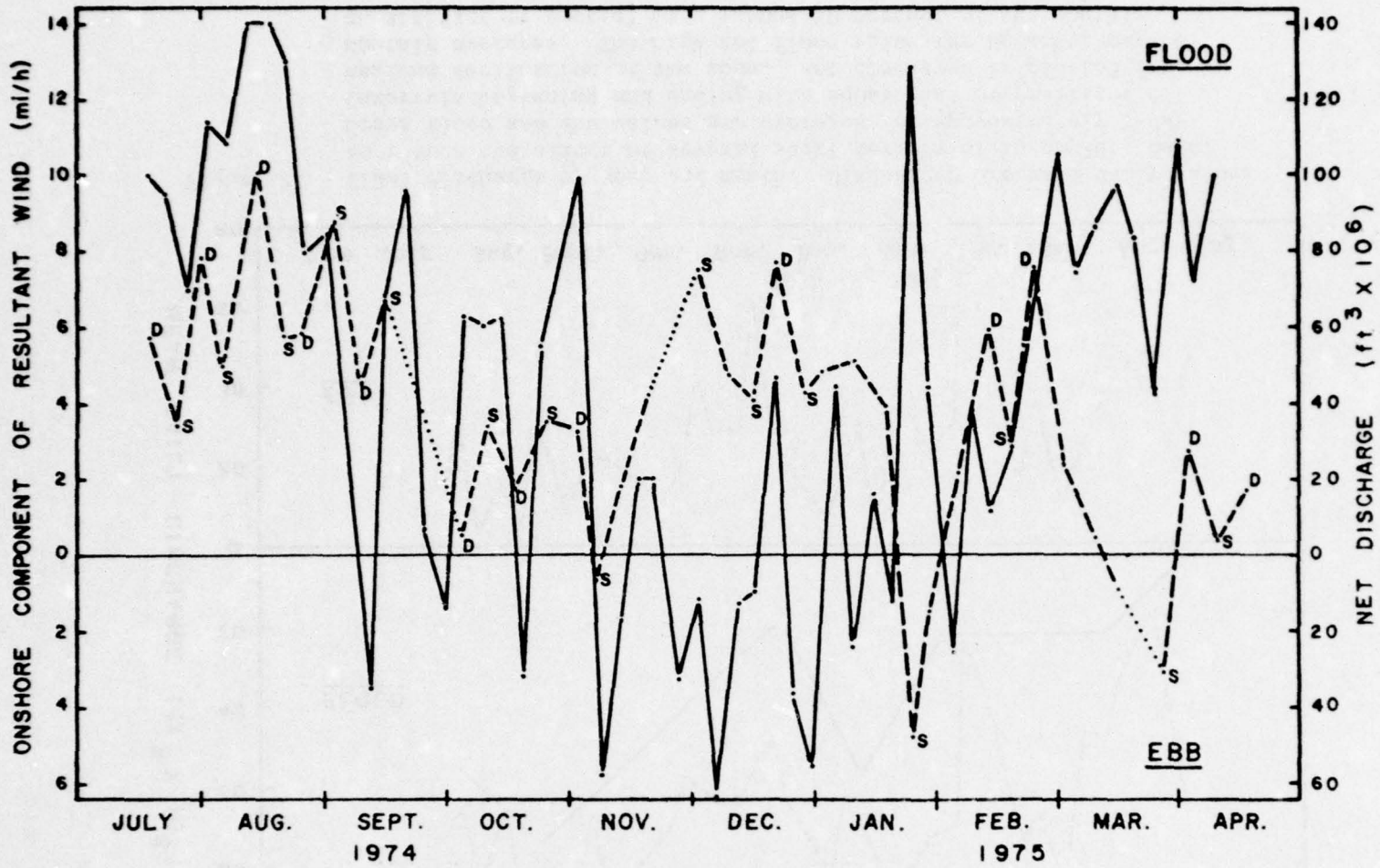

Figure 23. Weekly net tidal discharge (dashline; dotted where interpolated) and onshore component of resultant wind (solid line).
D = diurnal tide at times of maximum lunar declination;
S = semidiurnal tide at times moon crosses the equator.

As anticipated from tidal cycle velocity measurements and the average gulf and bay tide level difference, calculated flood minus ebb discharges show a net flood which averaged 36.6 X 10^6 cubic feet (1 X 10^6 cubic meters) per day.

The resultant, annual net flood discharge volume (13 X 10^9 cubic feet or 3.7 X 10^6 cubic meters) cannot be accounted for by evaporation, because it exceeds rainfall by only about 20 inches (51 centimeters) annually (Meyer, 1942), and thus could account for only about 6 X 10^9 cubic feet (1.7 X 10^6 cubic meters). Furthermore, Nueces River discharge into Corpus Christi and Nueces Bays (30 X 10^9 cubic feet or 8.5 X 10^6 cubic meters) (Collier and Hedgpeth, 1950) exceeds excess evaporation sufficiently to maintain salinities in Corpus Christi Bay below normal marine values except during periods of drought conditions.

Consequently, the excess flood discharge must flow through other outlets. Two channels could act effectively in this capacity. The Corpus Christi Ship Channel extends east from Corpus Christi to Port Aransas across the northern part of the bay. Thus, wind tides generated by the prevailing south-southeasterly winds could drain out this channel to the Gulf of Mexico. Corpus Christi Bayou connects the northeastern corner of the bay with Aransas Bay. Southerly winds would cause a water level differential between these bays and considerable northward discharge could take place.

Seasonally, the excess flood discharge is greatest from July to November (Fig. 22). The wind setups that lead to excess flood discharges cannot account entirely for this seasonal high, because the period of peak onshore winds creating the bay circulation away from the pass mouth begins sometime in March and extends only through August. However, mean water levels are rising from July to November due to storing effects (Whitaker, 1971) and this probably accounts for much of the peak in excess flooding at this time.

For shorter time intervals the amount of net discharge correlates both with resultant wind and with lunar positions. Figure 23 shows that over 70 percent of the short-term peaks in net flood discharge coincide with similar peaks of onshore resultant winds. Additionally, about 65 percent of the discharge peaks occurred at time intervals when the moon was progressing from an equatorial position to a position of maximum declination (semidiurnal to diurnal tides). The reason for this latter correlation is not apparent. Individual tidal cycle discharges are shown in Appendix B.

III. SEDIMENTATION AND EROSION

1. Introduction.

The amount of sedimentation and erosion was determined from

detailed bathymetric surveys within the channel, around the bay and gulf mouths, and up to 8,000 feet (2,438 meters) from each jetty along the gulf beach. Monthly surveys included from 19 to 24 channel cross sections (Fig. 24) and the shorter (500 feet or 150 meters) beach profiles 200, 400, 800, 1,200, 2,000, 4,000, 6,000, and 8,000 feet (61, 211, 244, 366, 610, 1,219, 1,829, and 2,438 meters) from each jetty. Bimonthly surveys were obtained of the bay and gulf mouths, and semiannual beach profiles 2,000 feet (610 meters) long were obtained at the same sites as the shorter, monthly profiles. Techniques are basically the same as those used during the 1972-73 study period (Behrens, Watson, and Mason, in preparation, 1976).

2. Gulf Beach Sedimentation.

a. Wave Climate and Longshore Transport. The most effective processes in the beach environment are wave action and wave-generated longshore transport. Consequently, daily visual wave observations were made 1 mile south of Aransas Pass between September 1972 and June 1975 as part of the CERC Littoral Environment Observation (LEO) program. These observations include significant wave height, wave period, angle between shoreline and wave orthogonal (measured from the left facing the ocean), wave type, longshore current speed and direction, and windspeed and direction.

Three years of data on wave climate (Table 4) show that from May to September waves are generally small, have a short period, and come from south of directly onshore. In other months the waves tend to be higher, have longer periods, and come from northeast of directly onshore. However, the most characteristic part of the data is the great range of values of all parameters for almost every month. The longer period winter waves are generally more refracted, the generating winds being most commonly directly alongshore; the shorter period summer winds commonly have a significant, short-fetch sea breeze component.

Monthly and annual rates of longshore transport to the north and south with net and gross rates in cubic yards (Table 5) were computed using the daily visual wave observation data and methods suggested by U.S. Army, Corps of Engineers, Coastal Engineering Research Center (1975). Longshore transport rates for missing days were estimated as the average of the previous day's rate and the following day's rate to produce an adjusted rate for entire month.

The pass is located about 30 miles (48 kilometers) north of a longshore transport convergence point on central Padre Island (Watson, 1971). As a result, the net longshore transport is directed to the south and is only about 8 percent of the gross rate.

b. Survey Results: 2,000-foot Profiles. Figures 25 to 30 show the changes in beach volumes determined from various pairs of sequential beach surveys and the longshore transport volumes computed from wave

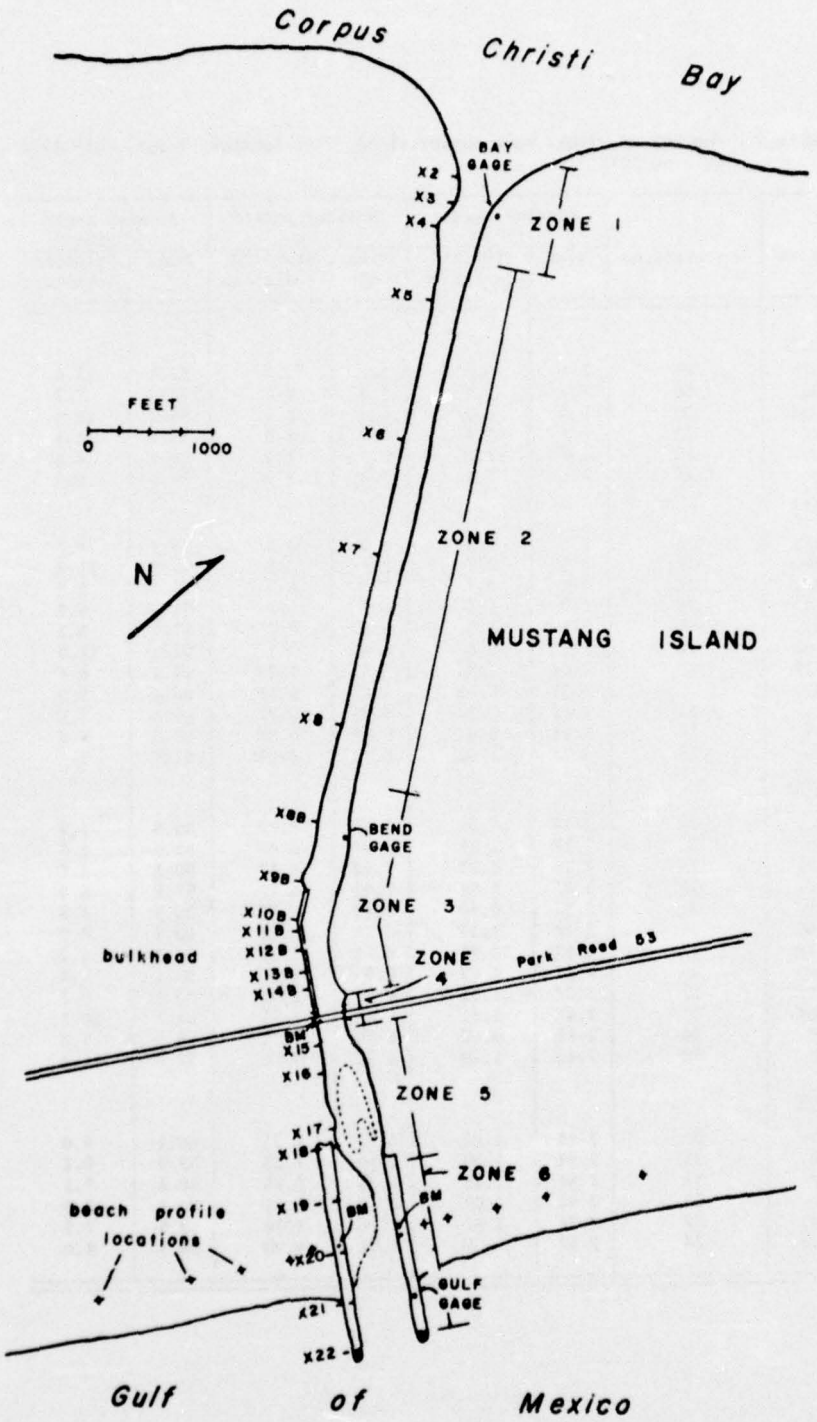

Figure 24. Corpus Christi Water Exchange Pass channel zones and cross-section survey locations.

Table 4. Summary of visual wave observations, Port Aransas, Texas, July 1972 to June 1975.

Month	Observations	Breaker height (ft)		Breaker period (s)		Breaker angle (degrees)	
		Mean	Standard Deviation	Mean	Standard Deviation	Mean	Standard Deviation
1972							
July	16	3.1	0.8	6.0	1.2	95.4	15.6
Aug.	30	2.1	1.4	5.4	1.2	102.6	7.2
Sept.	28	2.4	0.9	5.0	0.6	86.2	18.0
Oct.	27	2.6	1.4	5.9	1.0	89.0	11.5
Nov.	18	2.8	1.3	6.8	1.3	84.1	4.6
Dec.	27	2.8	1.5	7.4	1.0	85.0	6.9
1973							
Jan.	28	3.0	1.5	6.9	0.7	86.4	9.7
Feb.	27	2.5	1.1	7.3	0.9	85.0	11.4
Mar.	28	2.6	0.7	7.0	0.7	85.1	9.5
Apr.	28	2.7	1.5	6.7	.12	83.8	9.5
May	26	2.5	1.5	6.5	0.7	87.9	9.1
June	18	2.2	0.8	6.4	0.7	91.4	12.0
July		2.04	1.35	7.03	1.23	94.2	6.8
Aug.		2.31	0.60	7.03	1.10	86.4	7.9
Oct.	11	2.42	0.78	6.95	0.77	85.3	7.0
Nov.	30	3.14	0.95	6.88	0.80	88.6	8.3
Dec.	29	3.03	1.52	6.78	0.65	92.5	9.7
1974							
Jan.	28	2.10	1.01	6.49	0.79	86.8	6.8
Feb.	28	2.11	1.35	6.64	0.45	91.5	6.3
Mar.	25	2.19	0.95	6.92	0.47	90.2	5.1
Apr.	30	3.37	0.91	7.02	0.72	87.8	6.9
May	28	2.34	0.49	6.44	0.52	90.3	4.5
June	30	3.41	1.37	6.76	0.53	90.1	6.0
July	27	2.52	0.87	6.84	1.29	96.3	4.2
Aug.	26	2.11	1.22	5.80	0.97	93.1	5.4
Oct.	31	2.38	1.31	6.88	2.48	84.2	6.8
Sept.	37	2.47	1.41	6.44	1.71	85.7	10.1
Nov.	30	2.55	0.69	5.99	1.17	86.0	7.0
Dec.	30	2.41	1.29	6.51	1.06	92.0	11.4
1975							
Jan.	31	2.43	1.02	6.74	1.21	90.1	9.8
Feb.	25	1.84	1.00	6.50	1.23	88.9	9.2
Mar.	30	3.34	1.41	6.23	0.86	88.4	7.3
Apr.	23	2.91	0.97	6.17	1.21	86.7	3.6
May	27	2.29	1.50	5.36	2.16	92.6	7.5
June	24	2.37	1.07	5.51	0.90	96.3	8.0

Table 5. Longshore transport rates, Mustang Island, Texas.[1]

Date	Observations	To North[2]	To South[2]	Net[2]	Gross[2]
1972					
July	13	- 43.5	66.5	23.0	110.0
Aug.	25	- 71.0	0.0	-71.0	71.0
Sept.	28	- 28.8	65.1	+36.3	93.9
Oct.	26	- 22.6	43.9	+21.3	66.5
Nov.	18	- 1.5	58.3	+56.8	59.8
Dec.	27	- 28.4	53.7	+25.3	82.1
1973					
Jan.	29	- 47.5	72.9	+25.4	120.4
Feb.	27	- 19.2	68.3	+49.1	87.5
Mar.	28	- 15.1	49.8	+34.7	64.9
Apr.	30	- 59.5	55.5	- 4.0	115.0
May	26	- 38.9	27.8	-11.1	66.7
June	28	- 35.9	18.4	-17.5	54.3
July	28	- 24.2	.8	-23.4	25.0
Aug.	26	- 11.5	23.5	+12.0	35.0
Oct.	31	- 14.7	37.8	+23.1	52.5
Nov.	30	- 38.4	39.6	+ 1.2	78.0
Dec.	29	- 82.2	30.0	-52.2	112.2
1974					
Jan.	29	- 9.0	38.9	+29.9	47.9
Feb.	28	- 28.6	12.5	-16.1	41.1
Mar.	25	- 13.7	2.7	-11.0	16.4
Apr.	30	- 29.5	57.6	+28.1	87.1
May	29	- 13.0	6.9	- 6.1	19.9
June	30	- 31.1	38.8	+ 7.7	69.9
July	27	- 37.1	2.5	-34.6	39.6
Aug.	26	- 20.5	11.6	- 8.9	32.1
Sept.	29	- 39.1	61.6	+22.5	100.7
Oct.	31	- 6.5	41.0	+34.5	47.5
Dec.	29	- 45.1	11.1	-34.0	56.2
1975					
Jan.	31	- 15.1	41.6	+26.5	56.1
Feb.	23	- 18.1	6.9	-11.2	25.0
Mar.	30	- 9.5	50.4	+40.9	59.9
Apr.	24	- 40.5	30.7	- 9.8	71.2
May	27	- 17.5	10.5	- 7.0	28.0
June	24	- 27.0	9.0	-18.0	36.0
Monthly Mean		- 28.3	34.0	5.7	62.3
Annual Mean		-329.8	396.4	66.6	726.2

1. Data from U.S. Army, Corps of Engineers, Coastal Engineering Research Center (1975) and CERC LEO program.

2. Thousands of cubic yards.

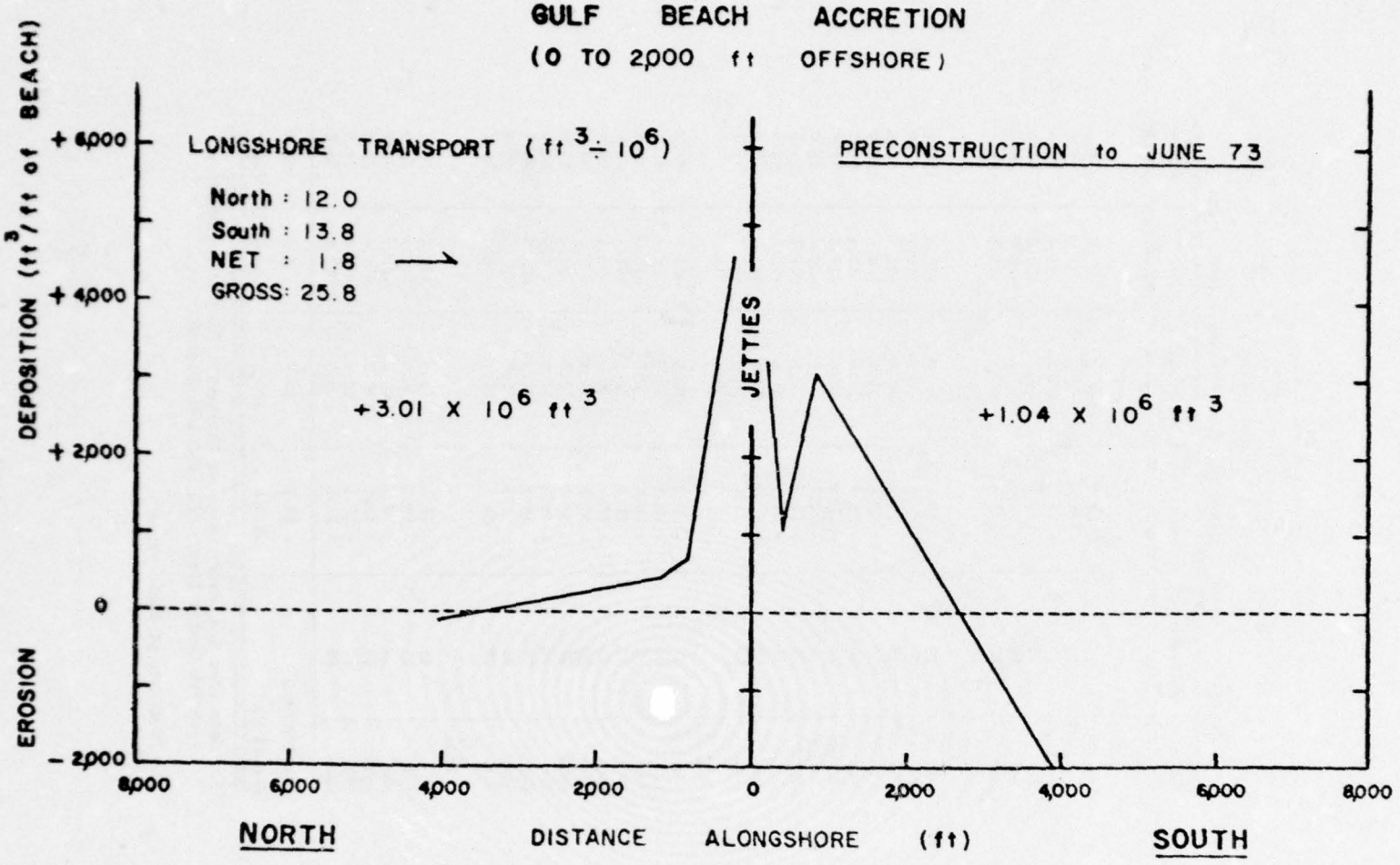

Figure 25. Gulf beach accretion, preconstruction to June 1973.

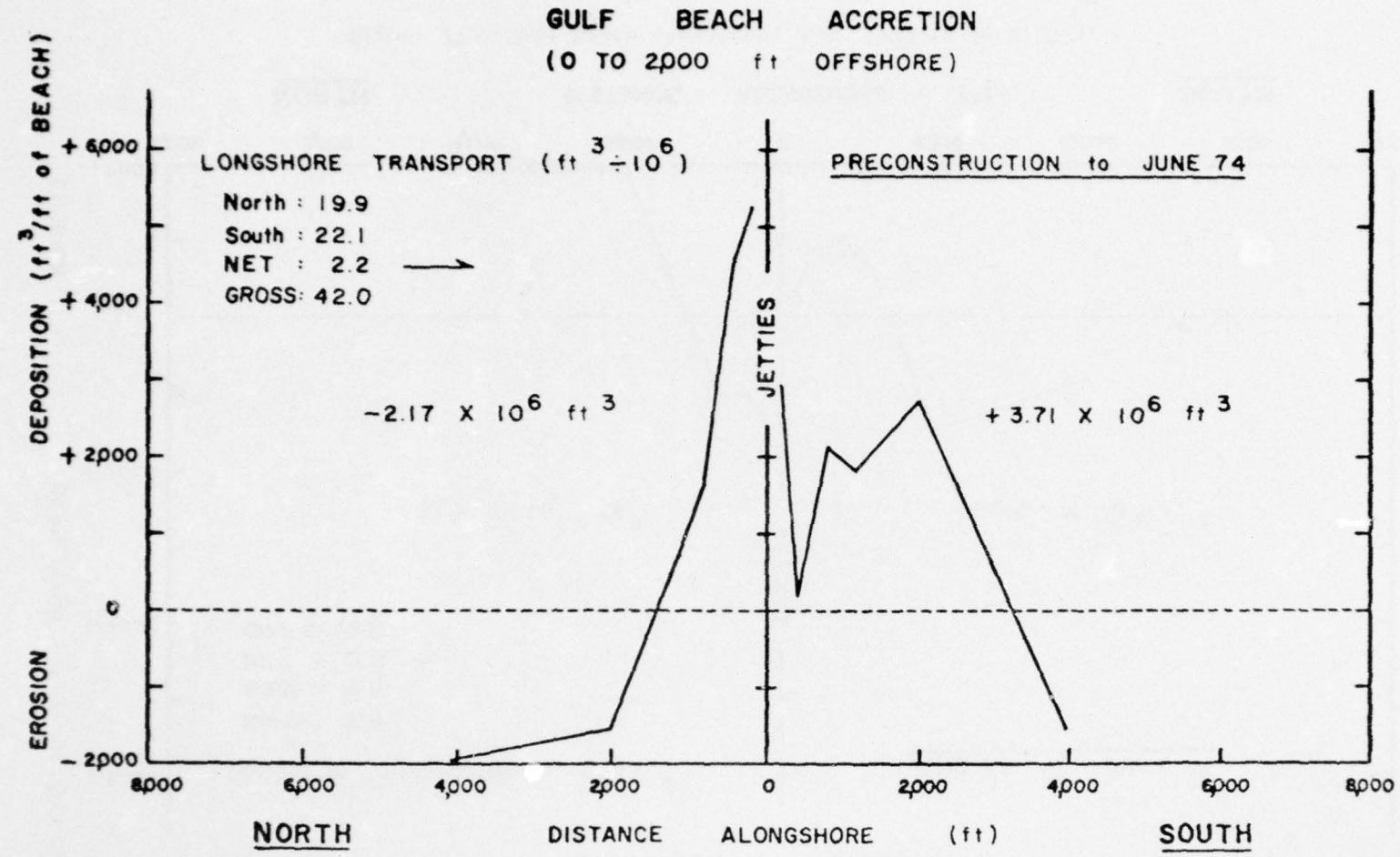

Figure 26. Gulf beach accretion, preconstruction to June 1974.

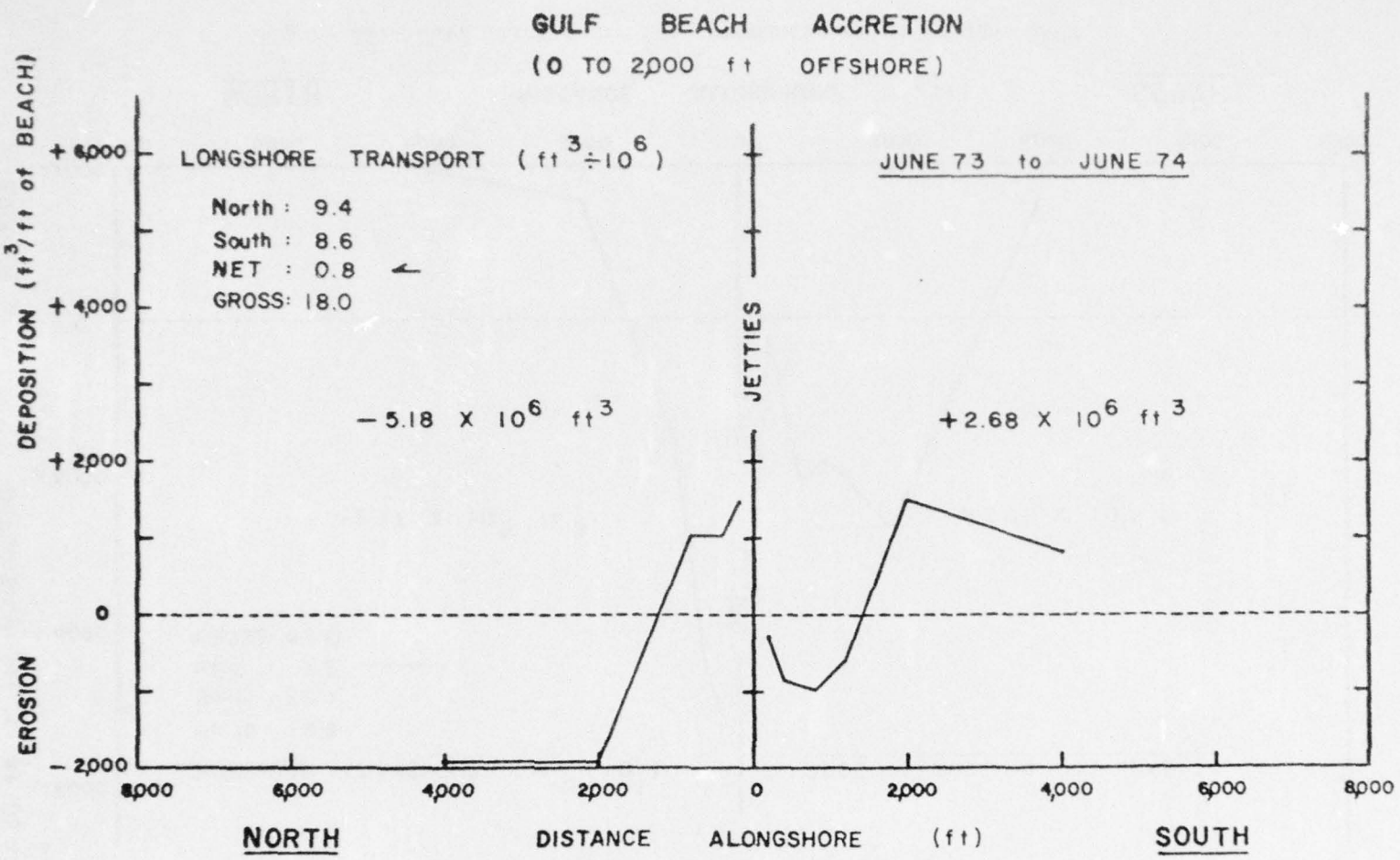

Figure 27. Gulf beach accretion, June 1973 to June 1974.

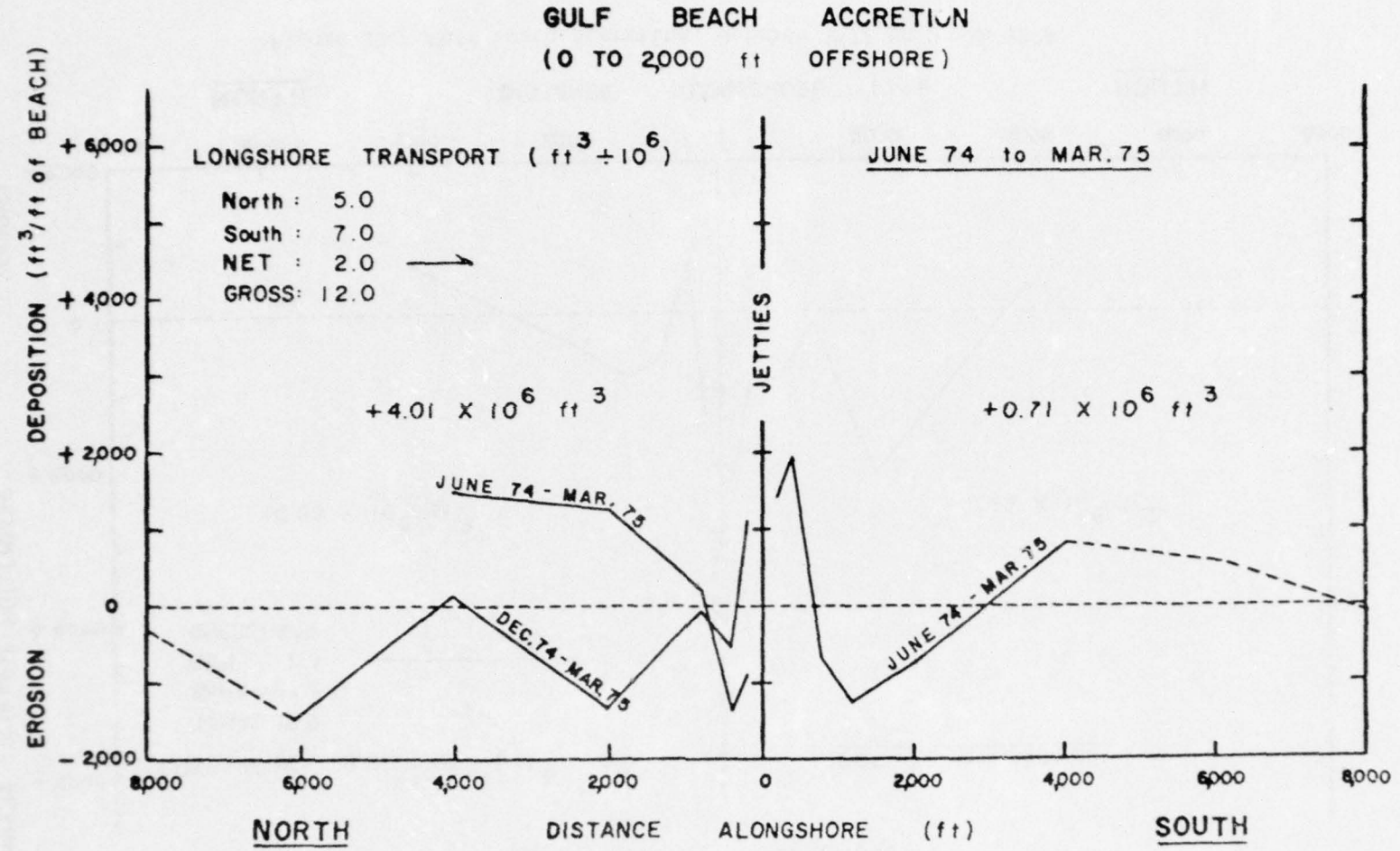

Figure 28. Gulf beach accretion, June 1974 to March 1975.

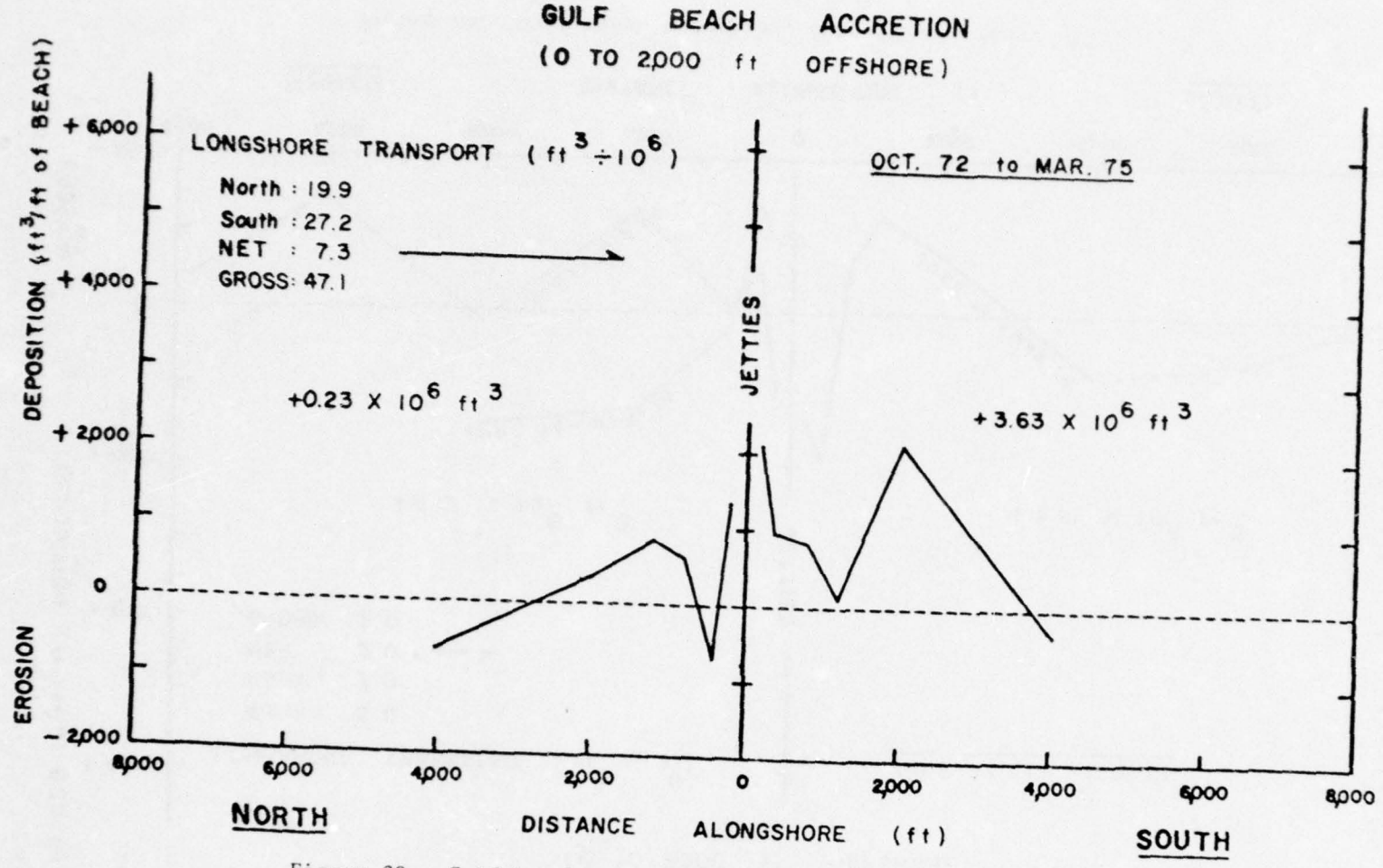

Figure 29. Gulf beach accretion, October 1972 to March 1975.

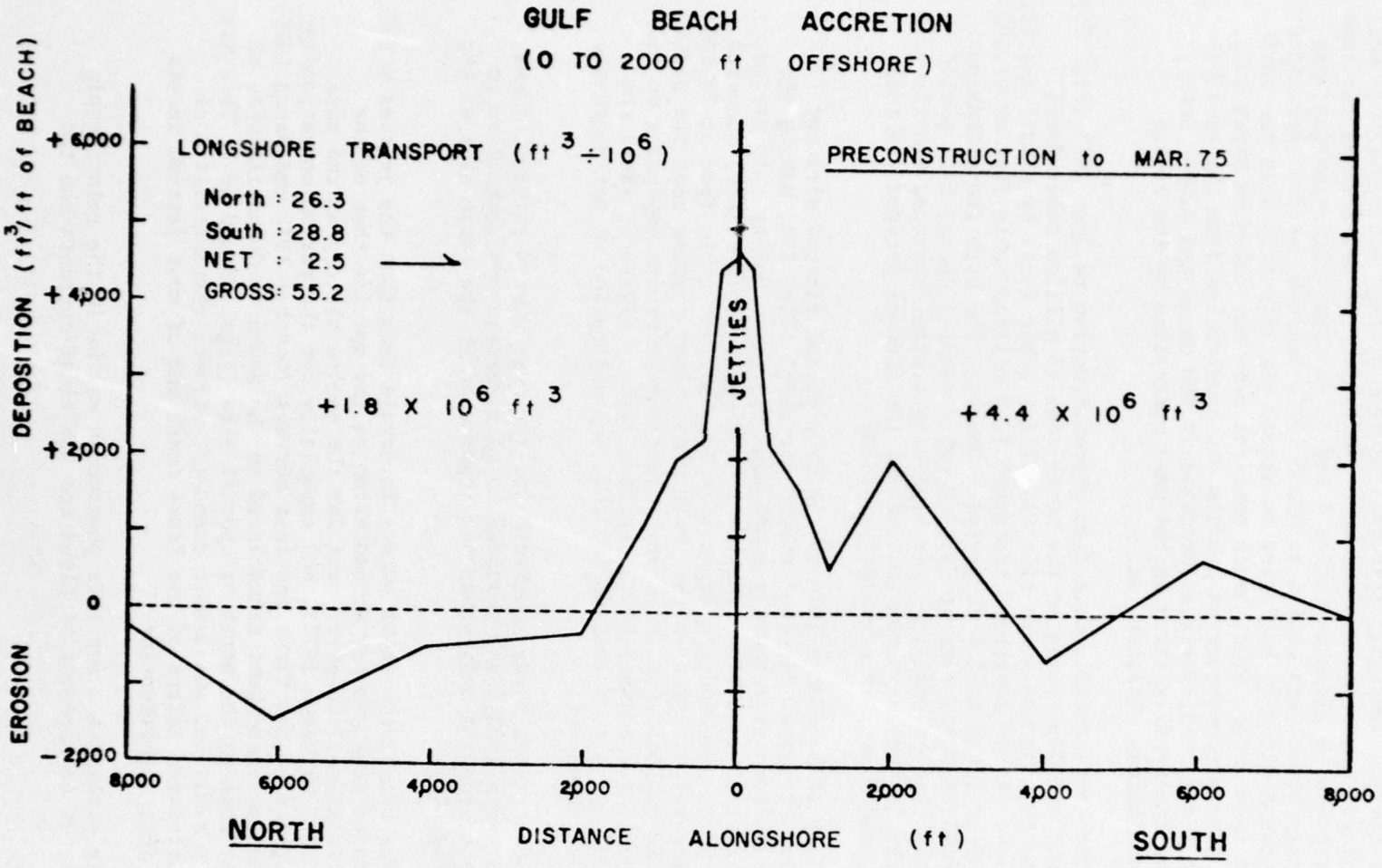

Figure 30. Gulf beach accretion, preconstruction to March 1975.

records for the same time intervals or from average monthly values when insufficient wave observations were available. Volume changes for each profile are also given in Tables 6 and 7. An arbitrary starting time (preconstruction) was chosen as March 1972, because jetties were under construction and only beginning to extend significantly into the surf zone on this date. Since beach profiles were not taken in March 1972, a composite preconstruction profile was constructed from the earliest, and least affected, surveyed profiles (4,000 north and 4,000 south), and from one profile taken on the pass centerline by the design engineers before construction.

The beach profile data from preconstruction to June 1973 (Fig. 25) show that net deposition on the north side (3 million cubic feet) exceeded that on the south side (1 million cubic feet) by almost exactly the volume of net longshore transport (1.8 million cubic feet or 51,000 cubic meters) for that time period. However, the high gross transport (25.8 million cubic feet or 731,000 cubic meters) during that period indicates that an efficient bar bypassing system developed shortly after the jetties were constructed and the channel dredged (Behrens, Watson, and Mason, in preparation, 1976).

June 1973 to June 1974 is the only period plotted with net longshore transport directed toward the north (Fig. 27), making the north side downdrift and the south side updrift. During this period, net erosion (5.2 million cubic feet or 147,000 cubic meters) occurred on the north side and net deposition (2.7 million cubic feet or 76,000 cubic meters) occurred on the south side. Some erosion near the south jetty was probably due to scour by longshore currents impinging on and being deflected seaward by the updrift jetty. Figure 26 shows the effect of north side loss during this unusual period of net northward longshore transport.

Net transport was southward for the next survey interval (June 1974 to March 1975), and resulted in considerable net deposition on the north side and only minor net deposition on the south side of the pass (Fig. 28).

The relatively short survey intervals show that the jetties acted like groins with greater accumulation on the updrift than on the downdrift sides. However, data for the entire history of the pass (March 1972 to March 1975), and especially for the period corresponding to the dates of the first and last surveys (October 1972 and March 1975), show that more sediment accumulated on the south or downdrift side of the pass than on the north or updrift side (Figs. 29 and 30). This has led to a small but measurable downdrift offset, characteristic of major unjettied inlets of the Texas coast and of most jettied inlets before jetty construction.

An explanation for this phenomenon may be in the relationship between the enhancement of flood and ebb tidal currents and the

Table 6. Gulf beach deposition[1], 0 to 2,600 feet offshore.

Station	Precon-struction Oct 72	Oct 72-Jan 73	Jan 73-Mar 73	Mar 73-June 73	June 73-June 74		June 74-Mar 75	Oct.72-Mar 75	
200 S	+2324	+1455	-1326	+ 770	- 255		+1445	+2089	
400 S	+1170	+1730	-1686	- 118	- 865		+1943	+1004	
800 S	+ 694	+1451	- 700	+1660	- 925		- 603	+ 883	
1200 S	+ 482	+ 998	- 741	+1684	- 600		-1231	+ 110	
2000 S	- 237	- 418	+ 594	+1246	+1500		- 744	+2178	
4000 S	- 240	- 970	- 86	-1009	+ 820		+ 860	- 385	
Deposition[2]	+1.62x10^6	+2.1x10^6	+0.83x10^6	+3.65x10^6	+3.74x10^6		2.73x10^6	+4.4x10^6	
Erosion[2]	-0.81x10^6	-2.5x10^6	-1.8x10^6	-2.05x10^6	-1.06x10^6		-2.02x10^6	-0.77x10^6	
Net[2]	+0.81x10^6	-0.4x10^6	-1.03x10^6	+1.6x10^6	+2.68x10^6		+0.71x10^6	+3.63x10^6	
	Precon-struction Oct 72	Oct 72-Dec 72	Dec 72-Apr 73	Apr 73-June 73	June 73-June 74	June 74-Dec 74	Dec 74-Mar 75	Oct 72-Mar 75	June 74-Mar 75
200 N	+3012	+ 531	-2403	+2688	+1430	-1983	+1131	+1394	- 852
400 N	+2935	- 245	-1934	+2823	+1045	-1888	- 539	- 729	-2427
800 N	+1282	+ 667	- 857	- 375	+1005	+ 233	- 27	+ 646	+ 206
1200 N	+ 288	± 193	+ 190	- 215	+ 85	+1069	- 506	+ 816	± 563
2000 N	- 755	+ 549	- 135	+ 678	-1885	+2566	-1364	+ 389	+1202
4000 N	+ 95	- 14	- 662	+ 473	-1870	+1331	+ 113	- 629	+1444
Deposition[3]	+2.66x10^6	+1.3x10^6	+0.11x10^6	+3.55x10^6	+1.20x10^6	+6.99x10^6	+0.56x10^6	+1.71x10^6	+4.99x10^6
Erosion[3]	-1.08x10^6	-0.1x10^6	-3.15x10^6	+0.28x10^6	-6.38x10^6	-1.16x10^6	-2.38x10^6	-1.48x10^6	-0.98x10^6
Net[3]	+1.58x10^6	+1.2x10^6	-3.04x10^6	+3.27x10^6	-5.18x10^6	+5.83x10^6	-1.82x10^6	+0.23x10^6	+4.01x10^6

1. Cubic feet per foot of beach.
2. Total volume south side, cubic feet.
3. Total volume north side, cubic feet.

Table 7. Cumulative gulf beach deposition[1], 0 to 2,000 feet offshore.

Station	Oct 72	Jan 73	Mar 73	June 73	June 74		Mar 75
200 S	+2324	+3779	+2453	+3223	+2968		+4413
400 S	+1170	+2900	+1214	+1096	+ 231		+2174
800 S	+ 694	+2145	+1445	+3105	+2180		+1577
1200 S	+ 482	+1480	+ 739	+2423	+1823		+ 592
2000 S	- 237	- 655	- 61	+1185	+2685		+1941
4000 S	- 240	-1210	-1296	-2305	-1485		- 625
Deposition[2]	$+1.62\times10^6$	$+3.75\times10^6$	$+2.1\times10^6$	$+5.65\times10^6$	$+6.68\times10^6$		$+5.6\times10^6$
Erosion[2]	-0.81×10^6	-3.3×10^6	-2.7×10^6	-4.61×10^6	-2.97×10^6		-1.2×10^6
Net[2]	$+0.81\times10^6$	$+0.45\times10^6$	-0.6×10^7	$+1.04\times10^6$	$+3.71\times10^6$		$+4.4\times10^6$

Station	Oct 72	Dec 72	Apr 73	June 73	June 74	Dec 74	Mar 75
200 N	+3012	+3543	+1140	+3828	+5258	+3275	+4406
400 N	+2936	+2691	+ 757	+3580	+4634	+2746	+2207
800 N	+1282	+1949	+1092	+ 717	+1722	+1955	+1928
1200 N	+ 288	+ 481	+ 671	+ 456	+ 541	+1610	+1104
2000 N	- 775	- 226	- 361	+ 317	-1568	+ 998	- 366
4000 N	+ 95	+ 81	- 581	- 108	-1978	- 647	- 534
Deposition[3]	$+2.66\times10^6$	$+3.10\times10^6$	$+1.41\times10^6$	$+3.23\times10^6$	$+3.98\times10^6$	$+4.95\times10^6$	$+3.42\times10^6$
Erosion[3]	-1.08×10^6	-0.32×10^6	-1.67×10^6	-0.22×10^6	-6.15×10^6	-1.29×10^6	-1.58×10^6
Net[3]	$+1.58\times10^6$	$+2.78\times10^6$	-0.26×10^6	$+3.01\times10^6$	-2.17×10^6	$+3.66\times10^6$	$+1.84\times10^6$

1. Cubic feet per foot of beach.

2. Total volume south side, cubic feet.

3. Total volume north side, cubic feet.

alternating longshore transport created by the bimodal wind system of the region. Southerly onshore winds enhance flood currents while generating northward-flowing longshore currents. Thus, littoral drift carried to inlets from the south would tend to be carried into or through the inlets, and beaches farther north would be starved. However, north winds enhance ebb currents while generating southward-flowing longshore currents, and littoral drift carried to inlets from the north would be more easily bypassed (and perhaps augmented by bay sediments) to the beaches farther south.

It would seem to follow that if the predominant loading of the channel was by longshore transport from the south, then the load would be deposited primarily on the south side of the channel. This has, indeed, been the case since early history of the pass (Behrens, Watson, and Mason, in preparation, 1976; Section II, 5).

Beach profile data of the 1972-73 study period showed that at depths of 11.1 feet (3.4 meters) south of the jetties and 11.8 feet (3.6 meters) north of the jetties, the beach profiles had a stable bottom elevation with neither accretion nor erosion, although the bottom elevations changed both landward and seaward of these depths. Later profiles taken in June and December 1974, and March 1975, showed no similar nodal point in elevation. This phenomenon may therefore be coincidental.

c. Survey Results: 500-foot Profiles. Although shorter beach profiles (App. C) do not provide an accurate estimate of quantities of erosion and deposition, they do reveal some seasonal variations in beach morphology and processes. Short-term studies by Davis and Fox (1972, 1975) showed that the innermost bar on Mustang Island beaches responds rapidly to increases in wave energy by increasing bar to trough relief and by seaward migration of the bar up to 50 feet (15 meters). Davis and Fox (1972) stated, "As energy subsides there is slow landward movement of the bar and filling of the trough"; furthermore, "high-energy conditions generally cause the shoreline to retreat between 15 and 25 feet. . . with low-energy conditions permitting the shoreline to return to its original position." These high-energy conditions referred to fall and winter northers, and observations were based on daily profiles. It might be expected that monthly profiles taken at random times relative to northers would show random patterns of bar heights, depths, and positions. However, examination of time-series diagrams (App. C) reveals several patterns of gradual change and consistent morphology.

The morphological elements traced were: (a) The backshore, which was wide near the jetties and narrow to almost nonexistent beyond 2,000 feet (610 meters) from them; (b) the berm crest, which may be either sharply or poorly defined; (c) the foreshore, of which the inner part was steepest and the outer part commonly formed a nearly flat toe at or just below mean sea level; (d) a trough between the toe of the

foreshore and the first bar; and (e) the first surf zone bar.

The least change took place on the backshore where the only major event was the widespread growth of small dunes which began in March 1974, the first month of the year when the southeasterly wind mode becomes dominant. A similar but more gradual development of backshore dunes occurred from February to April 1975. The berm crest and foreshore were the next most stable morphological elements. The berm crest retreated concurrently with a foreshore slope decrease or retreat shortly after the first strong, fall northers in September 1974. At the same time seasonal tide levels were rising rapidly (Fig. 7).

The shoreline, the foreshore toe, and the first bar did not always move in concert, but all showed distinct tendencies to advance seaward during falling seasonal water levels and to retreat landward during rising seasonal water levels. These trends are identified in Appendix C (Figs. C-17 to C-32). The tendency of offshore forms to migrate landward (especially but not exclusively with rising seasonal tide levels) is prevalent, but slow offshore migrations, even during rising tide levels, also occur (App. C, Figs. C-21 and C-31).

3. Gulf Mouth Deposition.

Contour maps of the gulf mouth region are presented in Appendix D. In the 1972-73 study period, mapping of the gulf mouth indicated that after initial fill of the deeply dredged channel, scour holes developed at the end of the updrift jetty during periods of strong wave action (Behrens, Watson, and Mason, in preparation, 1976). It was hypothesized that the holes were scoured by a combination of wave action, tidal currents, and longshore currents. The scour hole at the north jetty was 19 feet (5.8 meters) in late February 1973 (Behrens, Watson, and Mason, in preparation, 1976); depths off the south jetty were only 4 to 6 feet (1 to 2 meters). However, by 7 June 1973 (App. D, Fig. D-1) the hole at the north jetty had filled to -11 feet (-3.35 meters) and northward longshore currents typical of spring conditions had scoured a hole 15 feet (4.6 meters) deep at the end of the south jetty.

This pattern was repeated during 1974 and 1975, but to a lesser extent, perhaps reflecting the slow filling of the pass and reduced scouring ability of the tidal currents. On 28 June 1974 (App. D, Fig. D-2), 5- to 6-foot (1.5 to 1.8 meters) depths were at the ends of both jetties and no scour holes were present. This probably resulted from the low gross longshore transport rate for May and the low net rates for both May and June (Table 6). By 1 August 1974 (App. D, Fig. D-3) the area around the end of the south jetty had deepened to 8 feet (2.4 meters). Due to hazardous surf conditions, the surveys on 30 September (App. D, Fig. D-4) and 27 November 1974 (App. D, Fig. D-5) did not extend close enough to the jetties to determine the existence of scour holes, although they appeared to have been absent in September. In

February 1975 during very calm conditions, an accurate and detailed map of the entire gulf mouth area including the shoal inside the jetties was obtained (App. D, Fig. D-6). A deep scour hole had formed off the end of the north jetty; depths of only 6 feet (1.8 meters) existed near the south jetty. Winter waves and longshore currents had caused the third gulf bar to extend southward across the mouth of the pass seaward of the north jetty hole, and the main channel of the pass had shifted southward. A slight trough had developed just seaward of the third bar. By 12 May 1975 (App. D, Fig. D-7) the hole at the end of the north jetty had become considerably smaller and shoaled to -12 feet (-3.7 meters); the northward longshore currents of spring had scoured a hole to a depth of 9 feet (2.7 meters) off the south jetty. The crest of the third bar, at a depth of 6 feet (1.8 meters), extended completely across the pass mouth and the trough seaward of the third bar had disappeared.

A plot of the data given in Table 8 (Fig. 31) shows an initial period of predominant erosion through March 1973, followed by rapid, extensive deposition through June 1973. Although data were not collected between June 1973 and June 1974, subsequent data indicate that the gulf mouth region was generally shallower than the initial condition (net deposition between 10 and 20,000 cubic yards or 7,000 to 15,000 cubic meters). The only exception to this trend was in February 1975, when the large scour hole adjacent to the north jetty and the deep channel through the third bar contributed to a slight net erosion.

Although the volumetric changes within this region are small, the bathymetry changes continually with a deep hole usually found at the north jetty during winter, at the south jetty during summer, and transitional forms occurring during fall and spring.

4. Baymouth and Flood Tidal Delta.

Contour maps (App. E) derived from the approximately bimonthly baymouth surveys were used to graphically compute erosion and deposition volumes (Table 9; Fig. 32).

During the 1972-73 study period the controlling depth decreased from 8 to 2 feet (2.4 to 0.6 meters); about 63,000 cubic yards (48,000 cubic meters) of sediment were deposited (Behrens, Watson, and Mason, in preparation, 1976) in the form of a simple, single-lobed flood ramp. Between May 1973 and August 1974 the small remaining channel from the flood ramp to the bay disappeared, and a broad lip less than 2 feet (0.6 meter) deep became continuous around the ramp (App. E, Figs. E-1 and E-2). A shallow (2 to 3 feet; 0.6 to 1 meter) channel reformed across the lip from October to November, and a shoal less than 2 feet deep subsequently persisted around the flood ramp. Until this channel reformed, the flood ramp developed symmetrically along an extension of the channel axis across the approximately 1,000-foot-wide (300 meters) sandflat between the shoreline and the open bay. During the winter, the sediment carried to the distal end of the ramp through this channel was deflected southward by northerly wind-generated waves until by January the end had curved about 300 feet (100 meters) to the south and remained curved until the end of the study period.

Table 8. Gulf mouth erosion-deposition

Date	Erosion-deposition (ft^3)	Cumulative (yd^3)
1972		
15 Sept.	+121,200[1]	+ 4,500
26 Nov.	-675,200[2]	-20,500
22 Dec.	+356,400	- 7,300
1973		
29 Jan.	-672,400	-32,200
28 Feb.	+547,600	-11,900
5 Apr.	+395,400	+ 2,700
16 May	+121,200	+ 7,200
7 June	+217,560	+15,250
1974		
28 June	-199,560	+ 6,400
1 Aug.	+491,900	+10,200
30 Sept.	+ 91,600	+13,600
21 Nov.	-467,000	- 3,700
1975		
10 Feb.	+447,200	+12,900

1. Deposition (+).

2. Erosion (-).

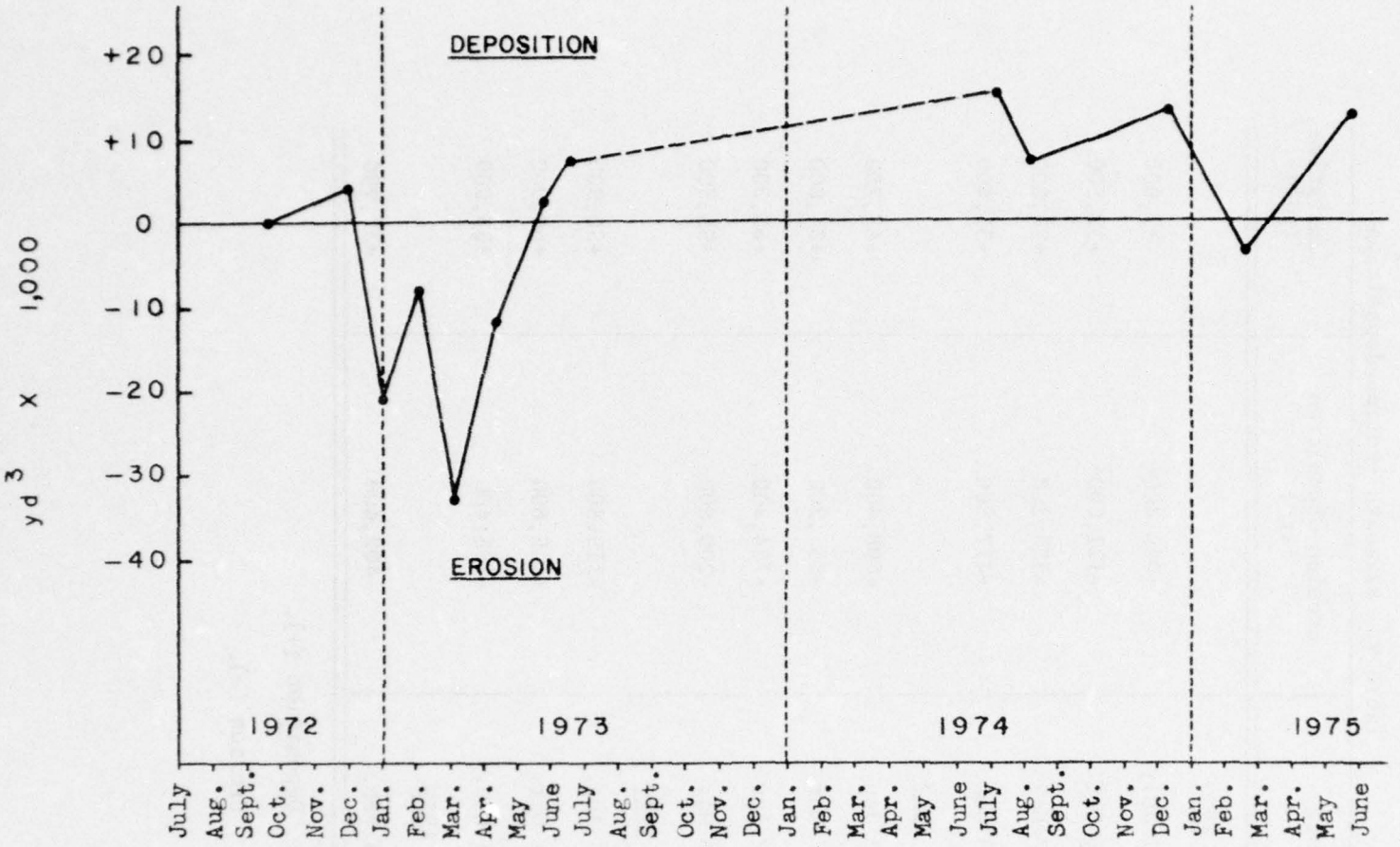

Figure 31. Gulf mouth sedimentation.

Table 9. Baymouth erosion-deposition.

Date	Erosion-deposition (ft^3)	Cumulative (yd^3)
1972		
21 July	+999,400[1]	37,000
16 Oct.	-121,000[2]	+32,500
27 Nov.	-338,200	+20,000
18 Dec.	+417,800	+35,400
1973		
26 Jan.	+898,400	+68,750
7 Mar.	-937,200	+34,000
12 Apr.	+784,800	+63,200
16 May	-209,600	+55,300
1974		
13 Aug.	-119,800	+50,900
1 Oct.	+145,600	+60,000
15 Nov.	-193,400	+53,000
1975		
13 Feb.	-402,600	+37,900

1. Deposition (+).

2. Erosion (-).

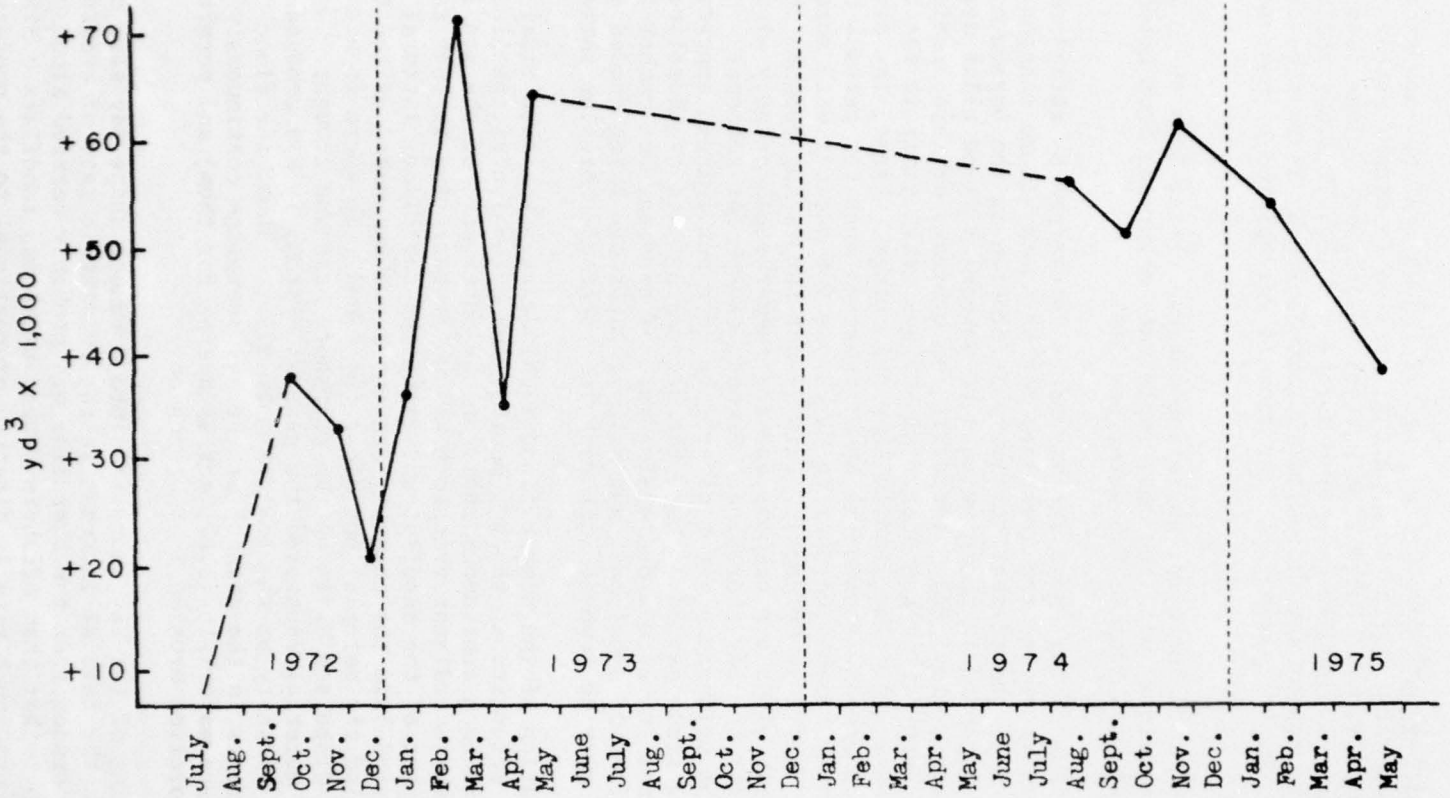

Figure 32. Baymouth sedimentation.

A plot of baymouth deposition (Fig. 32) shows that by late winter 1973, the flood tidal delta had apparently filled to approximately equilibrium dimensions. Later fluctuations in sediment volume seem to correlate with net floodflow measured during the 1974-75 study period (Fig. 32). Increasing net floodflow is accompanied by increasing baymouth deposition; decreasing net floodflow is accompanied by baymouth erosion.

Within the area surveyed, shoreline retreat varied from 60 to 250 feet (18 to 76 meters) with the most rapid rate occurring from October to December (up to 1 foot or 0.3 meter per day).

A comparison of bay shoreline movements determined by aerial photos and ground surveys beyond the area used for baymouth volume changes (App. E, Fig. E-1) showed that considerable erosion in the baymouth region is not included in the area used to determine flood tidal delta volumetric changes (Fig. 33). Therefore, an estimate of this erosion was made from bathymetric and subaerial surveys taken early in the first study year (Table 10). The results show two things. First, the average daily rate of shoreline erosion is about twice as much for periods of dominantly winter months (October to March) as for periods with more summer months (April to October). This is not surprising because the winter northerly winds are onshore and the summer southeasterly winds are offshore for the bay shoreline. Second, except for seasonal variations, the volumetric rates of erosion have not changed appreciably throughout the study period. Thus, the decreasing rate of shoreline retreat does not indicate a decreasing rate of erosion, but rather that higher elevations of spoil bank and natural dunes are being eroded and more material must be removed with each increment of shoreline retreat.

The formation of the simple flood tidal delta makes both tidal and bar bypassing effective at the bay mouth. The outer lip of the flood ramp reestablished a continuous shoal at the outer part of the sandflat so that alongshore sediment transport was not interrupted in that region. On the inner part of the sandflat and along the shoreline, littoral drift was carried into the channel, and the flood dominance of the tidal currents carried the material out along the flood ramp where it was picked up and dispersed again on the nearshore bars and troughs. Although this material reentered the general system, it was removed from the immediate vicinity of the baymouth shoreline. Thus, the flood-dominated currents in the channel at the bay shoreline continuously remove bay shore materials (i.e., act as a sink for them) and permit continuous shoreline erosion in that region.

The opening of the bay shoreline into a funnel shape may also have contributed to the initial increase in the volumetric rate of erosion. Most material eroded from the shoreline was probably carried alongshore by wave action rather than offshore across the broad sandflats. Since the longshore transport rate is directly proportional to the product of the sine and cosine of the angle of incidence of the waves with the

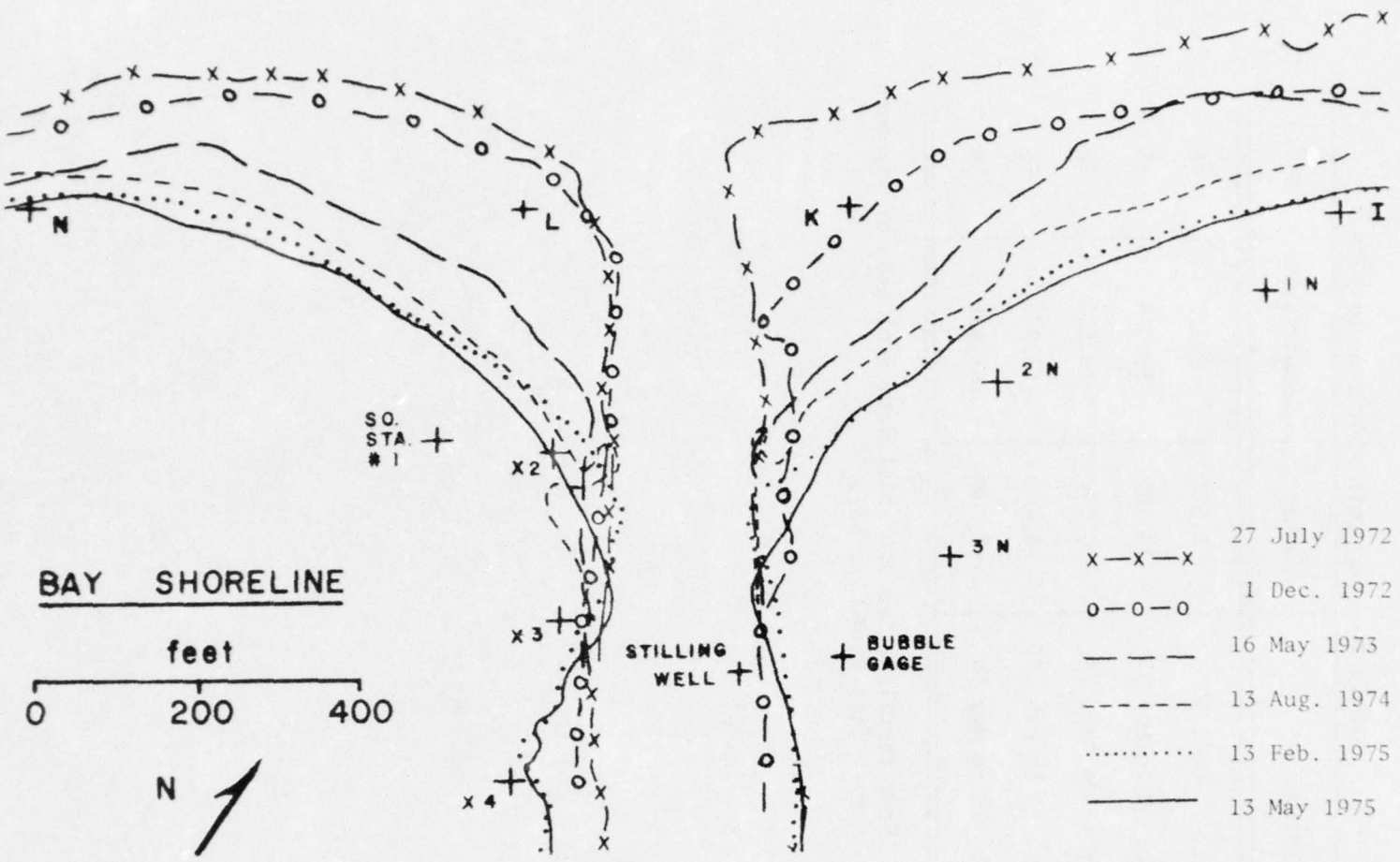

Figure 33. Bay shoreline erosion. Volumes for areas between successive pairs of shorelines and above mean sea level are given in Table 10. Baymouth volumes are taken from contour changes below mean sea level (see Fig. E-1 in App. E).

Table 10. Baymouth shoreline erosion.[1]

Interval	Change	Cumulative	Yd^3/d
July to Dec. 72	- 5,325	- 5,325	43
Dec. 72 to May 73	-13,700	-19,025	83
May 73 to Aug. 74	-20,900	-39,925	46
Aug. 74 to Feb. 75	-14,000	-53,925	78
Feb. 75 to May 75	- 8,000	-61,925	89

1. From shoreline and subaerial data exclusive of baymouth survey data (see Fig. 33).

shoreline, the change in shoreline orientation from the initial right-angle junction with the channel margin to a funnel-shaped channel entrance at an angle of about 45° to the open bay increased the longshore component of wave power to a maximum.

5. Channel.

a. Long-Term Changes. In the 1972-73 study the channel analysis was subdivided into six morphologically distinct zones which responded differently to sedimentological controls (see Fig. 24 for locations and extent). The volume of water between the bottom contours and +0.8 foot MSL (24 centimeters) in each zone was computed for each survey to determine deposition and erosion.

By June 1975, zone I was within 2,000 cubic yards (1,500 cubic meters) of its original dredged volume and almost never differed from this by more than 5,000 cubic yards (3,800 cubic meters) (Fig. 34). Depositional peaks occurred in winter (January to March) when north winds blowing onto the bay shore caused high longshore transport rates and increased ebb discharges which prevented material transported to the unjettied entrance from efficiently returning to the bay surf zone via the flood ramp. However, in summer, the bay longshore transport was nearly zero, and flood dominance produced erosional peaks.

Zone II had the most uniform cross section, a trapezoid the smaller base of which rose and fell to account for most of the sediment accumulation or erosion. Zone II had the largest volume, and the changes which correspond almost exactly to changes in the entire channel, will be discussed later in this section.

Zone III (channel bend) reflects many of the short-term (monthly) changes of the entire channel and zone II. However, a major modification controlled much of its behavior from mid-1974 to mid-1975. Since the opening of the pass until mid-1974 the bend behaved as a meander, migrating southwestward by eroding its outer bank. The erosion endangered a gas pipeline, requiring the Texas Parks and Wildlife Department to fill in the eroded part and bulkhead the southwest bank in June and July 1974. This zone subsequently remained quite stable, generally less than 3,000 cubic yards (2,300 cubic meters) difference from its original dredged volume.

Initially, the small bridge section of zone IV compensated for its narrowness by deepening and eroding about 2,000 cubic yards (1,500 cubic meters). This volume remained until April 1974 when a gradual shoaling began which reduced the volume to about the original level by August 1974. A very slight shoaling trend has continued since then (Fig. 35).

Near the gulf mouth there was a seasonal effect opposite to that at the bay mouth. Zone V shows erosional peaks (or depositional lows) in winter and depositional peaks in summer and fall (Fig. 35). This

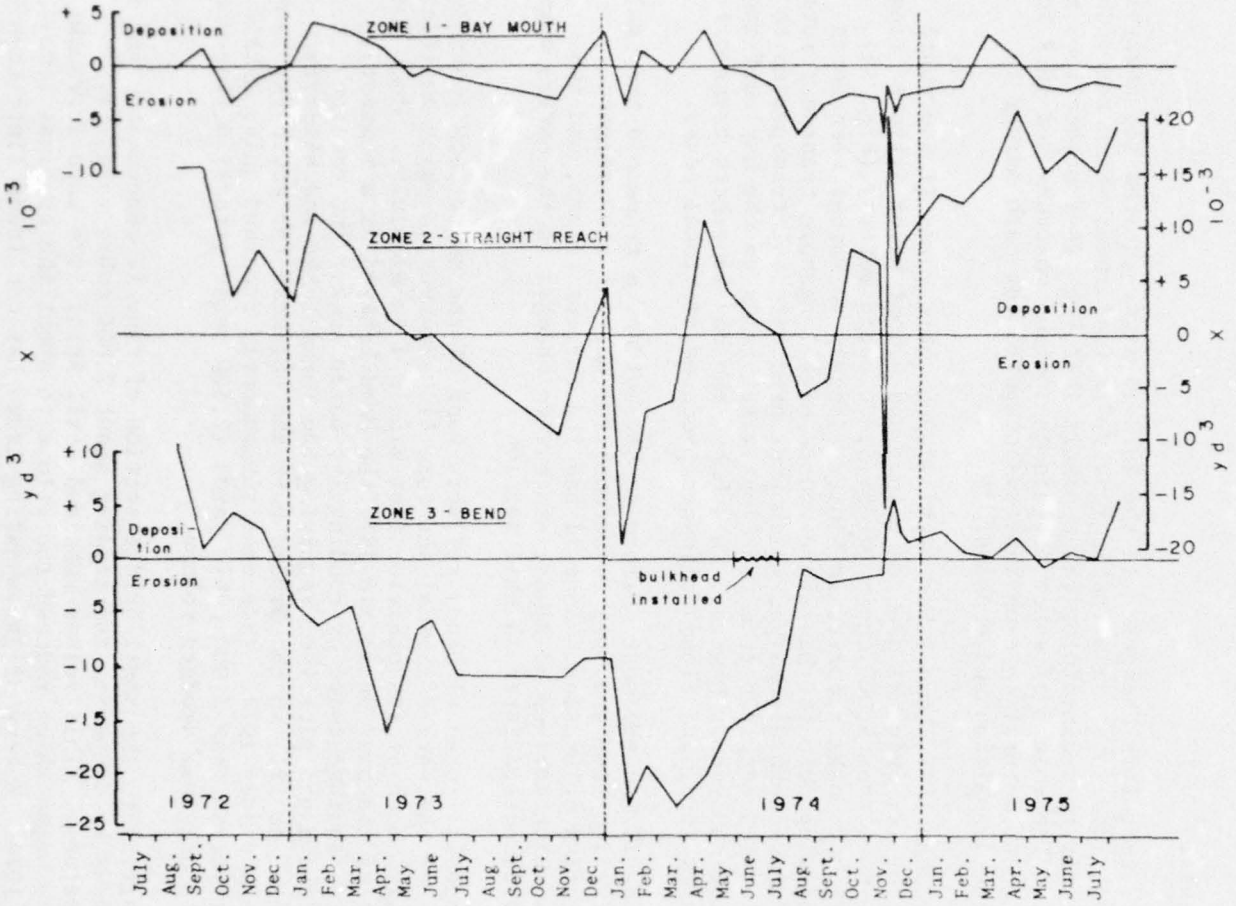

Figure 34. Channel zones 1, 2, and 3. Cumulative sedimentation-erosion.

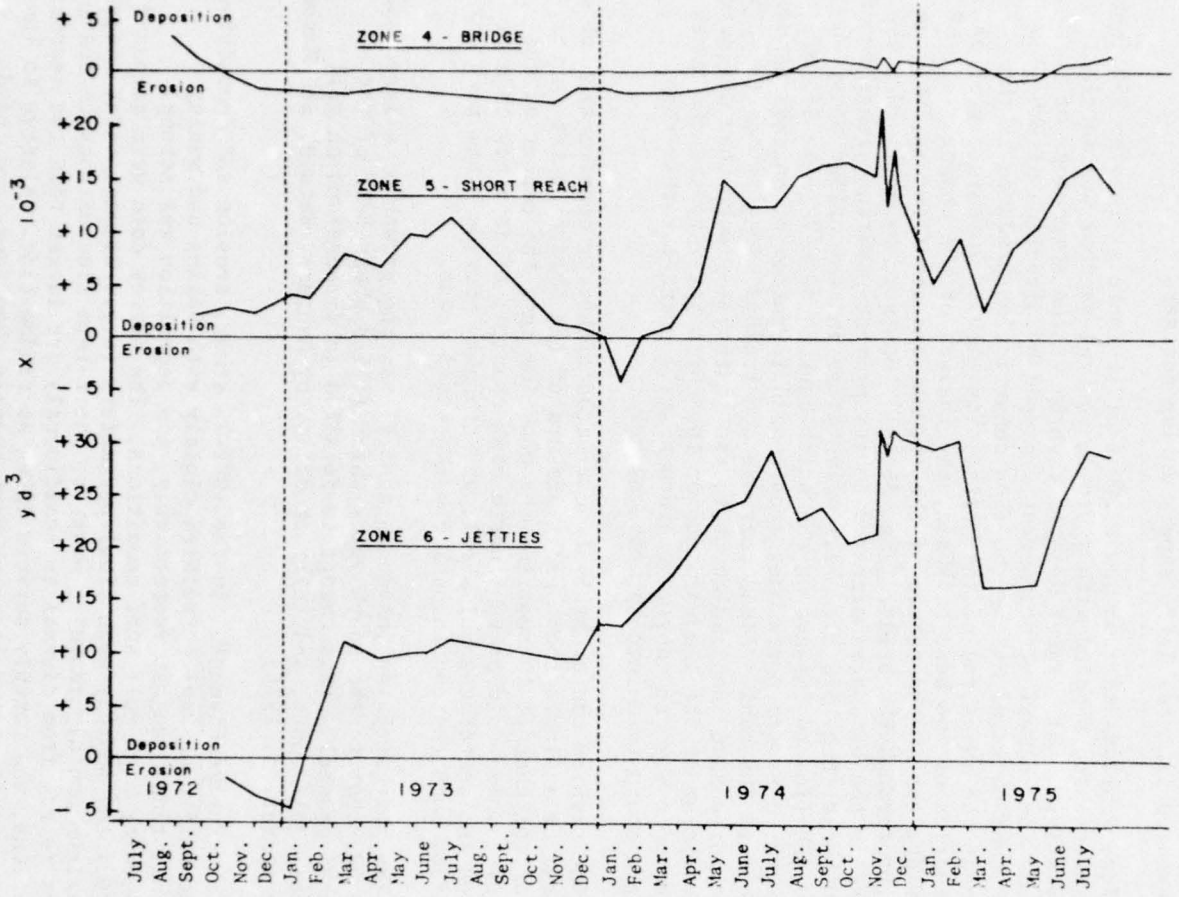

Figure 35. Channel zones 4, 5, and 6. Cumulative sedimentation-erosion.

was probably a simple response to greater sediment supply from the gulf during periods of floodtide dominance, and a scouring of the channel or decreased littoral drift supply during northers.

Zone V broadened from about 200 feet (60 meters) to over 350 feet (100 meters) and shoaled with a broad, central sandbar and marginal channels (Fig. 35). These drastic changes in the morphology of this reach of the channel were apparently caused by direction of ebb flow by the bend bulkhead and by the flow constriction produced by the riprap at the inner end of the north jetty (X19). Immediately after construction of the bend bulkhead, the thalweg of the channel west of the bridge was in the center of the channel and ebb flow was directed straight through the bridge (Fig. 36, A). However, by April 1975 the thalweg in the bend area migrated to its present position alongside of the bulkhead (Fig. 36, B). This orientation and the bridge position forced ebb flow to impinge on the north bank in zone V (Fig. 36, B), which caused severe north bank erosion and formation of an ebb channel adjacent to the bank. Flood currents constrained along the north jetty by the large sand shoal adjacent to the south jetty were then deflected by the riprap at the landward end of the north jetty toward the south bank of zone V where they maintained a small channel rather than making a sharp turn into the ebb channel.

The problem can probably be corrected either by construction of a bulkhead or a single short groin seaward of the bridge on the north side of the channel to reorient the ebb flow into the center of the channel. This would prevent north bank erosion, erode a new channel through the center channel shoal, and probably provide a new path for floodflow such that south bank erosion would cease.

The most striking change in zone VI was the growth of a large sand shoal adjacent to the south jetty which filled about half of the original channel. This change is detailed in discussions on gulf beaches, gulf mouth, and inlet stability by Behrens, Watson, and Mason (in preparation, 1976).

b. Entire Channel. In the 1972-73 study, erosion and deposition in the entire channel correlated closely with waxing and waning seasonal tidal ranges, respectively, and deposition was strongly enhanced by high gulf surf conditions. The survey data were compared to predicted monthly mean tidal parameters (e.g., diurnal tidal ranges or maximum monthly range). However, short-term fluctuations in tidal ranges (e.g., from diurnal to semidiurnal) are larger than the seasonal variations, and monthly surveys taken at random times relative to lunar positions will show more short-term scatter than long-term trends. Unfortunately, this was not realized until data analysis was well underway. Therefore, monthly erosion-deposition data were compared with differences in predicted daily tidal ranges between each pair of successive survey dates (Fig. 37).

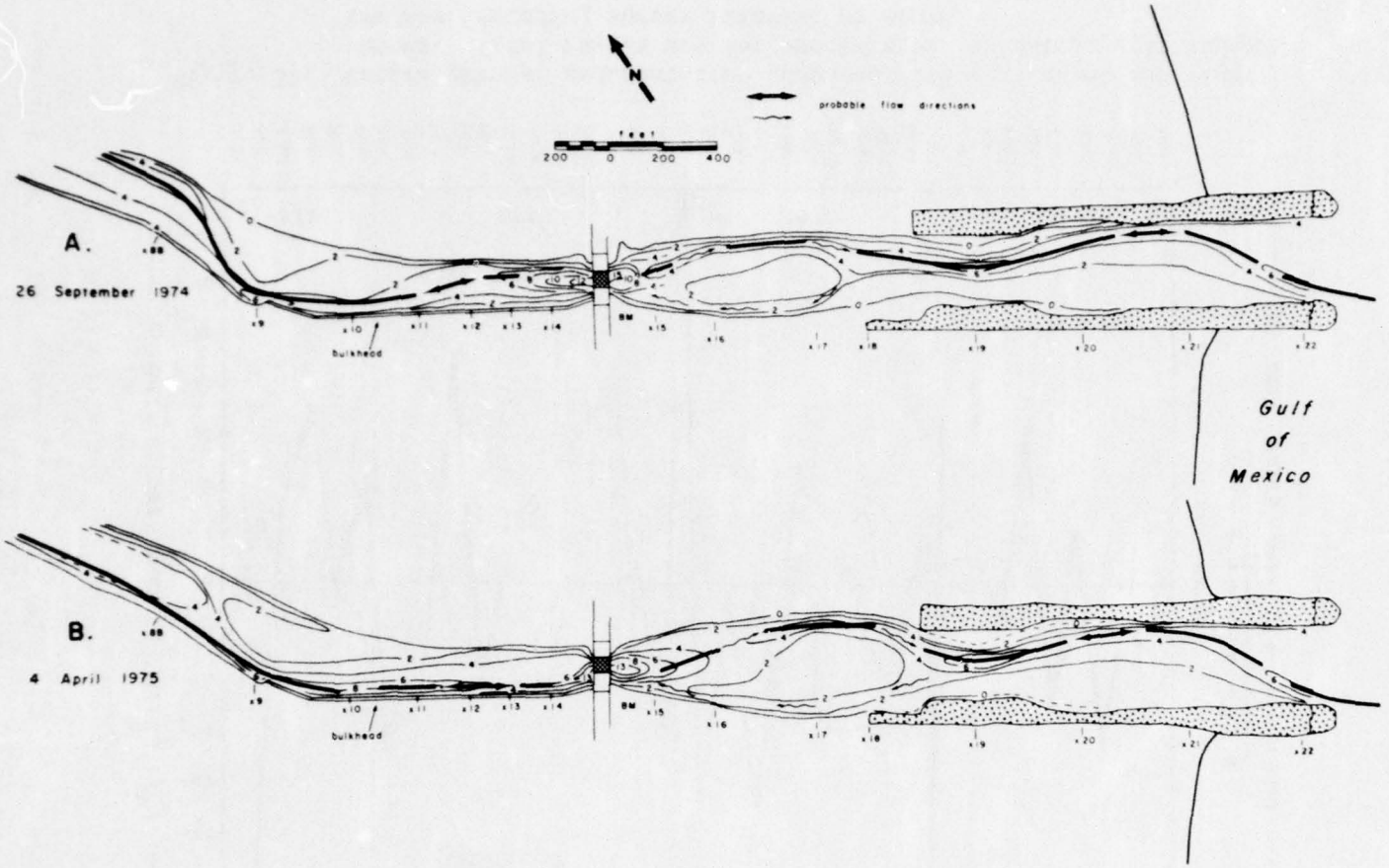

Figure 36. Bend to jetties thalwegs. Changes in channel axes loci and alinement of alternative channels with ebb flow and floodflow directions.

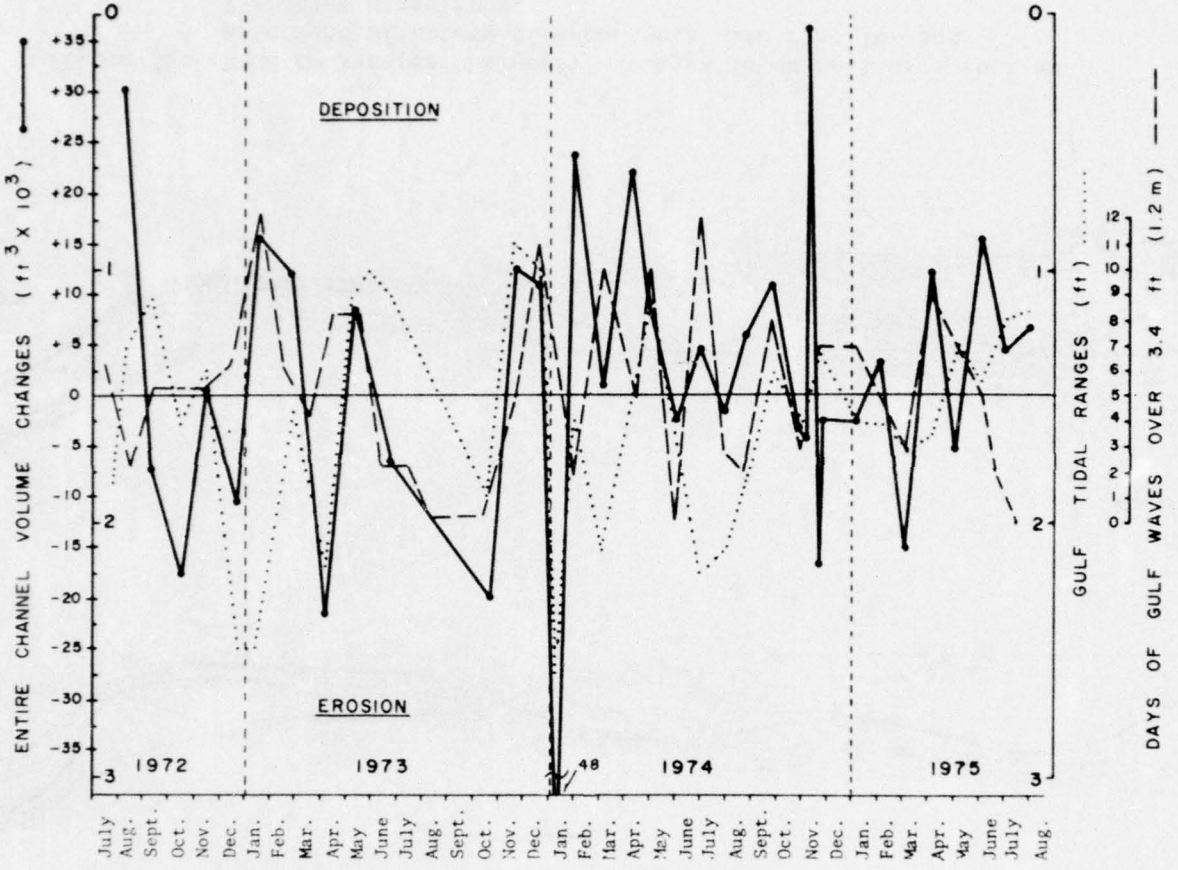

Figure 37. Entire channel sedimentation compared with gulf waves and tidal ranges. Tidal ranges are for specific survey dates; gulf waves are for preceding survey interval or month.

The results show that peaks in tidal range correlate very well with peaks in erosion (especially April and October 1973; January 1974) and low tidal ranges correlate well with peaks of deposition (especially May, November, and December 1973; February and September 1974). Furthermore, when these correlations are poor, there is usually an obvious gulf surf effect, e.g., the coincidence of depositional peaks with high-surf conditions in July 1974 and April 1975 and coincidence of erosional peaks with low-surf conditions in June 1974 and March 1975. It appears that during periods when each tidal discharge was less than the preceding one (waning range) there was less sediment moved with each succeeding cycle, thus more remained behind (i.e., deposited). Conversely, during waxing ranges each succeeding discharge was greater, could carry more sediment, and thus eroded the channel.

In addition to these short-term effects, the trend seems to have changed from a slow, net erosional phase from 1972 through the fall or winter of 1973 to a long-term, net depositional phase in 1974 and 1975 (Fig. 38).

Correlations for this pattern were sought in long-term trends in breaker height, computed longshore transport rate, observed longshore current speed, northerly wind frequency, and annual rainfall. Two parallel trends were found (Fig. 39). Annual rainfall was high at the beginning of the study and increased while the channel expanded in 1973. Decreases from wet to normal to almost dry conditions through 1974 and 1975 diminished runoff enhancement of ebbtide scouring capacity and correlate with the period of channel filling.

Observed gross longshore current speeds also parallel sedimentation by decreasing during channel erosion and increasing during channel filling (Fig. 39). An explanation for this correlation might be that faster longshore currents carry more sediment to the channel mouth. If this is true, a more direct measure of potential sediment supply, computed longshore transport rates should also show this correlation. However, the rates do not show the correlation, and it remains unexplained at this time.

c. Short-Term Changes. Weekly channel surveys were made from 29 October to 25 November 1974 to evaluate the magnitude of short-term erosion-deposition responses to environmental variables. The diurnal tidal ranges, resultant onshore winds, lunar positions, gulf wave heights, and daily discharges are plotted on Figure 40.

During the beginning of the first study period (29 October to 5 November) two opposing conditions existed: (a) Two days of high gulf waves favoring deposition; and (b) tidal ranges waxing from semidiurnal to diurnal and favoring erosion. Thus, little net effect might be expected. Little further change might also have been predicted because tidal ranges, although predicted to wane toward another semidiurnal tide in the next week, actually stayed high to the end of the period, probably because of wind tide effects of an intense norther on 4

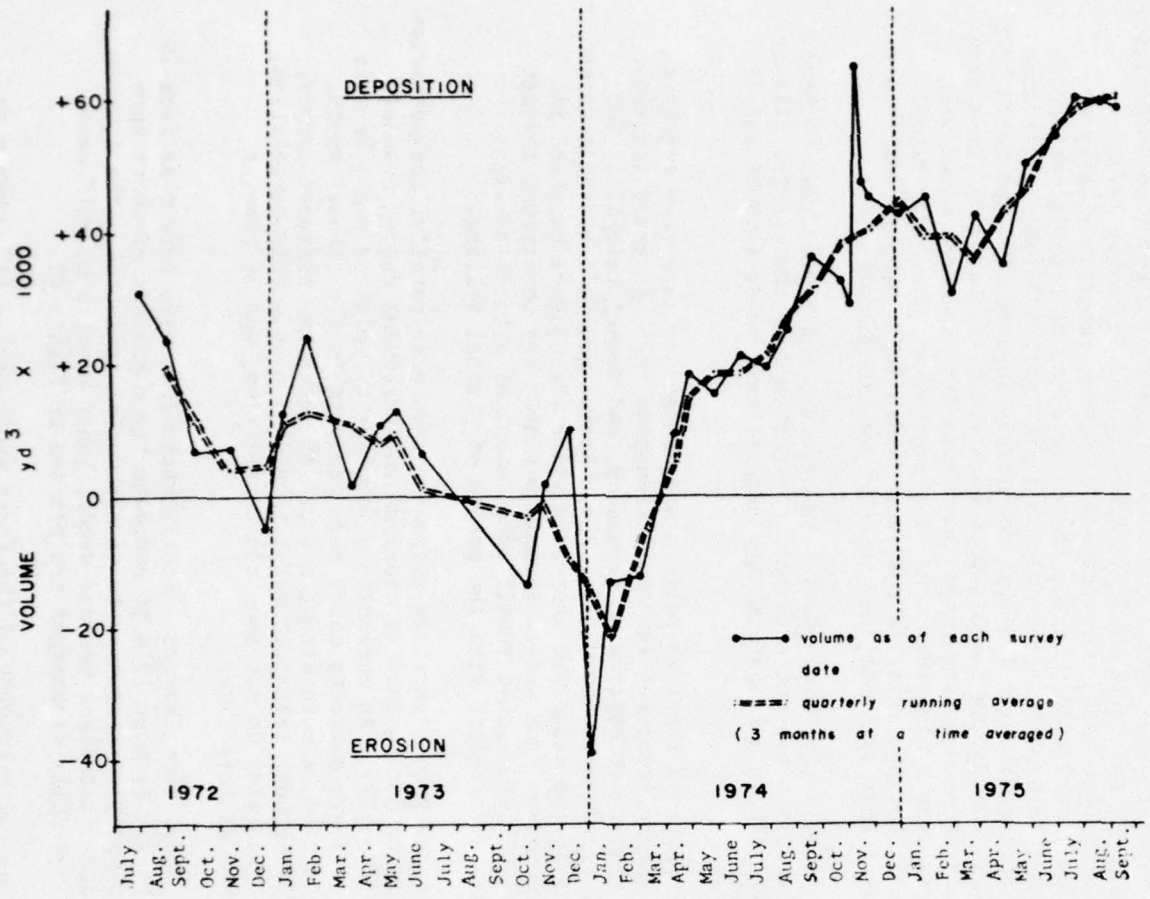

Figure 38. Total channel cumulative sedimentation.

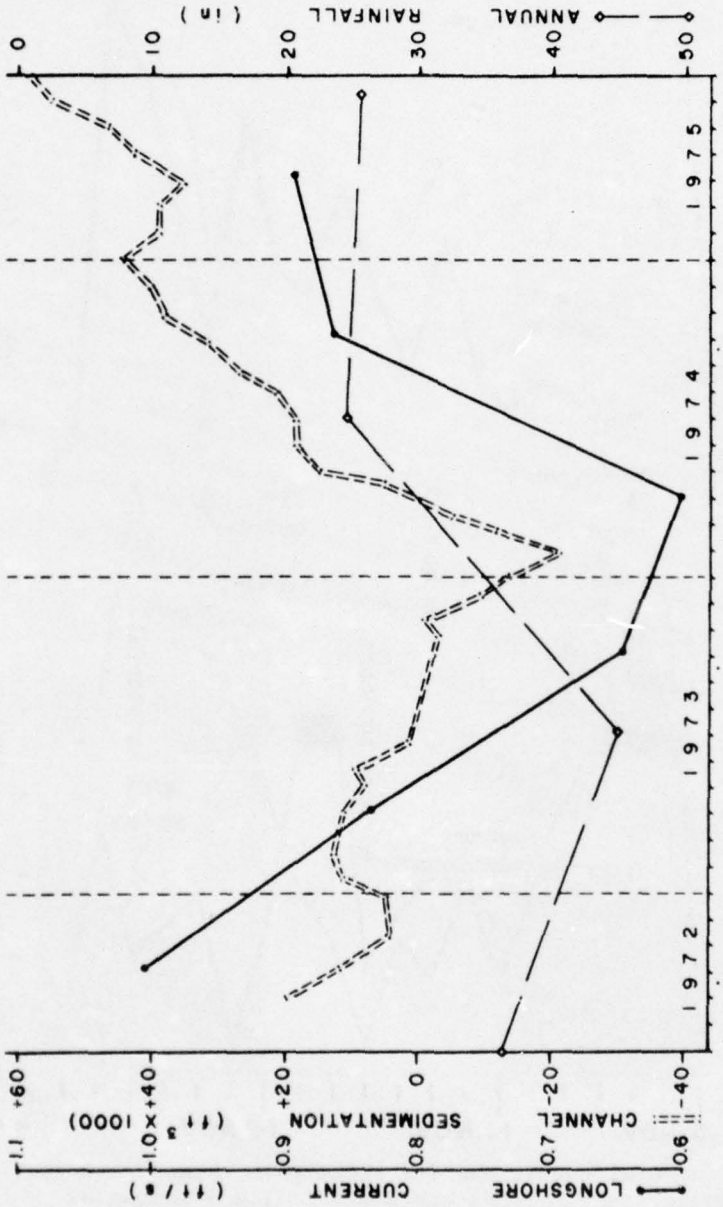

Figure 39. Annual rainfall and gross longshore current compared to total channel sedimentation. Sedimentation values are cumulative, 3-month running averages; longshore current values are 6-month averages.

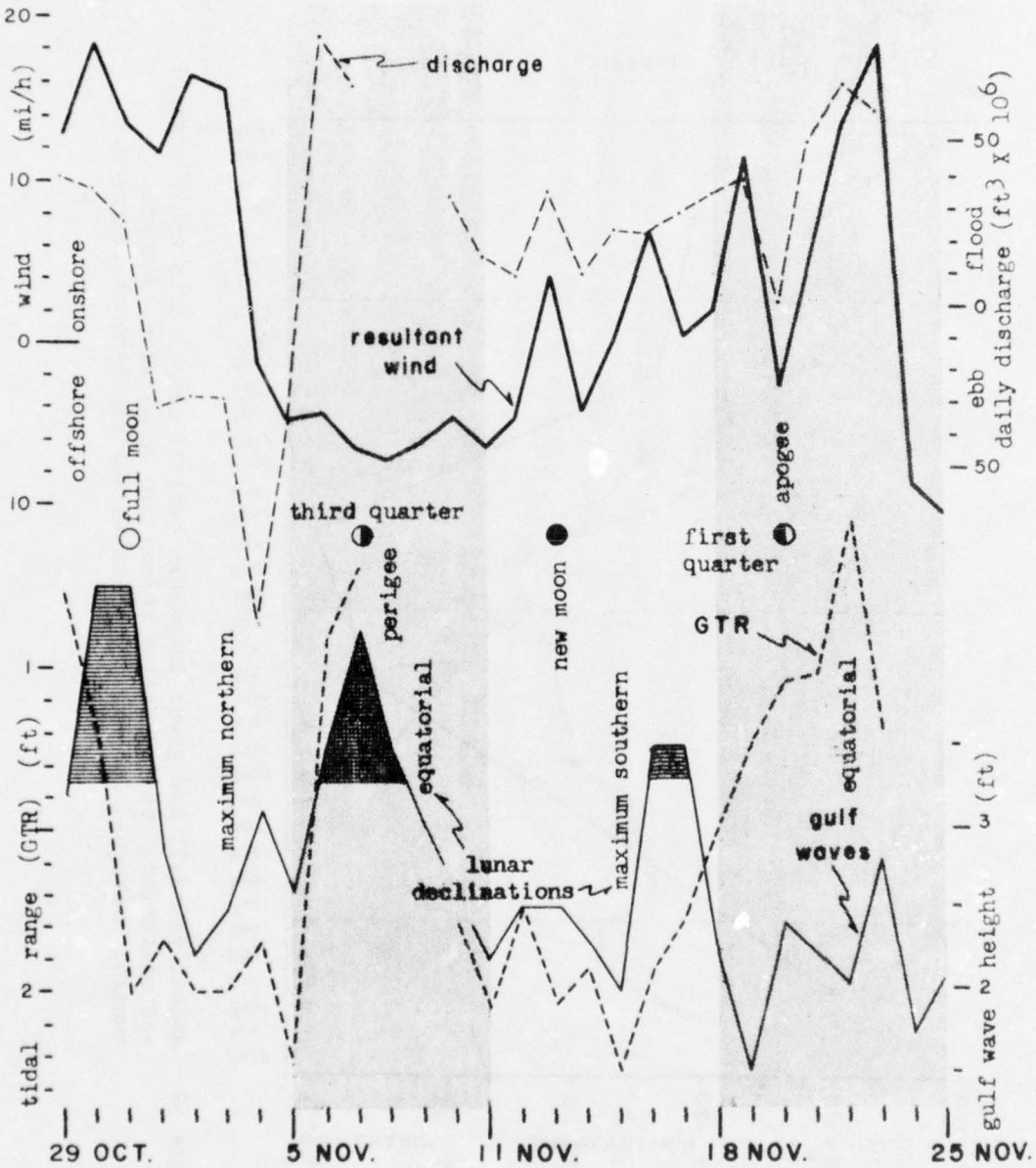

Figure 40. Environmental conditions for short-term channel studies. Alternate study periods are shaded. Tidal ranges are from $CCWEP_G$ gulf gage: discharges are computed from gulf and bay gage data; wind data are from Corpus Christi; gulf waves are from daily beach observations (periods of time when waves were higher than 1 meter are horizontally lined); and lunar data are from National Oceanic and Atmospheric Administration (1972-75).

November. However, the norther produced a net ebb tidal discharge of 69 million cubic feet (2 million cubic meters) which should have moved sediment in the channel gulfward. Apparently this was the case (Fig. 41, A), since material eroded from zones I and II was deposited in zones III to VI. Net erosion of 5,000 cubic yards (3,800 cubic meters) indicates the incapacity of bay shore longshore transport to replace material removed rapidly from the bay end of the channel.

In the second period (5 to 11 November; Fig. 41, B) apparently the opposite sediment movement took place as there was erosion in zones IV, V, and VI and deposition in zones I, II, and III with a large net deposition of over 36,000 cubic yards (28,000 cubic meters). Deposition was highly favored during the first part of the period when waning tidal ranges coincided with 3 days of gulf wave heights over 3.3 feet (1 meter). A mass of sediment probably moved into the gulf end of the pass at that time and was subsequently carried bayward by flood-dominated tides (flood exceeded ebb by about 52 million cubic feet (1.5 million cubic meters) per day); low-wave conditions did not enable much sand to enter the channel the last 2 days of the period.

In the third period (11 to 18 November; Fig. 41, C) tidal ranges were high during the first 4 days and then waned the last 3 days. Two days of gulf waves over 3.3 feet (1 meter) during the waning part of the period should have caused sedimentation in the pass, but there was net erosion of about 17,000 cubic yards (13,000 cubic meters). The net erosion probably resulted from transport of the material deposited in zones I, II, and III during the previous period to the flood tidal delta. At the same time, material from the surf zone was being deposited at the gulf mouth. Flood dominance averaged 24 million cubic feet (0.68 million cubic meters) per day.

Tides during the last period (18 to 25 November; Fig. 41, D) were like those of the second, in that first waning then waxing tidal ranges bracketed a low-amplitude, semidiurnal tide. However, low gulf waves persisted throughout the period, and winds were more onshore leading to greater flood dominance than in the preceding period (51 million cubic feet or 1.4 million cubic meters). Consequently, the material deposited in the gulf end of the channel during the previous period was apparently distributed bayward throughout the rest of the pass resulting in only a small net erosion (2,400 cubic yards or 1,800 cubic meters).

These short-term studies not only support the general correlations of deposition with high gulf waves and waning tidal ranges and erosion with waxing tidal ranges, but also show some of the detailed movement of sediment from one zone to another within the channel and how the direction of movement correlates with the wind-affected discharge asymmetry. The large magnitude of the changes illustrates the importance of basing longer observations on surveys made during equivalent parts of the monthly lunar tidal cycle and of strict attention to short-term wave climate.

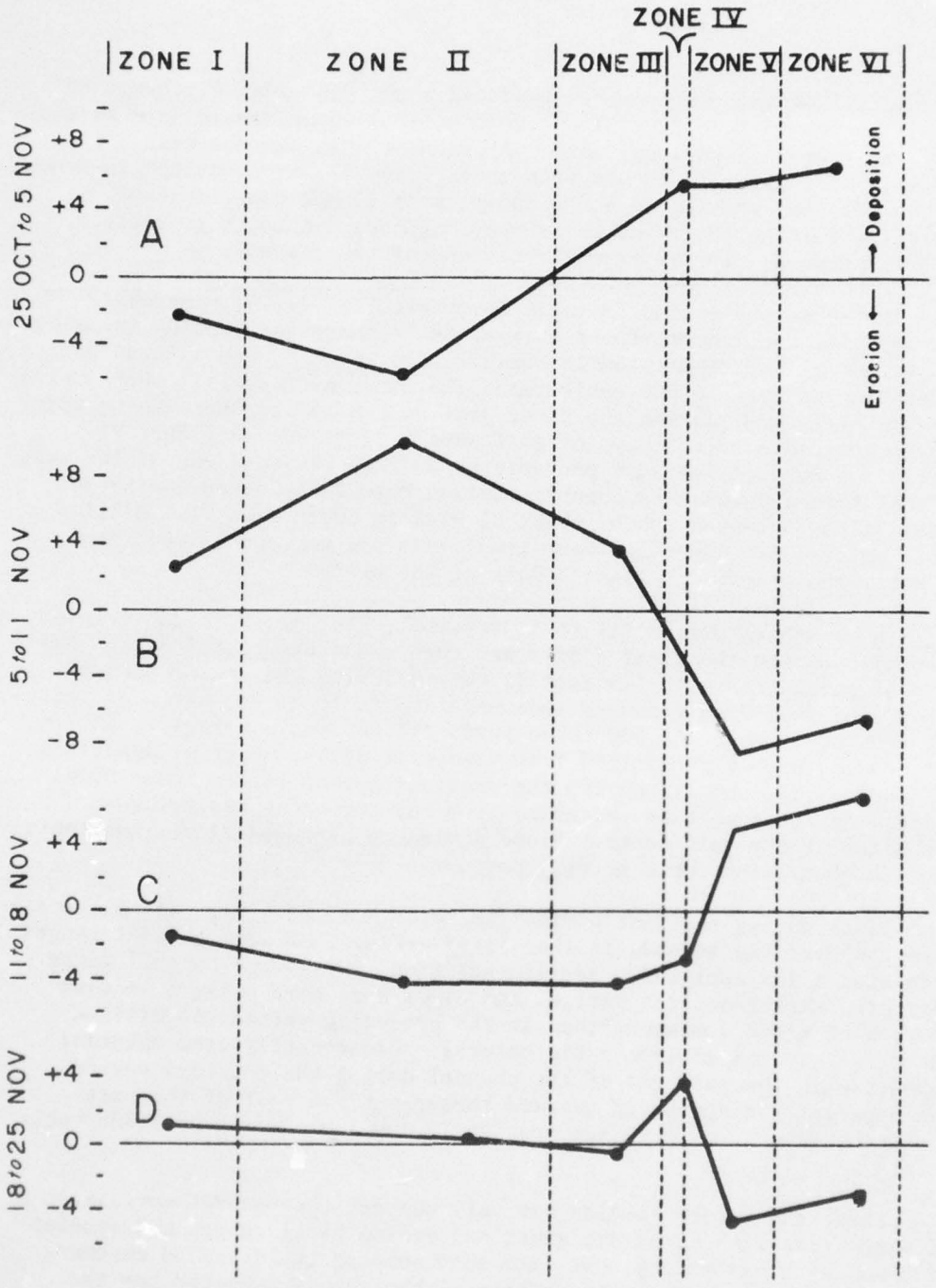

Figure 41. Deposition (+) and erosion (-) in cubic feet per linear foot of channel for the short-term study periods.

IV. INLET STABILITY CONSIDERATIONS

1. Introduction.

The factors controlling inlet stability include: (a) bed material size; (b) tidal prism; (c) longshore sediment transport rate; (d) wave characteristics; (e) inlet and bay geometry; and (f) flood-to-ebb current ratio. Parameters of several of these variables have been compared to see if consistent relationships correlate with equilibrium conditions at apparently stable inlets.

2. Tidal Prism-Cross-Sectional Area Relationships.

To determine whether or not differences exist between the tidal prism-inlet area relationships for inlets on the Atlantic, gulf, and Pacific coasts of the United States, Jarrett (1976) used and supplemented data of O'Brien (1931) to form empirical relationships of:

$$A = CP^n,$$

where A is the minimum cross-sectional area below MSL in square feet, P is the spring tidal prism in cubic feet, and C and n are constants which differ for all inlets, unjettied and single-jettied inlets, and twin-jettied inlets. Furthermore, he grouped Pacific, Atlantic, and gulf coast inlets separately.

To determine if the pass conformed to one of these relationships, spring tidal prisms were used to calculate minimum areas according to each equation (Table 11). Two spring tidal prisms were used: (a) The average value for the prisms measured during spring tides included in the diurnal discharge studies (49×10^6 cubic feet or 1.4×10^6 cubic meters); and (b) the average maximum monthly prism computed from tide gage records (75×10^6 cubic feet or 2.1×10^6 cubic meters). The difference results from the lack of coincidence of the measured spring-tides and maximum lunar declinations. The minimum monthly cross section (731 square feet or 68 square meters) is the average of all those measured, and this varies from less than 300 to over 1,000 square feet (28 to 93 square meters).

The comparisons show that the pass most nearly fits Jarrett's (1976) relationship for all unjettied inlets, and that the minimum cross-sectional area seems to be much less than an equilibrium value. The similarity to unjettied inlets is reasonable, because the short jetties do not cross the entire surf zone, surf processes are not excluded from the pass mouth region, and the entire inlet is not lined with jetties.

3. Comparisons with Other Empirical Relationships.

Harwood (1973) found that for Pass Cavallo, Texas, and other Texas inlets that the ratio of maximum discharge to channel length ranged from

Table 11. Tidal prism - inlet cross-sectional area relationships.

Equation: $A =$	Group	Source	Computed area (ft^2) for tidal prism of:		Surveyed areas (ft^2)	
			$49X10^6$ (ft^3)	$75X10^6$ (ft^3)	minimum	mean
$4.69 \times 10^{-4} P^{0.85}$	Pacific inlets	O'Brien, (1931)	1,613	2,323	731	1,061
$2.0 \times 10^{-5} P$	Atlantic, Pacific, and Gulf;unjettied	O'Brien, (1969)	980	1,504	731	1,061
$1.04 \times 10^{-5} P^{1.03}$	All coasts;un-jettied	Jarrett, (1976)	867	1,347	731	1,061
$5.77 \times 10^{-5} P^{0.95}$	All coasts;un-jettied	Jarrett, (1976)	1,166	1,752	731	1,061
$3.51 \times 10^{-4} P^{0.86}$	Gulf coast (east); unjettied	Jarrett, (1976)	1,442	2,084	731	1,061

4 to 7 square feet per second (0.37 to 0.65 square meters per second) and that longer relative channel lengths tended to shoal. With a maximum discharge of 2,500 cubic feet per second (71 cubic meters per second) and a channel length of 10,000 feet (3,048 meters), the ratio for the water exchange pass is 0.25 and thus the pass may be unstable, with shoaling tendencies.

Bruun and Gerritsen (1960) and Bruun (1966) related inlet stability to the ratios between annual gross littoral drift rate, M, and maximum discharge, Q_{max}, and between spring tidal prism and maximum discharge as follows:

M/Q_{max} greater than 200 to 300 implies bar bypassing;

M/Q_{max} less than 10 to 20 implies tidal bypassing;

where M is the annual gross littoral drift (cubic feet per year) and Q_{max} is the maximum discharge (cubic feet per second). From Section III, 2, the annual gross littoral drift rate at the water exchange pass is about 19.5 million cubic feet per year (55 million cubic meters). Maximum spring tidal discharge is about 2,000 to 2,500 cubic feet per second (57 to 71 cubic meters per second) yielding a M/Q_{max} ratio of about 7,700 indicating that the pass is strongly bar bypassing. Similarly, Bruun and Gerritsen (1960) found that the ratio Q_{max}/M greater than 0.01 implied stability; a ratio of less than 0.01 implied instability. The Q_{max}/M ratio for the pass is 1.3×10^{-4} implying that the pass is highly unstable with regard to shoaling by littoral drift. Bruun and Gerritsen also defined stability on the basis of the ratio between spring tidal prism, Ω, and annual littoral drift as follows:

$\Omega/2M$ greater than 300, highly stable;

$\Omega/2M$ less than 100, unstable and barred.

This ratio for the water exchange pass is 1.26 indicating instability. It is suggested that although the ratio of spring tidal prism and discharge to the littoral drift rate suggests extreme instability, the pass has remained open because it is partially protected from the littoral drift by short jetties. If the beaches were to accrete seaward to the ends of the jetties so that they no longer functioned, the pass would probably close immediately.

Regardless of the tidal prism and maximum discharge, the flow velocity and channel dimensions must be such that the bottom shear stress is adequate to initiate and sustain sediment transport or the pass will not be self-scouring. Bruun and Gerritsen (1960) suggest that the minimum shear stress should be 0.092 to 0.103 pounds per square foot (44 to 50 dynes per square centimeter). Assuming a maximum mean velocity of 2 feet per second (61 centimeters per second), hydraulic radius 4.76 feet (145 centimeters) Manning's n of 0.028, and the following

relationship for shear stress:

$$\tau_o = \frac{29.0\ n^2\ V_{max}^2}{R^{1/3}} \quad ,$$

the maximum shear stress is equal to 0.075 pounds per square foot which is less than the minimum required for marginal stability.

4. Escoffier Diagram Analysis.

Escoffier (1940) presented a unique concept of inlet stability, relating the maximum mean velocity in the channel to the cross-sectional flow area for a given spring tidal prism (Fig. 42). Above a critical area, A_c^*, a reduction in cross-sectional area is accompanied by an increase in velocity, and the section tends to be self-scouring. Below the critical area a decrease in cross section results in a further decrease in flow velocity with closure as a result. If the initial or equilibrium area is far to the right of the critical area, the pass can support considerable shoaling during periods of reduced tidal flow or excessive longshore transport, since with the next spring tidal prism, flow velocity will increase and scour the inlet. O'Brien and Dean (1972) utilized the tidal prism-cross-sectional area relationships of O'Brien (1969) and the inlet hydraulics of Keulegan (1967) to define a method to produce the Escoffier diagram for real inlets. They also developed relationships to compute additional curves to indicate the stability of a pass which is undergoing cross-sectional area reduction along any channel length, Δl. This enables one to start with an equilibrium cross-sectional area and evaluate the effect of hypothetical shoaling on the ability of the inlet to remain self-scouring. Finally, O'Brien and Dean (1972) defined a stability index, β, as:

$$\beta = \int_{A_c^*}^{A_{ce}} (V_{max} - V_t)^3 dA_c \quad , \qquad (2)$$

where V_{max} is the maximum mean velocity from the Escoffier diagram, V_t is the threshold velocity to erode the pass sediment, A_c is the pass minimum cross-sectional area, A_c^* is the critical area previously defined, and A_{ce} is the equilibrium cross section defined by O'Brien's relationship or through measurement of the prototype.

Although the equations used for the calculation of a stability curve were developed for the simplified system of a bay with a single inlet, the method was attempted to see what empirical relationships might exist between its predictions and the observed behavior of the pass.

In construction of an Escoffier diagram the ordinate, V_{max}, is calculated from:

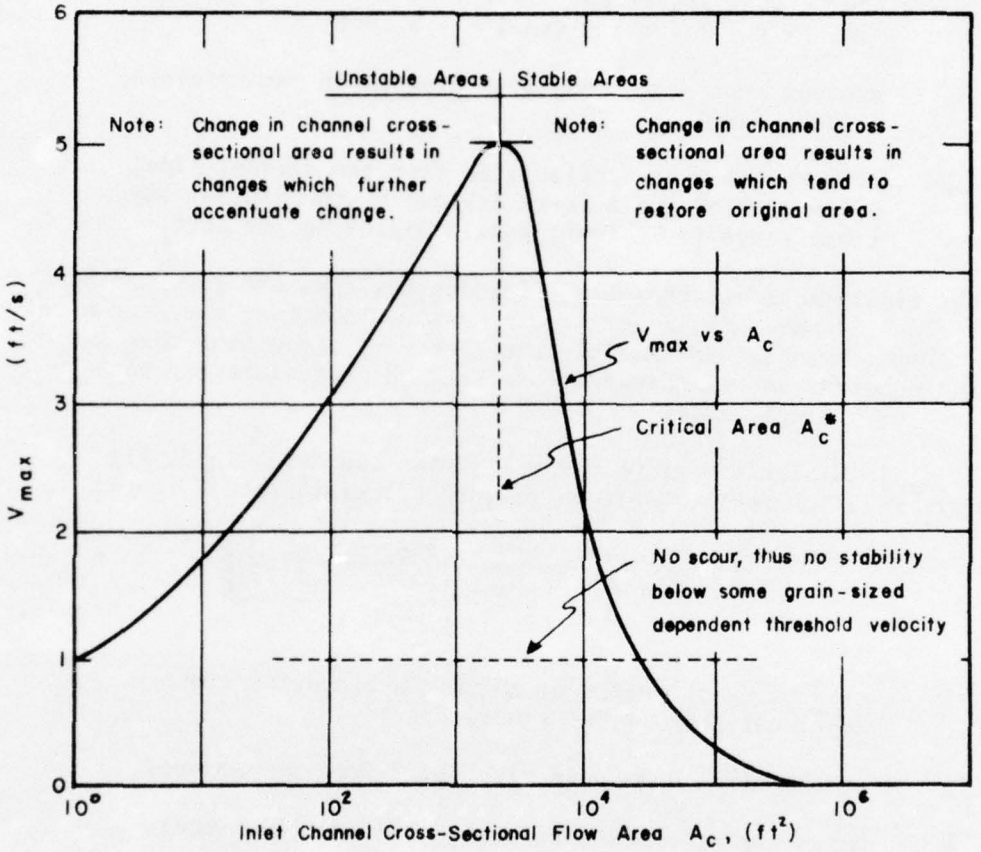

Figure 42. Illustration of Escoffier's stability concept (after O'Brien and Dean, 1972).

$$V_{max} = V'_{max} \frac{2\pi}{T} a_o \frac{A_b}{A_c}$$

T = diurnal tidal period (89,280 seconds)

a_o = ocean tidal amplitude measured at the $CCWEP_G$ gulf gage (mean = 0.717 foot; diurnal = 1.3 feet)

A_c = minimum cross-sectional area plotted on the abscissa (square feet)

A_b = effective bay area calculated from the diurnal tidal prism ($75X10^6$ cubic feet) divided by the diurnal bay tidal range (0.79 feet) equals $95X10^6$ square feet.

The bay tidal range and thus the effective bay area are governed by the tidal flows at the much larger Aransas Pass. Therefore they are more independent variables and satisfy the necessary assumption that A_b remains constant as the channel cross section changes better than in the case of a single inlet.

V'_{max} is determined graphically (O'Brien and Dean, 1972, Fig. 3) from its relation to the Keulegan repletion coefficient, K, where

$$K = \frac{T}{2\pi a_o} \frac{A_{ce}}{A_b} \left(\frac{2ga_o}{\frac{\Sigma K_e}{k^2} + \frac{f\Delta l}{4\, k\, R_e k^2} + \frac{f(l-\Delta l)}{4R_e}} \right)^{\frac{1}{2}}$$

A_{ce} = mean of over 2 years of monthly averages of cross-sectional area (1,061 square feet)

g = acceleration due to gravity (32.2 feet per second)

k = parameter of cross-sectional area reduction equals A_c divided by A_{ce}

f = Darcy-Weisbach friction factor = $\frac{116\ n^2}{R^{1/3}}$ (0.054 for n = 0.028)

R_e = equilibrium hydraulic radius (mean of over 2 years of monthly means = 4.76 feet)

l = length of channel between tide gages (8,900 feet)

K_e = coefficients of head losses due to acceleration of flow at channel irregularities such as the entrances, bridge, and bend (5).

The Keulegan repletion coefficient can also be estimated independently from tidal records giving the timelag (ε) between high or low water and the following slack. For diurnal tides at the pass this averaged 5.4

hours or 79° which is equivalent to K = 0.16. The sum of head loss coefficients is estimated from this repletion coefficient by:

$$\Sigma K_e = \left(\frac{T}{\pi}\right) \frac{2ga_{o_{mean}}}{K} \cos\varepsilon \left(\frac{A_c}{P_{mean}}\right)^2 - \frac{f1}{4R} .$$

A family of curves (Fig. 43) for various values of $\Delta 1$ (Fig. 43) presents the relationship between the mean velocity and the cross-sectional area for values of A_c between 100 and 1,000 square feet (9 and 93 square meters respectively). Useful information about the potential stability can be gained by comparing the cross-section history of the pass to the Escoffier diagram (Figs. 8 and 43; App. F). The minimum areas reflect the field observations that since May 1974, there has been a significant constriction about 200 feet (61 meters) long in the vicinity of X19, and a less severe constriction for another 800 feet (244 meters) between the jetties (X20 and X21).

During June 1975 the section at X19 was reduced to 277 square feet (26 square meters) and the longer section to about 700 square feet (65 square meters). For all depositional lengths less than 1,000 feet (305 meters), the critical area is less than 200 square feet (19 square meters) (Fig. 43). Interpolating between the curves in the figure indicates that a cross-section reduction to about 300 square feet (28 square meters) would lead to a current velocity over 3 feet per second (0.9 meters per second) which should scour quite effectively. Reduction to 700 square feet (65 square meters) would produce, at most, about one-half this velocity which would probably scour only against a moderate, continued wash load from longshore currents and waves. Thus, the 277-square-foot (26 square meters) cross section should have been reexpanded rapidly, and it was by the following month (586 square feet or 54 square meters by 2 July 1975), while the 700-square-foot (65 square meters) reach remained well below the equilibrium area. At the longer $\Delta 1$'s, such as 3,000 feet (914 meters) and 5,000 feet (1,524 meters), the increase in flow velocity with increasing channel constriction is very slight due to the high frictional losses, and self-scouring is far less likely than for $\Delta 1$'s of 100, 500, or 1,000 feet (30, 152, or 305 meters, respectively) where the increase in velocity is high for a small decrease in channel section.

5. Future Inlet Stability.

All indices of stability indicate that the water exchange pass is marginally stable or unstable with a tendency toward closure. Survey data support this by showing summer shoaling and winter scouring resulting in a net reduction in average and minimum cross-sectional area each year. Closure by restriction of short reaches is unlikely as shown by Escoffier diagram analysis and observed recovery of cross-sectional areas reduced to less than 300 square feet (28 square meters).

Since the tidal flow was flood dominated, more littoral drift

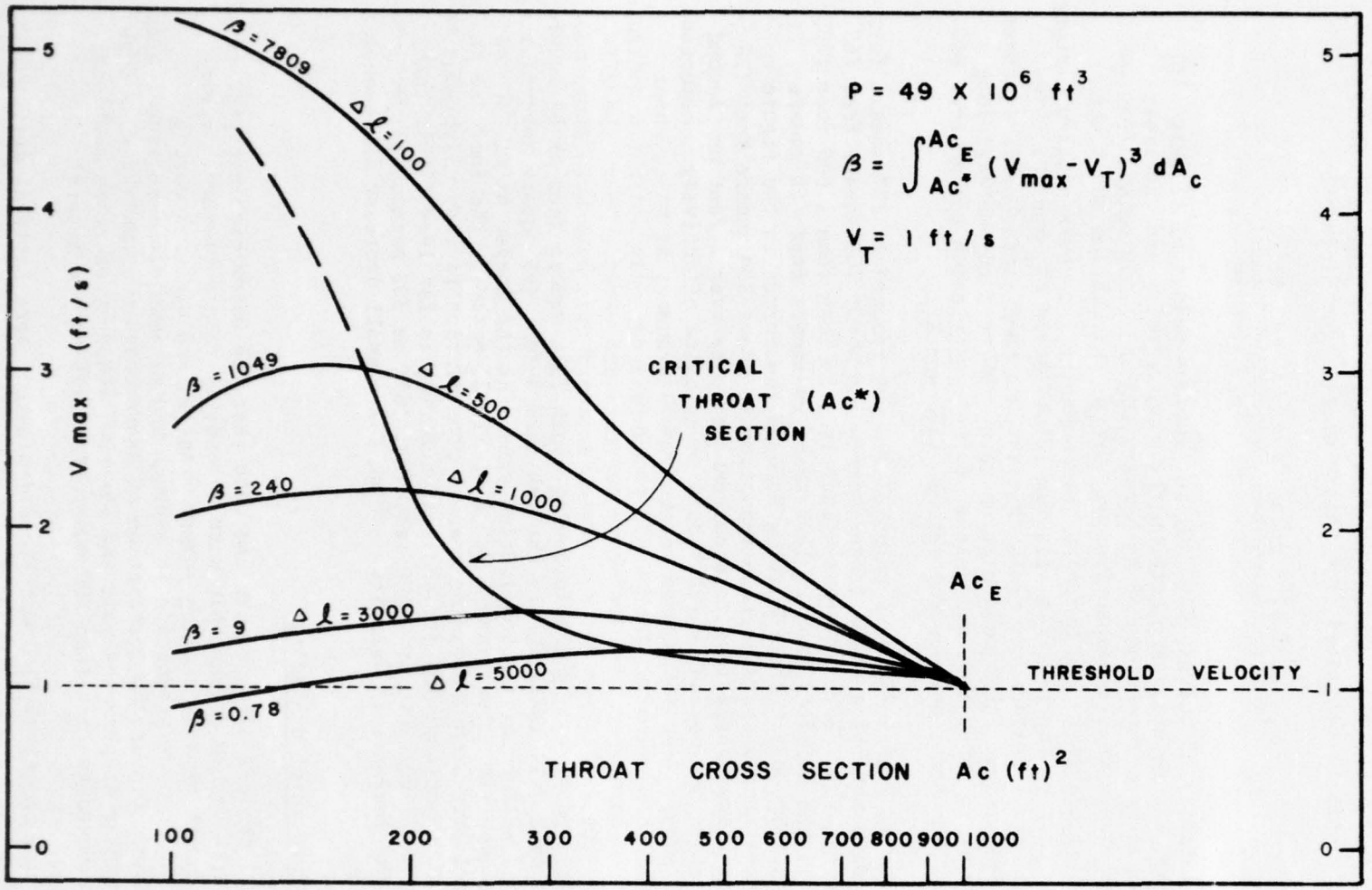

Figure 43. Escoffier stability diagram for the Corpus Christi Water Exchange Pass.

entered the channel on floodtides than was removed on ebbtides. Continuation of this phenomenon will probably lead to closure by restriction of cross-sectional areas over a greater length of channel. This will probably be the bridge to gulf section (zones V and VI), but shoaling may extend farther bayward, especially into the bend zone where some meander point bar morphology already exists. Since shoaling is most favored by waning tidal ranges and strong, southerly, onshore winds predominate in summer, closure is most likely then.

Total self-scouring ability can probably be achieved only by the construction of long jetties to keep littoral drift out of the pass. However, this might eventually require installation of a bypassing plant or regular dredging with downdrift disposal to prevent beach erosion and continued growth of the beach to the end of the jetties.

V. CONCLUSIONS

1. The location of Corpus Christi Water Exchange Pass relative to Corpus Christi Bay is such that each of the two wind modes in this region creates gulf and especially bay water surface slopes that enhance one direction of tidal flow. The dominance of the onshore, southerly wind leads to the dominance of flood over ebb tidal discharge by about 1.6 to 1.

2. While the first year's study (Behrens, Watson, and Mason, in preparation, 1976) documented the well-known groin effect on the gulf beaches of the newly created pass jetties, subsequent studies have revealed the potential danger of updrift beach erosion due to the formation of a downdrift offset at the gulf mouth of the pass. This formation was apparently due to the tidal discharge asymmetry caused by intracoastal wind tidal circulation and by longshore transport reversals such that net northward (updrift) transport coincided with maximum flood discharges and net southward (downdrift) transport coincided with maximum ebb discharges. Monthly, inner surf zone and beach changes seem to reflect both widespread shoreward migration of inner bars and troughs, and upward and downward migration of forms in response to seasonal changes in mean water levels.

3. Earlier conclusions by Behrens, Watson, and Mason (in preparation, 1976) that low gulf surf and waxing tidal ranges cause channel erosion, and high surf and waning tidal ranges cause channel deposition continue to explain most of the bathymetric changes occurring within the channel and its several parts during both weekly and monthly intervals. A third factor, local winds, explains much of the short-term, detailed, erosion-deposition observations because of its control on the direction and amount of discharge and on surf conditions.

4. A simple, single-lobed, flood tidal delta seems to have contributed to a stable bypassing system at the bay mouth. However, material eroded from the bay shoreline entered this system through the small ebb channels and was flushed out of the pass by the dominant flood discharges to be deposited on the outer bay bars or be transported away from the area by longshore currents. Thus, the eroded material was lost to the system and the bay shore continued to erode at a constant volumetric rate.

5. Although most stability indices suggest that the pass is not stable, it has maintained itself for 3 years. Escoffier diagram analysis gives the greatest indication of stability and explains some critical, short-term fluctuations in cross-sectional area. Thus, it seems to be the best predictor of the Corpus Christi Exchange Pass behavior.

LITERATURE CITED

BAYAZIT, M., "Resistance to Reversing Flows Over Movable Beds," *Journal of the Hydraulic Division*, ASCE, Vol. 95, No. HY 4, Paper 6649, 1969, pp. 1109-1127.

BEHRENS, E.W., WATSON, R.L., and MASON, C., "Hydraulics and Dynamics of Corpus Christi Water Exchange Pass, Texas," GITI Report, U.S. Army, Corps of Engineers (in preparation, 1976).

BRUUN, P., *Tidal Inlets and Littoral Drift*, Universit ets forlaget, Oslo, Norway, 1966.

BRUUN, P., and GERRITSEN, F., *Stability of Coastal Inlets*, North Holland, Amsterdam, 1960.

COLLIER, A., and HEDGPETH, J., "An Introduction to the Hydrography of Tidal Waters," *Publications of the Institute of Marine Sciences*, Vol. 1, No. 2, Nov. 1950, pp. 121-177.

DAVIS, R.A., and FOX, W.T., "Coastal Dynamics along Mustang Island, Texas," Contract NONR 388-092, Office of Naval Research, Washington, D.C., 1972.

DAVIS, R.A., and FOX, W.T., "Process Response Patterns in Beach and Nearshore Sedimentation: I. Mustang Island, Texas," *Journal of Sedimentary Petrology*, Vol. 45, No. 4, Dec. 1975, pp. 852-865.

ESCOFFIER, F.F., "The Stability of Tidal Inlets," *Shore and Beach*, Vol. 8, No. 4, 1940, pp. 114-115.

HARWOOD, P.J., "Stability and Geomorphology of Pass Cavallo and Its Flood Delta Since 1956," Unpublished Master's Thesis, University of Texas, Austin, Tex., 1973.

JARRETT, J.T., "Tidal Prism - Inlet Area Relationships," GITI Report 3, U.S. Army, Corps of Engineers, Vicksburg, Miss., Feb. 1976.

KEULEGAN, G.H., "Tidal Flow in Entrances: Water-level Fluctuations of Basins in Communication with Seas," Technical Bulletin No. 14, U.S. Army Committee in Tidal Hydraulics Coastal Engineers, July 1967.

MEYER, A.F., "Evaporation from Lakes and Reservoirs. A Study Based on Fifty Years' Weather Bureau Records," St. Paul: Minnesota Resources Commission, St. Paul, Minn., 1942.

NATIONAL OCEANIC AND ATMOSPHERIC ADMINISTRATION, "Tide Tables, High and low Water Predictions," National Ocean Survey, Norfolk, Va., 1972, 1973, 1974, and 1975.

O'BRIEN, M.P., "Estuary Tidal Prisms Related to Entrance Areas," *Civil Engineering*, Vol. 1, No. 8, May 1931, pp. 738-739.

O'BRIEN, M.P., "Equilibrium Flow Areas of Inlets on Sandy Coasts," *Journal of Waterways Harbors Division*, ASCE, Vol. 95, No. WW1, Feb. 1969, pp. 43-52.

O'BRIEN, M.P., and DEAN, R.G., "Hydraulics and Sedimentary Stability of Coastal Inlets," *Proceedings of the 13th Coastal Engineering Conference*, ASCE, Vol. 2, 1972, pp. 761-780.

SMITH, N.P., "Intracoastal Tides of Corpus Christi Bay," *Contributions in Marine Science*, Vol. 18, Sept. 1974, pp. 205-219.

U.S. ARMY, CORPS OF ENGINEERS, COASTAL ENGINEERING RESEARCH CENTER, *Shore Protection Manual*, Vols. I, II, and III, 2d ed., Stock No. 008-022-00077, U.S. Government Printing Office, Washington, D.C., 1975, 1,160 pp.

WATSON, R.L., "Origin of Shell Beaches, Padre Island, Texas," *Journal of Sedimentary Petrology*, Vol. 41, No. 4, 1971, pp. 1105-1111.

WHITAKER, R.E., "Seasonal Variations of Steric and Recorded Sea Level of the Gulf of Mexico," NRC Contract, NOOOO14-68-A-03C38-0002, Project 700-3, Texas A&M University, College Station, Tex., 1971.

APPENDIX A

DIURNAL DISCHARGE STUDIES RESULTS

Plots of instantaneous tidal discharge and differential versus time.

AD-A033 607 TEXAS UNIV PORT ARANSAS MARINE SCIENCE INST F/G 8/3
HYDRAULICS AND DYNAMICS OF NEW CORPUS CHRISTI PASS, TEXAS: A CA--ETC(U)
SEP 76 R L WATSON, E W BEHRENS DACW72-74-C-0017
UNCLASSIFIED WES-6ITI-9 NL

2 OF 2
AD
A033607

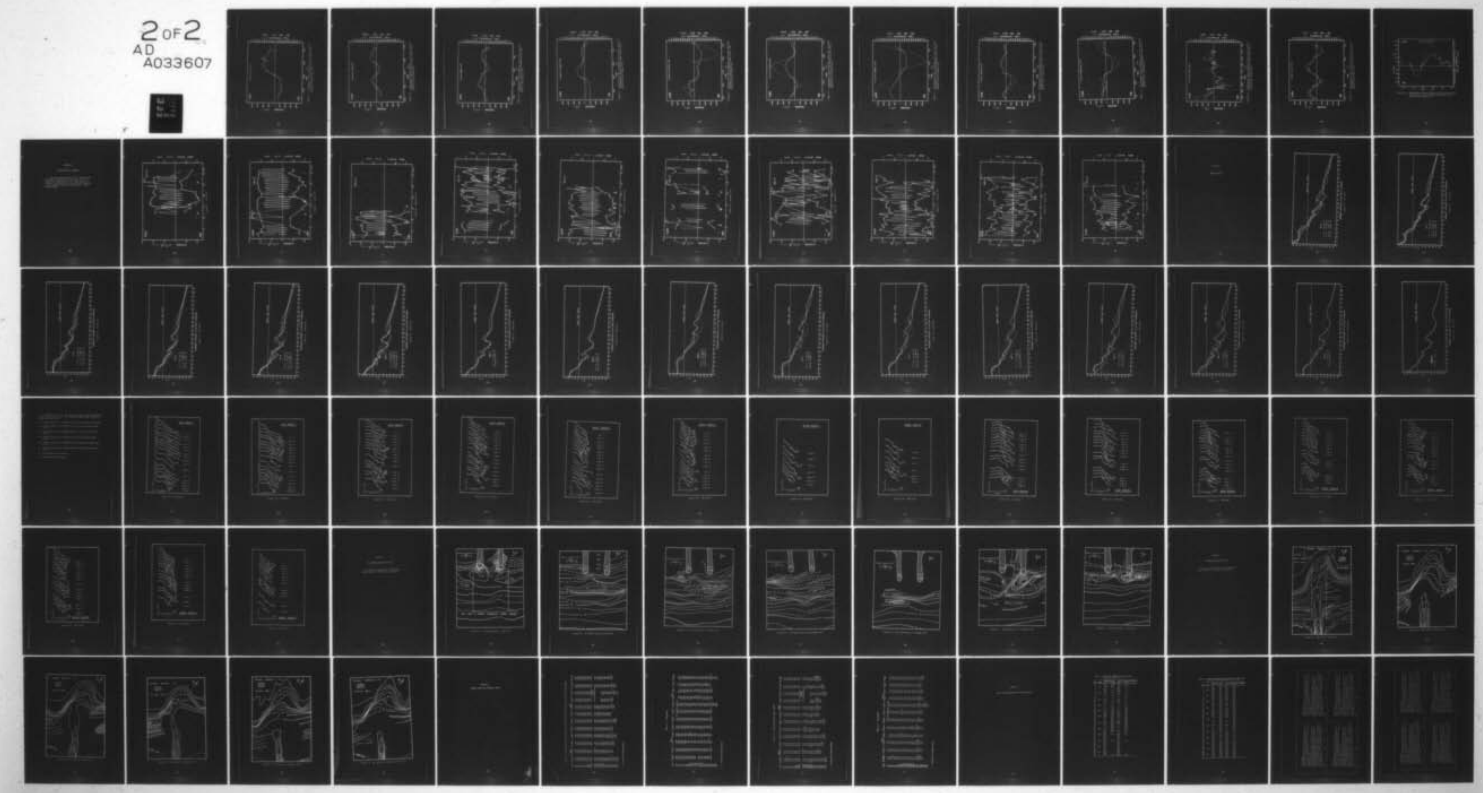

END

DATE
FILMED
2-77

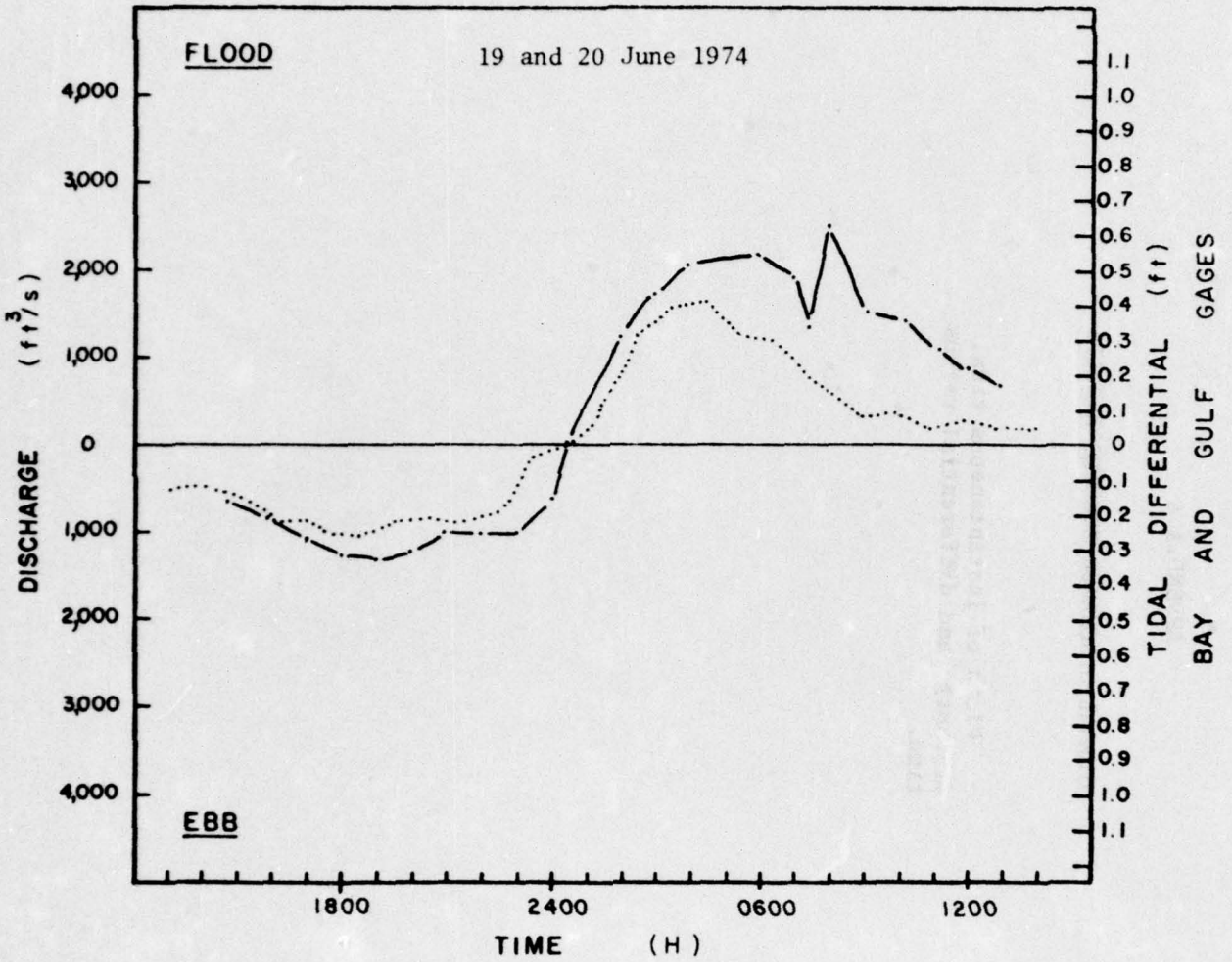

Figure A-1. Instantaneous tidal discharges (solid line) and tidal differentials (dotted line) through diurnal study period, 19 and 20 June 1974.

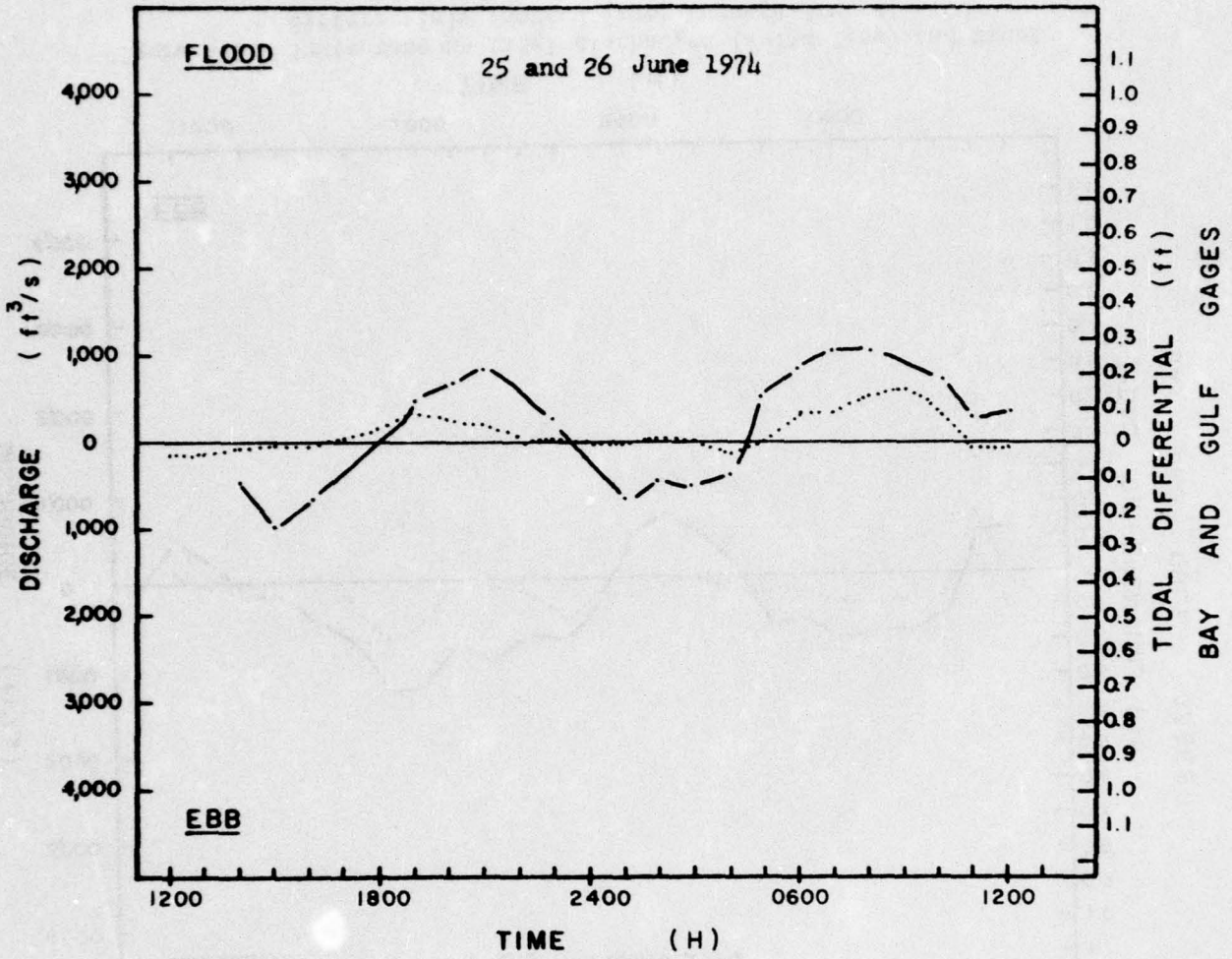

Figure A-2. Instantaneous tidal discharges (solid line) and tidal differentials (dotted line) through diurnal study period 25 and 26 June 1974.

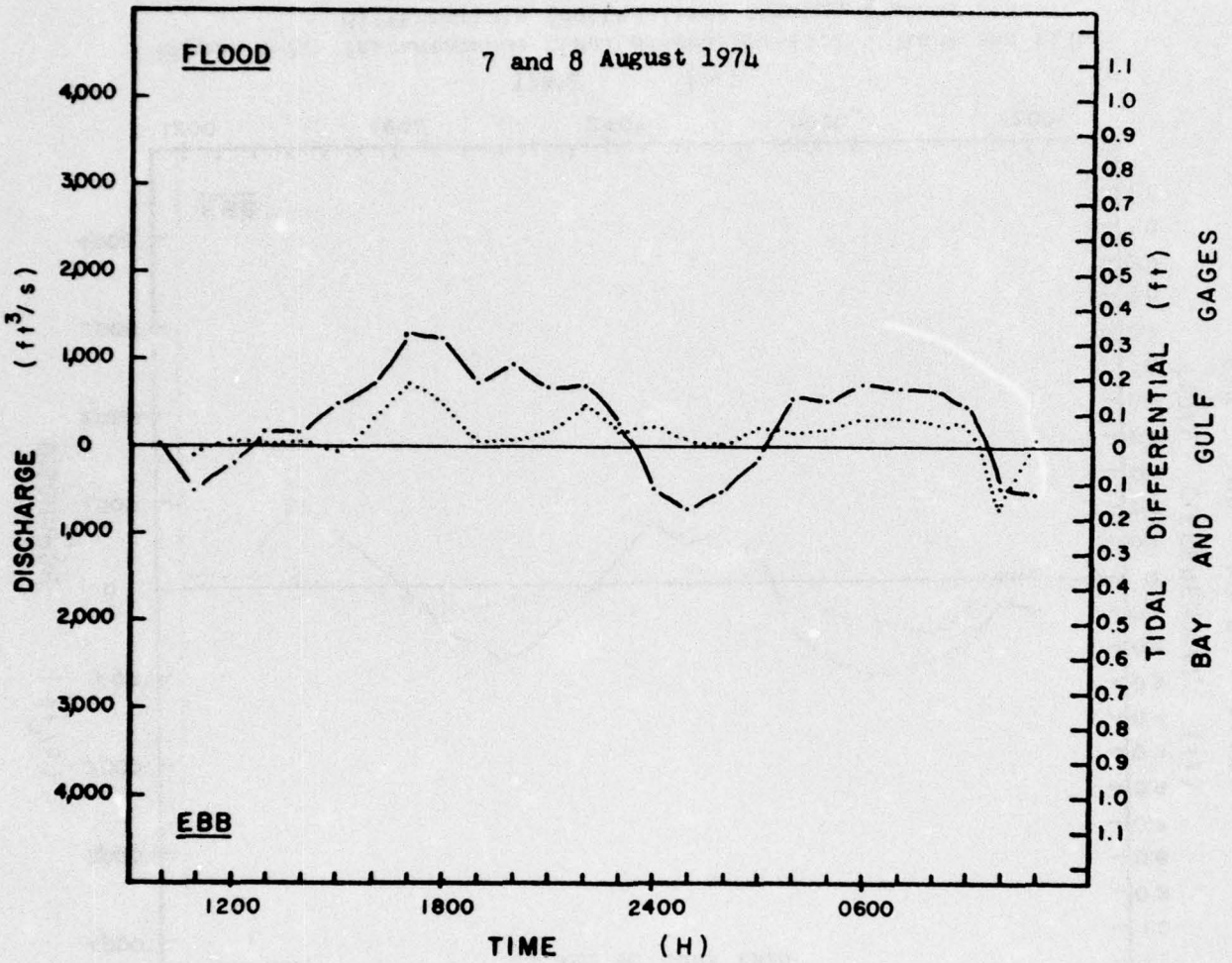

Figure A-3. Instantaneous tidal discharges (solid line) and tidal differentials (dotted line) through diurnal study period 7 and 8 August 1974.

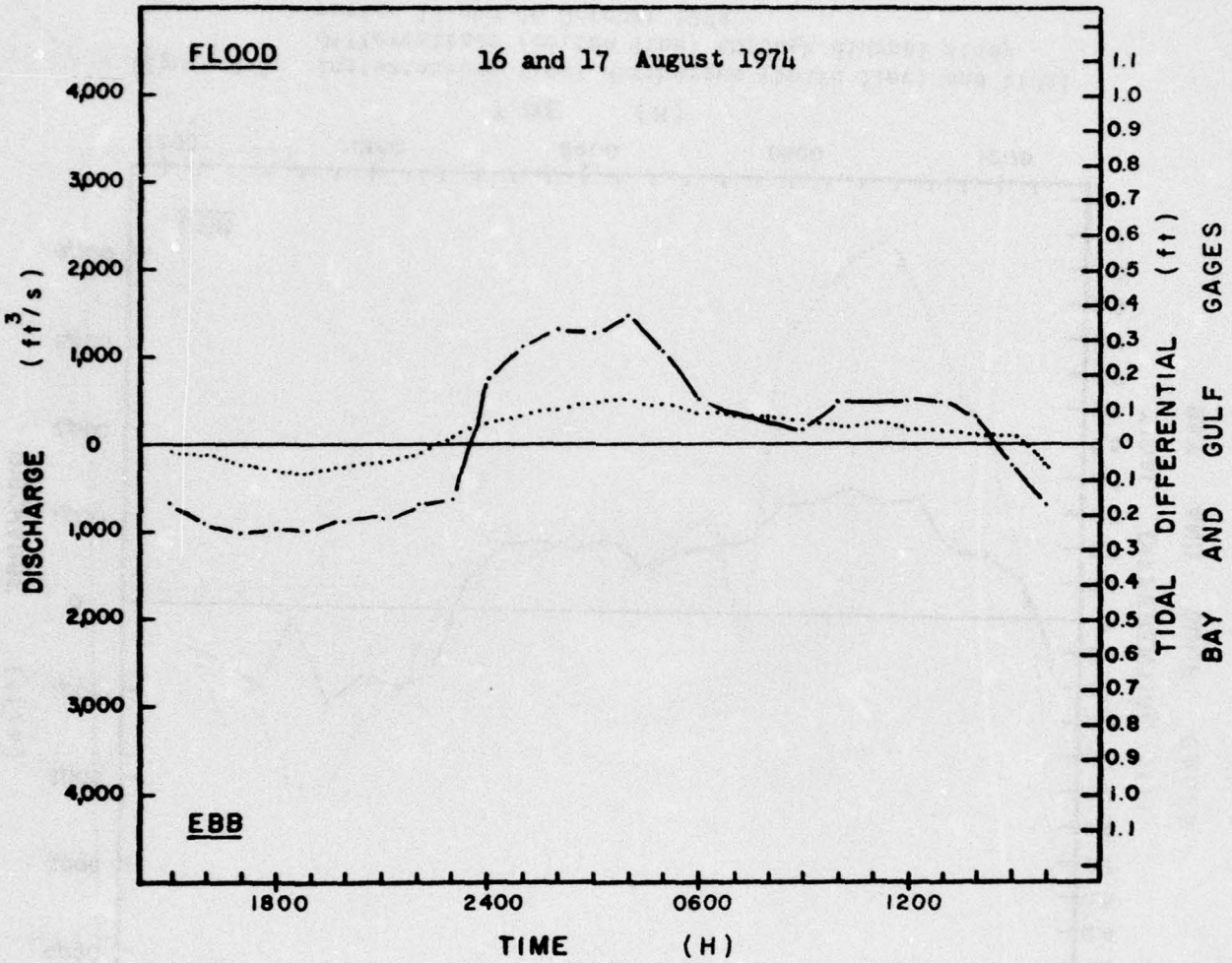

Figure A-4. Instantaneous tidal discharges (solid line) and tidal differentials (dotted line) through diurnal study period 16 and 17 August 1974.

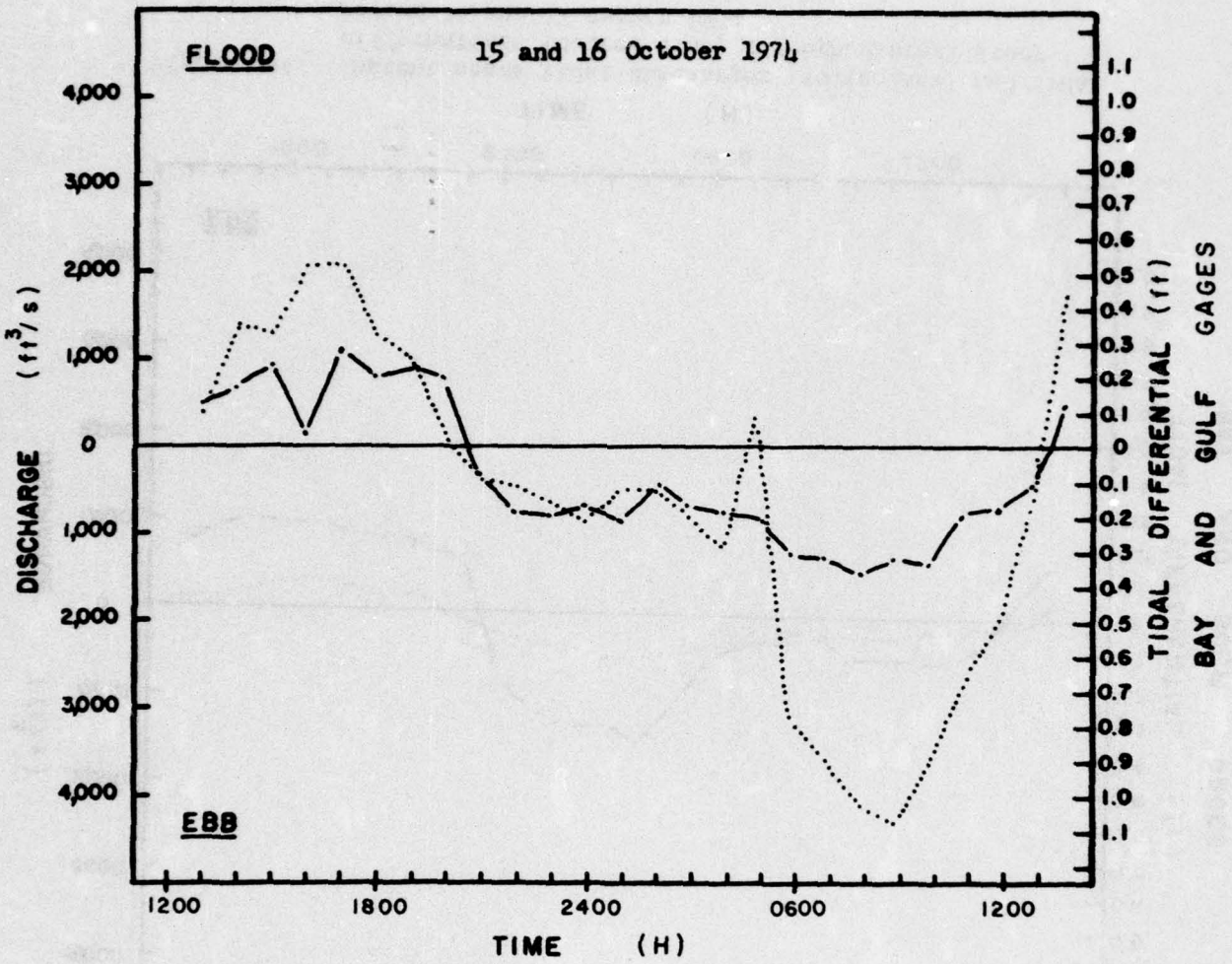

Figure A-5. Instantaneous tidal discharges (solid line) and tidal differentials (dotted line) through diurnal study period 15 and 16 October 1974.

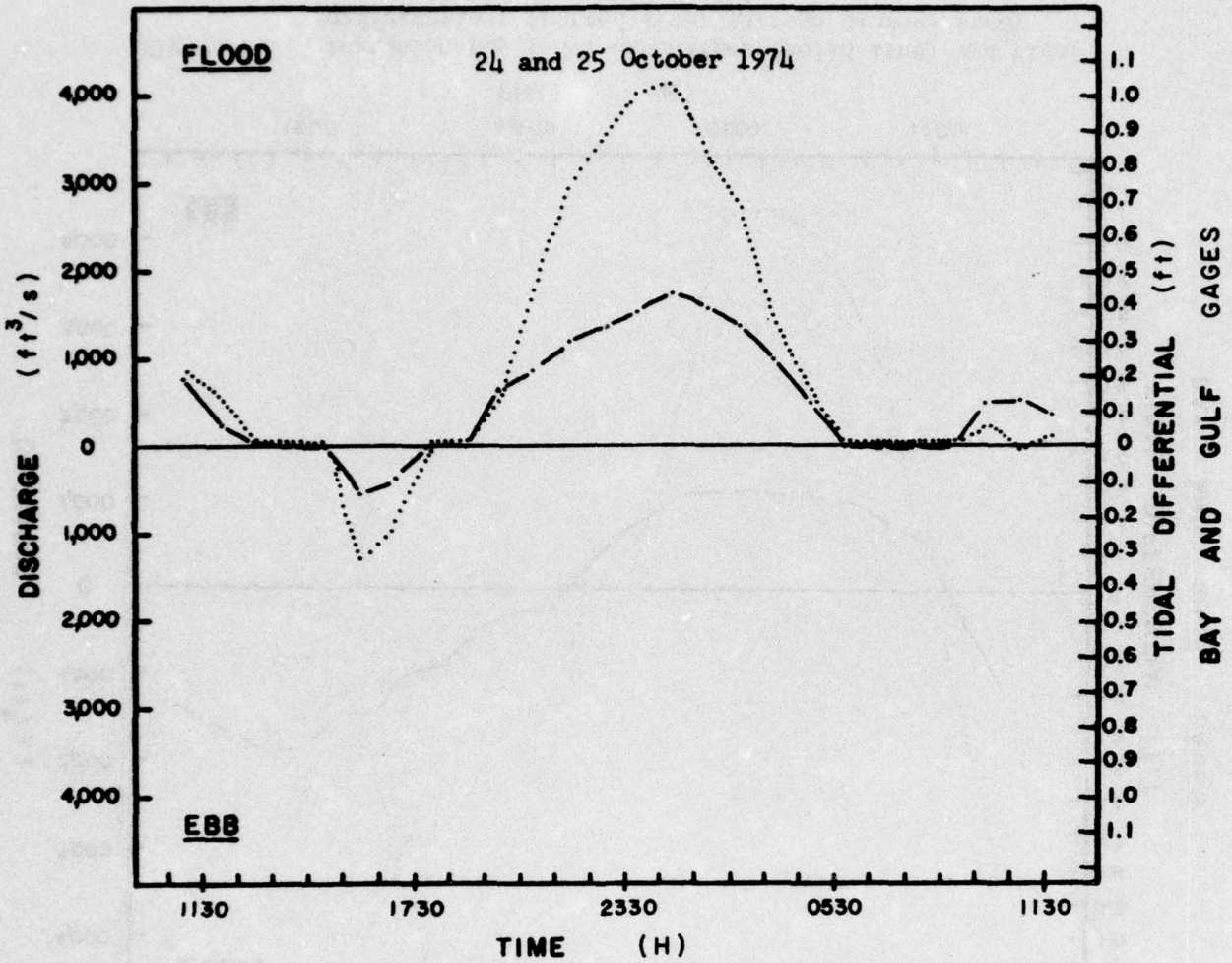

Figure A-6. Instantaneous tidal discharge (solid line) and tidal differential (dotted line) through diurnal study period 24 and 25 October 1974.

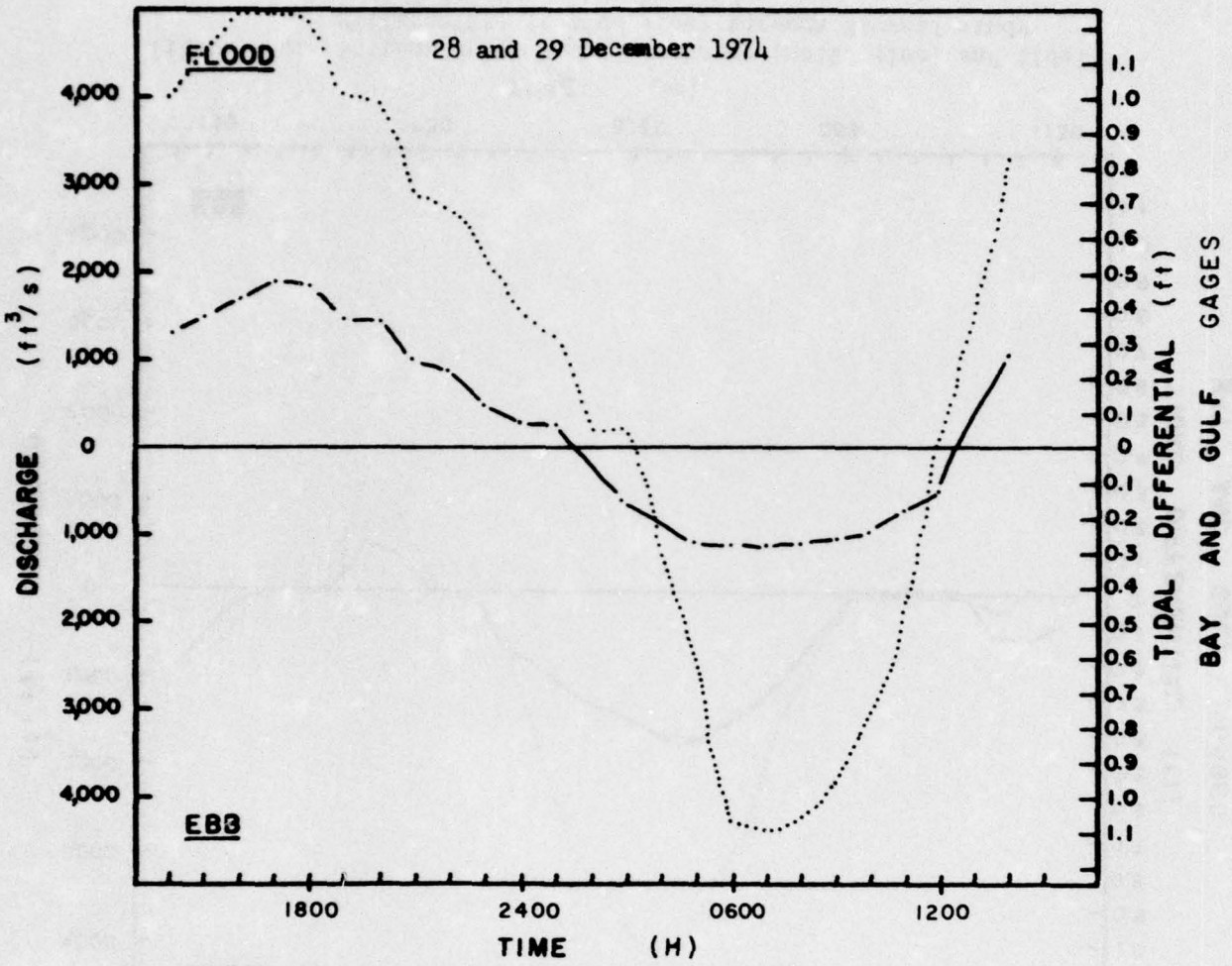

Figure A-7. Instantaneous tidal discharges (solid line) and tidal differentials (dotted line) through diurnal study period 28 and 29 December 1974.

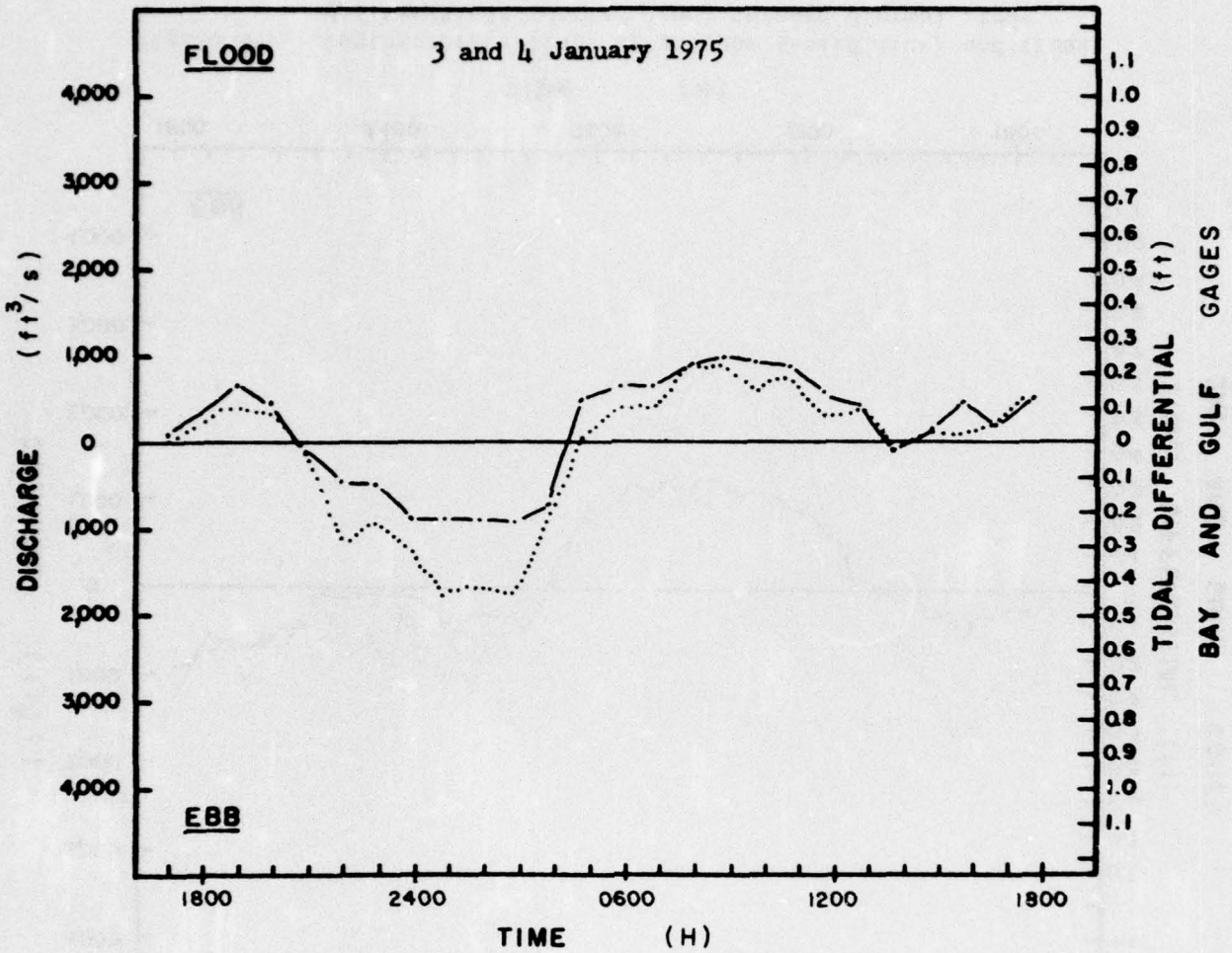

Figure A-8. Instantaneous tidal discharges (solid line) and tidal differentials (dotted line) through a diurnal study period 3 and 4 January 1975.

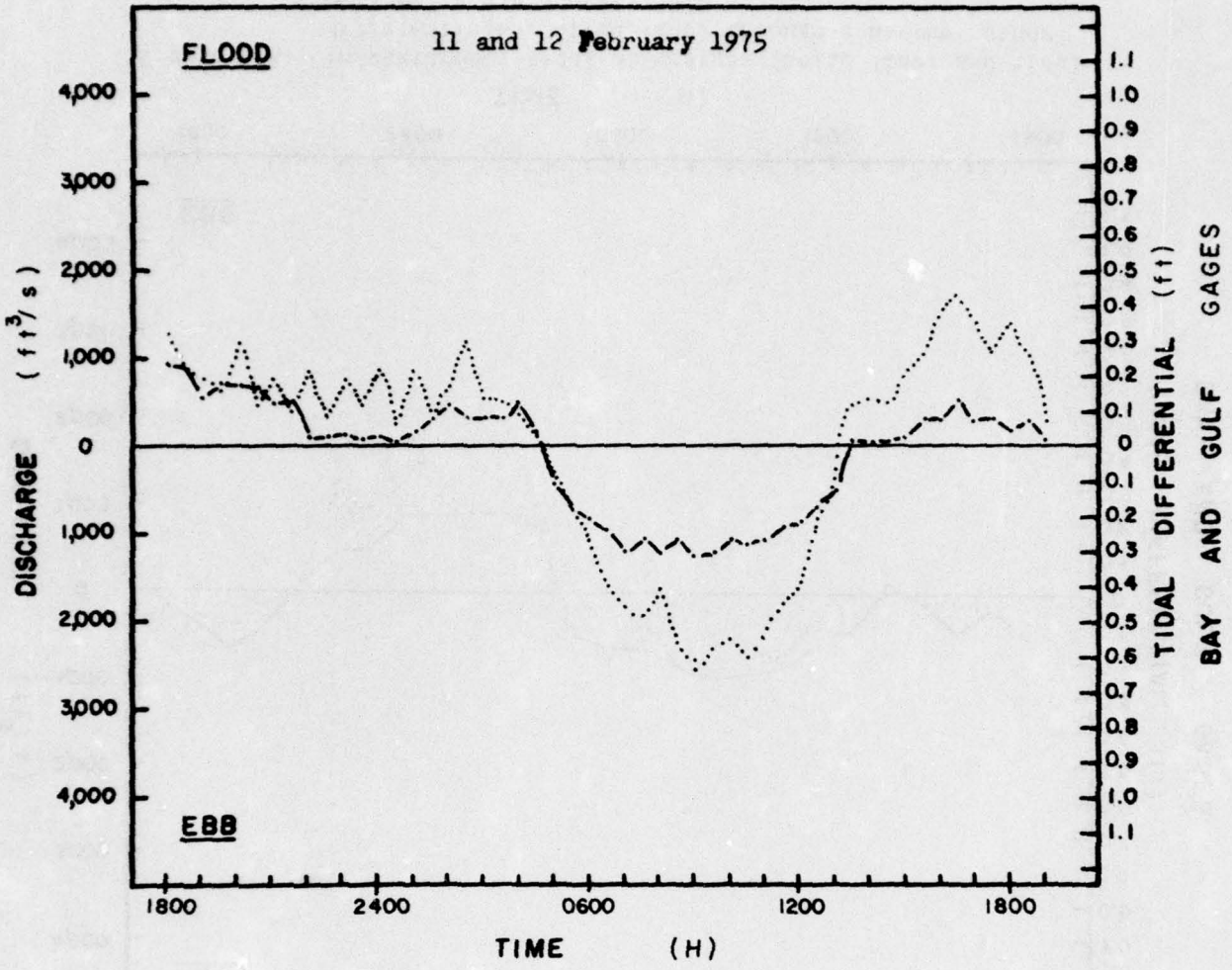

Figure A-9. Instantaneous tidal discharges (solid line) and tidal differentials (dotted line) through diurnal study period 11 and 12 February 1975.

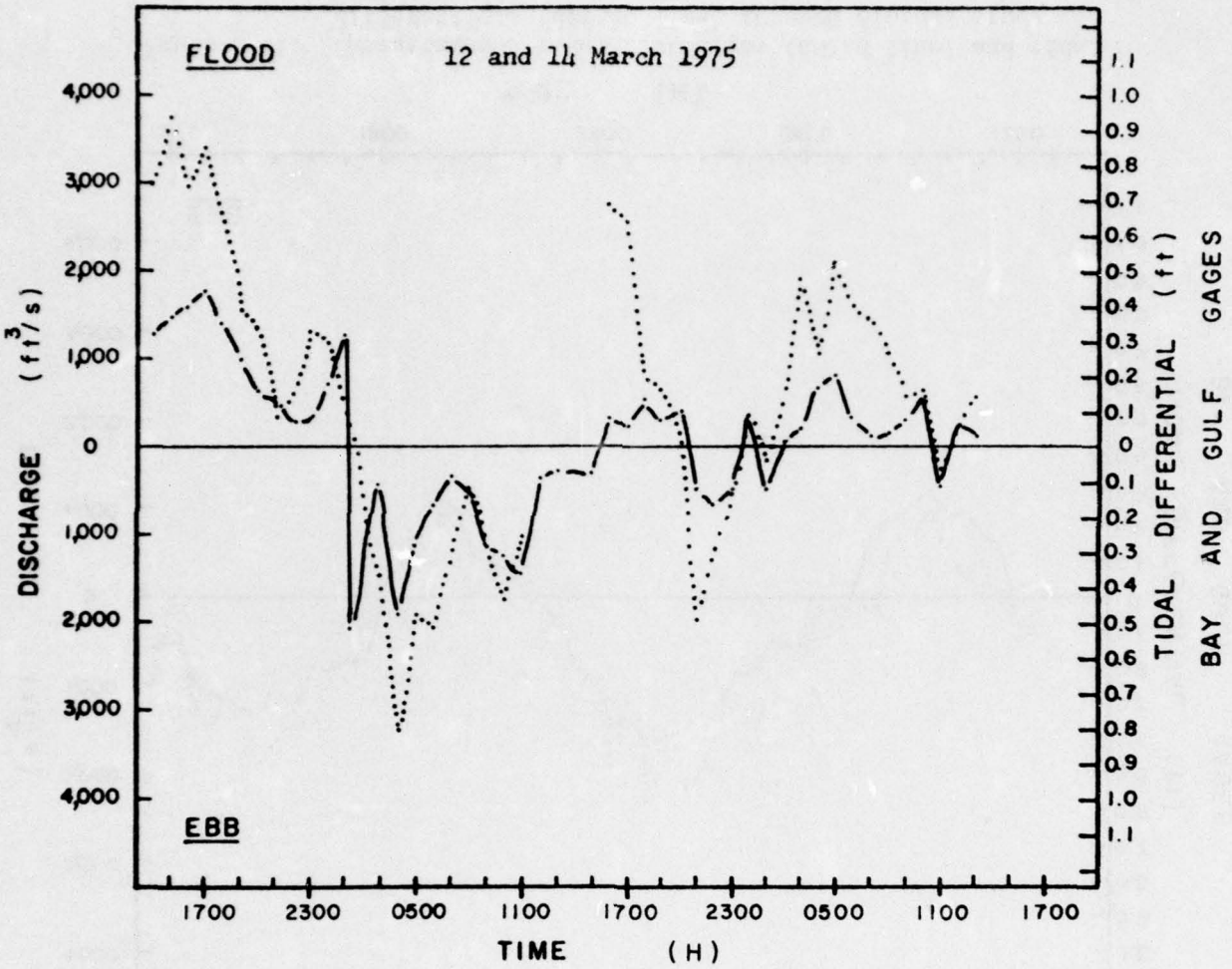

Figure A-10. Instantaneous tidal discharges (solid line) and tidal differentials (dotted line) through diurnal study period 12 and 14 March 1975.

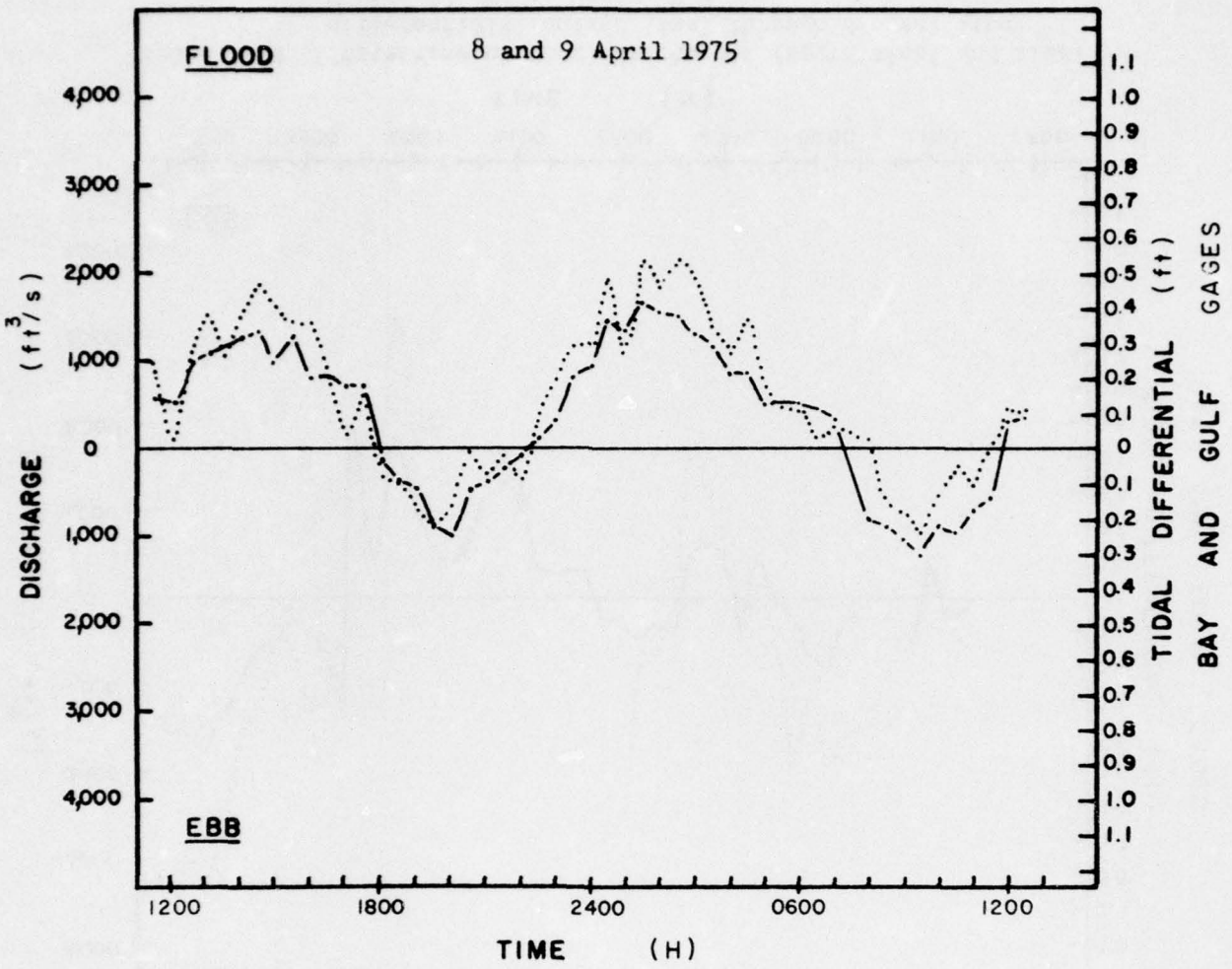

Figure A-11. Instantaneous tidal discharges (solid line) and tidal differentials (dotted line) through diurnal study period 8 and 9 April 1975.

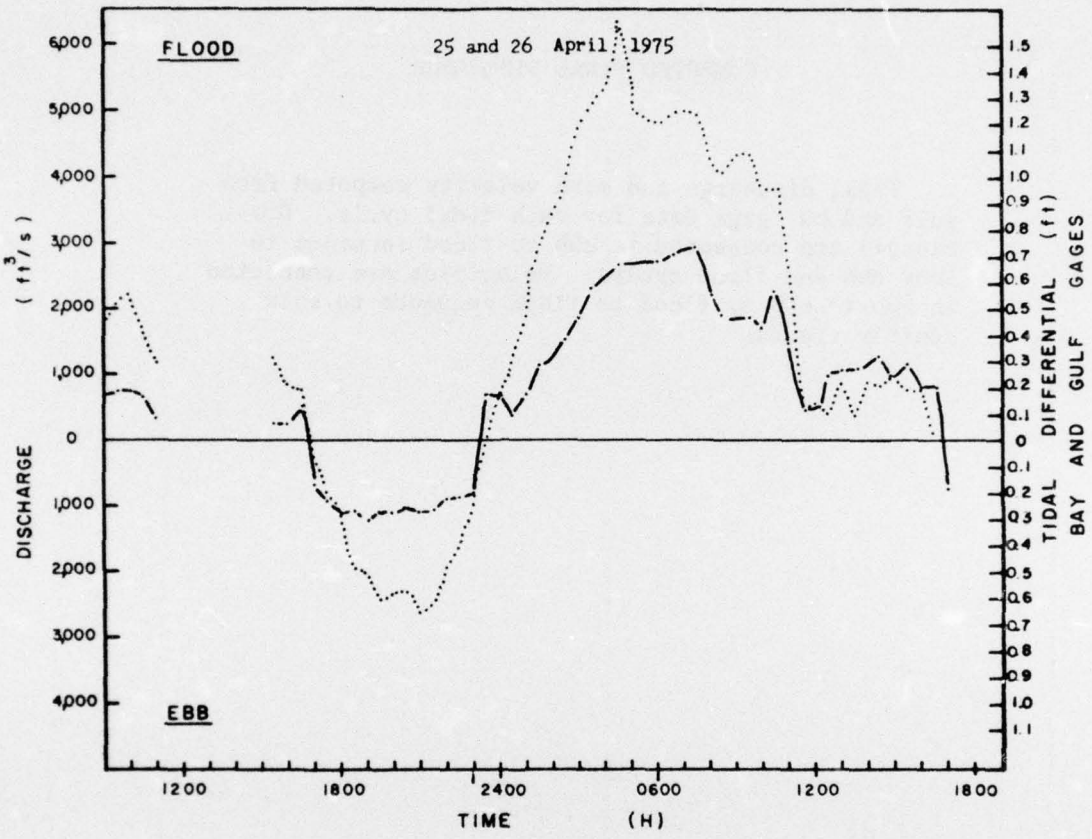

Figure A-12. Instantaneous tidal discharges (solid line) and tidal differentials (dotted line) through diurnal study period 25 and 26 April 1975.

APPENDIX B

COMPUTED TIDAL DISCHARGE

Tidal discharge and mean velocity computed from gulf and bay gage data for each tidal cycle. Discharges are connected in ebb to flood sequence to show ebb and flood cycles. Velocities are connected in ebb to ebb or flood to flood sequence to show monthly trends.

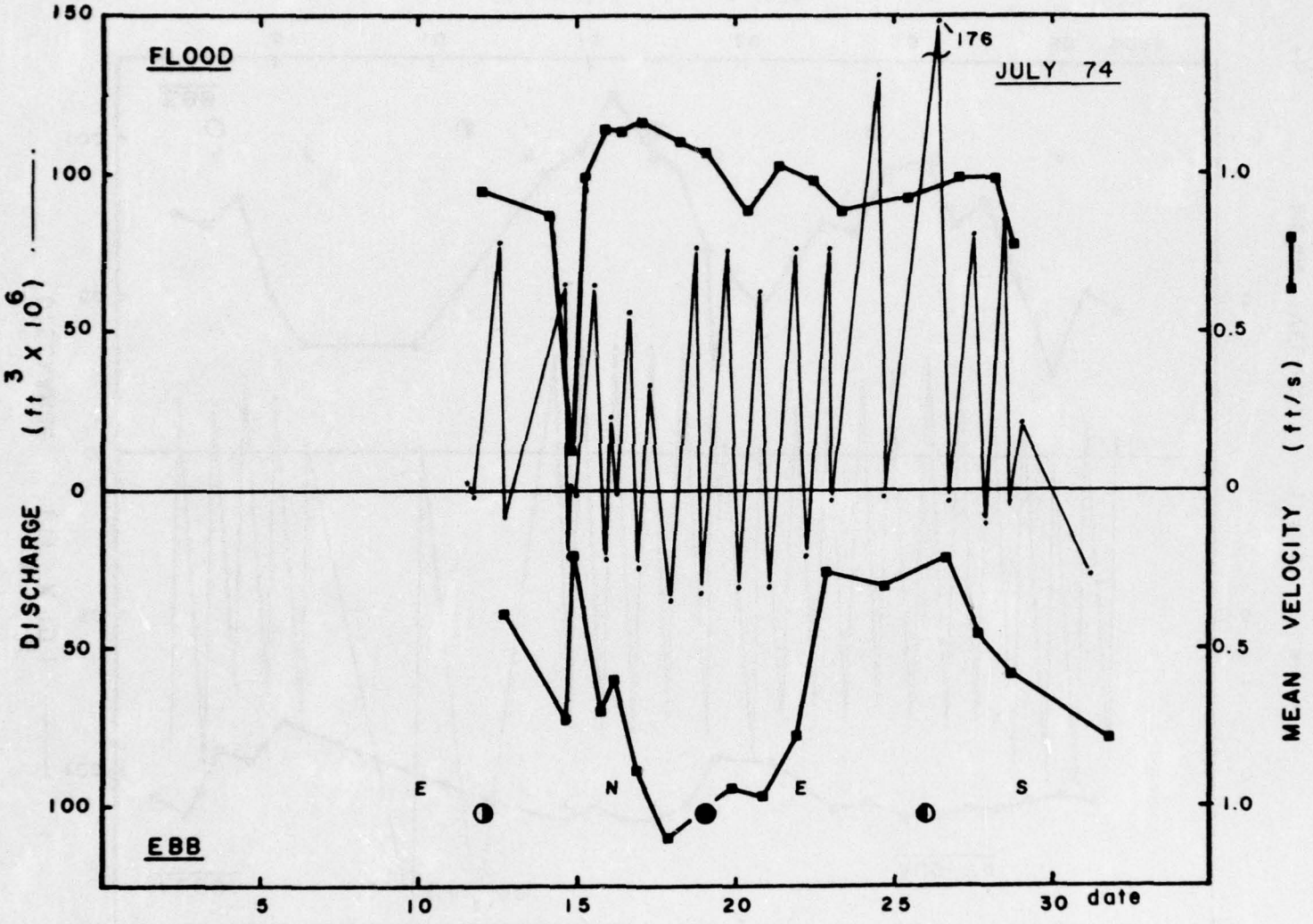

Figure B-1. July 1974.

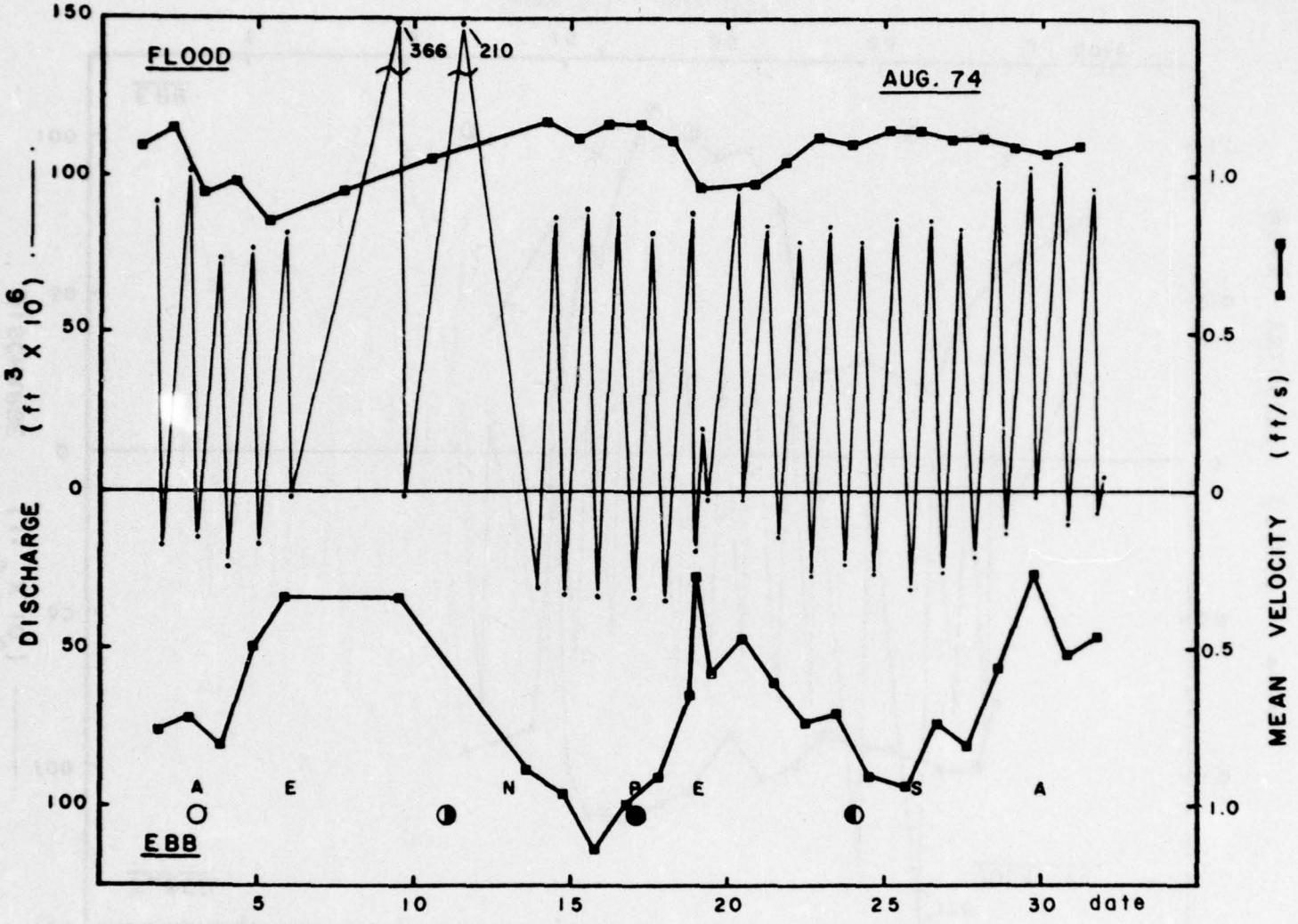

Figure B-2. August 1974.

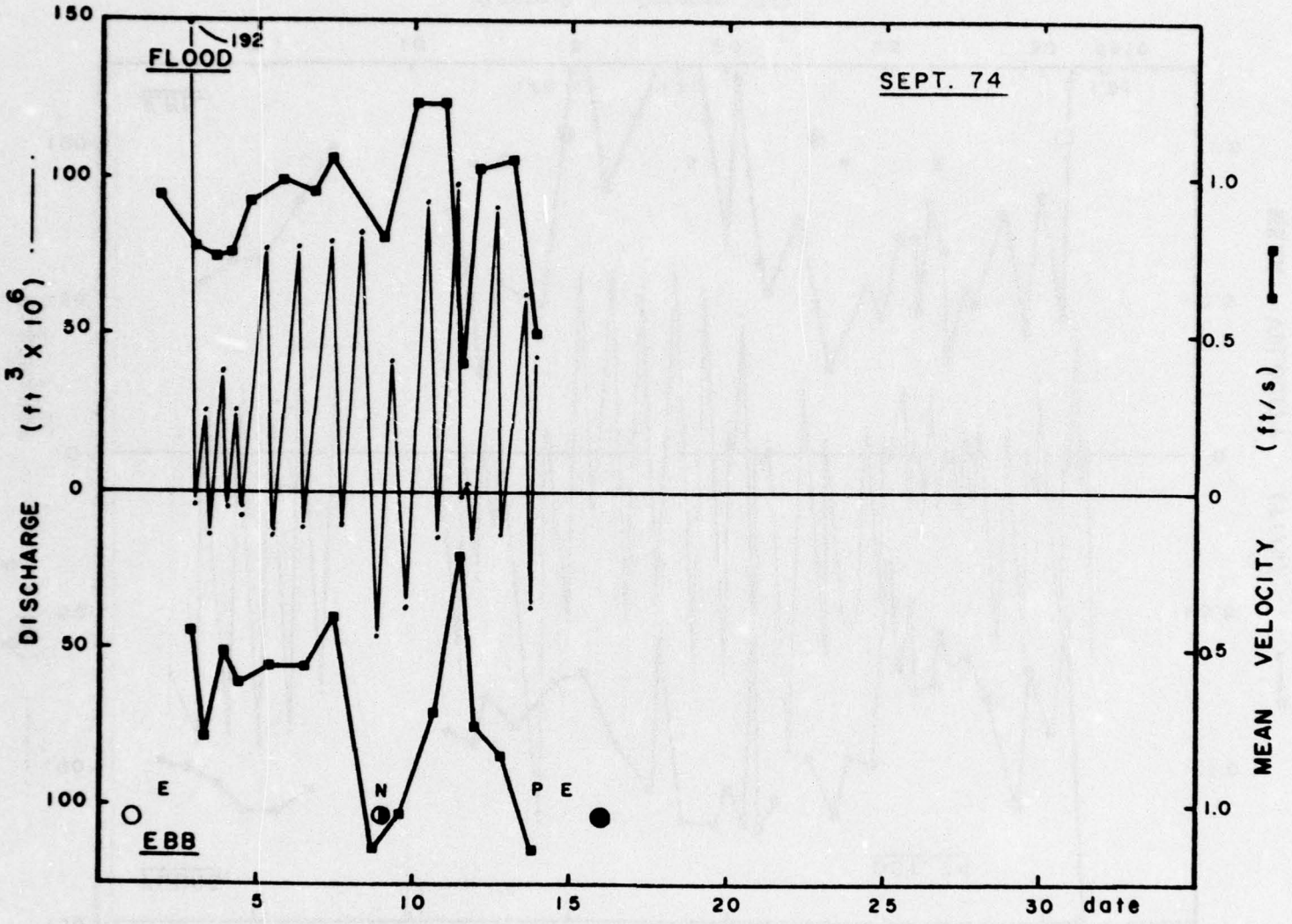

Figure B-3. September 1974.

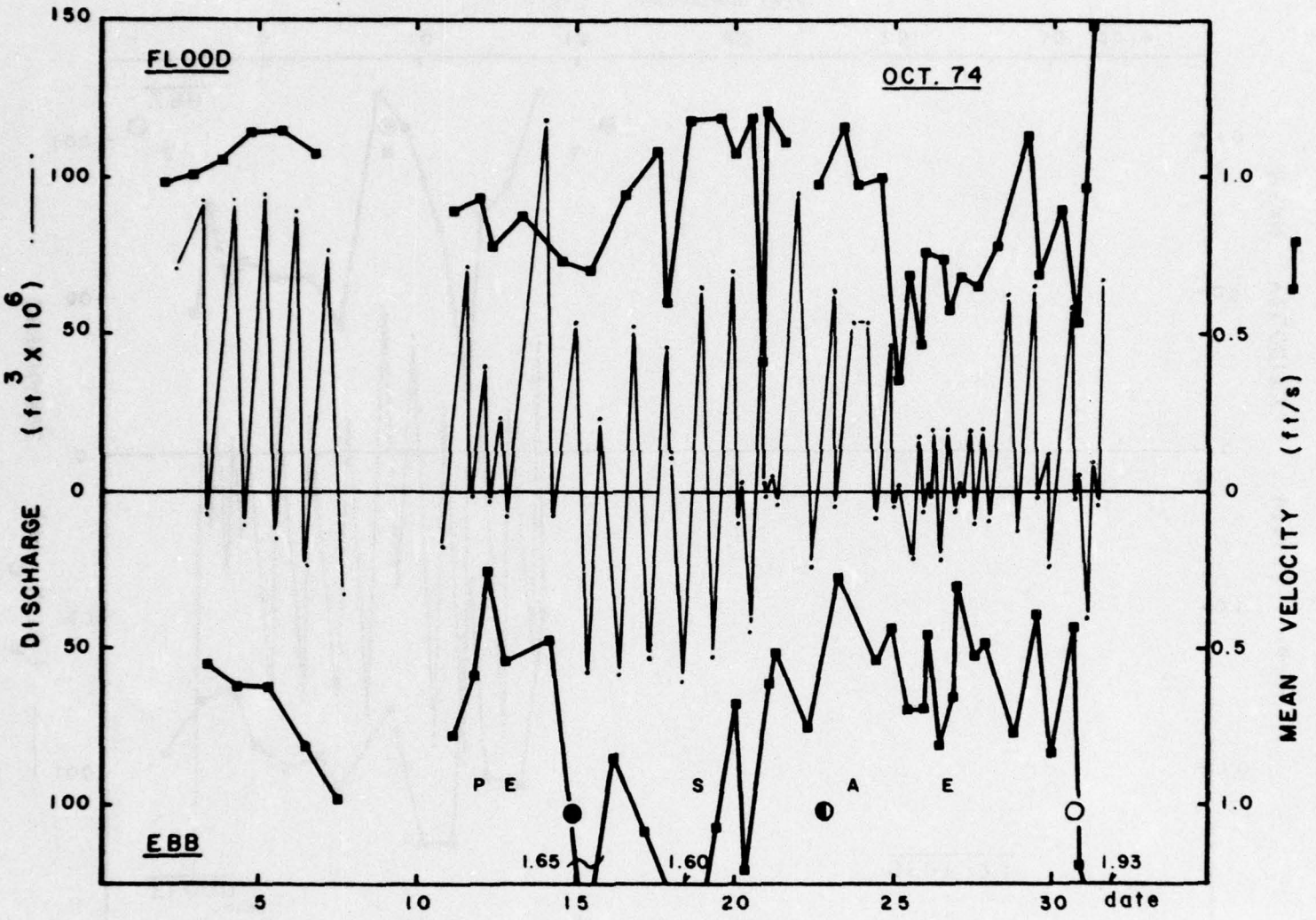

Figure B-4. October 1974.

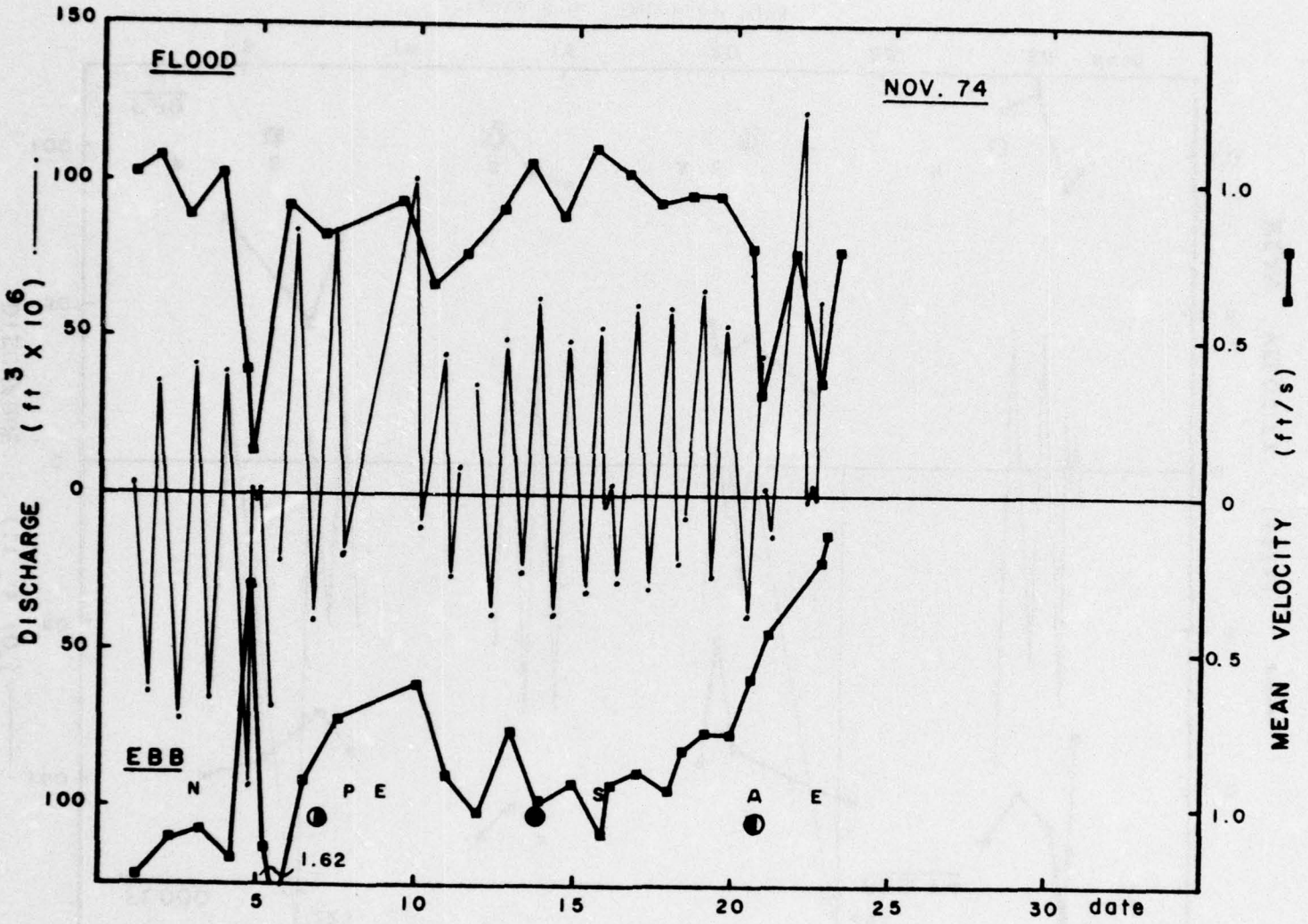

Figure B-5. November 1974.

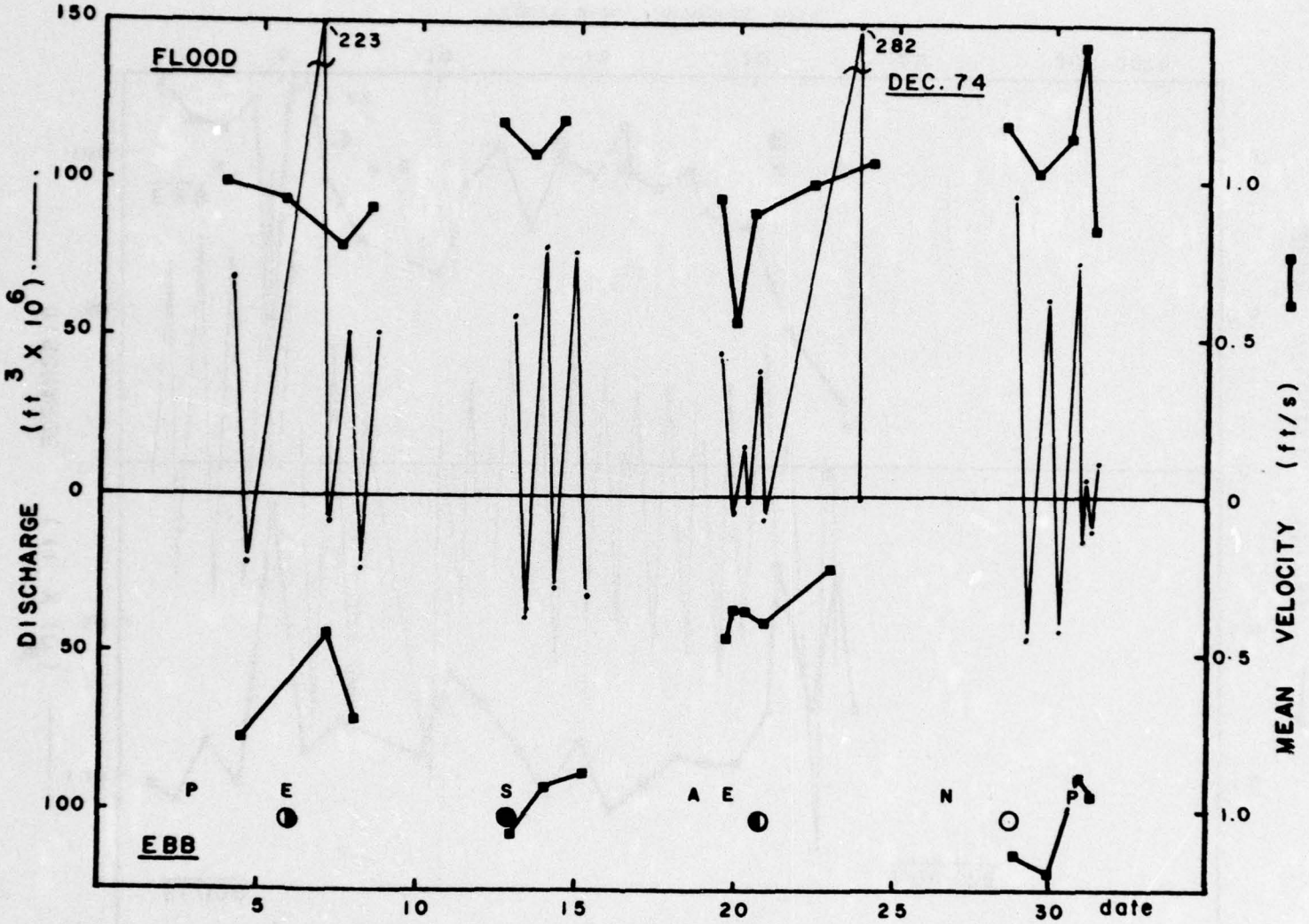

Figure B-6. December 1974.

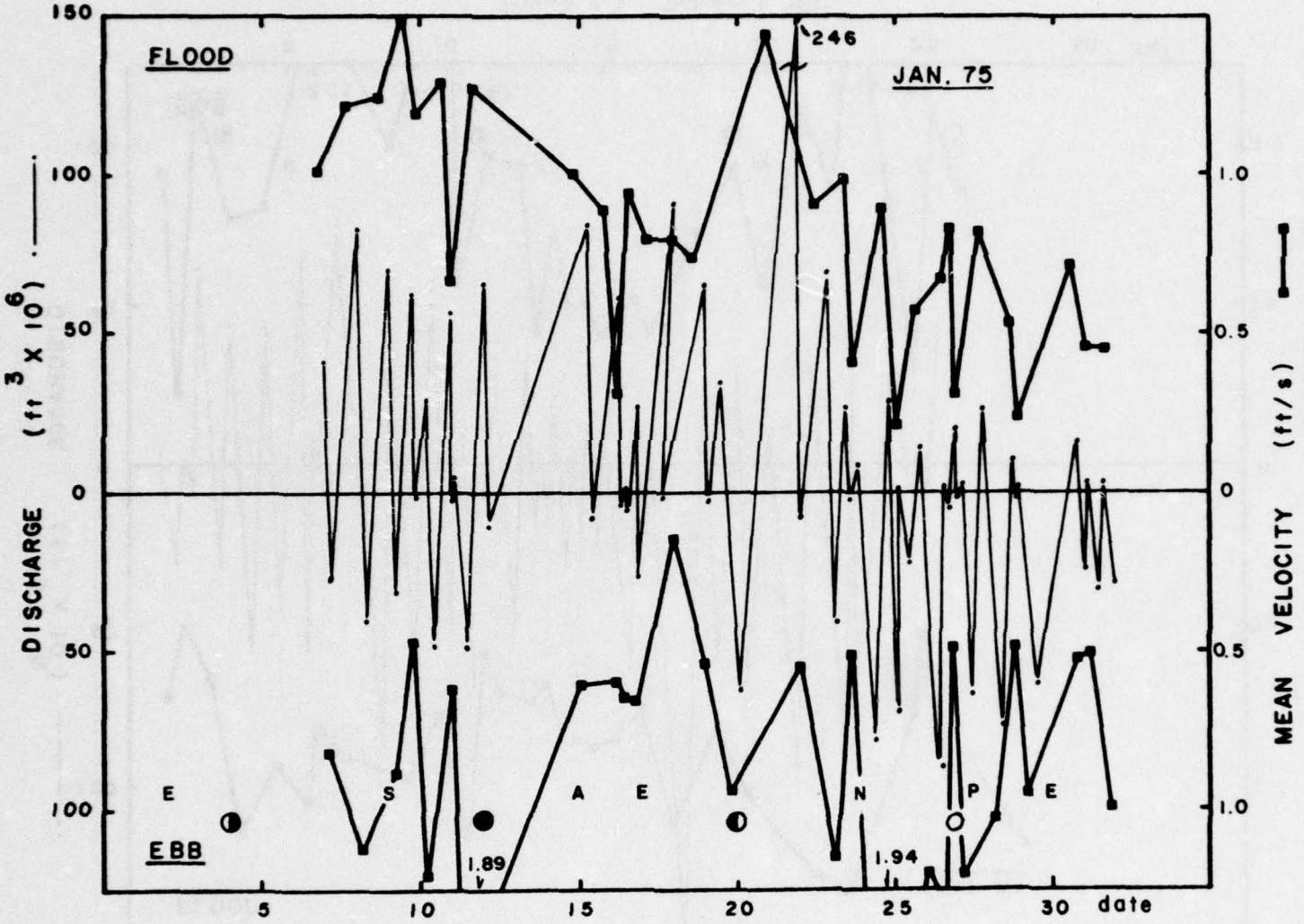

Figure B-7. January 1975.

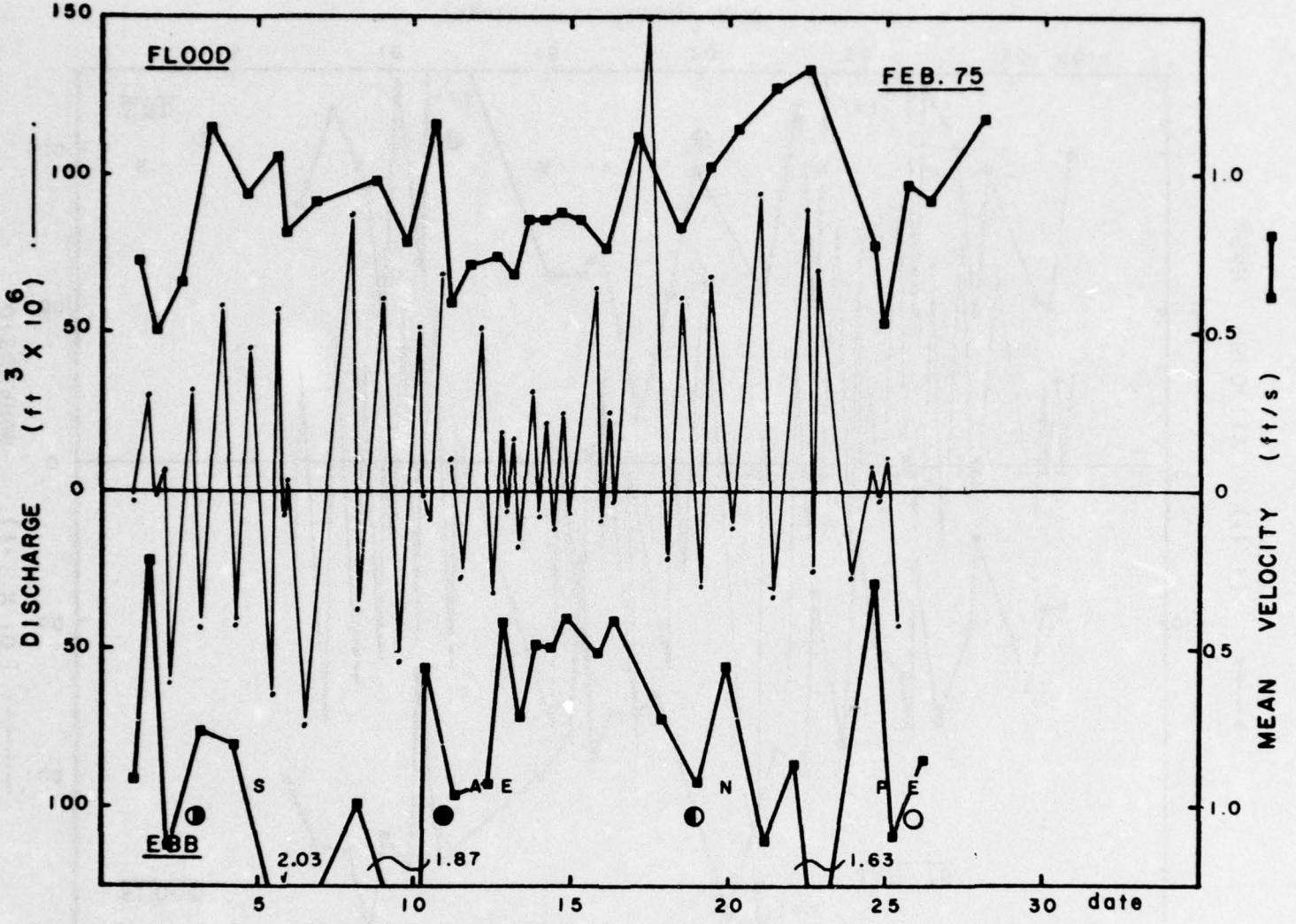

Figure B-8. February 1975.

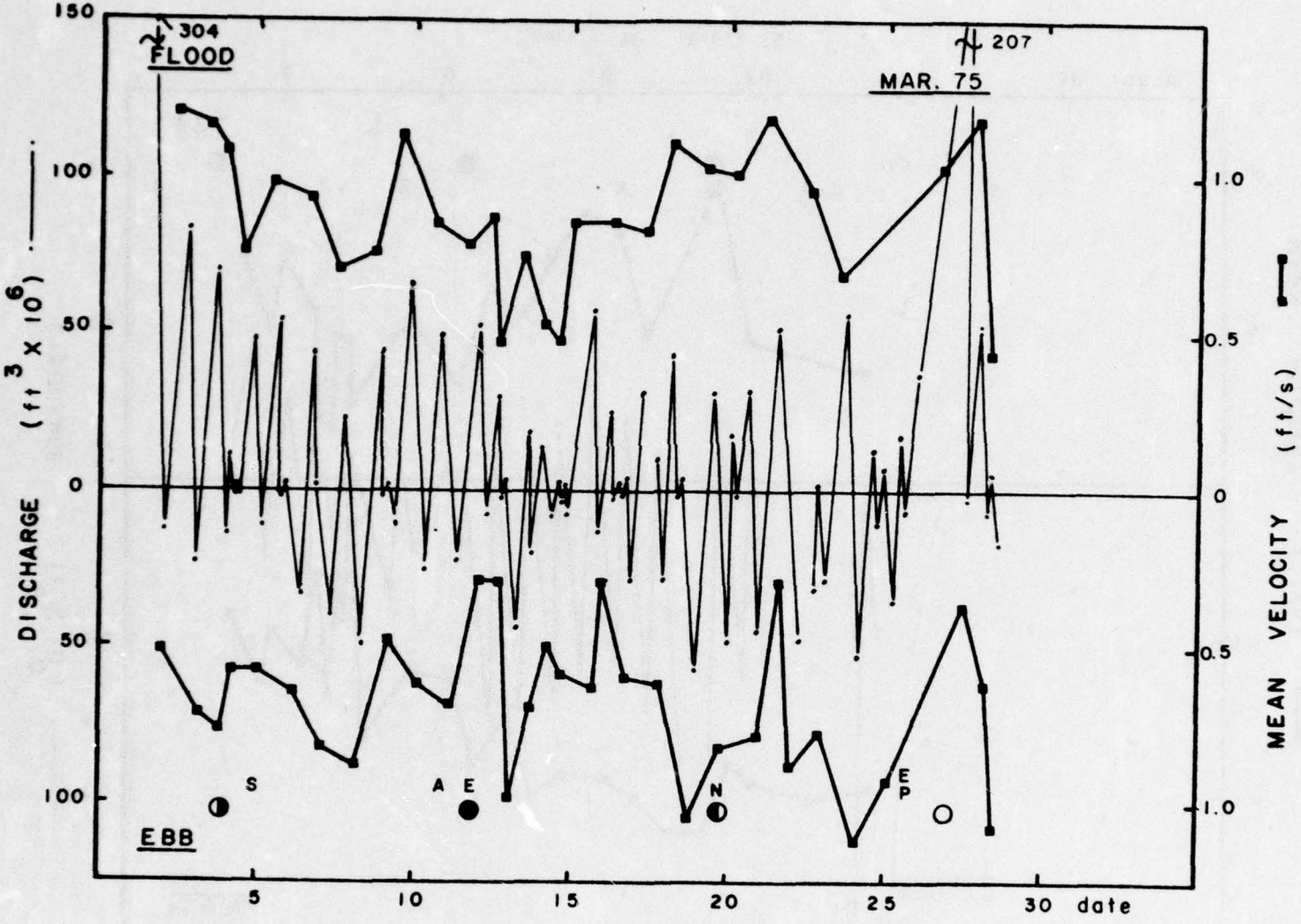

Figure B-9. March 1975.

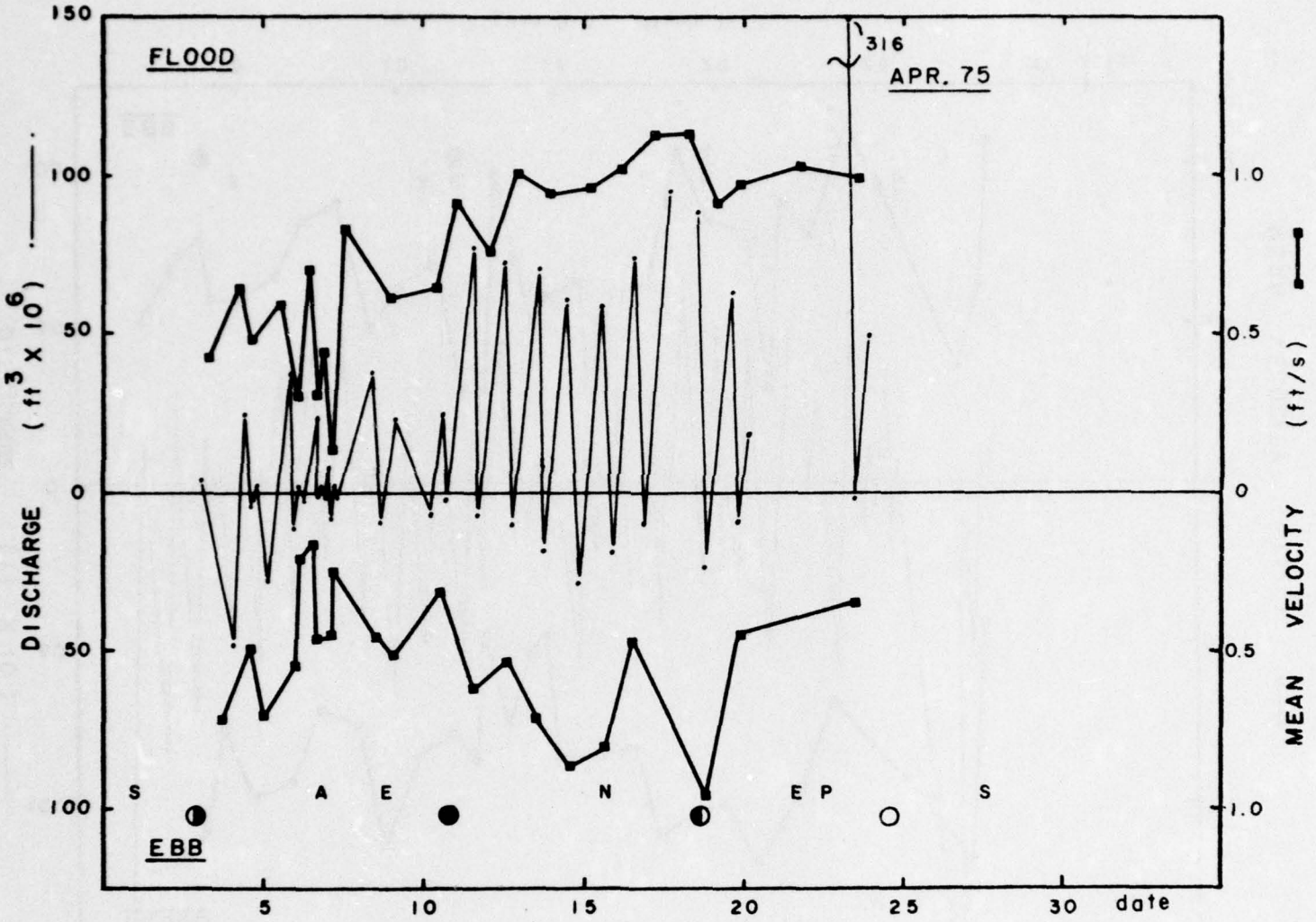

Figure B-10. April 1975.

APPENDIX C

BEACH PROFILES

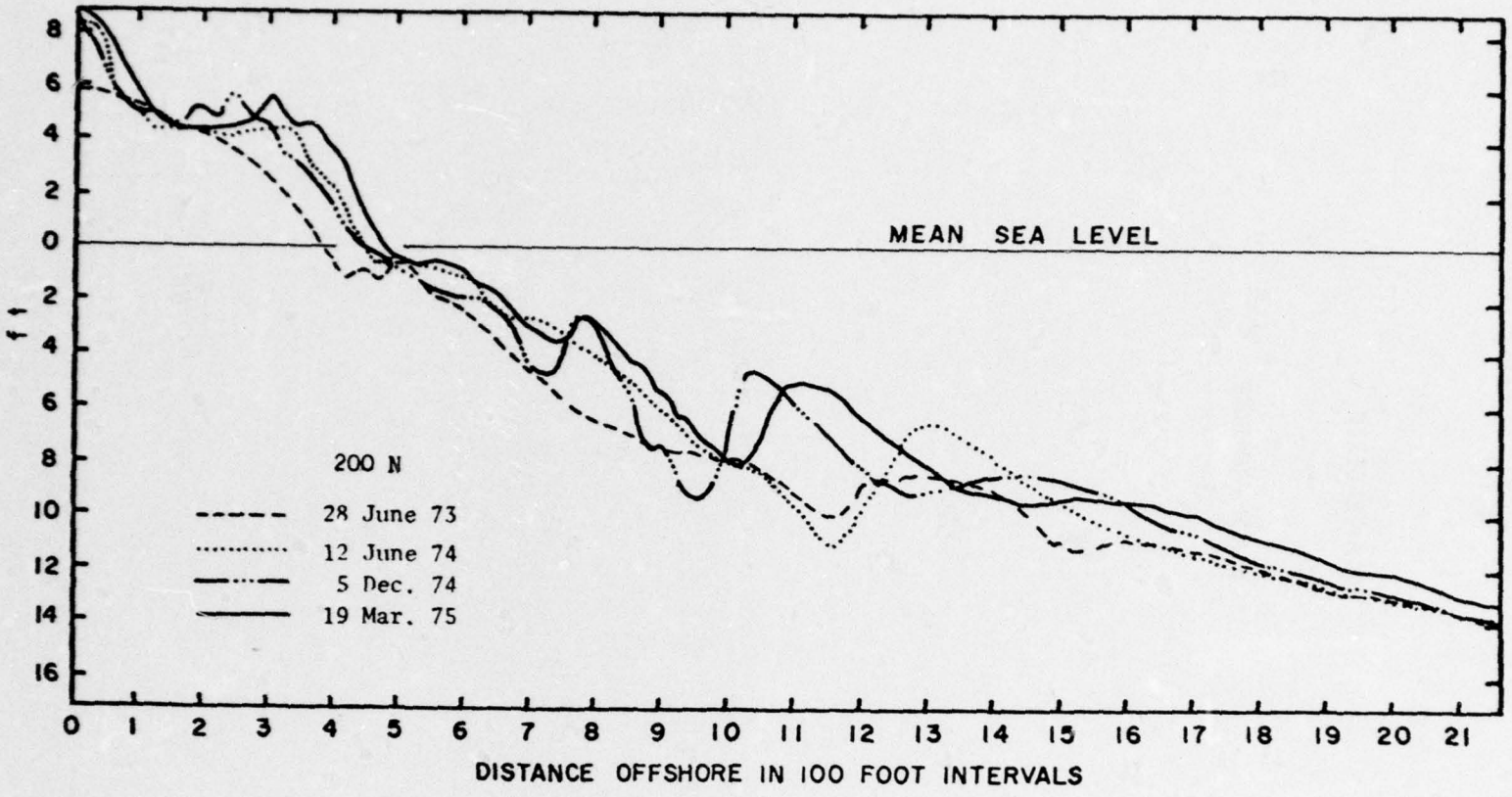

Figure C-1. 200 North.

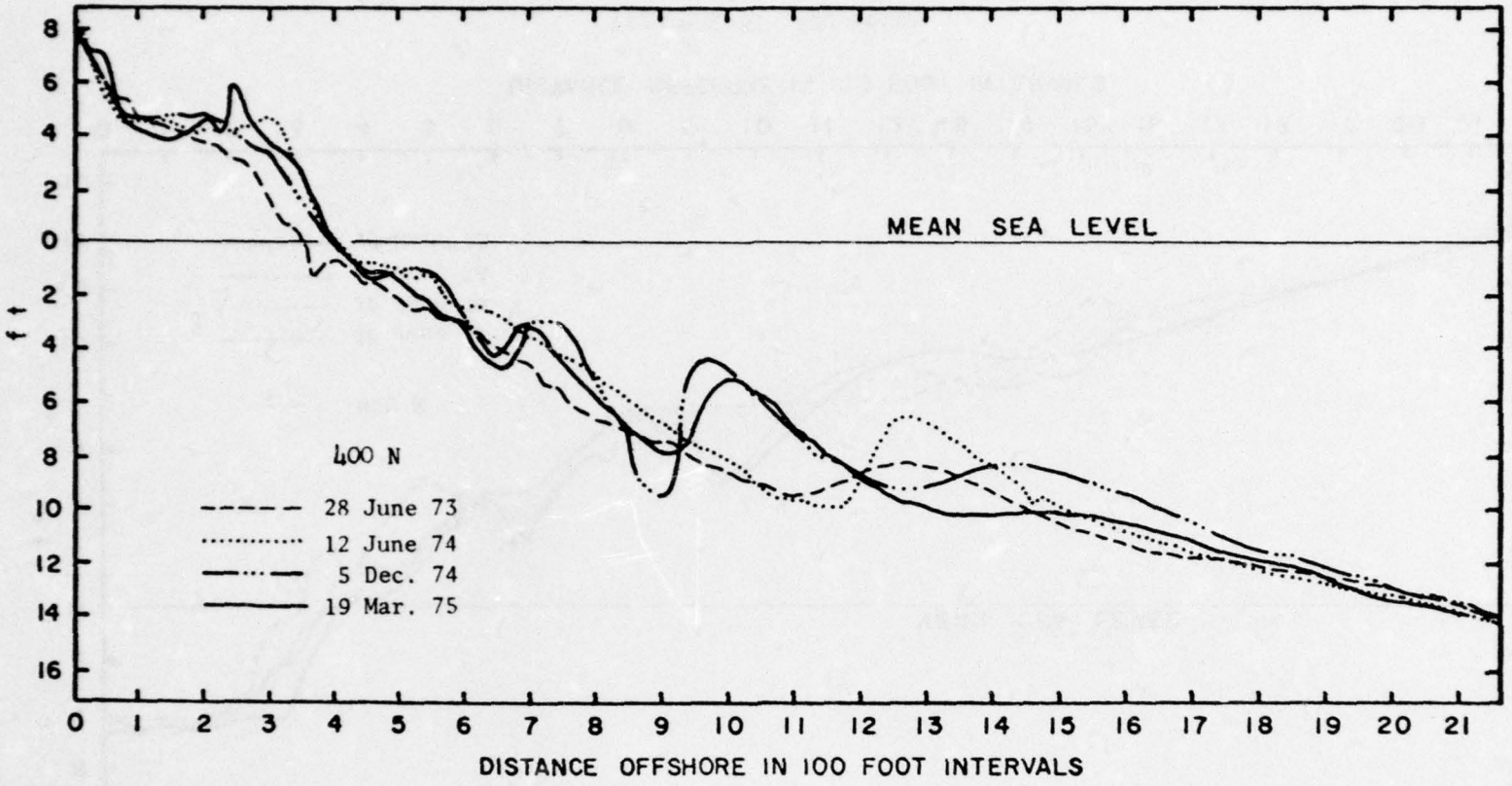

Figure C-2. 400 North.

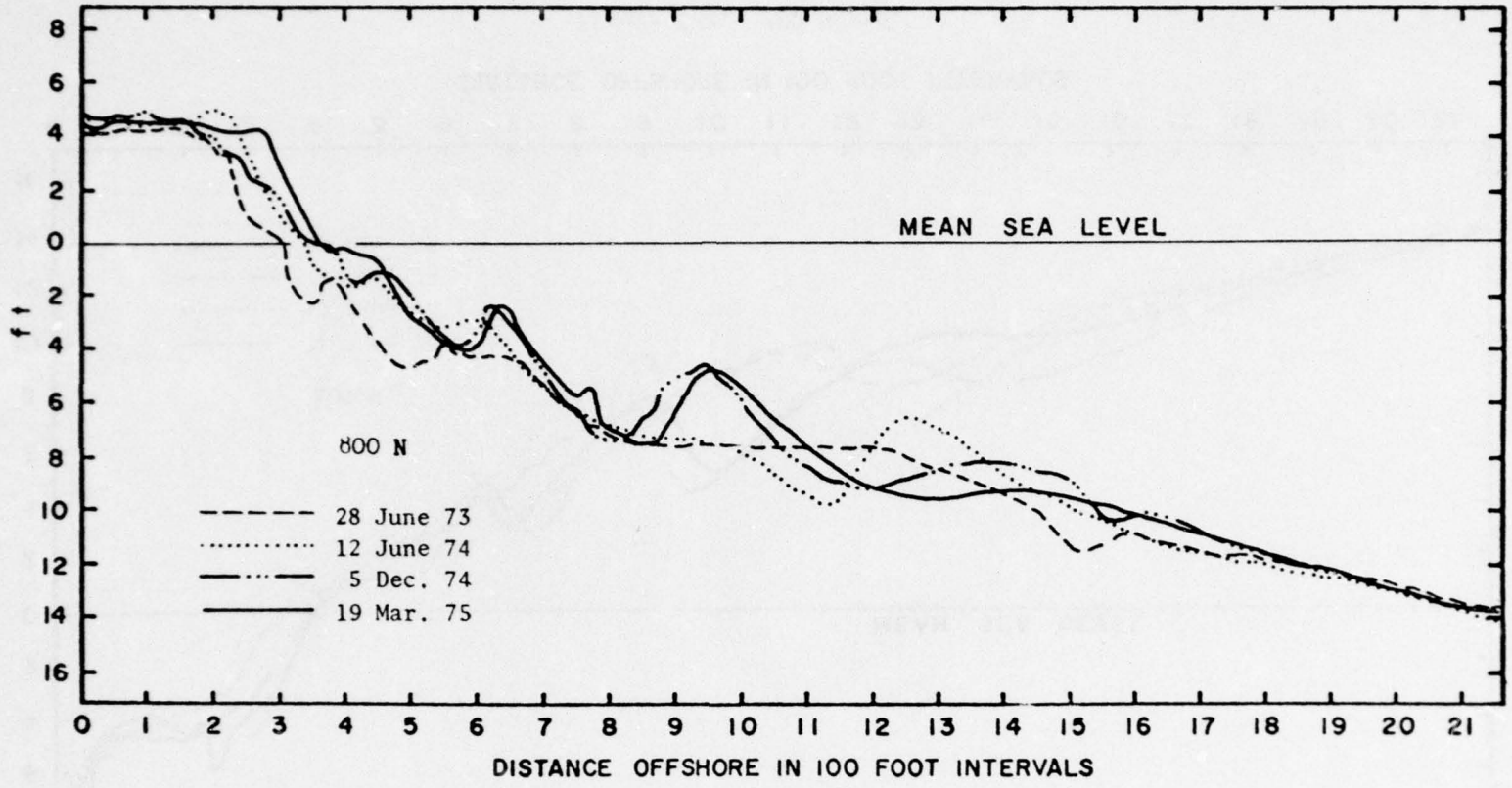

Figure C-3. 800 North.

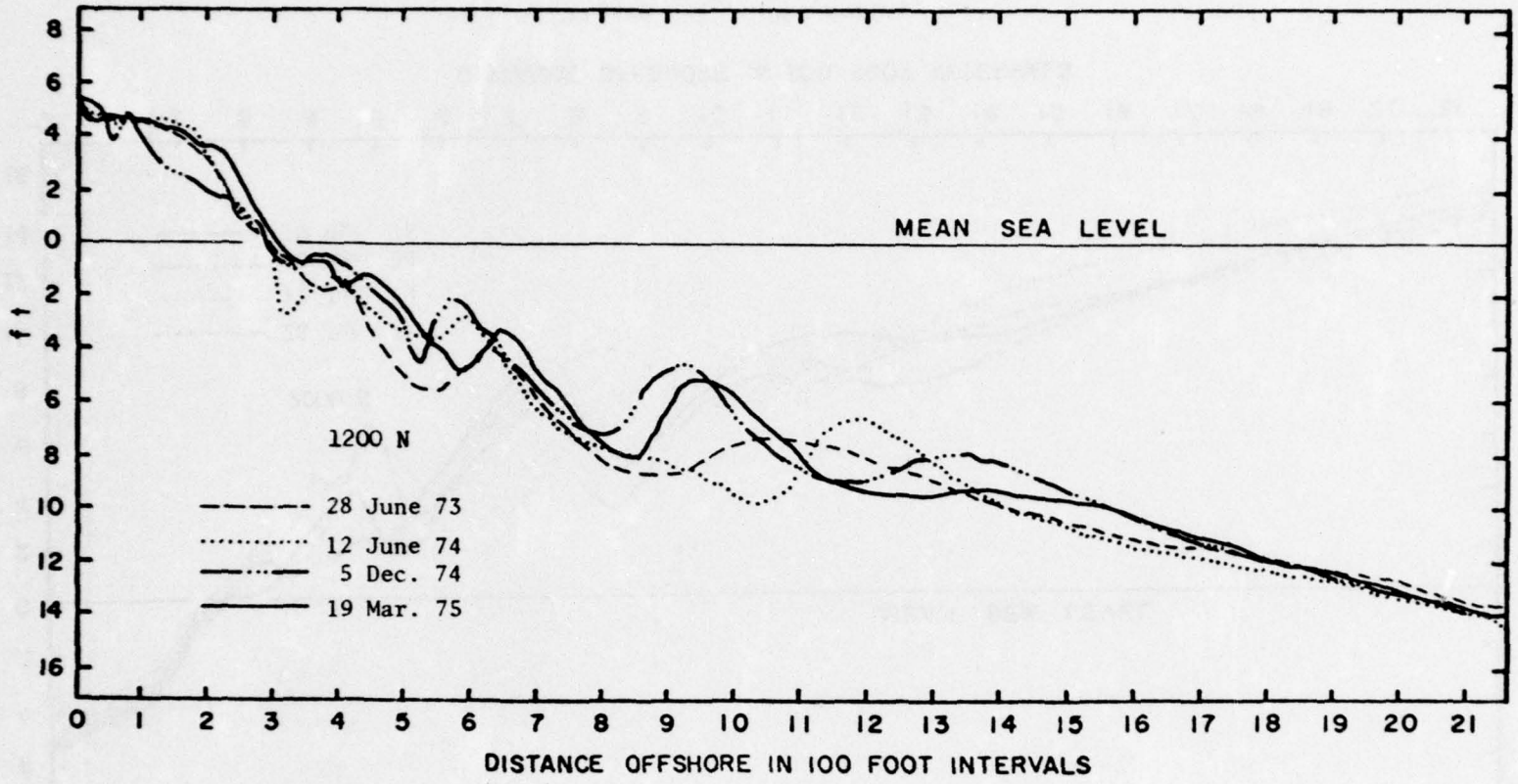

Figure C-4. 1200 North.

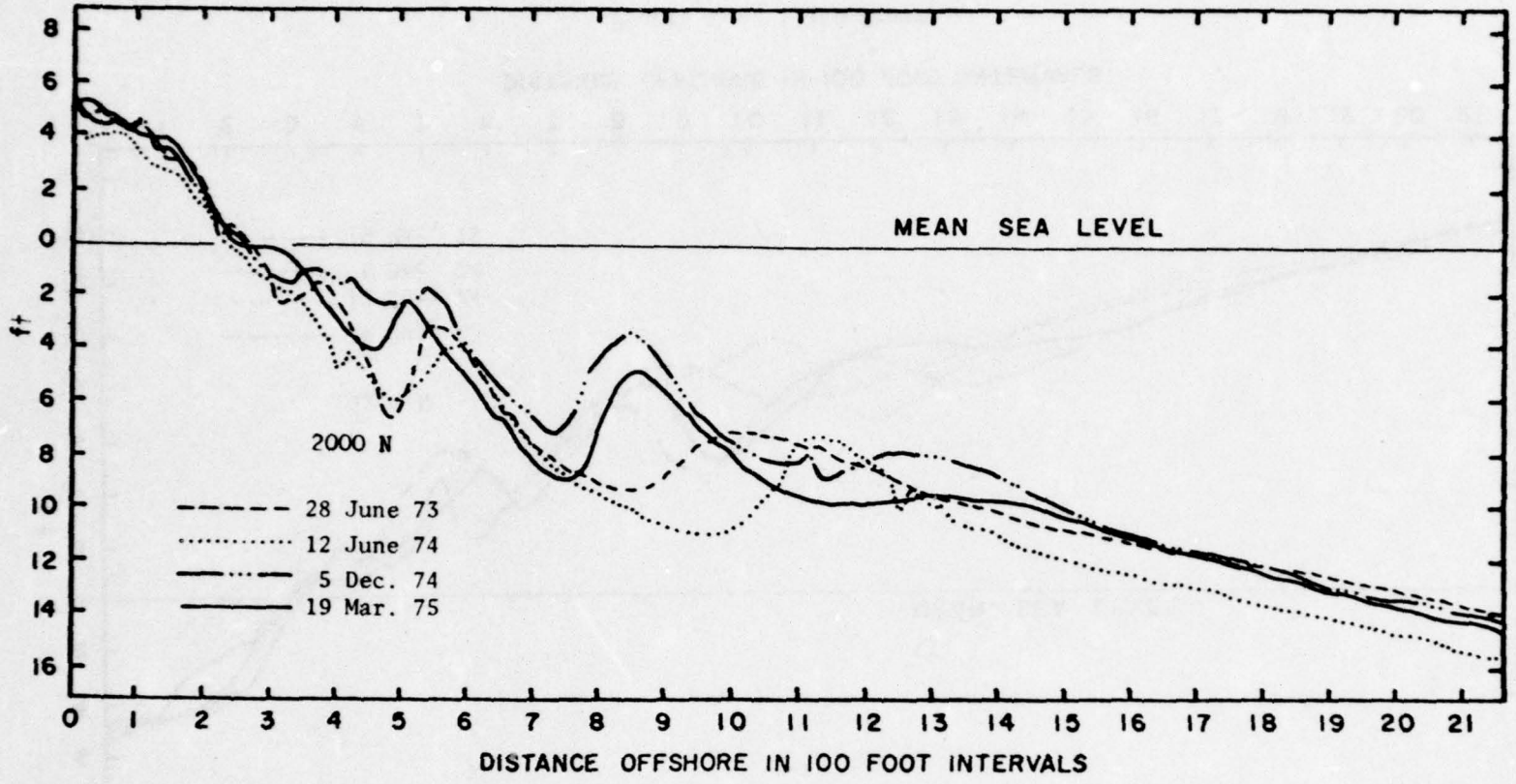

Figure C-5. 2000 North.

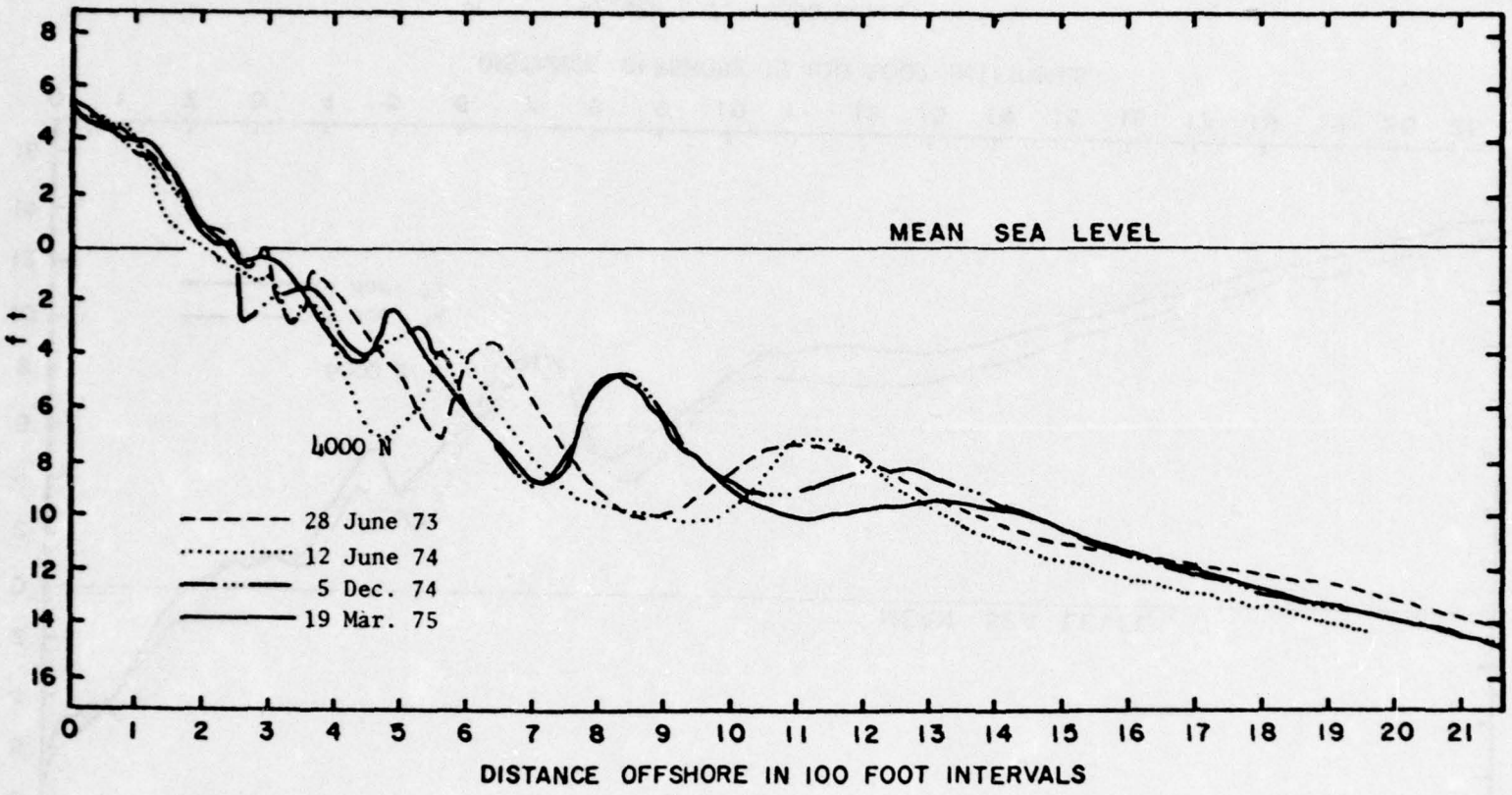

Figure C-6. 4000 North.

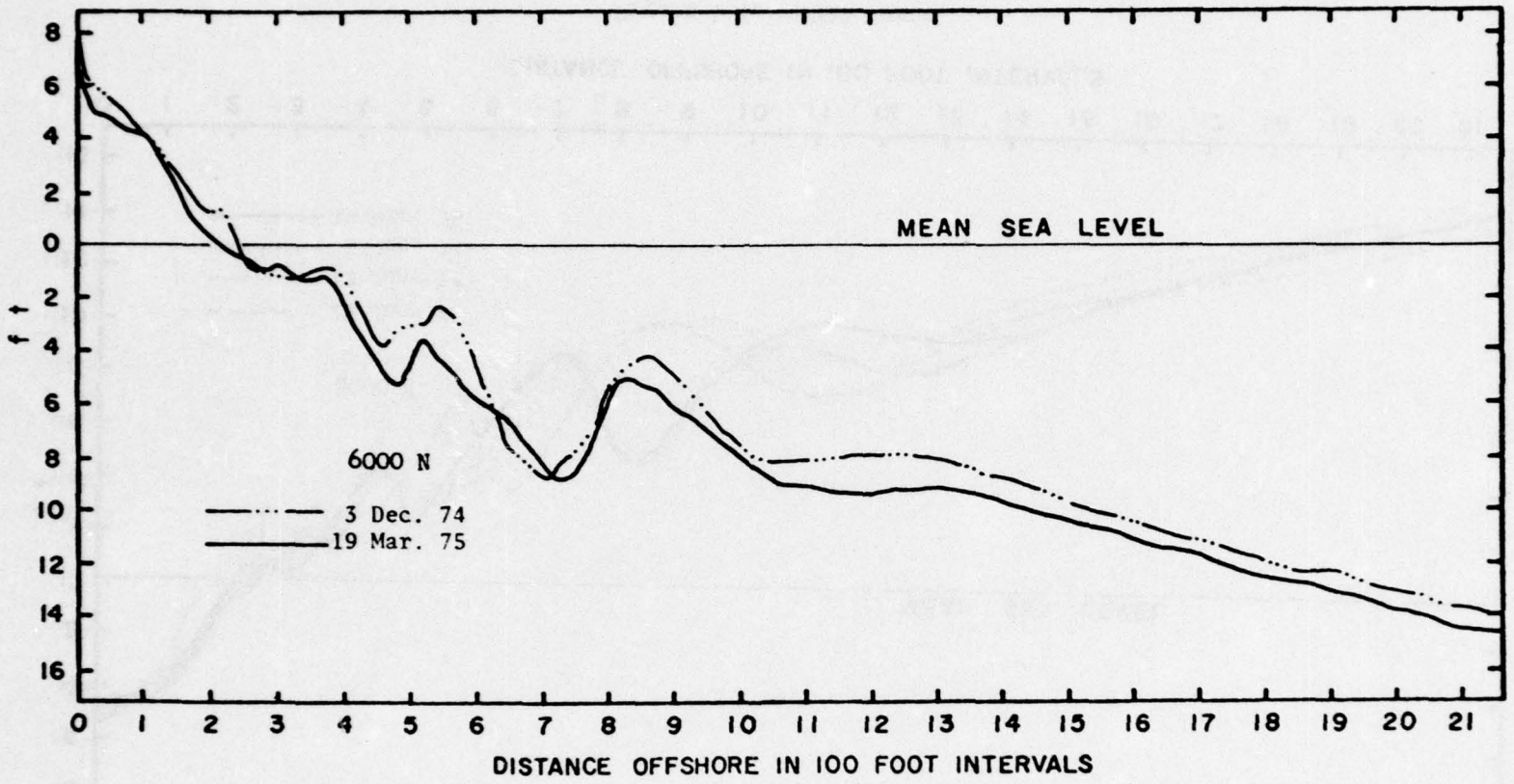

Figure C-7. 6000 North.

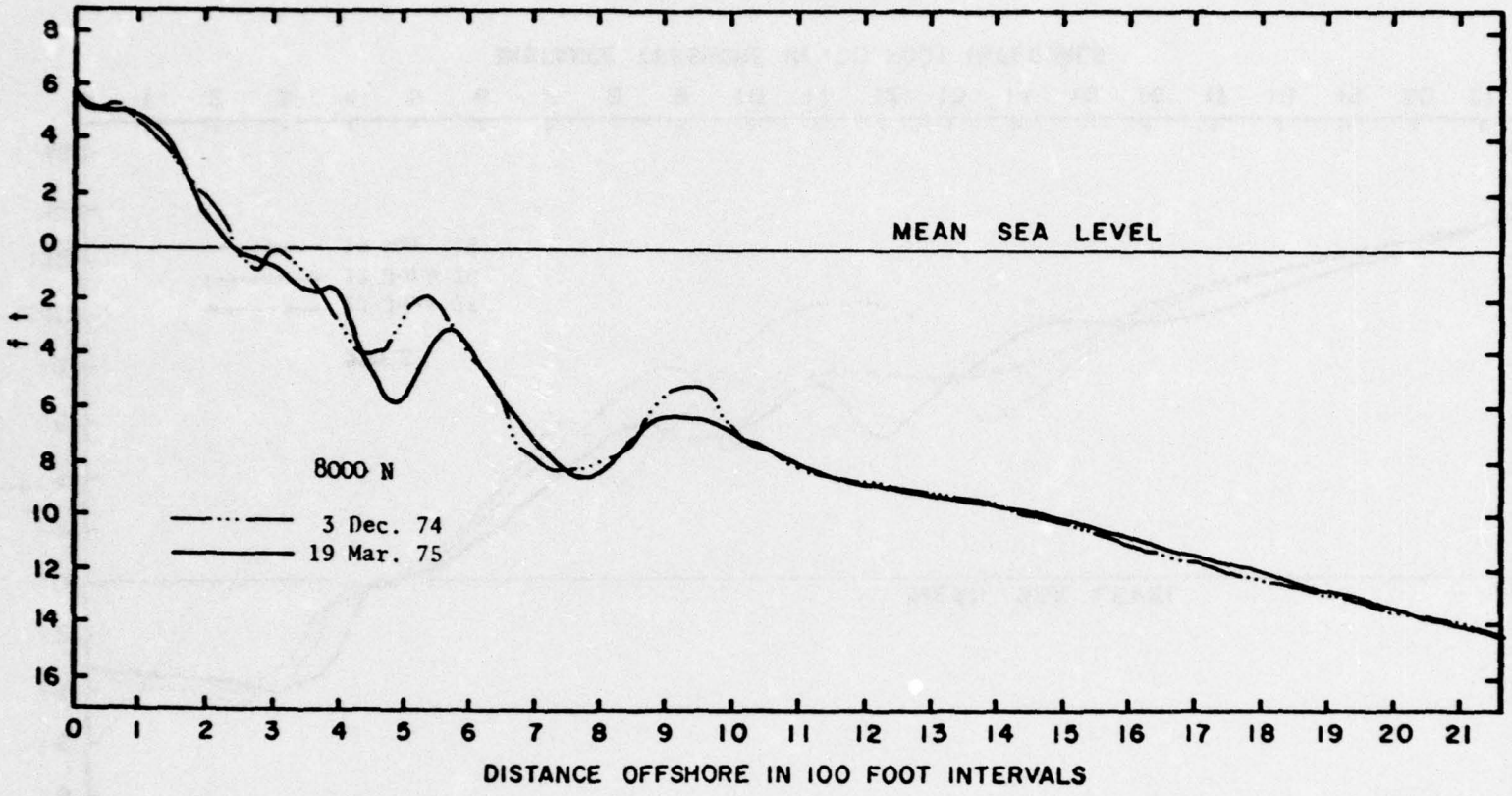

Figure C-8. 8000 North.

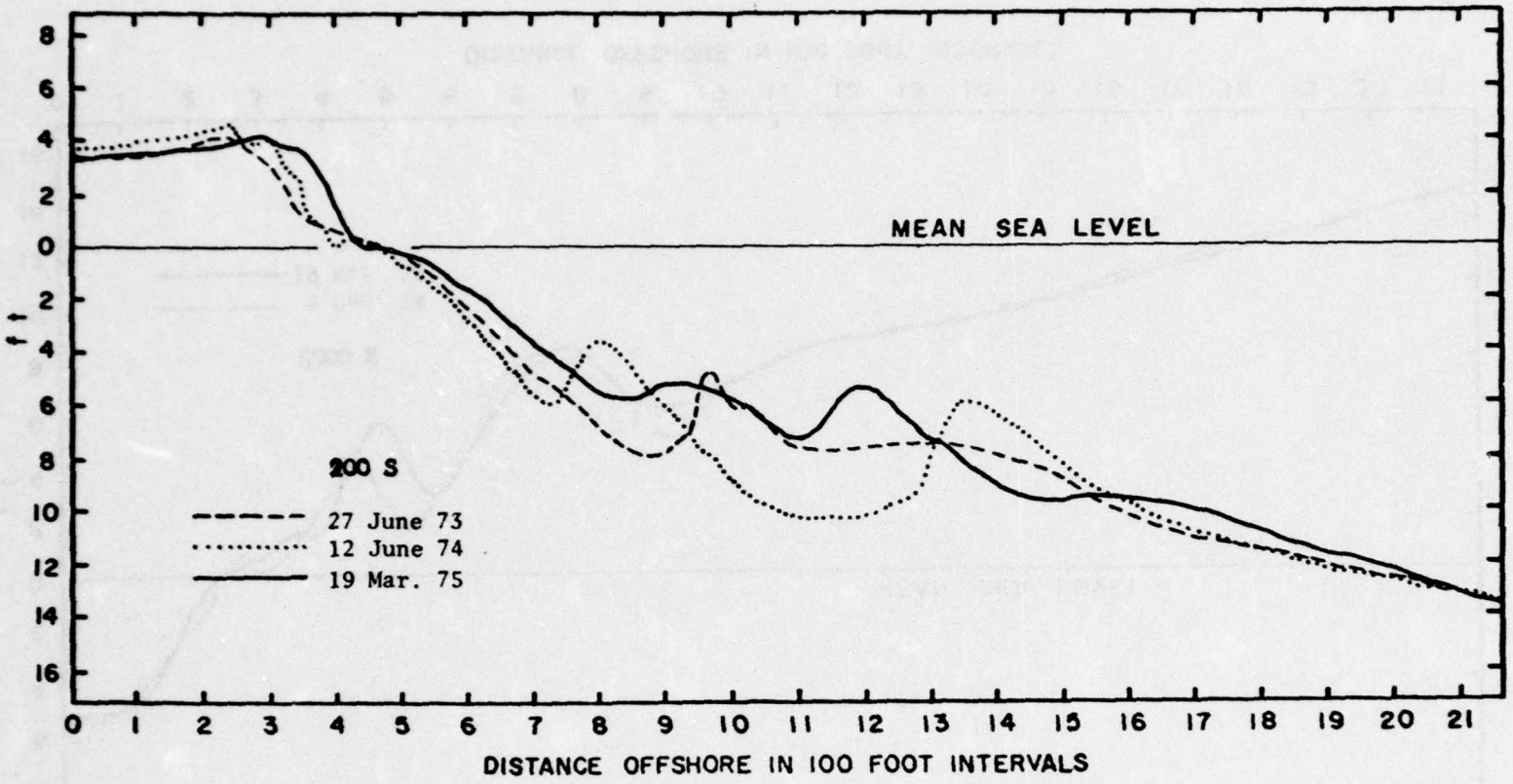

Figure C-9. 200 South.

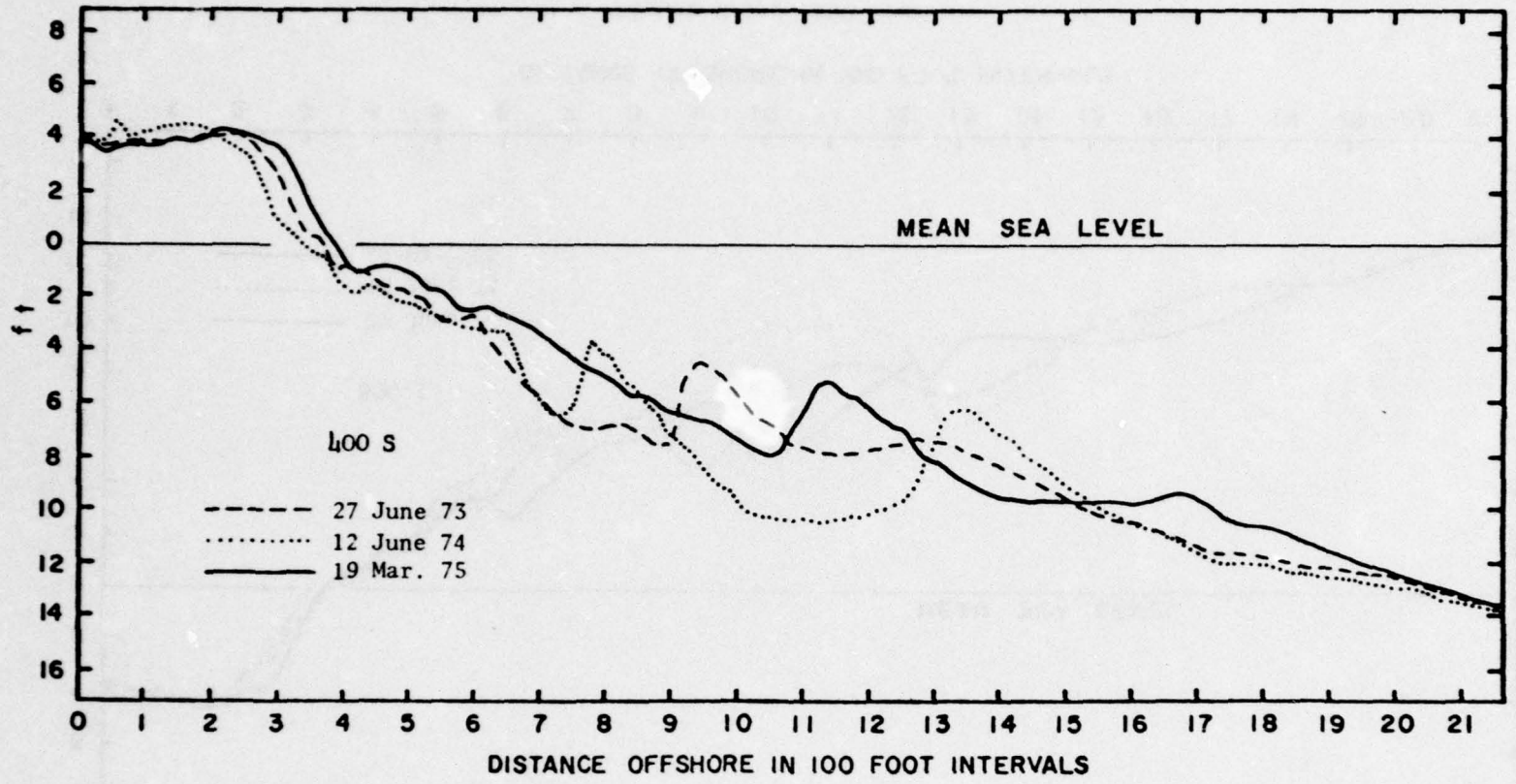

Figure C-10. 400 South.

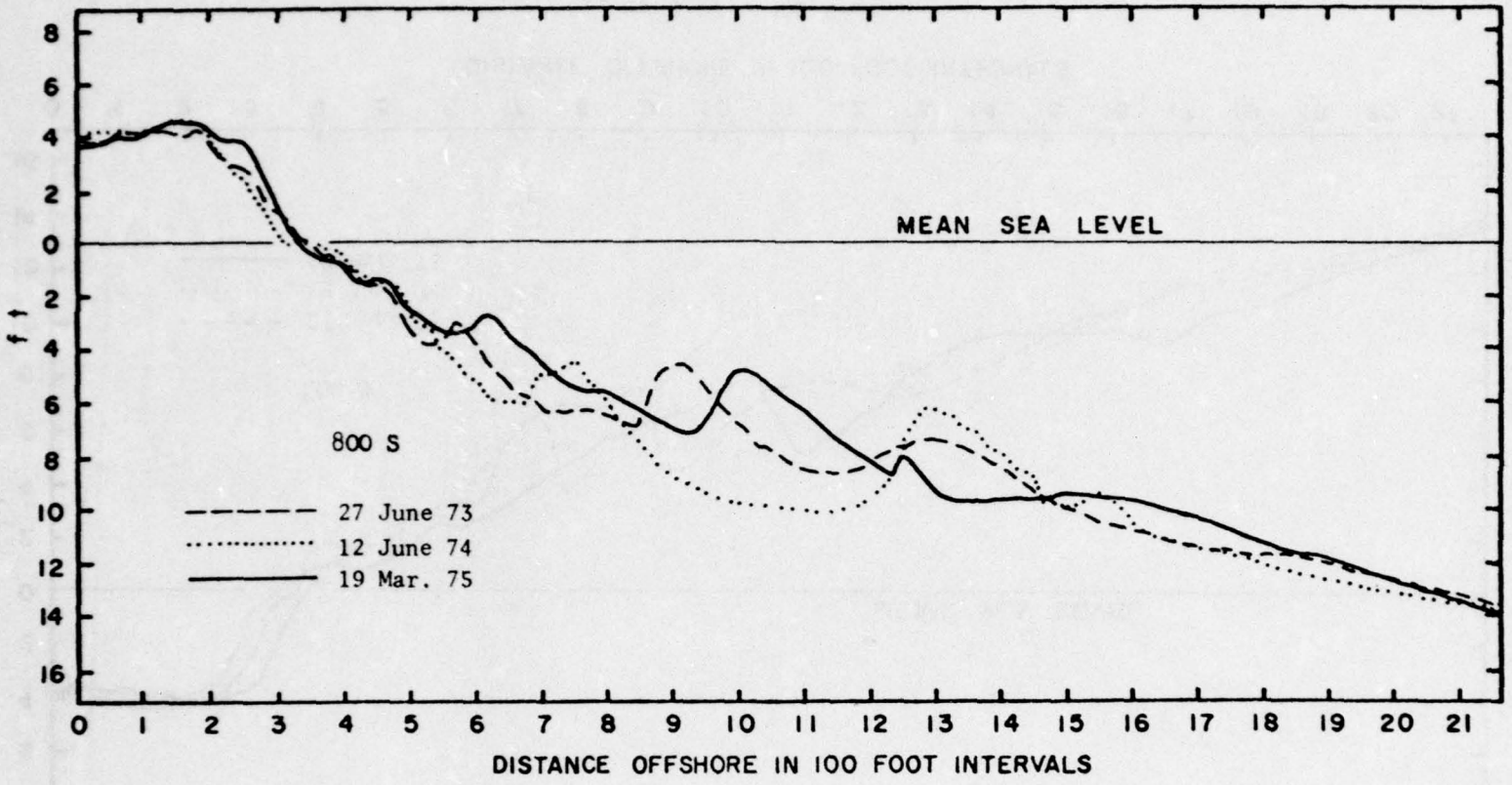

Figure C-11. 800 South.

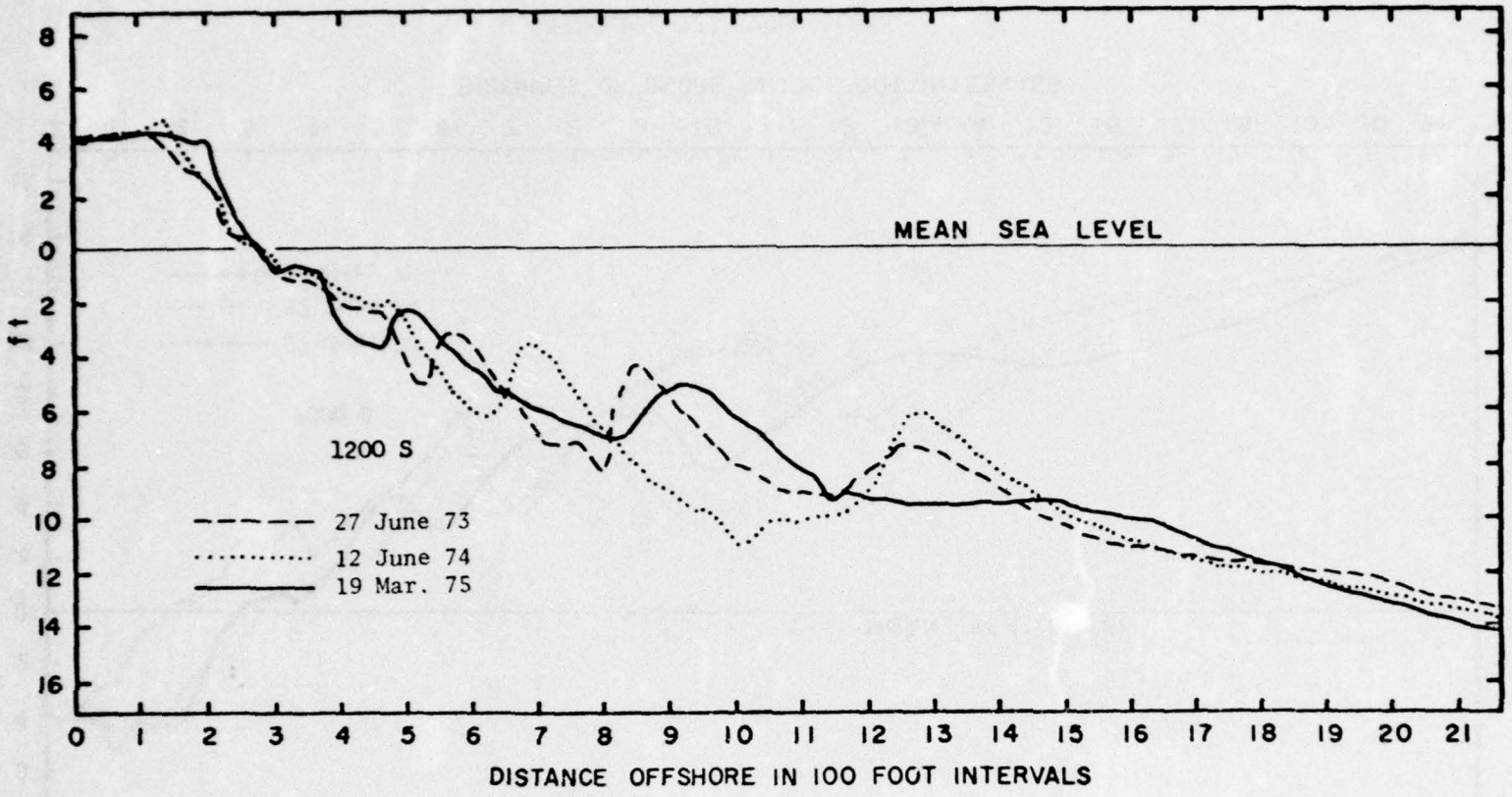

Figure C-12. 1200 South.

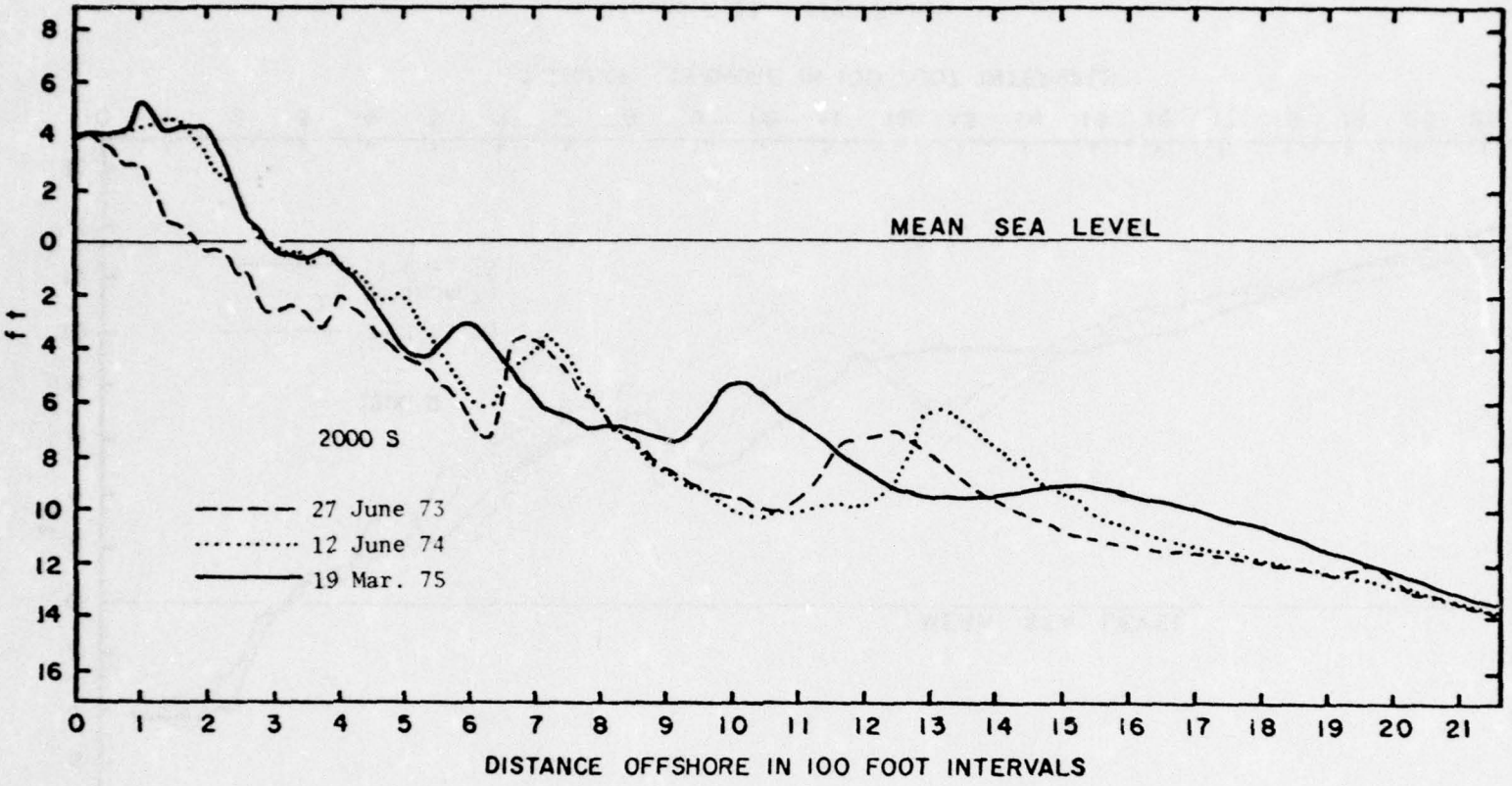

Figure C-13. 2000 South.

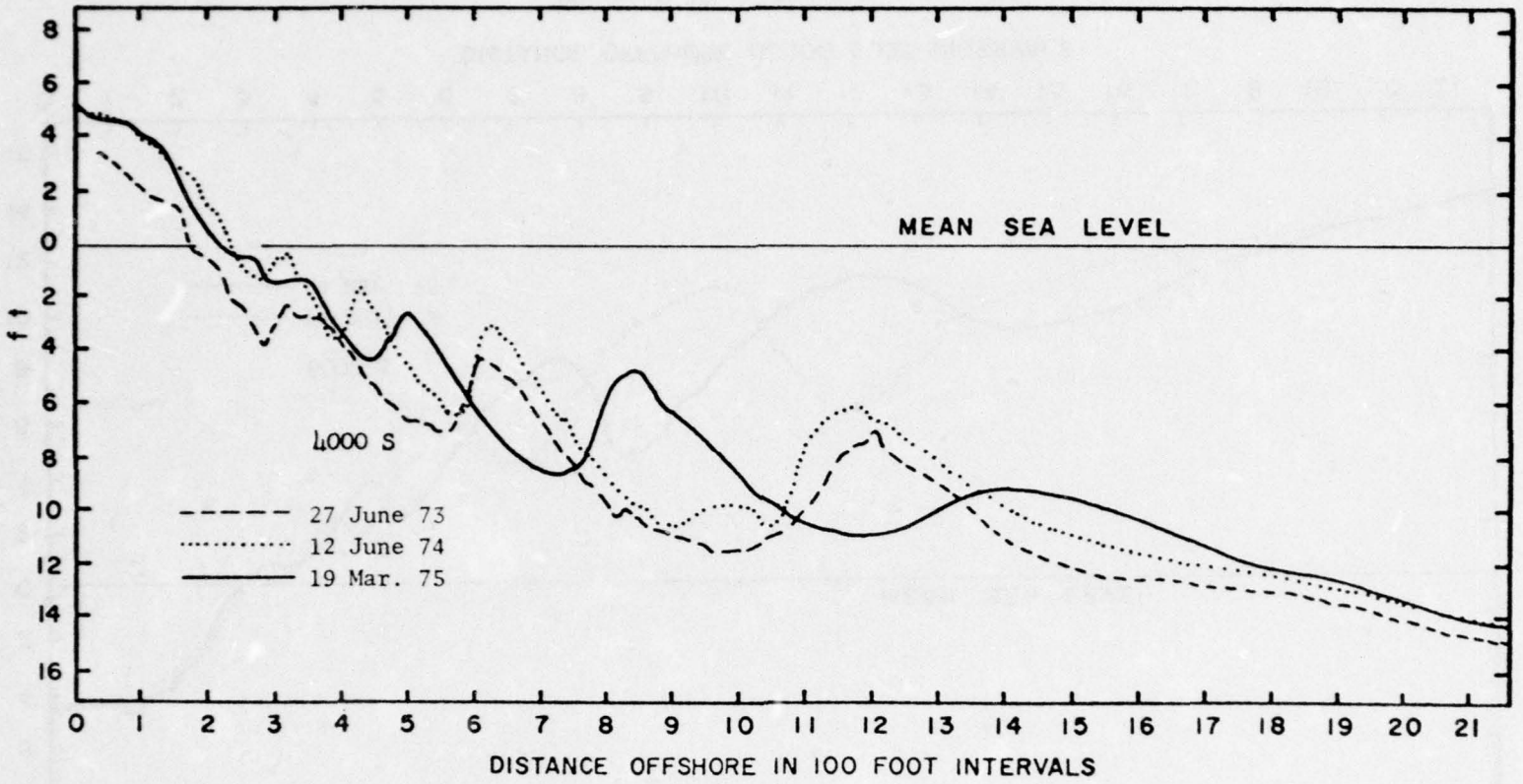

Figure C-14. 4000 South.

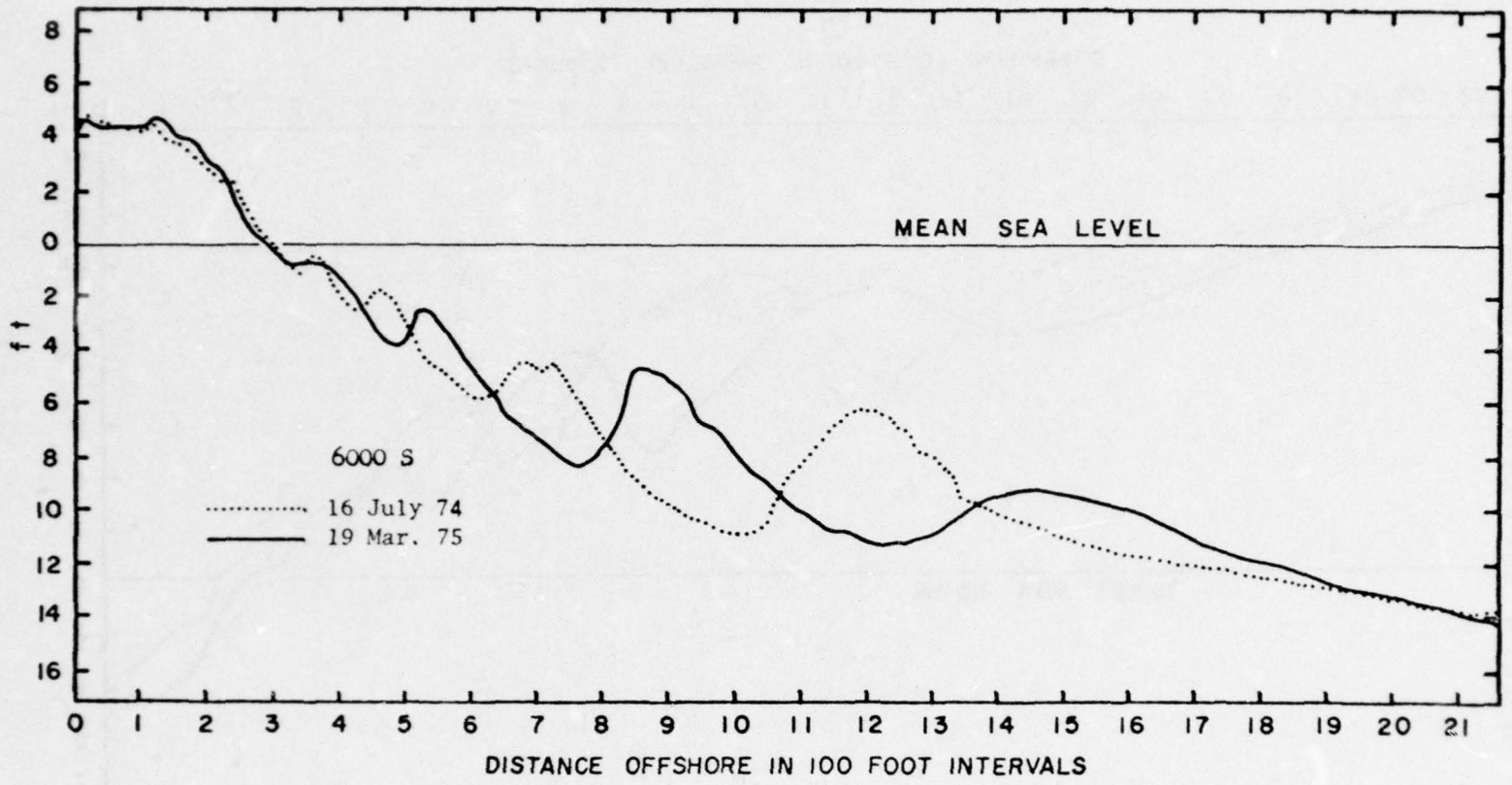

Figure C-15. 6000 South.

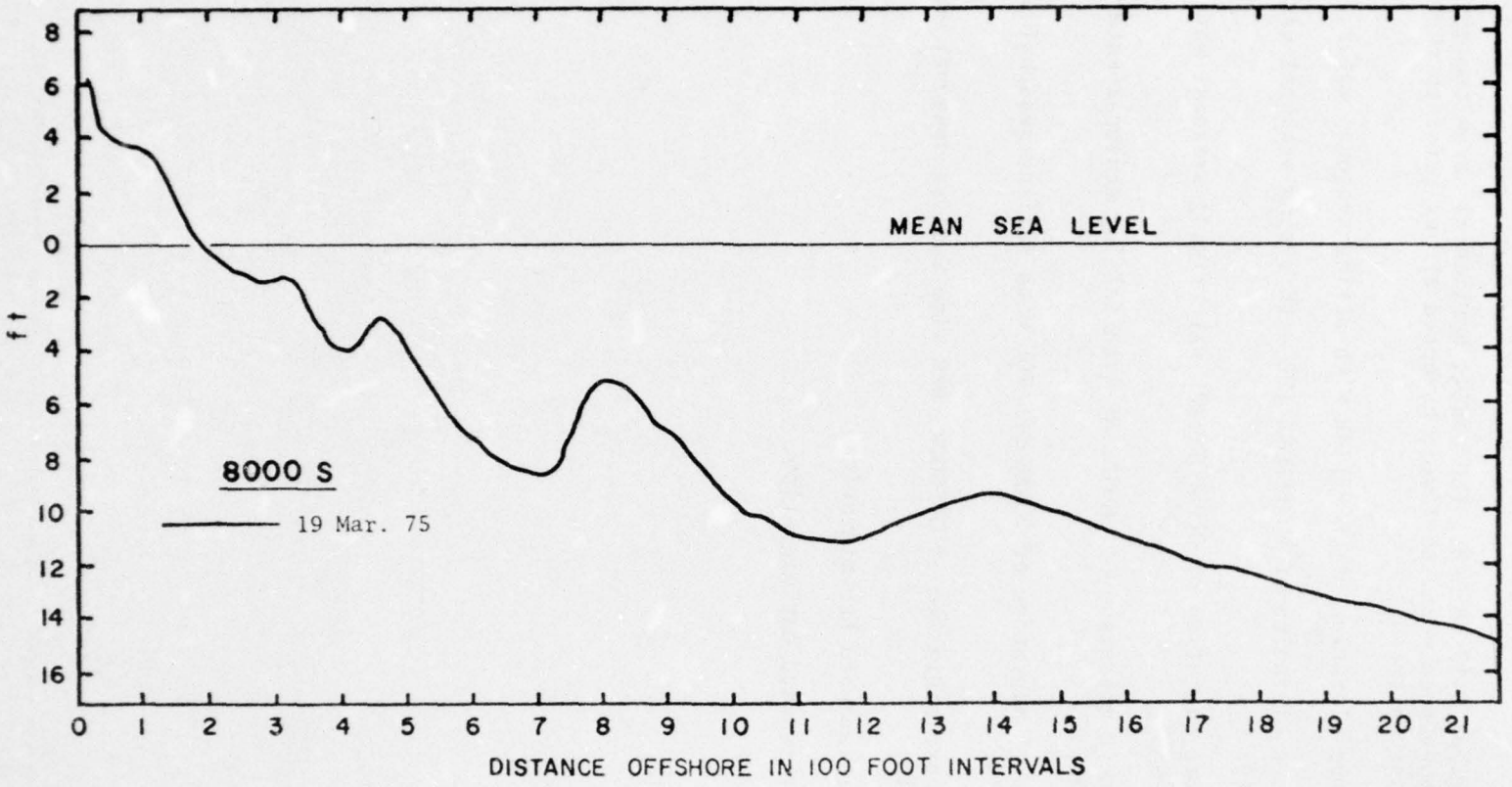

Figure C-16. 8000 South.

In Figures C-17 to C-32, the small, horizontal arrow touching each profile represents mean sea level; numbered arrows refer to the following observed trends:

(1) Onshore migration of SHORELINE with rising seasonal water levels;

(2) onshore migration of FORESHORE TOE with rising seasonal water levels;

(3) onshore migration of OFFSHORE BAR with rising seasonal water levels;

(4) offshore migration of SHORELINE with falling seasonal water levels;

(5) offshore migration of FORESHORE TOE with falling seasonal water levels;

(6) offshore migration of OFFSHORE BAR with falling seasonal water levels;

(7) other landward bar migration;

(8) other seaward bar migration.

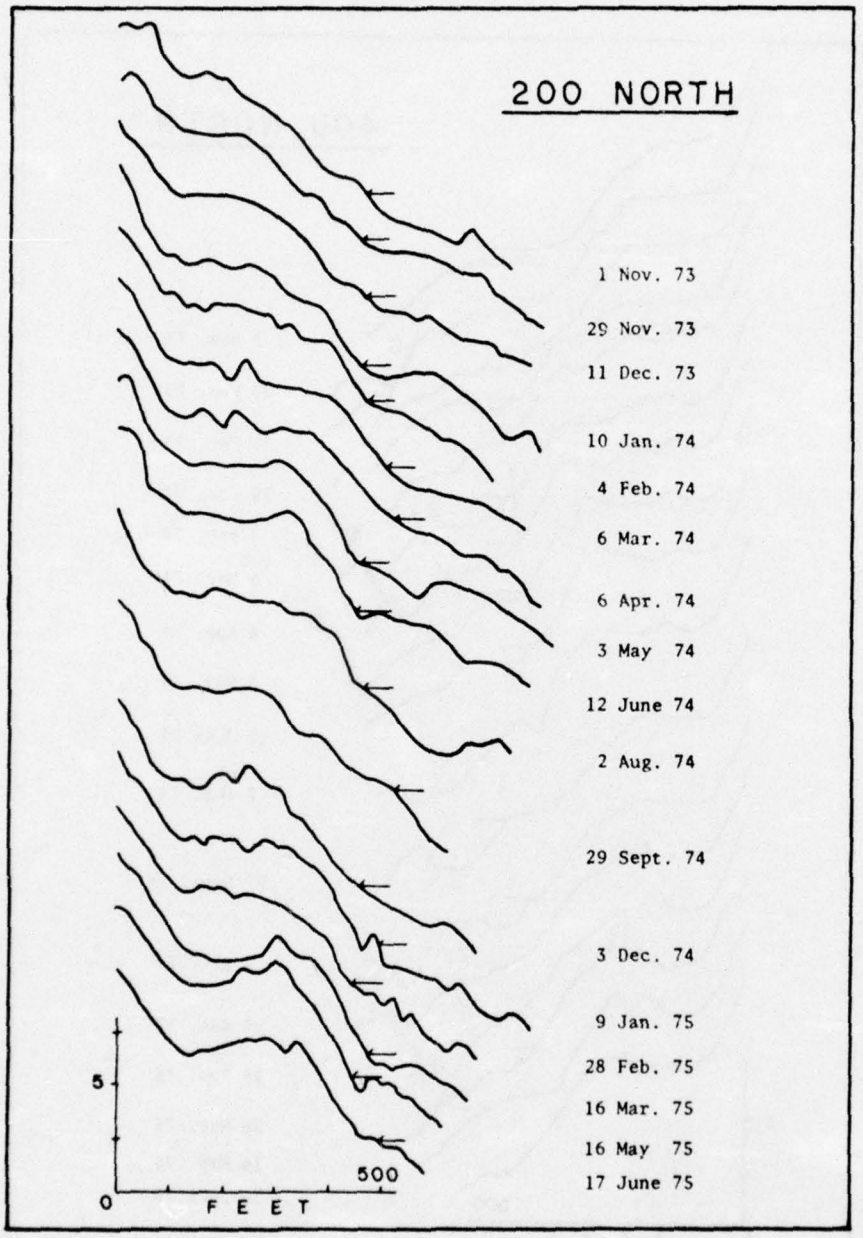

Figure C-17. 200 North.

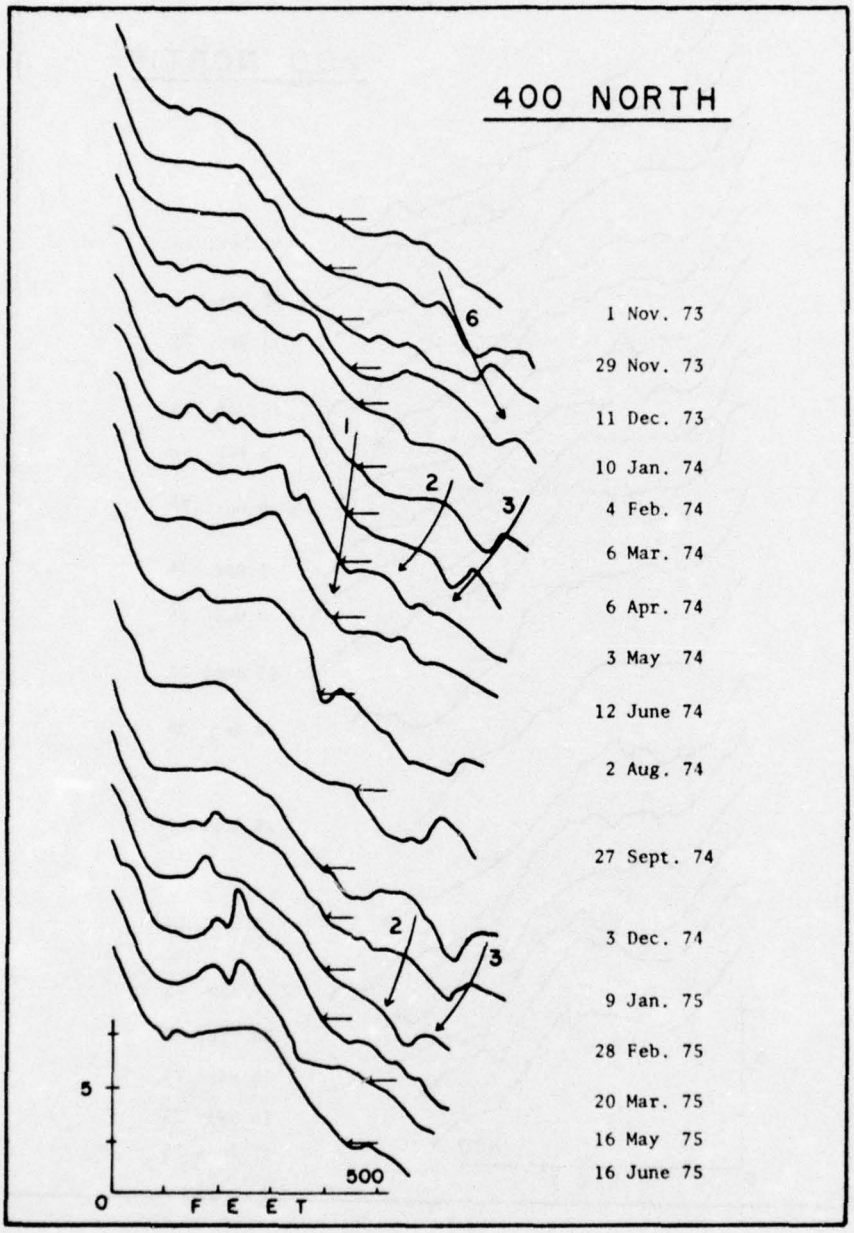

Figure C-18. 400 North.

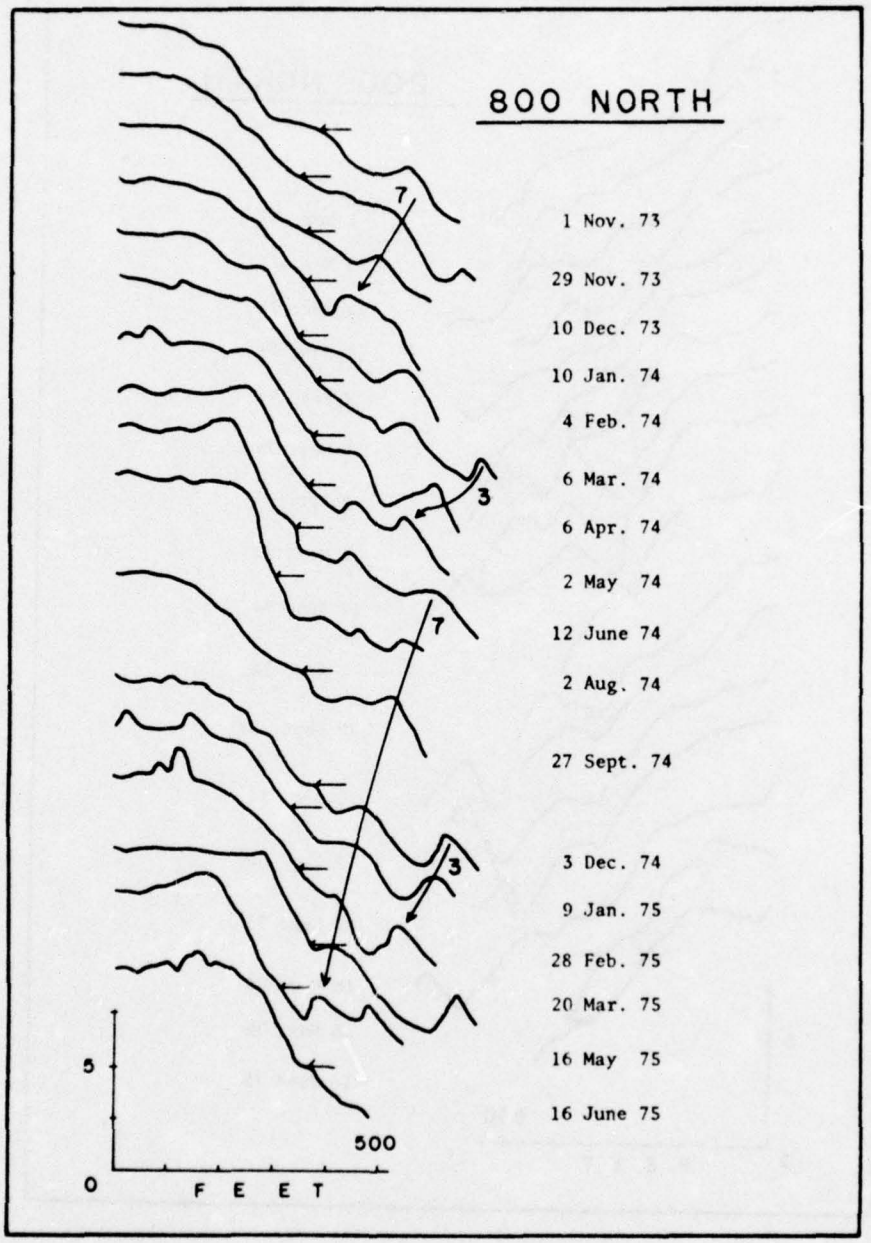

Figure C-19. 800 North.

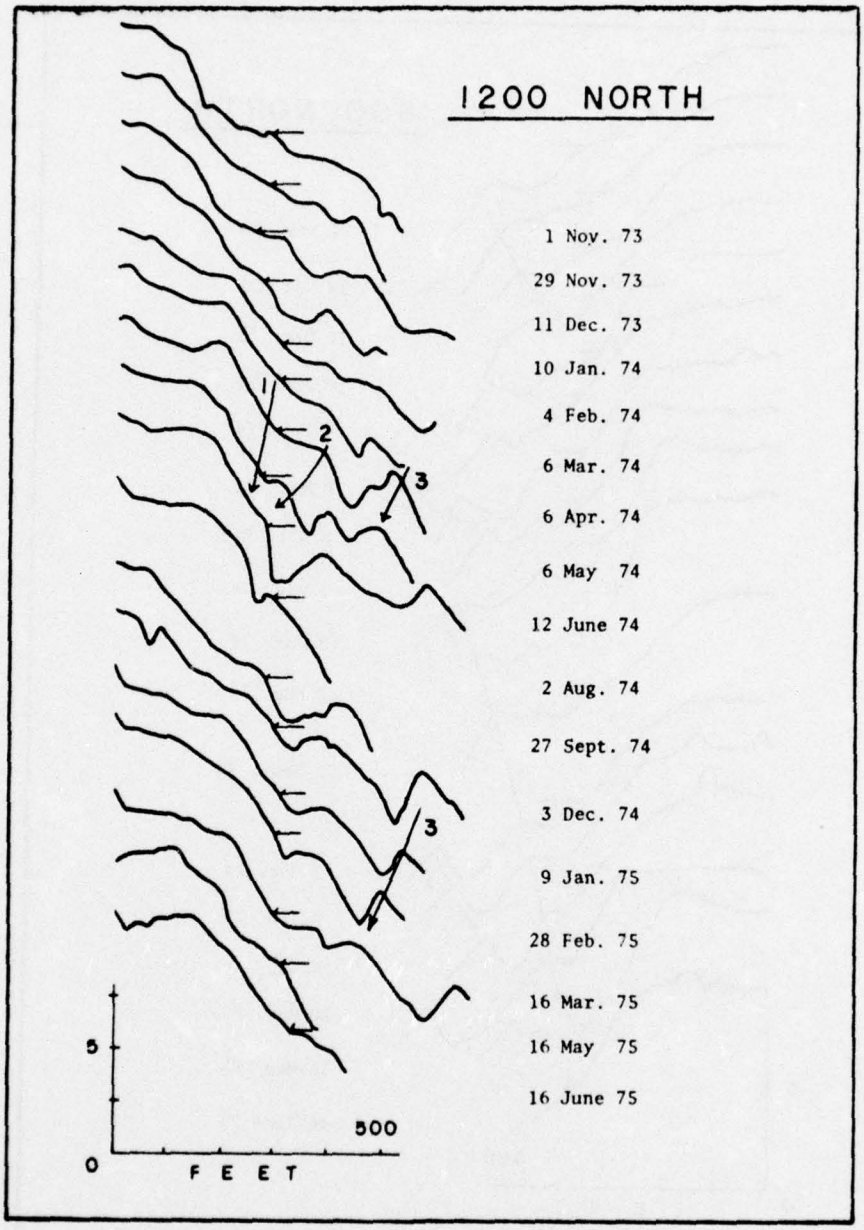

Figure C-20. 1200 North.

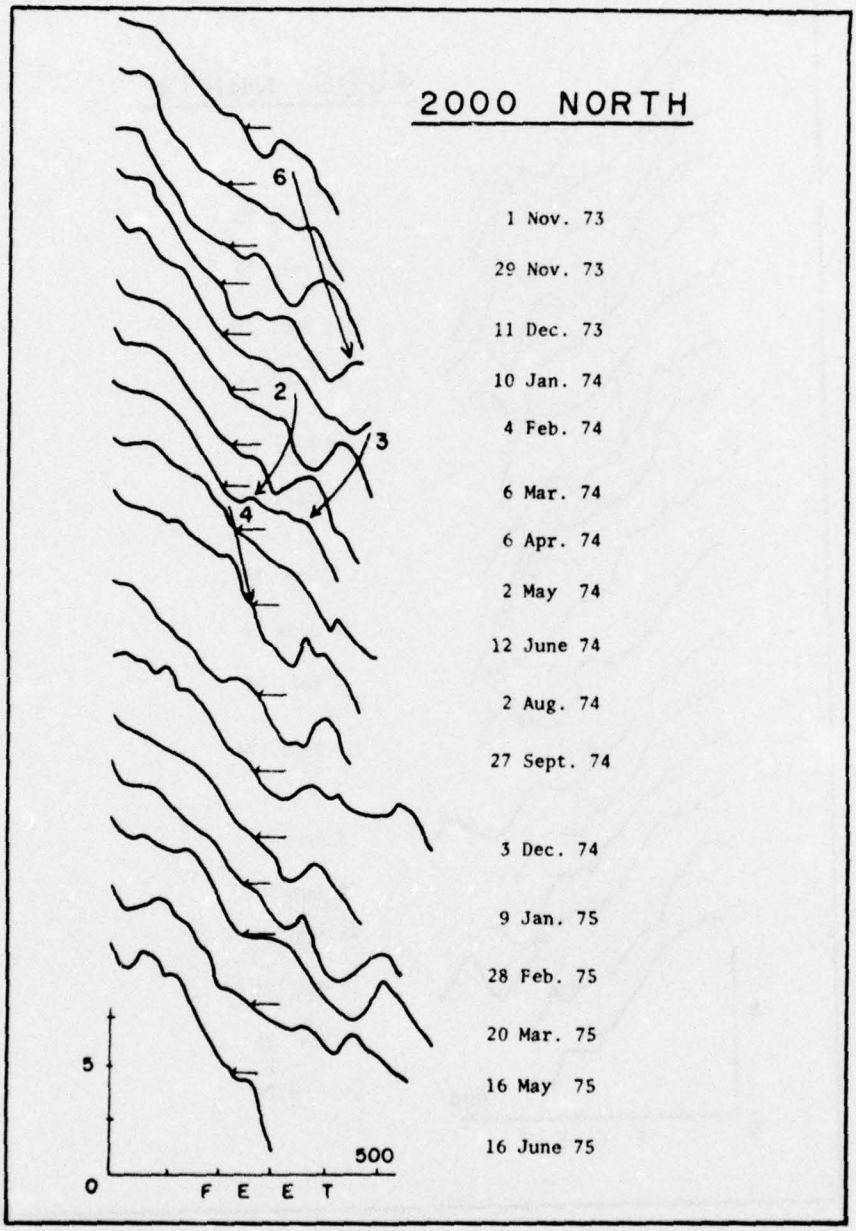

Figure C-21. 2000 North.

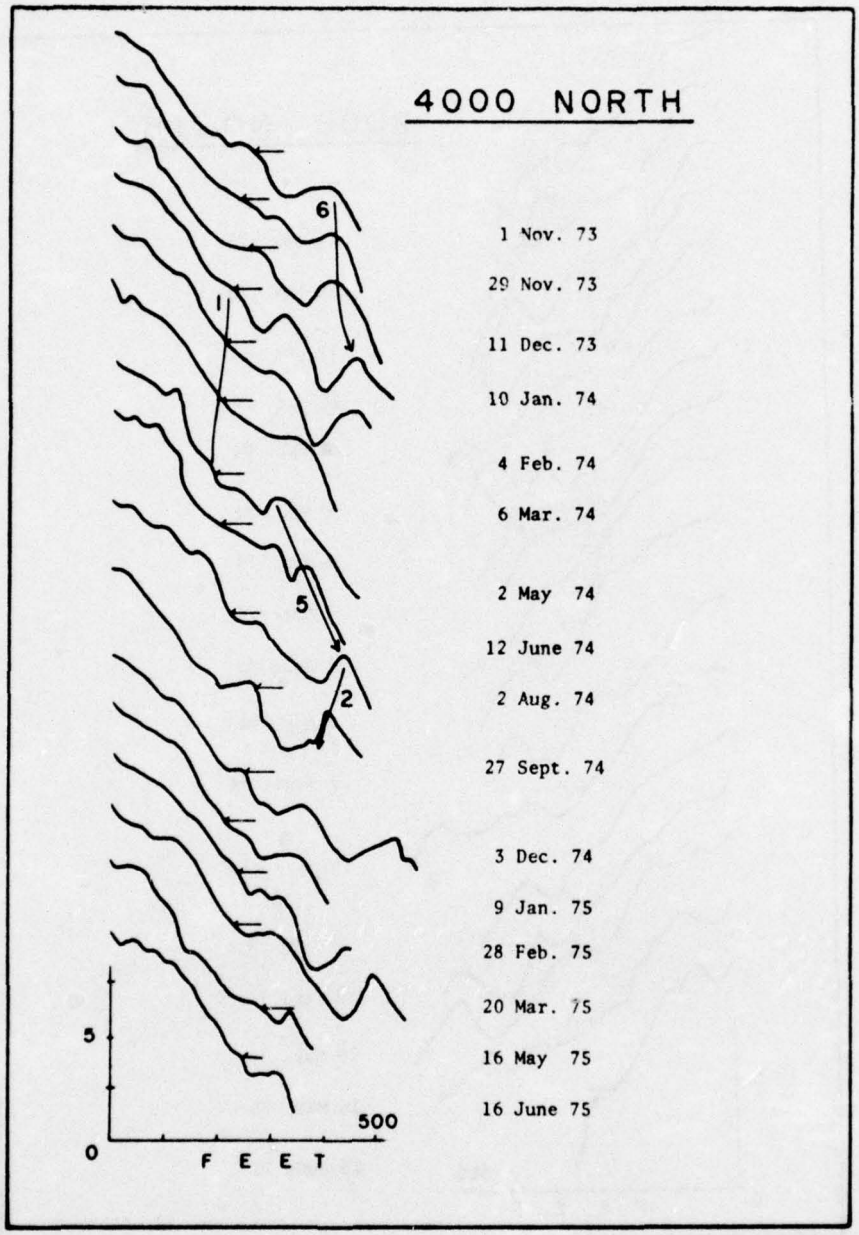

Figure C-22. 4000 North.

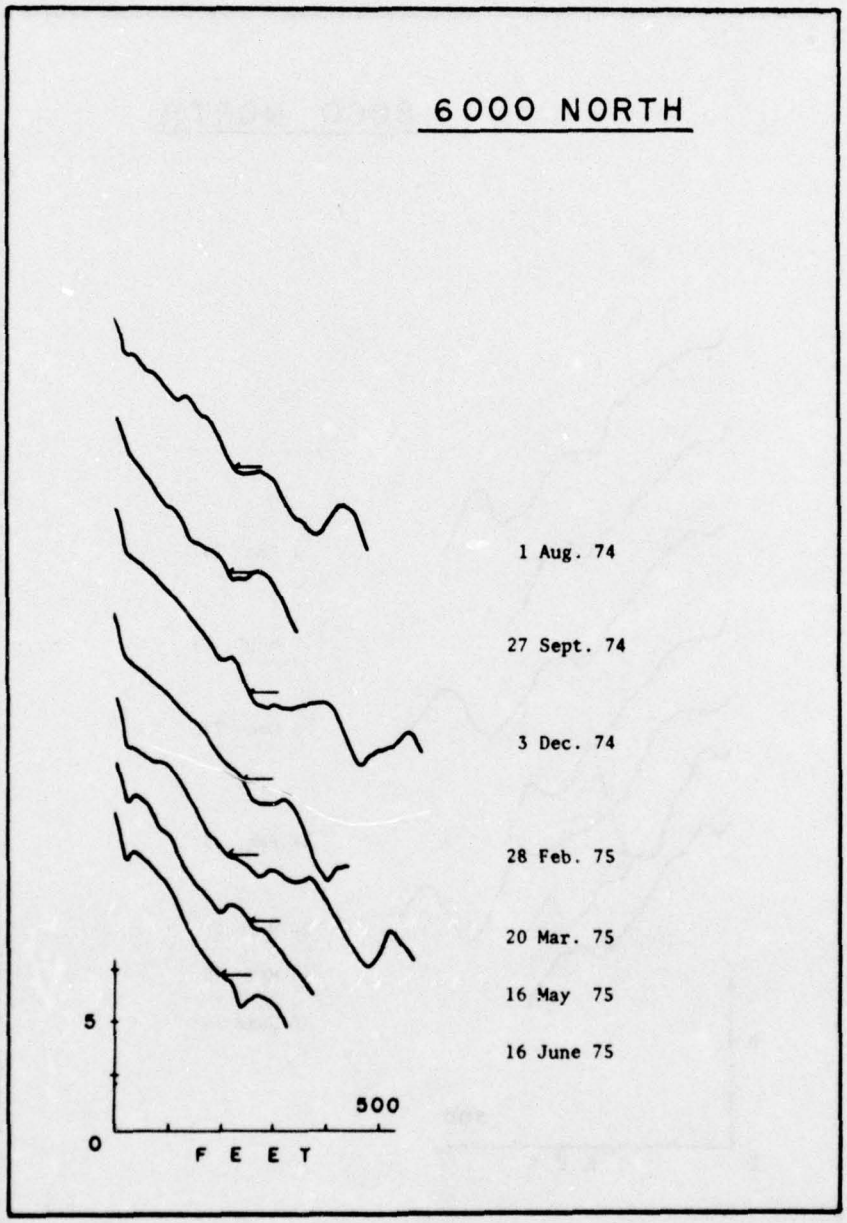

Figure C-23. 6000 North.

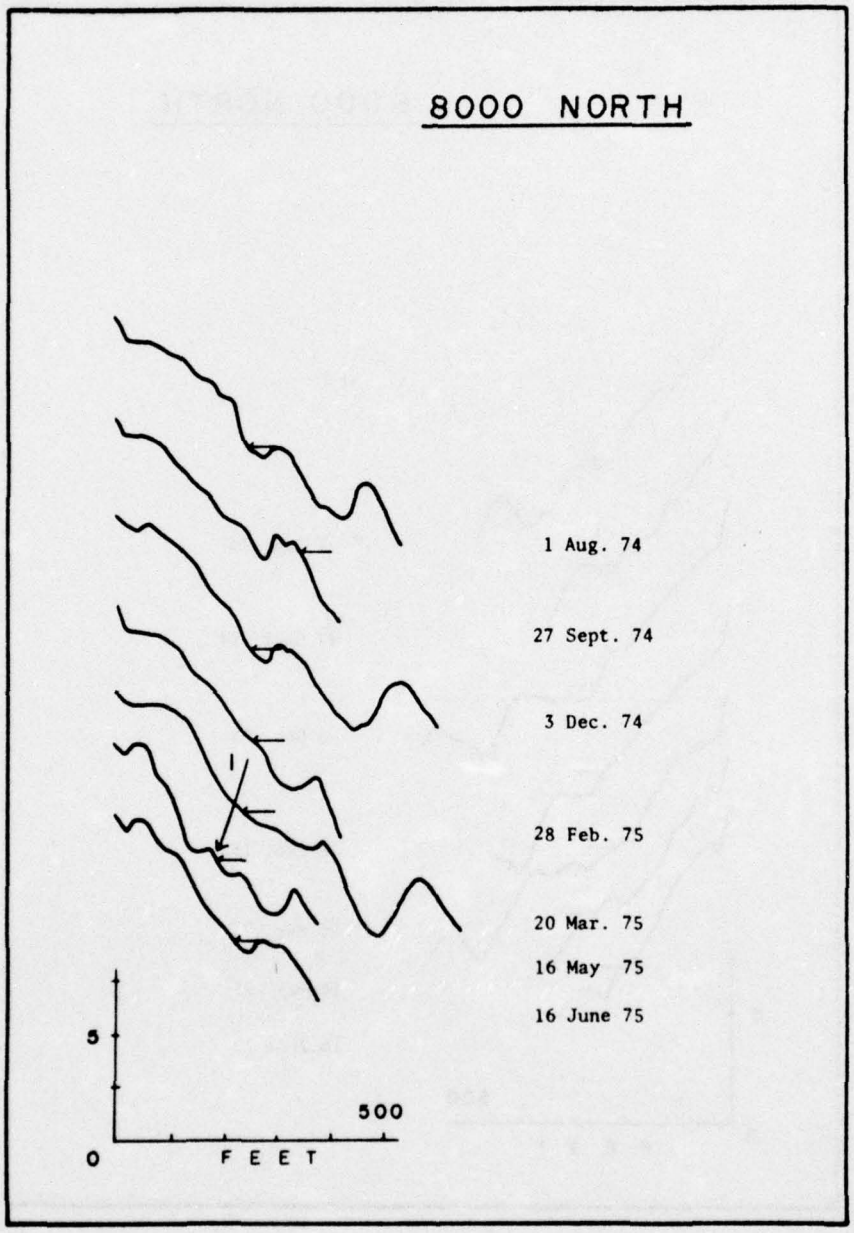

Figure C-24. 8000 North.

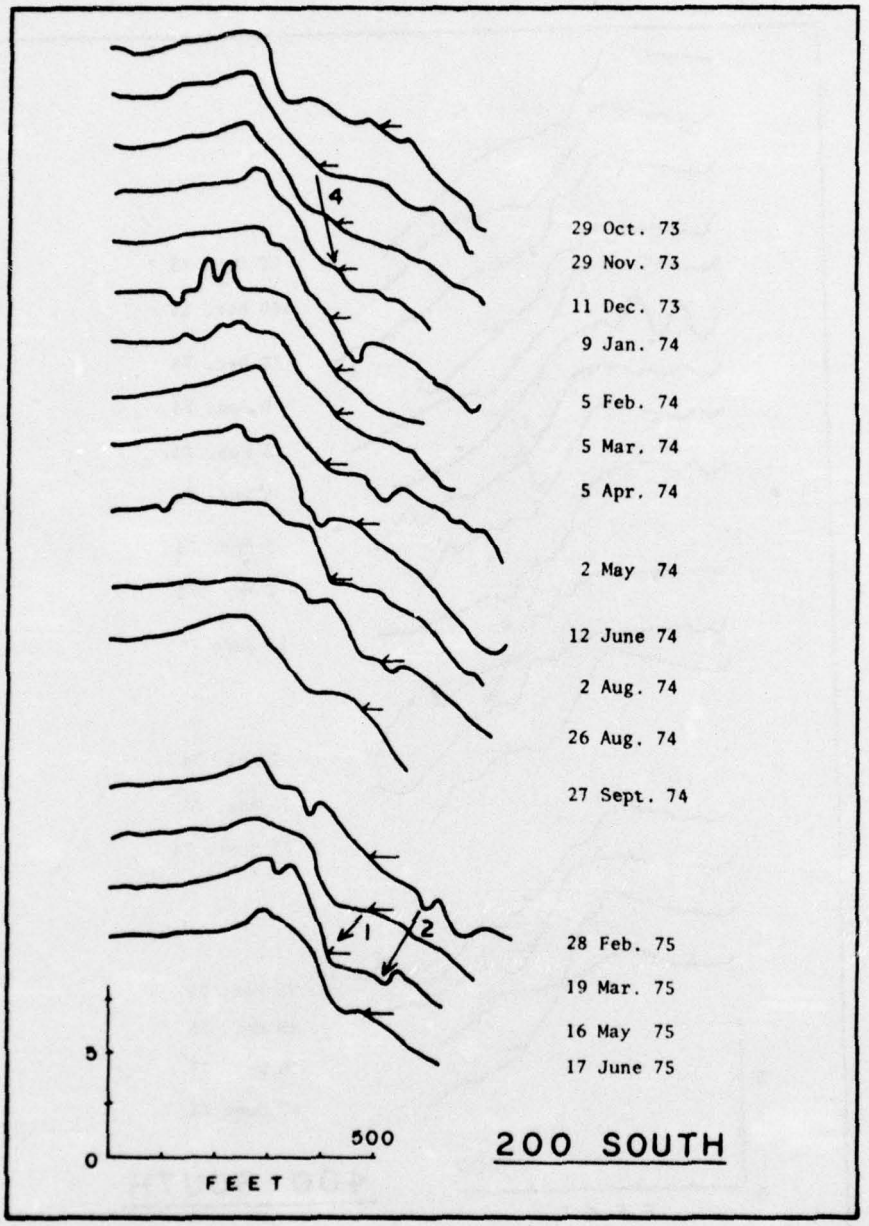

Figure C-25. 200 South.

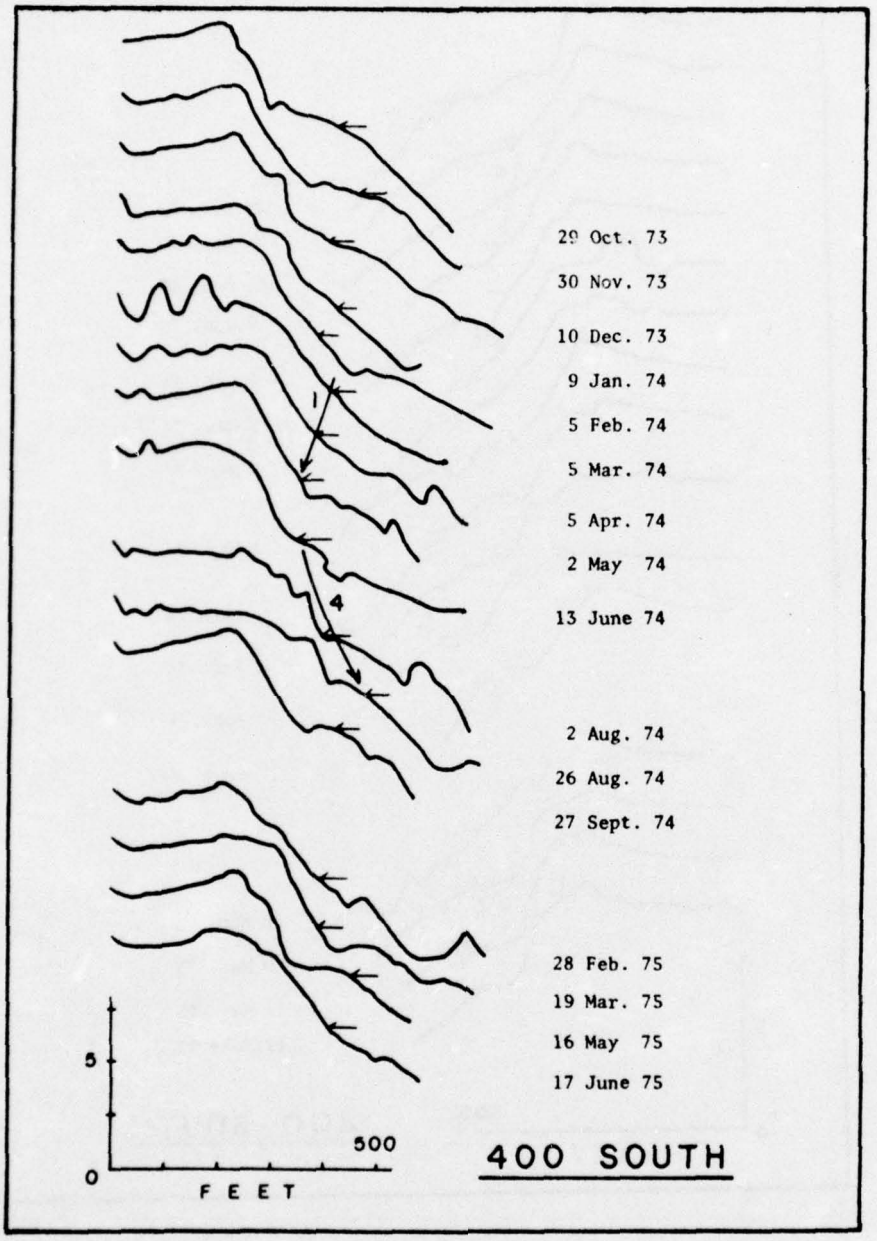

Figure C-26. 400 South.

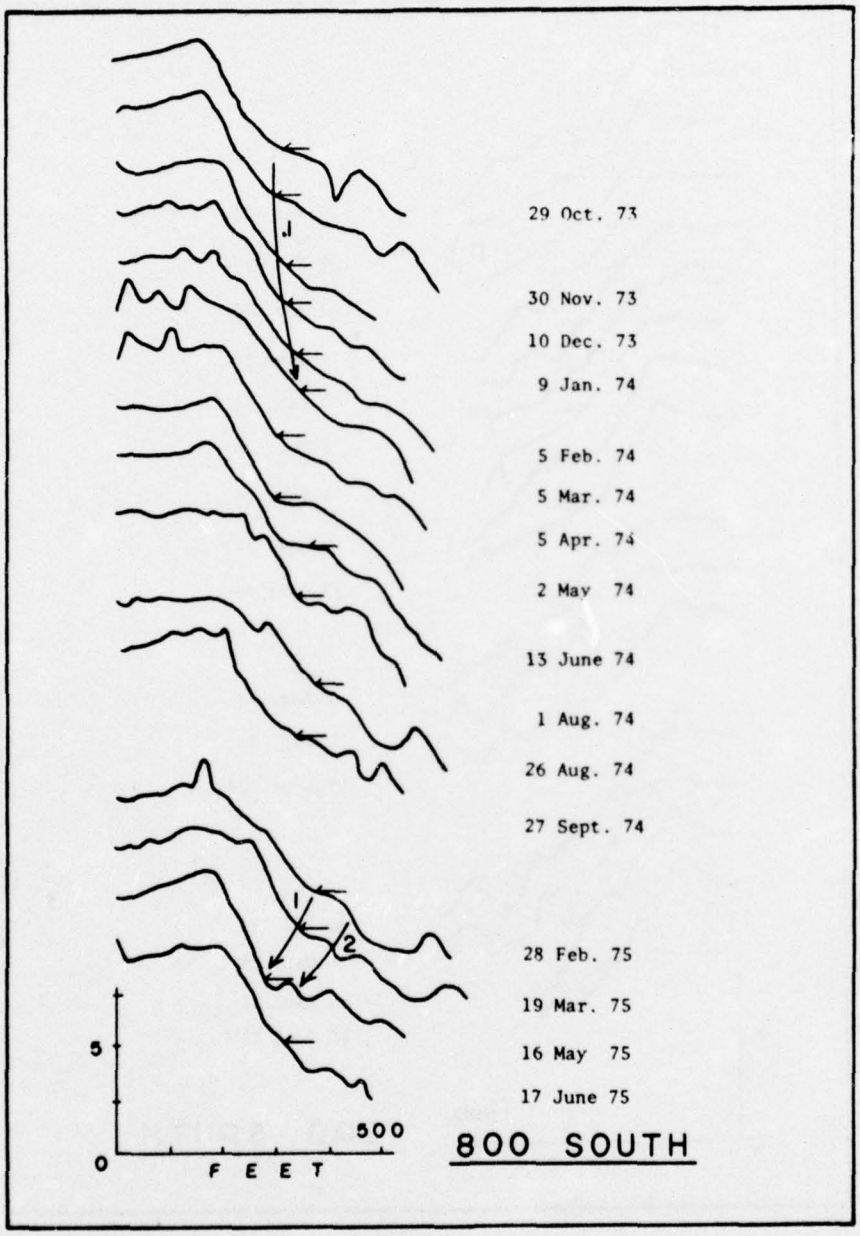

Figure C-27. 800 South.

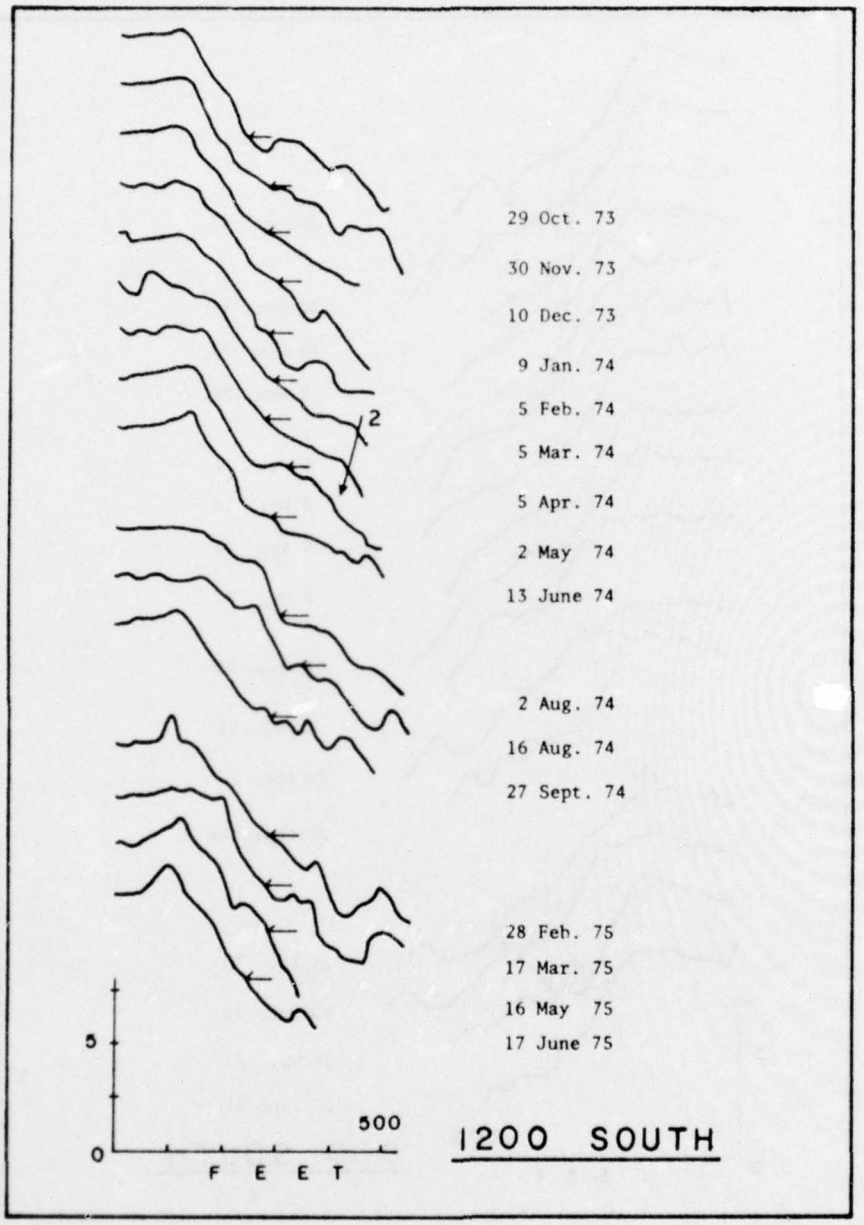

Figure C-28. 1200 South.

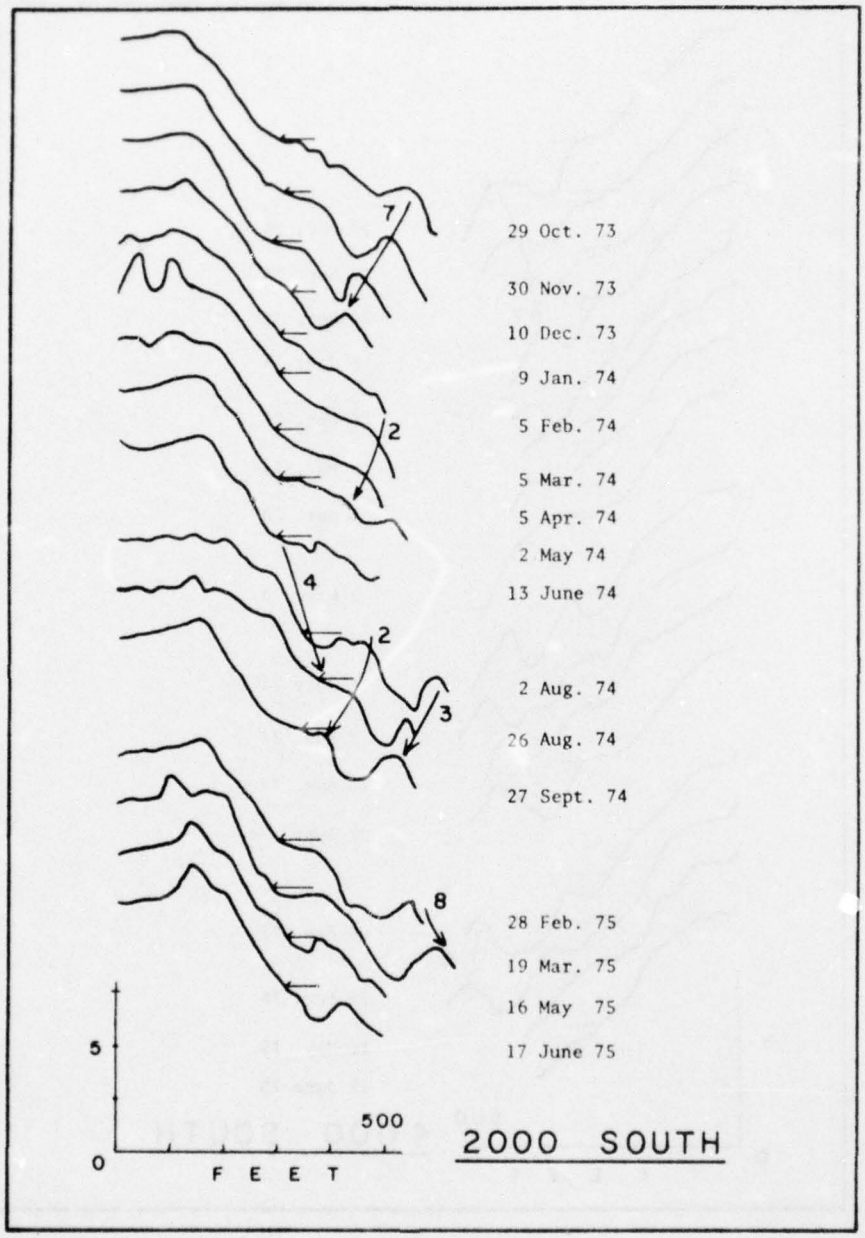

Figure C-29. 2000 South.

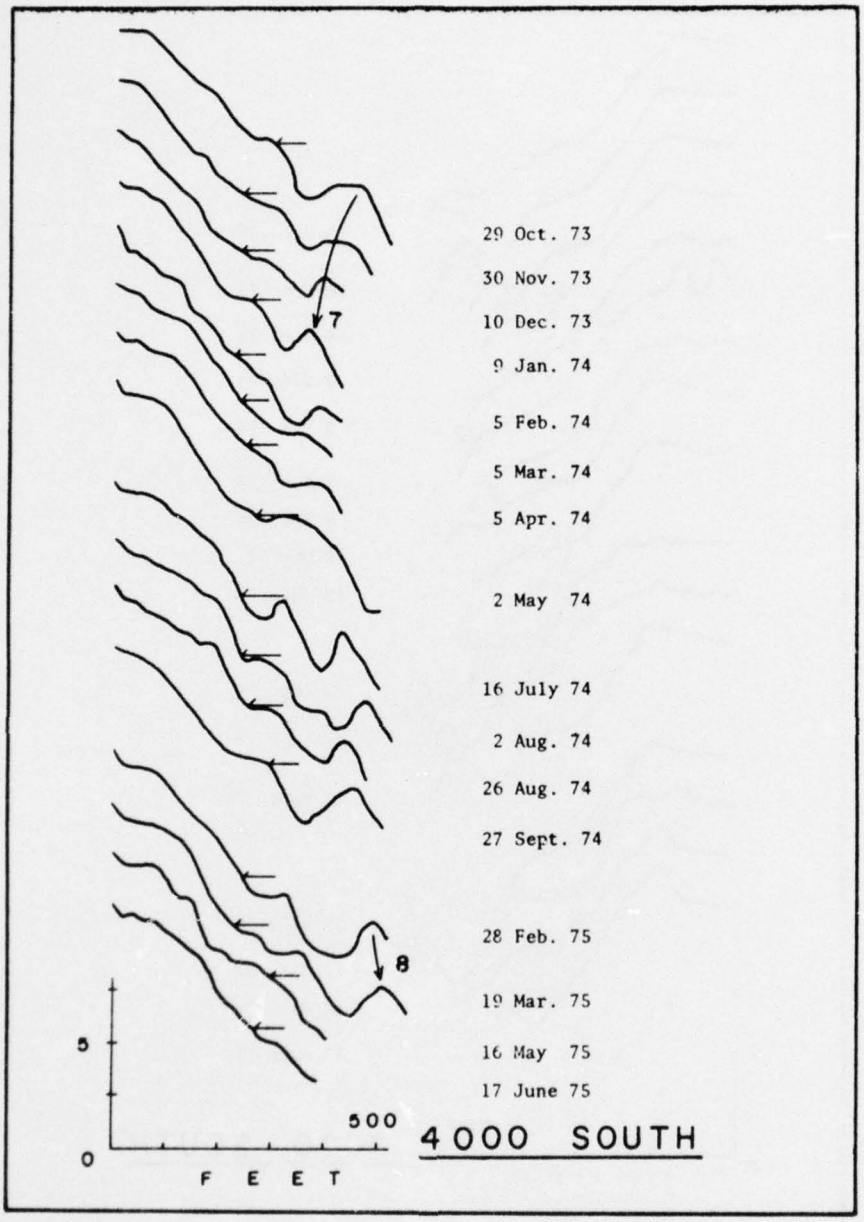

Figure C-30. 4000 South.

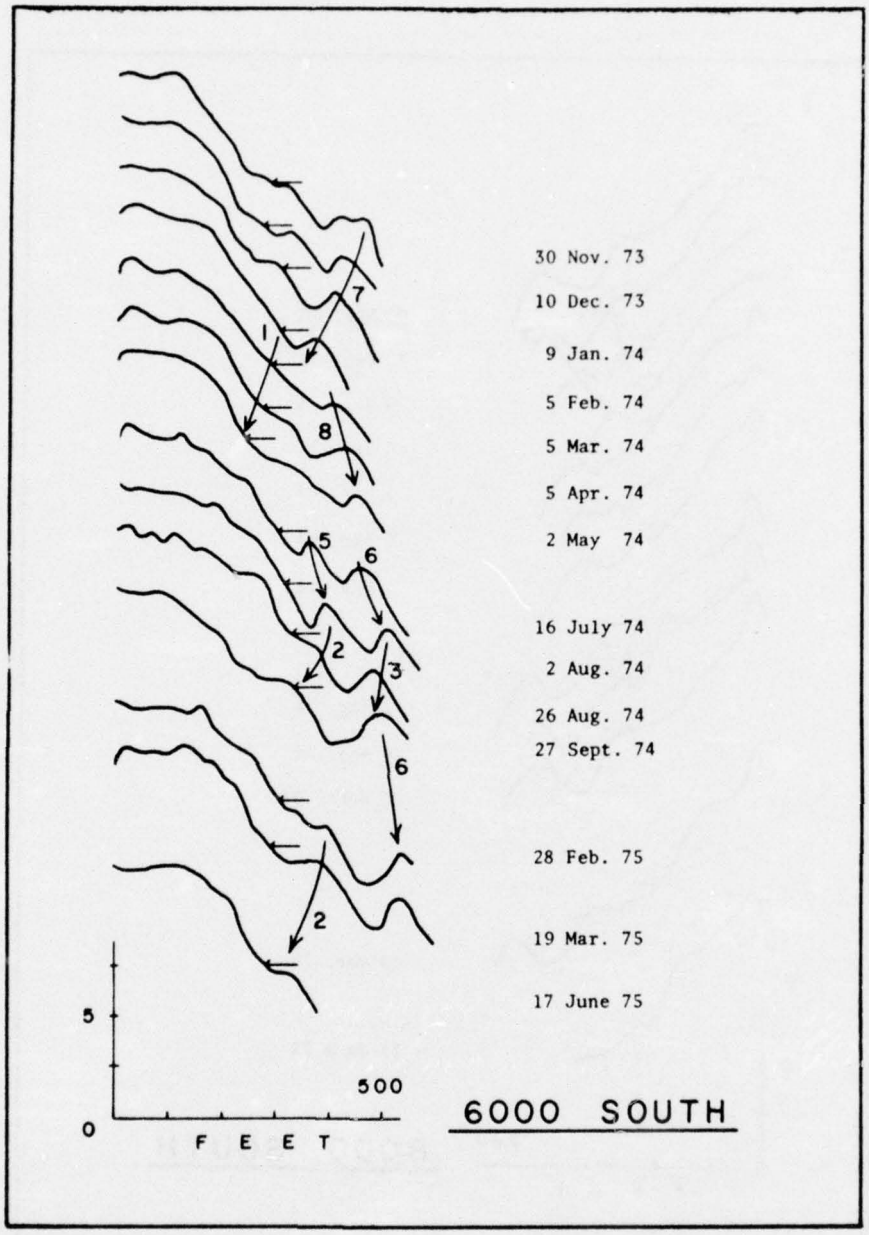

Figure C-31. 6000 South.

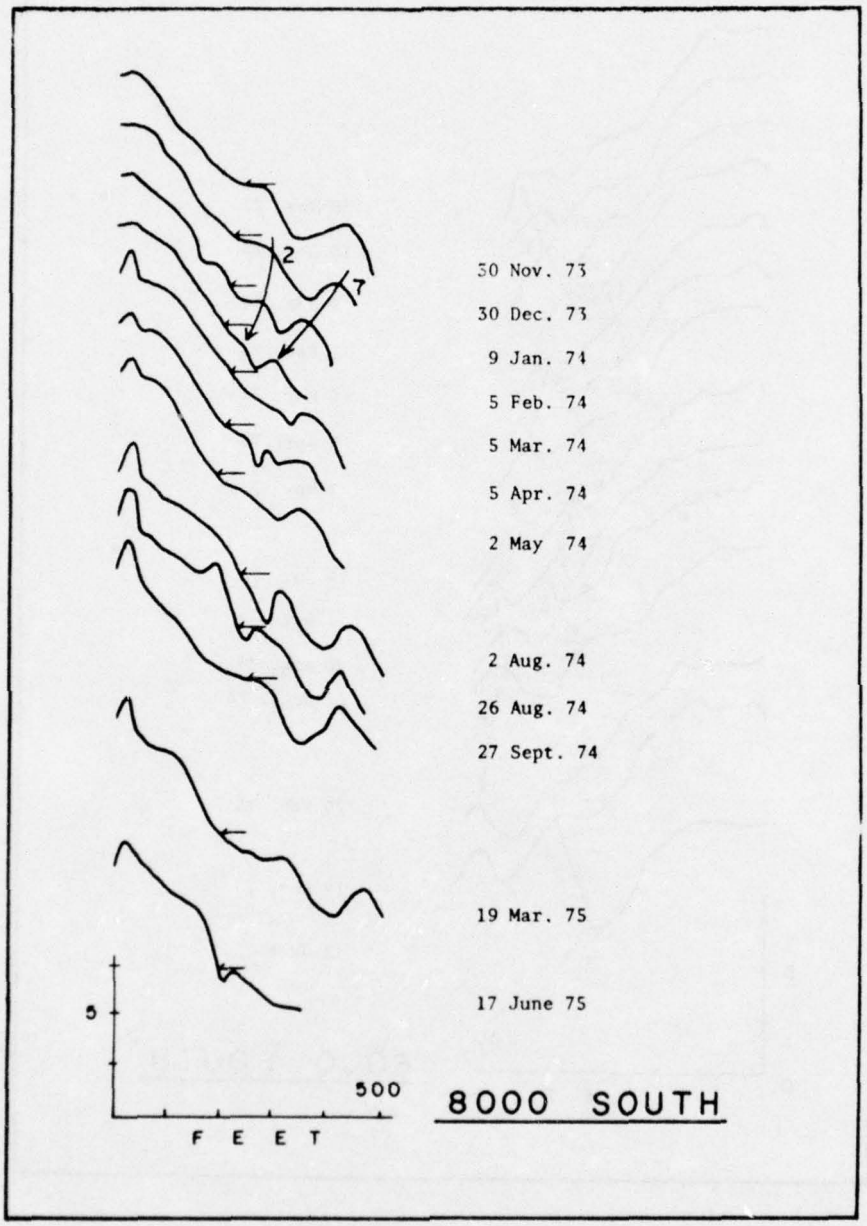

Figure C-32. 8000 South.

APPENDIX D

GULF MOUTH BATHYMETRIC MAPS

Area used for computation of sedimentary volume changes is outlined in Figure D-1.

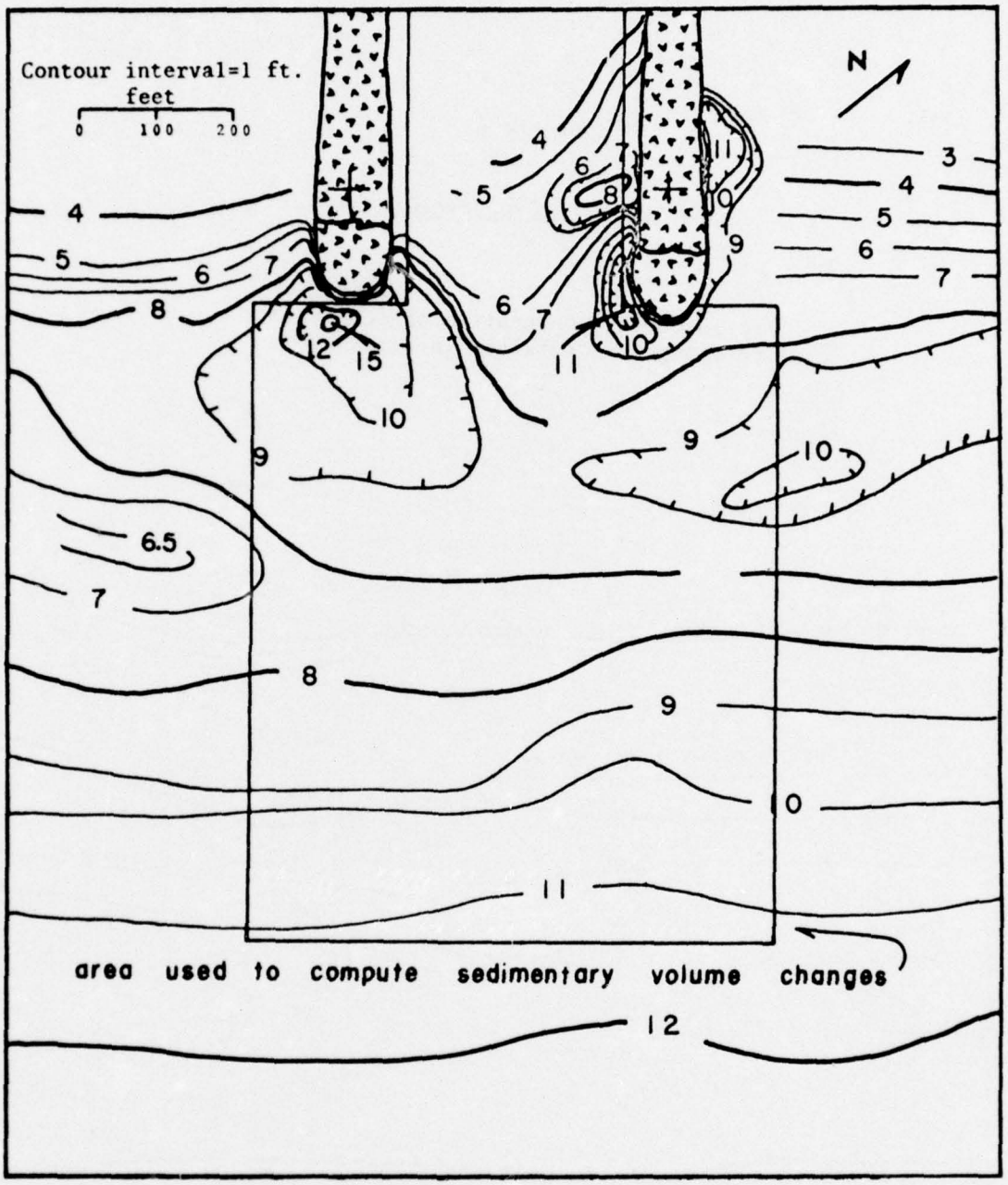

Figure D-1. Gulf mouth survey, 7 June 1973.

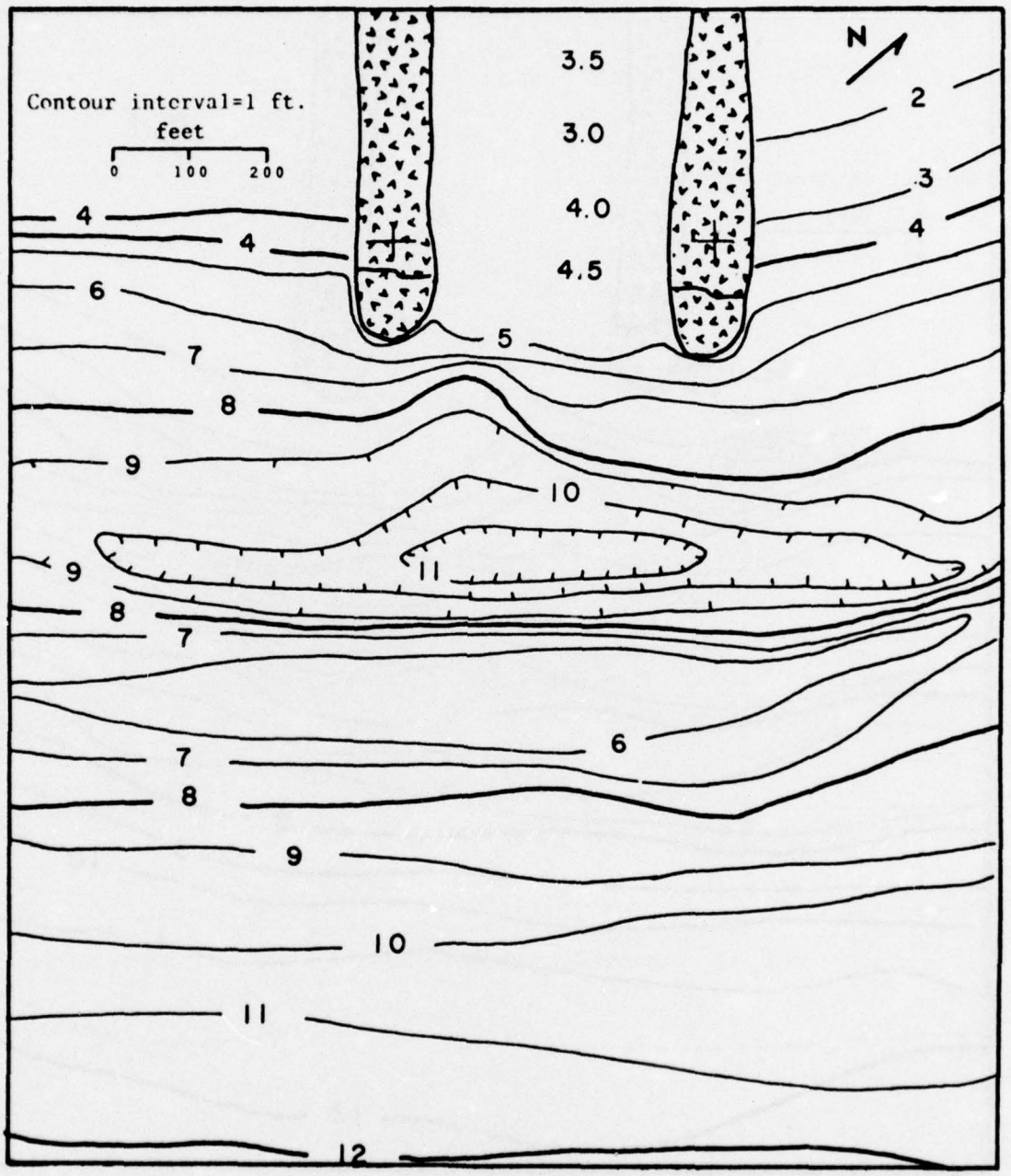

Figure D-2. Gulf mouth survey, 28 June 1974.

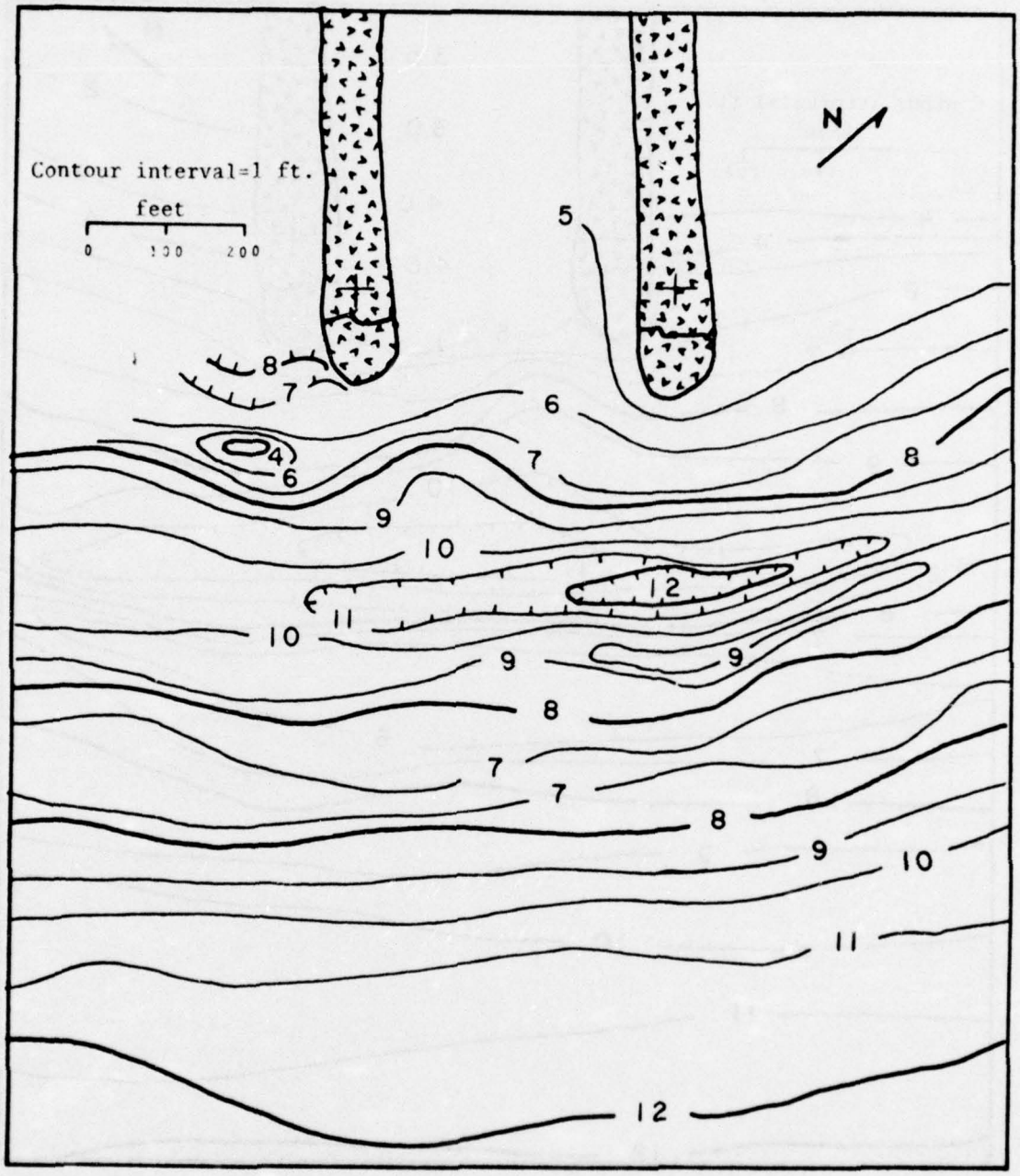

Figure D-3. Gulf mouth survey, 1 August 1974.

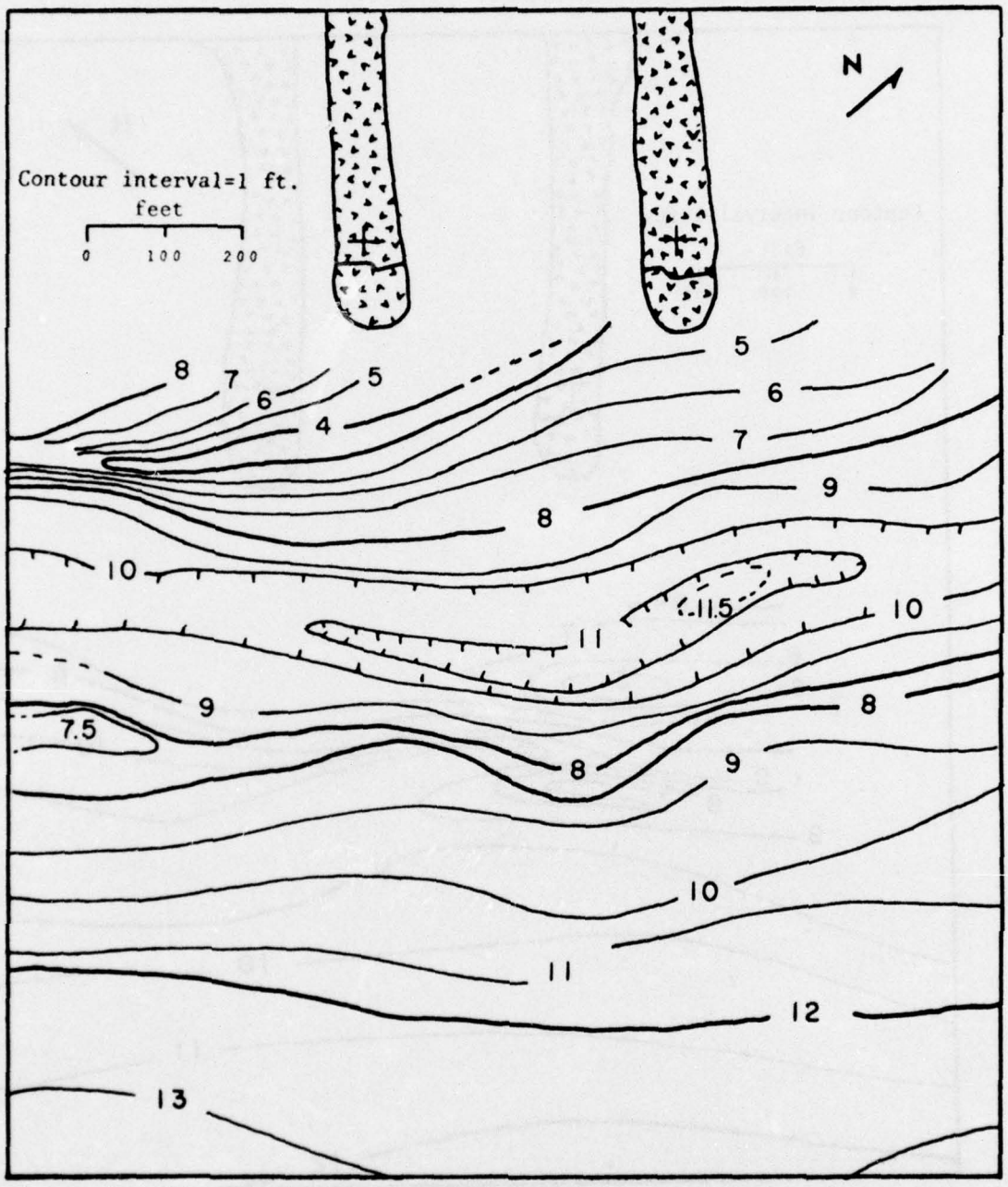

Figure D-4. Gulf mouth survey, 30 September 1974.

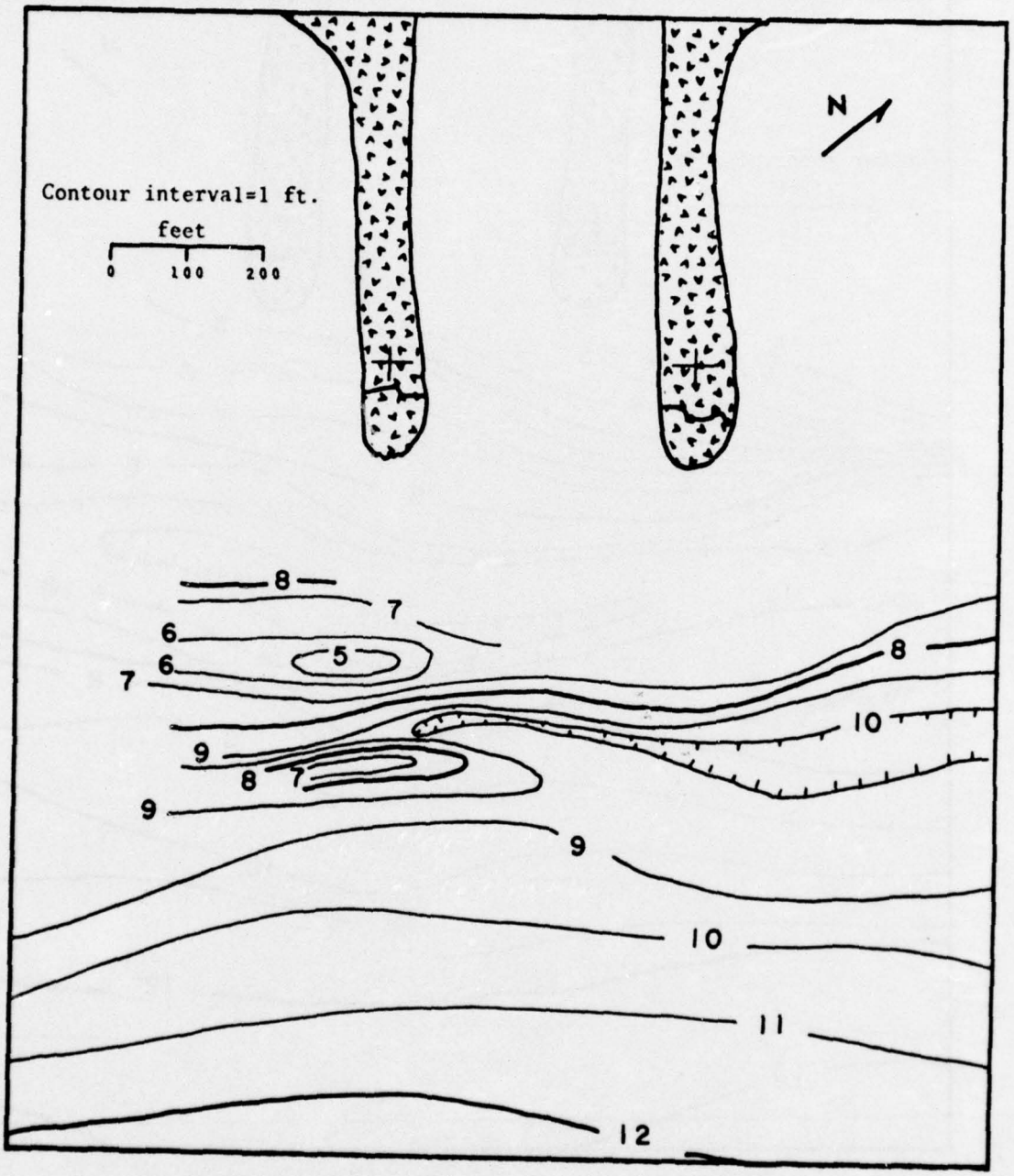

Figure D-5. Gulf mouth survey, 27 November 1974.

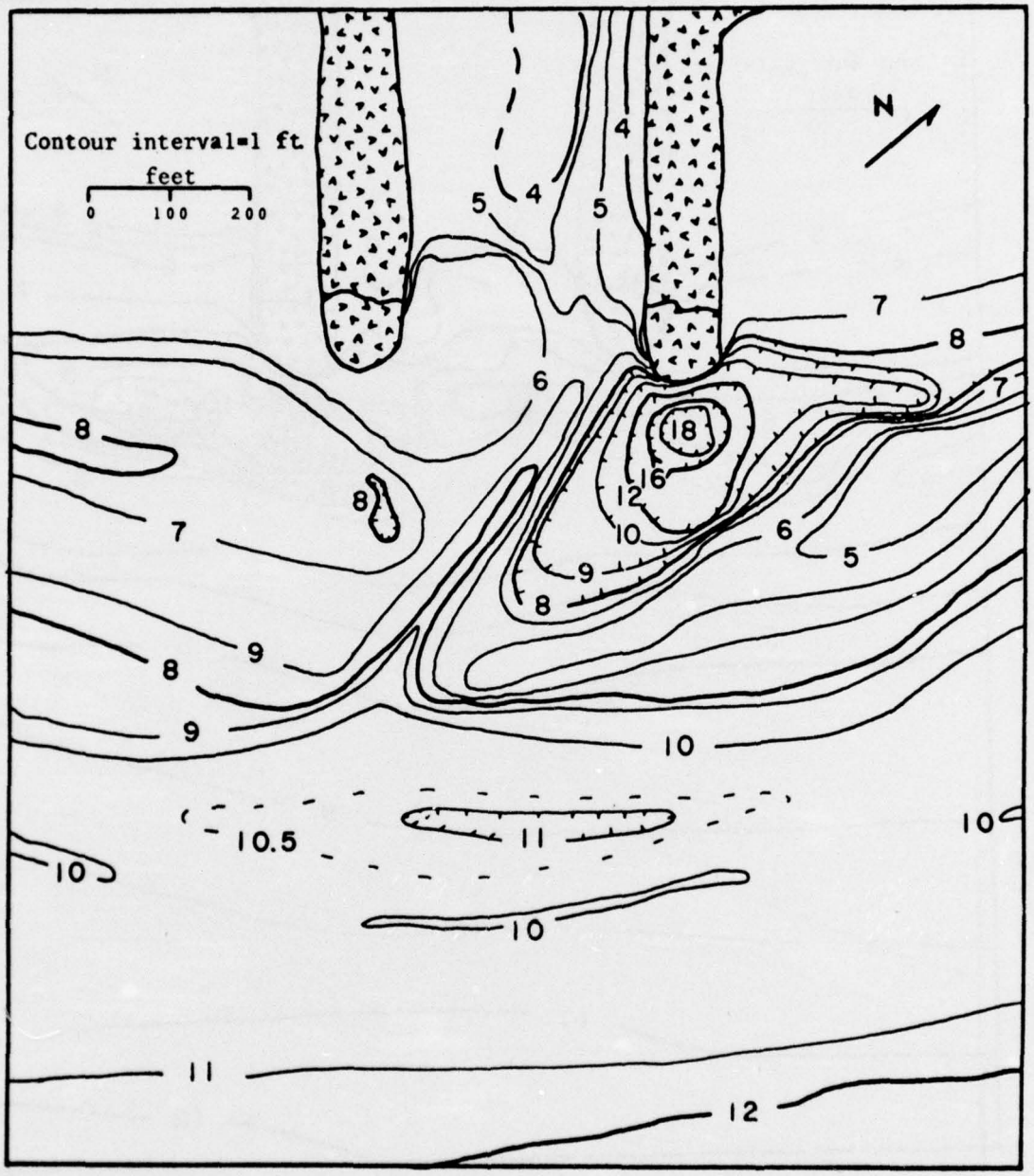

Figure D-6. Gulf mouth survey, 10 February 1975.

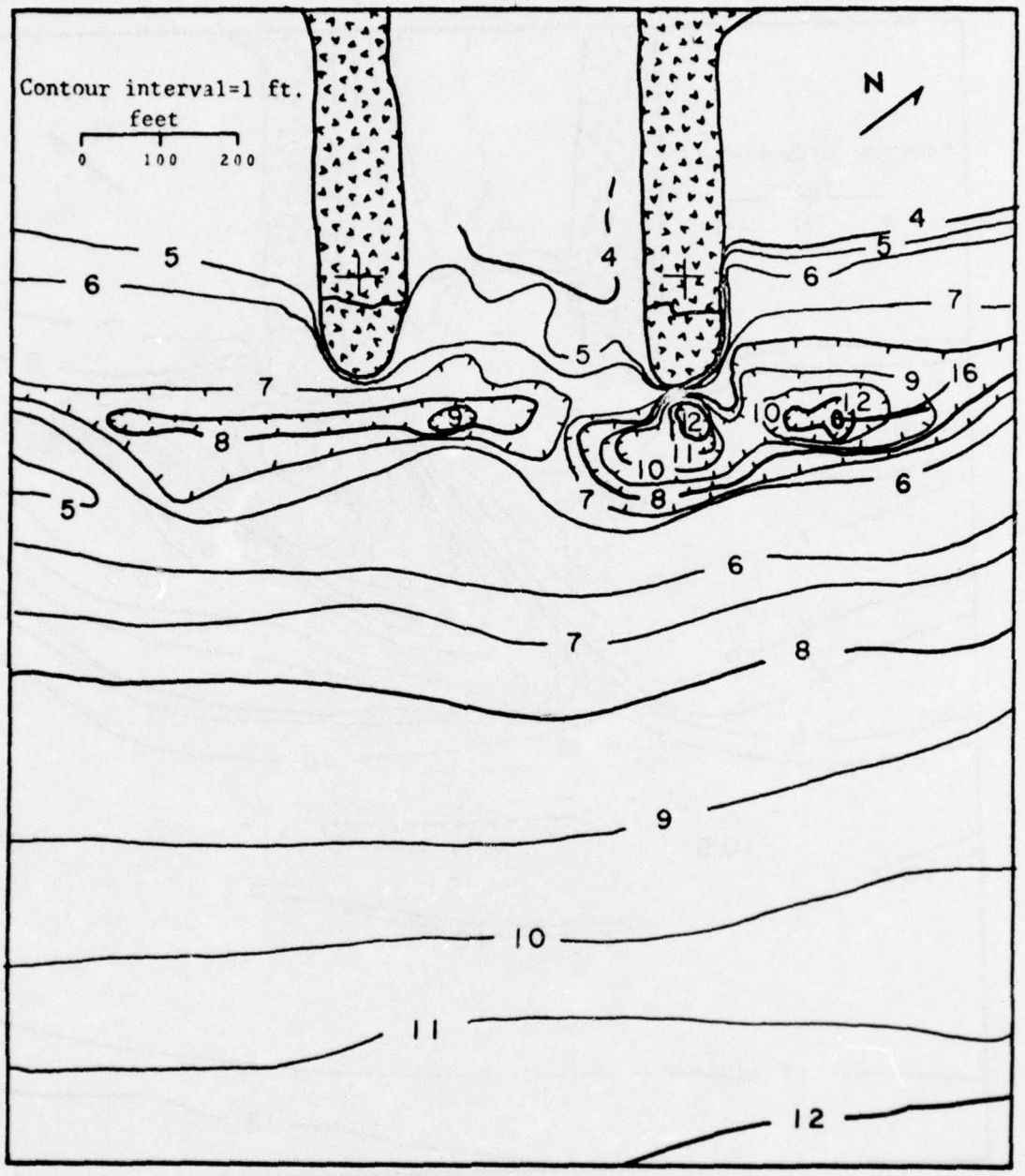

Figure D-7. Gulf mouth survey, 12 May 1975.

APPENDIX E

BAYMOUTH BATHYMETRIC MAPS

Area used for computation of sedimentary volume changes is outlined in Figure E-1.

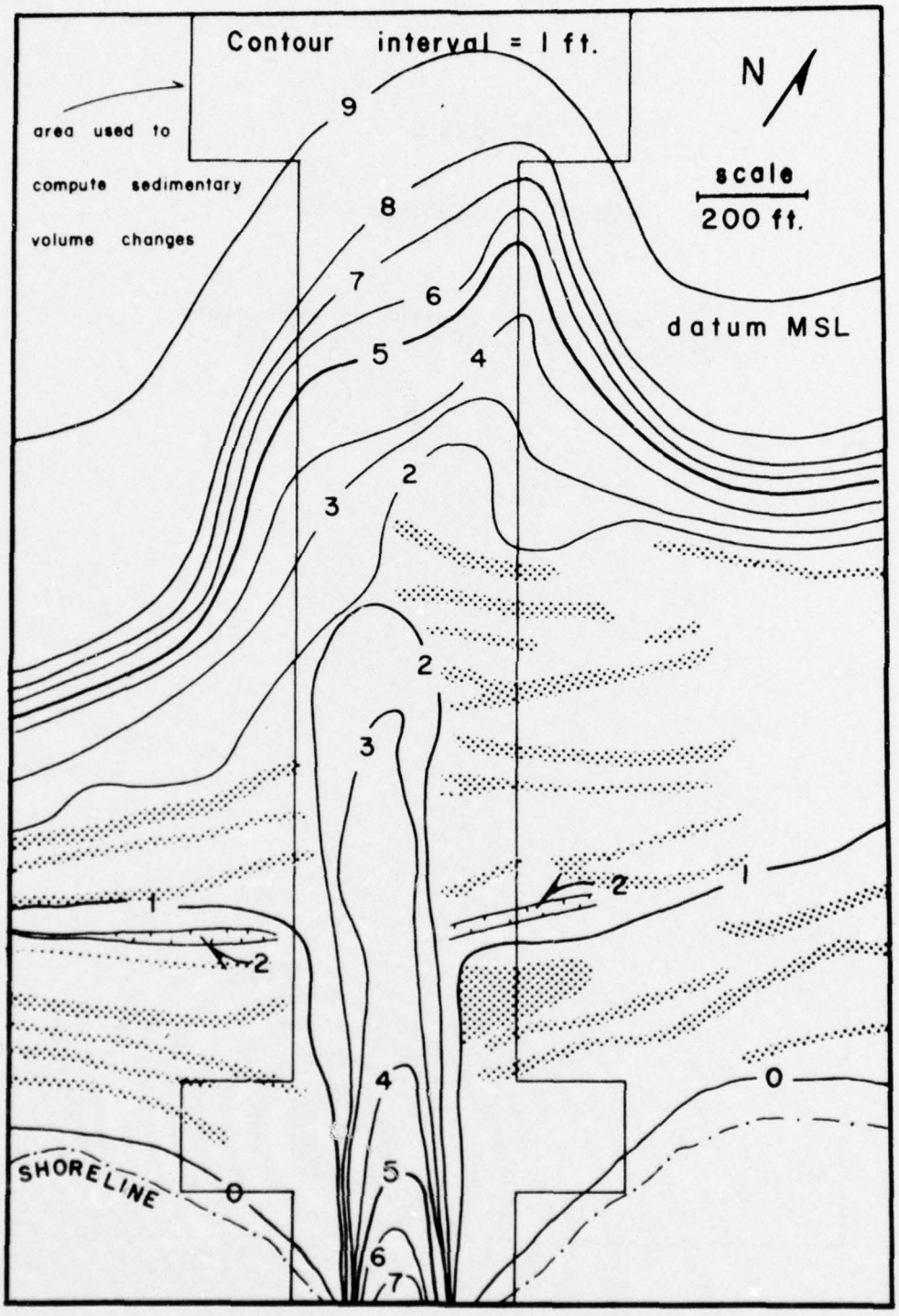

Figure E-1. Bay survey, 16 May 1973.

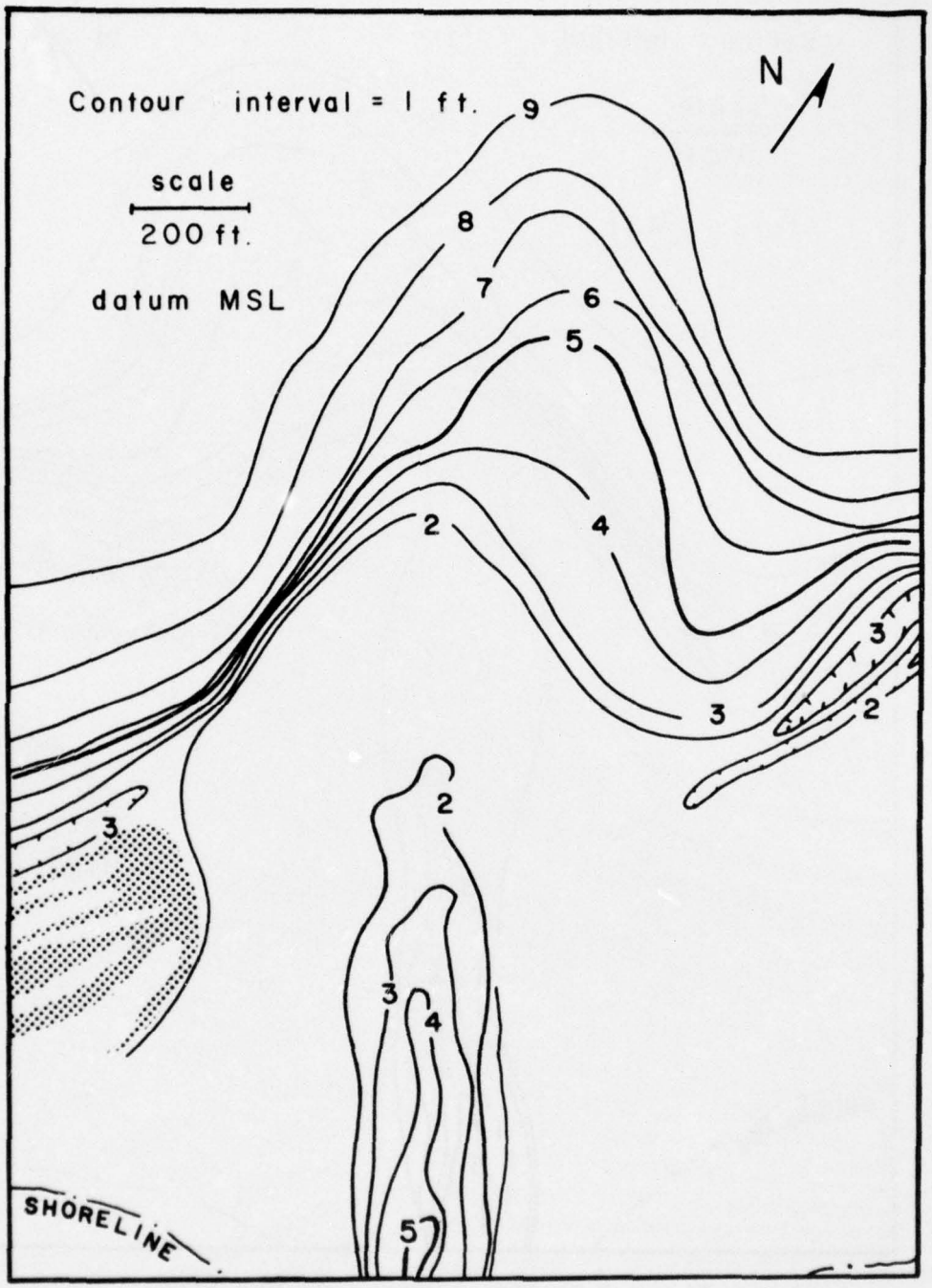

Figure E-2. Bay survey, 13 August 1974.

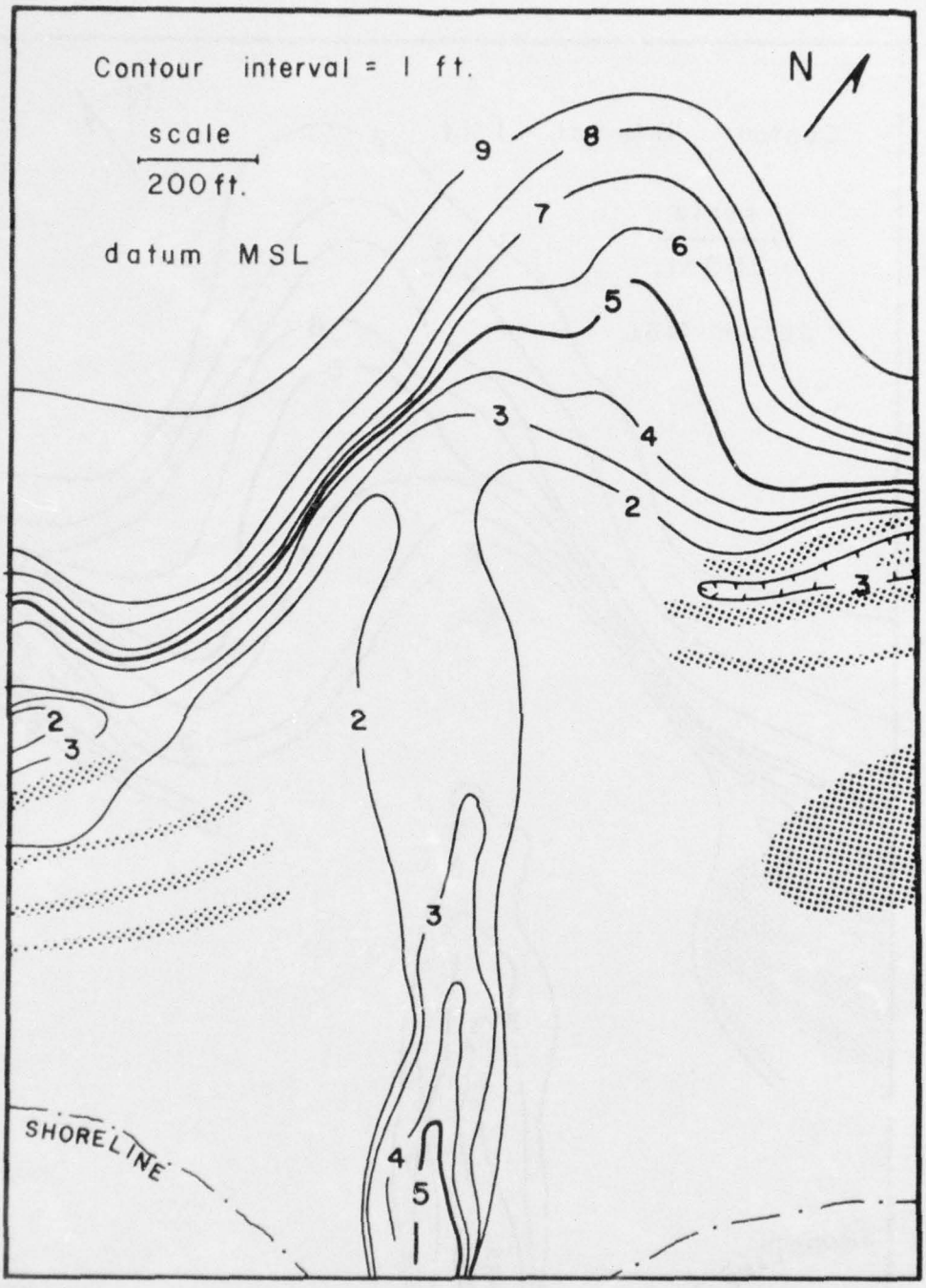

Figure E-3. Bay survey, 1 October 1974.

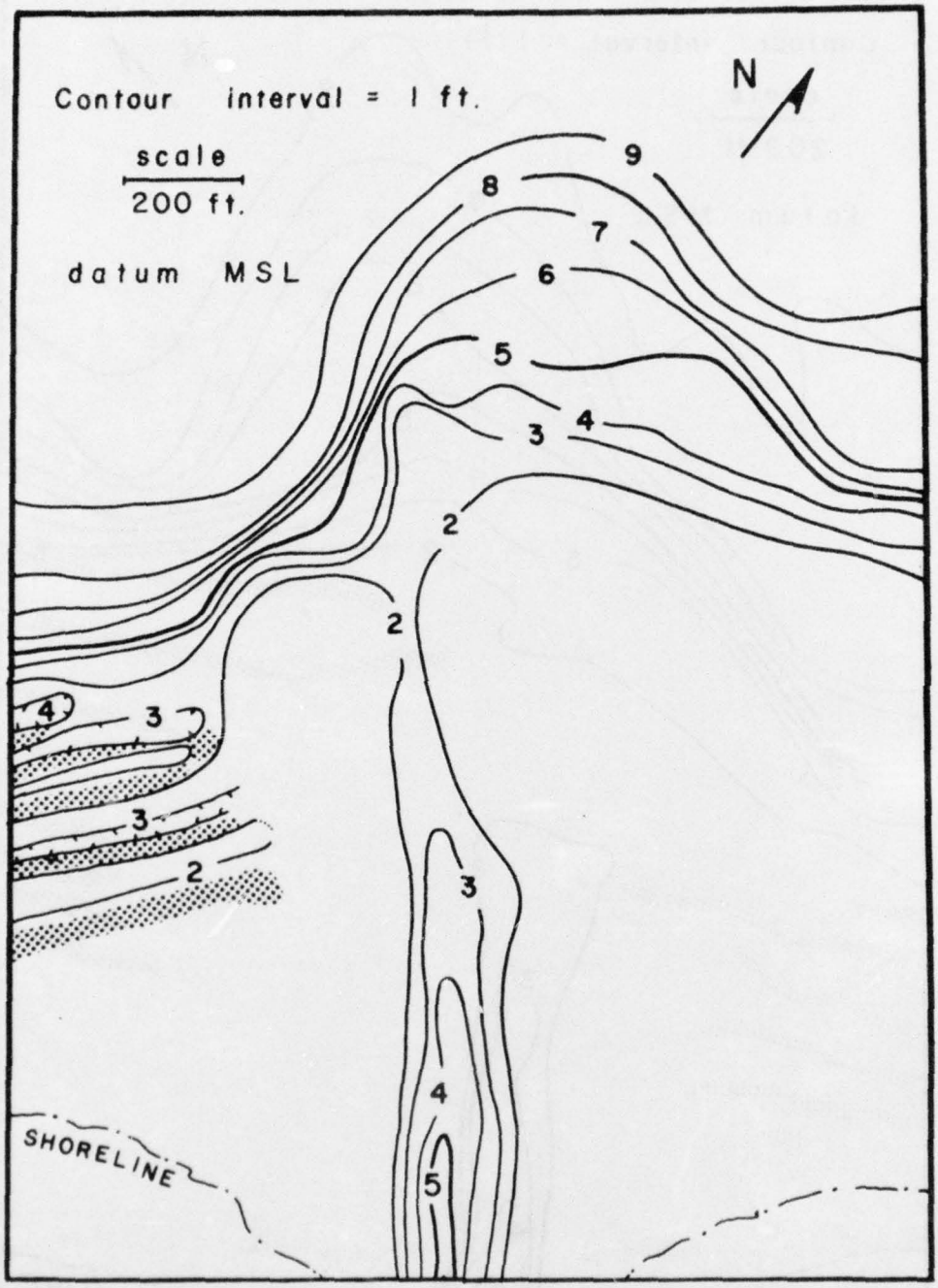

Figure E-4. Bay survey, 21 November 1974.

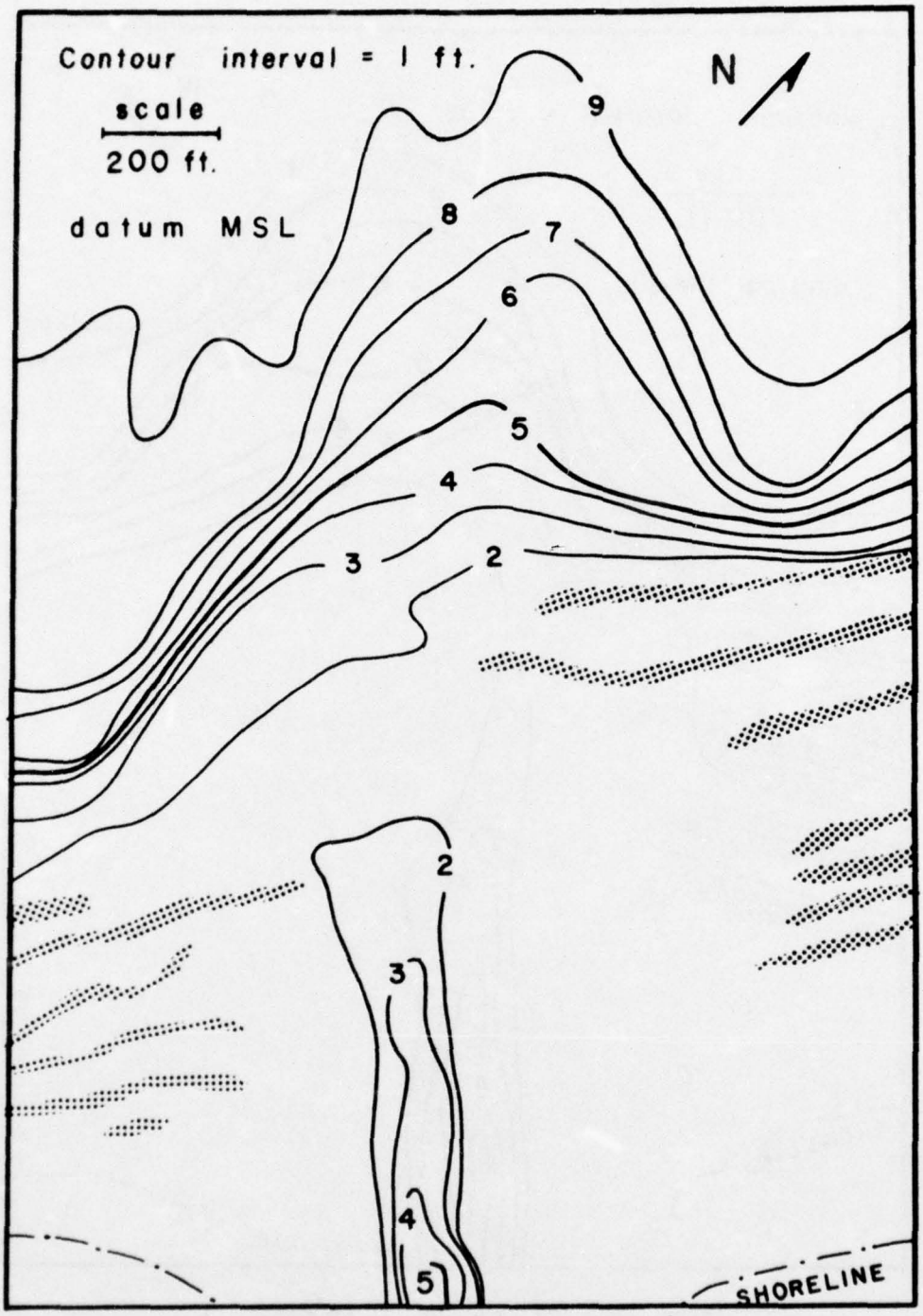

Figure E-5. Bay survey, 2 February 1975.

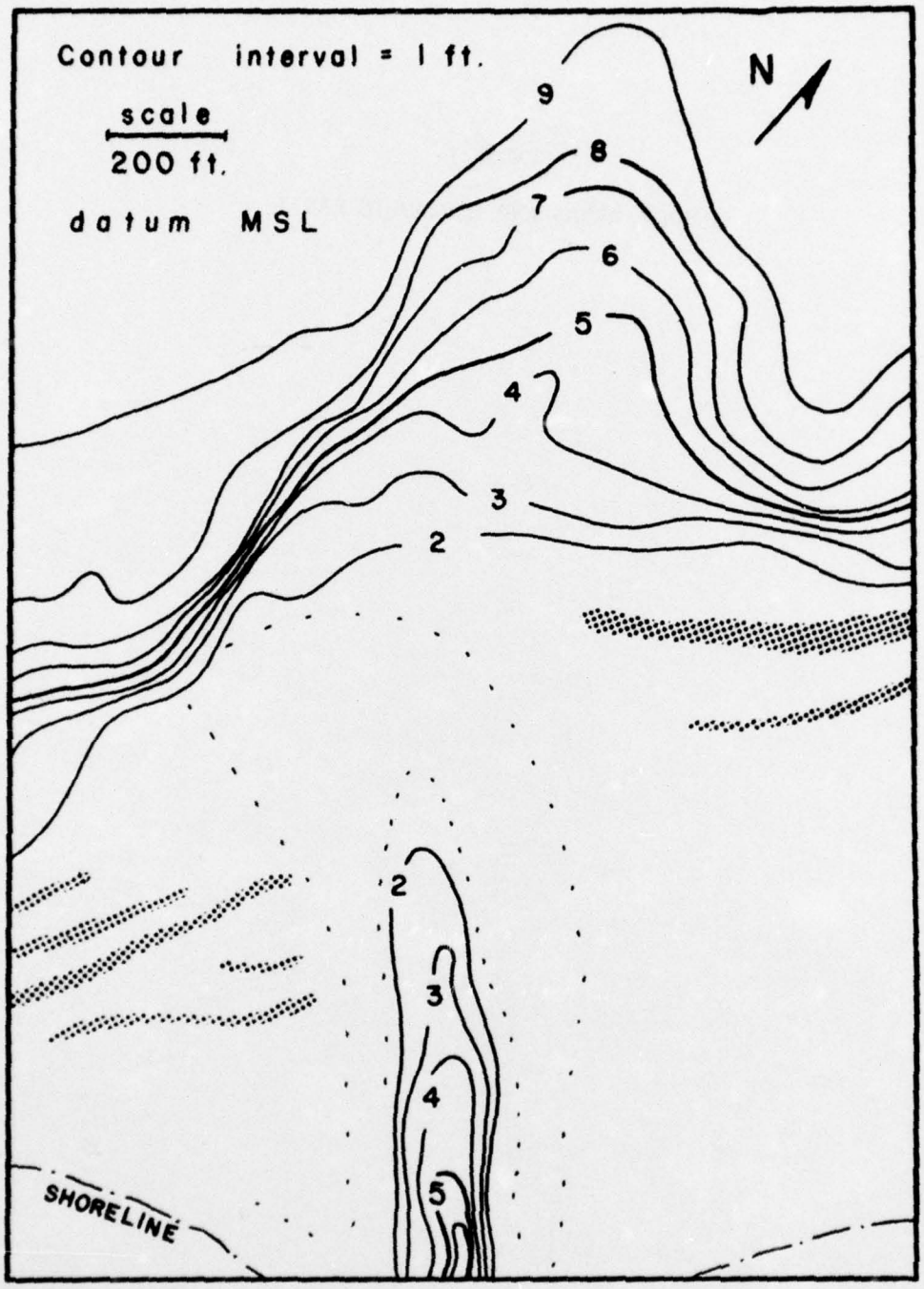

Figure E-6. Bay survey, 30 April and 13 May 1975.

APPENDIX F

CHANNEL AREAS AND HYDRAULIC RADII

Table F-1. Channel cross-sectional areas (square feet) below mean water level (+0.8 foot MSL).

	1973			1974								
Site	29 Oct.	19 Nov.	17 Dec.	8 Jan.	31 Jan.	5 Mar.	10 Apr.	2 May	1 June	3 July	31 July	27 Aug.
X2	1174	1148	994	1066	973	1109	937	1019	1081	1081	1156	1161
X3	1304	1180	1001	1214	1091	1183	943	1102	1133	1106	1214	1155
X4	1163	1043	1033	1319	1098	1125	1043	1161	1139	1183	1393	1223
X5	1108	1010	978	1188	1092	1072	1006	1095	1096	1121	1206	1187
X6	1186	1148	1062	1264	1160	1129	1063	1157	1131	1155	1199	1177
X7	1092	1094	1071	1220	1140	1127	1082	1115	1137	1136	1213	1209
X8	1191	1101	1084	1165	1134	1151	1087	1076	1137	1136	1102	1105
X8b	1112	1167	1111	1219	1171	1241	1218	1163	1149	1093	1137	1154
X9b	1172	1140	1145	1309	1284	1319	1218	1013	965	960	880	928
X10b	1050	1004	1063	1238	1238	1168	1058	1045	974	bulkhead	1093	1020
X11b	1168	(924)[1]	971	1183	1219	1244	1208	1180	1227	under construction	867	911
X12b	1161	1124	1054	1305	1216	1272	1354	1298			820	877
X13b	1136	1141	1213	1484	1410	1397	1498	1463			874	898
X14b	1055	1181	1217	1569	1472	1652	1600	1743			1108	1104
bri.b	1444	1241	1290	1294	1261	1388	1371	1308	1300	1254	1171	1168
bri.b	1520	1350	1298	1357	1415	1355	1358	1278	1207	1080	950	764
X15	1362	1537	1359	1311	1293	1296	1002	896	1265	947	888	956
X16	1220	1225	1309	1330	1162	1148	1088	845	929	896	901	760
X17	1197	1172	1194	1369	1242	1245	1040	865	891	850	848	899
X18	1130	1047	1170	1417	1261	1239	1136	937	857	1068	887	852
X19	(917)[1]	958	(926)[1]	(1052)[1]	(971)[1]	877		(743)[1]	(666)[1]	765	(593)[1]	(519)[1]
X20	1398		1189	1077		1188		840		(556)[1]	953	
X21	1102			1103		(843)[1]				765	958	
X22	1249									1172		

1. Location of minimum area.

Table F-1. (Continued)

Site	1974						1975					
	26 Sept.	29 Oct.	5 Nov.	11 Nov.	18 Nov.	25 Nov.	6 Jan.	3 Feb.	3 Mar.	2 Apr.	2 May	2 June
X2	1040	1050	1189	1190	1190	lost to bayshore erosion						
X3	1155	1093	1250	1098	1147	1102	1105	1097	862	926	1072	1038
X4	1221	1266	1361	1137	1276	1181	1145	1134	930	1024	1121	1175
X5	1094	1085	1204	994	1139	1118	1172	1070	1070	1024	1081	1104
X6	1112	1109	1296	970	1120	1134	1093	1136	1088	1055	1057	1085
X7	1170	1206	1503	1046	1188	1118	1114	1142	1103	1057	1097	1048
X8	980	982	963	949	949	984	864	887	906	869	936	893
X8b	1090	1083	996	967	1024	1036	999	1018	1071	1027	1011	961
X9b	912	999	872	(618)[1]	914	940	1001	1006	1008	964	1056	1037
X10b	990	978	952	893	964	942	917	968	969	971	951	928
X11b	880	1015	934	931	935	972	879	958	882	871	955	877
X12b	893	865	981	886	897	898	888	881	899	879	959	957
X13b		868	871	911	860	864	867	853	915	880	905	946
X14b	1069	983	880	921	838	858	869	915	(847)[1]	873	962	1040
bri.b	919	1209	953	1024	1089	1048	968	1029	957	1185	1174	1162
bri.b	973	962	894	1021	1114	962	1081	900	1210	1153	1148	866
X15	910	1000	879	995	924	1028	1041	1020	1221	1140	961	872
X16	893	894	782	998	749	944	1087	1100	1159	1106	(887)[1]	688
X17	836	798	790	903	869	921	1320	1018	1221	1060	942	942
X18	764	850	(503)[1]	917	768	894	1055	978	1189	920	1072	1032
X19	(706)[1]	(768)[1]	617	787	(600)[1]	(676)[1]	(737)[1]	(705)[1]	872	(824)[1]		(277)[1]
X20								849				707
X21								922				747
X22								1630				1252

1. Location of minimum area.

Table F-2. Channel hydraulic radii (feet).

Site	1973			1974								
	29 Oct.	19 Nov.	17 Dec.	8 Jan.	31 Jan.	5 Mar.	10 Apr.	2 May	1 June	3 July	31 July	27 Aug.
X2	5.2	5.4	5.4	6.2	5.0	5.1	4.6	4.2	3.5	4.3	6.0	5.0
X3	6.0	5.9	5.6	6.5	5.8	6.0	5.2	5.2	5.1	5.1	5.5	5.4
X4	(3.1)[1]	3.4	4.4	5.4	4.5	4.6	4.0	3.8	3.6	3.6	5.5	4.3
X5	5.6	5.2	5.8	6.9	6.1	6.3	5.6	5.6	5.5	5.8	6.9	6.3
X6	5.4	5.1	5.0	5.9	5.6	5.2	4.8	5.2	5.0	5.1	5.6	5.3
X7	5.5	5.5	5.7	6.3	5.8	5.8	5.4	5.3	5.5	5.4	6.1	5.7
X8	7.3	6.6	6.9	7.4	7.0	7.3	6.7	6.5	6.8	6.9	6.6	6.5
X8B	4.9	4.9	5.1	5.6	5.1	5.4	5.2	5.0	5.0	4.9	5.1	4.9
X9B	4.3	4.0	4.3	4.8	4.6	4.7	4.3	3.6	3.3	3.2	3.2	3.2
X10B	4.0	3.6	4.0	4.6	4.4	4.1	3.7	3.6	3.3	bulkhead under	4.3	4.0
X11B	4.1	(3.3)[1]	3.5	4.1	4.1	4.1	3.9	3.8	3.9	construction	4.7	4.8
X12B	4.0	3.8	3.7	4.3	(3.9)[1]	4.1	4.2	4.0			4.7	4.9
X13B	3.8	3.7	4.2	5.0	4.5	4.35	4.6	4.6			5.3	5.2
X14B	4.1	3.4	4.6	5.4	4.6	5.3	4.7	5.2			6.8	6.4
XBrB	11.6	9.9	10.3	11.2	10.9	12.1	11.0	11.0	11.1	10.7	10.5	10.4
XBrG	12.2	11.0	10.7	11.5	12.1	11.8	10.6	10.5	10.2	8.7	8.4	7.1
X15	6.1	5.7	5.6	4.9	4.7	4.8	4.0	3.3	4.6	4.0	3.9	4.0
X16	4.6	4.4	5.0	5.0	4.5	4.2	3.9	3.1	3.3	3.2	3.2	(3.0)[1]
X17	4.2	3.9	4.1	4.7	4.2	4.3	(3.5)[1]	(3.0)[1]	(2.9)[1]	3.0	3.1	(3.0)[1]
X18	3.6	(3.3)[1]	3.8	4.7	4.1	4.1	3.6	3.3	(2.9)[1]	2.8	3.2	(3.0)[1]
X19	4.1	4.4	4.7	6.4		4.8		3.5	4.3	3.6	4.8	6.2
X20	4.0		(3.4)[1]	4.3		3.5				2.6	(2.9)[1]	
X21	3.2			(3.6)[1]		(2.7)[1]				(2.4)[1]	3.1	
X22	(3.6)[1]									3.8		

1. Location of minimum radius.

Table F-2. (Continued)

	1974						1975					
Site	26 Sept.	29 Oct.	5 Nov.	11 Nov.	18 Nov.	25 Nov.	6 Jan.	3 Feb.	3 Mar.	2 Apr.	2 May	2 June
X2	4.1	5.0	5.3		5.0	lost to bayshore erosion						
X3	5.2	5.1	5.7	4.9	5.5	5.6	5.3	5.3	4.6	5.3	5.4	5.2
X4	3.6	3.9	4.3	3.6	4.0	4.4	4.1	4.0	3.8	3.6	3.0	3.6
X5	5.45	5.4	5.8	4.9	4.9	6.3	5.6	5.7	5.2	5.0	4.8	5.3
X6	4.8	4.8	5.4	4.3	5.2	4.6	4.8	5.0	4.7	4.5	4.2	4.5
X7	5.4	5.6	7.1	5.0	5.7	5.5	5.3	5.3	5.0	4.7	4.9	4.7
X8	5.8	5.7	5.7	5.5	5.7	5.8	5.1	5.1	5.2	4.9	5.2	5.1
X8B	4.5	4.4	4.2	4.0	4.4	4.4	4.2	4.2	4.2	4.0	3.6	3.6
X9B	2.9	3.3	2.9	(2.0)[1]	3.0	3.1	(3.2)[1]	3.3	3.3	3.1	3.3	3.2
X10B	3.8	3.8	3.7	3.5	3.8	3.7	3.5	3.8	3.7	3.7	3.6	3.5
X11B	4.5	5.2	5.0	4.8	4.8	5.0	4.6	5.0	4.4	4.3	4.8	4.4
X12B	4.8	5.0	5.4	4.8	5.2	4.9	4.9	4.6	4.7	4.7	4.9	5.1
X13B	6.4	4.8	5.2	5.3	5.1	5.0	4.8	4.4	4.8	4.5	4.5	4.8
X14B	4.8	4.0	5.3	4.1	5.0	5.1	4.4	4.5	3.7	3.7	3.6	4.7
XBrB	8.5	9.7	8.0	9.3	9.95	9.7	8.7	9.5	7.6	9.9	9.2	9.5
XBrG	8.7	8.1	8.3	9.0	8.7	8.7	9.5	8.4	9.8	9.4	9.1	7.2
X15	3.5	3.4	3.2	3.8	3.4	3.7	3.7	4.1	4.7	4.0	2.5	3.2
X16	3.0	2.9	(1.6)[1]	3.2	(2.4)[1]	2.9	3.3	3.3	3.8	3.5	2.6	1.9
X17	(2.8)[1]	(2.4)[1]	(1.6)[1]	2.7	2.6	(2.6)[1]	3.4	(2.6)[1]	(3.0)[1]	2.7	(2.4)[1]	2.4
X18	(2.8)[1]	2.8	2.0	3.2	2.8	3.0	(3.2)[1]	2.9	3.2	(2.5)[1]	3.0	2.9
X19	3.4	3.7	3.2	3.7	3.7	4.1	4.7	3.4	4.2	3.9		(1.8)[1]
X20								(2.6)[1]				
X21								2.9				
X22								5.4				

1. Location of minimum radius.

APPENDIX G

WEEKLY WATER TEMPERATURES AND SALINITIES

Table G-1. Weekly water temperatures and salinities at Aransas Pass Inlet for 1974.

Week	Month	Temperature (°C) ebb	Temperature (°C) flood	Salinity (parts per thousand) ebb	Salinity (parts per thousand) flood
1		8.0	11.0	21.0	27.0
2		13.0	14.0	27.5	24.5
3	Jan.	13.0	12.0	24.5	21.5
4		14.5		25.0	
5		17.0	16.5	20.5	23.5
6		15.5		21.5	
7	Feb.	18.0	16.0	28.5	27.0
8		18.0		28.0	
9			16.0		30.0
10		19.5		32.5	
11			21.0		28.5
12	Mar.	21.0		25.0	
13		17.0	16.5	26.5	25.5
14		21.0		29.0	
15			21.0		30.5
16	Apr.	20.5		31.0	
17			23.0		25.5
18		24.5	25.5	22.0	23.0
19			25.0		26.0
20	May	27.0	26.5	26.5	26.0
21		27.5	28.0	26.0	23.0
22		28.5	28.0	25.0	28.0
23		28.5	28.0	33.5	32.5
24	June	29.0	27.0	28.0	29.5
25		29.5	28.0	32.0	33.0
26			28.0		33.0
27		28.5	28.5	33.0	33.5
28		29.0	28.5	34.0	34.0
29	July	29.5	28.3	35.0	34.5
30		29.0	28.5	35.0	35.5
31			27.5		36.0
32		28.0	28.5	37.0	37.0
33	Aug.		29.0		37.5
34		29.5	29.5	37.5	37.5
35		29.5	29.5	37.5	37.5
36		27.0		37.0	
37	Sept.	26.5	26.5	36.0	36.0
38		28.0		30.5	
39		24.5		26.0	
40		24.5		27.0	
41		25.5		27.5	
42	Oct.	24.0	22.0	26.5	22.0
43		24.0		29.0	
44		24.0		27.0	
45		20.5		23.0	
46	Nov.	17.0		19.5	
47		19.5		26.0	
48		16.0		20.0	
49		15.5		29.5	
50	Dec.	13.5		25.5	
51		15.0		31.0	
52		13.5	17.0	24.0	28.5

Table G-2. Weekly water temperatures and salinities at Aransas Pass and Corpus Christi Water Exchange Pass for 1975.

Week	Month	Temperature (°C) ebb	Temperature (°C) flood	Salinity (parts per thousand) ebb	Salinity (parts per thousand) flood
1		12.2	12.9	27.0	25.8
2		15.6	16.0	25.5	30.0
3	Jan.	12.5	13.4	27.2	26.8
4		12.8	13.0	24.0	29.0
5		17.5	18.7	30.0	30.8
6		14.0	17.0	25.7	25.0
7	Feb.	15.8	16.1	26.7	27.5
8		15.0	14.2	28.0	28.8
9		15.9	16.9	27.8	31.5
10		16.6	18.5	29.0	28.5
11	Mar.	15.2	16.1	29.5	28.7
12			17.6		27.5
13		20.5	18.0	27.0	31.0
14		17.2	18.4	24.5	26.5
15		20.2	20.0	25.7	25.8
16	Apr.		20.6		27.5
17		21.4	23.1	26.0	26.0
18		23.9	23.9	24.0	21.5
19		25.6	25.8	21.0	20.0
20	May	26.1	25.8	21.5	22.0
21		25.6	25.8	30.0	29.5
22		27.8	26.9	28.0	28.5
23		27.5	26.9	28.0	25.5
24	June		26.4		33.0
25			26.4		35.5
26		29.4	28.9	33.0	33.0
27			29.4		29.0
28		28.9	27.2	33.5	36.5
29	July	29.2	25.8	35.5	35.5
30			28.1		36.0
31		29.4	28.9	36.5	36.0
32			26.9		37.0
33	Aug.	28.1	28.1	36.5	36.0
34		28.9	29.2	37.0	37.0
35		28.9		36.0	
36		28.9	29.8	28.5	27.5
37		29.1	28.9	27.0	27.0
38	Sept.	28.7	29.0	27.0	27.0
39		24.4		23.0	
40		25.5	24.5	25.5	26.0
41		25.7	24.3	29.0	27.5
42	Oct.	26.7	25.9	28.5	24.0
43		24.7	24.6	28.5	27.0
44		23.3	24.0	27.0	27.0
45		24.2	24.6	27.0	29.0
46	Nov.	22.9	19.6	26.5	24.0
47		17.4	22.5	24.5	29.5
48		16.7	18.9	26.5	29.5
49		17.7	16.8	27.0	28.0
50	Dec.	17.0	18.6	25.5	29.5
51		12.6	17.6	23.5	28.0
52		13.5	13.0	26.5	26.0

Watson, Richard L.
Hydraulics and dynamics of New Corpus Christi Pass, Texas : a case history, 1973-1975 / by Richard L. Watson and E. William Behrens. – Ft. Belvoir, Va. : U.S. Coastal Engineering Center, 1976.
175 p. : ill. (GITI report 9) Also (Contract - Coastal Engineering Research Center ; (DACW72-74-C-0017)
Bibliography : p. 93.
A case history of the hydraulics and sedimentation of the Corpus Christi Water Exchange Pass, Texas, from 1973-75 is presented. Qualitative data are given on longshore sediment transport, tidal differentials, flood and ebb tidal discharge, wind waves, and local winds to explain bathymetric changes in the Pass.
1. Corpus Christi Pass, Texas. 2. Tidal inlets. 3. Tidal hydraulics. I. Title. II. Behrens, E. William, joint author. III. Texas. University. Marine Science Institute. IV. U.S. Army. Corps of Engineers. GITI report no. 9. V. U.S. Coastal Engineering Research Center. Contract DACW72-74-C-0017.

GB454 .I5 U581r no. 9 551.4

Watson, Richard L.
Hydraulics and dynamics of New Corpus Christi Pass, Texas : a case history, 1973-1975 / by Richard L. Watson and E. William Behrens. – Ft. Belvoir, Va. : U.S. Coastal Engineering Center, 1976.
175 p. : ill. (GITI report 9) Also (Contract - Coastal Engineering Research Center ; (DACW72-74-C-0017)
Bibliography : p. 93.
A case history of the hydraulics and sedimentation of the Corpus Christi Water Exchange Pass, Texas, from 1973-75 is presented. Qualitative data are given on longshore sediment transport, tidal differentials, flood and ebb tidal discharge, wind waves, and local winds to explain bathymetric changes in the Pass.
1. Corpus Christi Pass, Texas. 2. Tidal inlets. 3. Tidal hydraulics. I. Title. II. Behrens, E. William, joint author. III. Texas. University. Marine Science Institute. IV. U.S. Army. Corps of Engineers. GITI report no. 9. V. U.S. Coastal Engineering Research Center. Contract DACW72-74-C-0017.

GB454 .I5 U581r no. 9 551.4

Watson, Richard L.
Hydraulics and dynamics of New Corpus Christi Pass, Texas : a case history, 1973-1975 / by Richard L. Watson and E. William Behrens. – Ft. Belvoir, Va. : U.S. Coastal Engineering Center, 1976.
175 p. : ill. (GITI report 9) Also (Contract - Coastal Engineering Research Center ; (DACW72-74-C-0017)
Bibliography : p. 93.
A case history of the hydraulics and sedimentation of the Corpus Christi Water Exchange Pass, Texas, from 1973-75 is presented. Qualitative data are given on longshore sediment transport, tidal differentials, flood and ebb tidal discharge, wind waves, and local winds to explain bathymetric changes in the Pass.
1. Corpus Christi Pass, Texas. 2. Tidal inlets. 3. Tidal hydraulics. I. Title. II. Behrens, E. William, joint author. III. Texas. University. Marine Science Institute. IV. U.S. Army. Corps of Engineers. GITI report no. 9. V. U.S. Coastal Engineering Research Center. Contract DACW72-74-C-0017.

GB454 .I5 U581r no. 9 551.4

Watson, Richard L.
Hydraulics and dynamics of New Corpus Christi Pass, Texas : a case history, 1973-1975 / by Richard L. Watson and E. William Behrens. – Ft. Belvoir, Va. : U.S. Coastal Engineering Center, 1976.
175 p. : ill. (GITI report 9) Also (Contract - Coastal Engineering Research Center ; (DACW72-74-C-0017)
Bibliography : p. 93.
A case history of the hydraulics and sedimentation of the Corpus Christi Water Exchange Pass, Texas, from 1973-75 is presented. Qualitative data are given on longshore sediment transport, tidal differentials, flood and ebb tidal discharge, wind waves, and local winds to explain bathymetric changes in the Pass.
1. Corpus Christi Pass, Texas. 2. Tidal inlets. 3. Tidal hydraulics. I. Title. II. Behrens, E. William, joint author. III. Texas. University. Marine Science Institute. IV. U.S. Army. Corps of Engineers. GITI report no. 9. V. U.S. Coastal Engineering Research Center. Contract DACW72-74-C-0017.

GB454 .I5 U581r no. 9 551.4

Watson, Richard L.
Hydraulics and dynamics of New Corpus Christi Pass, Texas : a case history, 1973-1975 / by Richard L. Watson and E. William Behrens. – Ft. Belvoir, Va. : U.S. Coastal Engineering Center, 1976.
175 p. : ill. (GITI report 9) Also (Contract - Coastal Engineering Research Center ; (DACW72-74-C-0017)
Bibliography : p. 93.
A case history of the hydraulics and sedimentation of the Corpus Christi Water Exchange Pass, Texas, from 1973-75 is presented. Qualitative data are given on longshore sediment transport, tidal differentials, flood and ebb tidal discharge, wind waves, and local winds to explain bathymetric changes in the Pass.
1. Corpus Christi Pass, Texas. 2. Tidal inlets. 3. Tidal hydraulics. I. Title. II. Behrens, E. William, joint author. III. Texas. University. Marine Science Institute. IV. U.S. Army. Corps of Engineers. GITI report no. 9. V. U.S. Coastal Engineering Research Center. Contract DACW72-74-C-0017.

GB454 .I5 U581r no. 9 551.4

Watson, Richard L.
Hydraulics and dynamics of New Corpus Christi Pass, Texas : a case history, 1973-1975 / by Richard L. Watson and E. William Behrens. – Ft. Belvoir, Va. : U.S. Coastal Engineering Center, 1976.
175 p. : ill. (GITI report 9) Also (Contract - Coastal Engineering Research Center ; (DACW72-74-C-0017)
Bibliography : p. 93.
A case history of the hydraulics and sedimentation of the Corpus Christi Water Exchange Pass, Texas, from 1973-75 is presented. Qualitative data are given on longshore sediment transport, tidal differentials, flood and ebb tidal discharge, wind waves, and local winds to explain bathymetric changes in the Pass.
1. Corpus Christi Pass, Texas. 2. Tidal inlets. 3. Tidal hydraulics. I. Title. II. Behrens, E. William, joint author. III. Texas. University. Marine Science Institute. IV. U.S. Army. Corps of Engineers. GITI report no. 9. V. U.S. Coastal Engineering Research Center. Contract DACW72-74-C-0017.

GB454 .I5 U581r no. 9 551.4

Watson, Richard L.
Hydraulics and dynamics of New Corpus Christi Pass, Texas : a case history, 1973-1975 / by Richard L. Watson and E. William Behrens. – Ft. Belvoir, Va. : U.S. Coastal Engineering Center, 1976.
175 p. : ill. (GITI report 9) Also (Contract - Coastal Engineering Research Center ; (DACW72-74-C-0017)
Bibliography : p. 93.
A case history of the hydraulics and sedimentation of the Corpus Christi Water Exchange Pass, Texas, from 1973-75 is presented. Qualitative data are given on longshore sediment transport, tidal differentials, flood and ebb tidal discharge, wind waves, and local winds to explain bathymetric changes in the Pass.
1. Corpus Christi Pass, Texas. 2. Tidal inlets. 3. Tidal hydraulics. I. Title. II. Behrens, E. William, joint author. III. Texas. University. Marine Science Institute. IV. U.S. Army. Corps of Engineers. GITI report no. 9. V. U.S. Coastal Engineering Research Center. Contract DACW72-74-C-0017.

GB454 .I5 U581r no. 9 551.4

Watson, Richard L.
Hydraulics and dynamics of New Corpus Christi Pass, Texas : a case history, 1973-1975 / by Richard L. Watson and E. William Behrens. – Ft. Belvoir, Va. : U.S. Coastal Engineering Center, 1976.
175 p. : ill. (GITI report 9) Also (Contract - Coastal Engineering Research Center ; (DACW72-74-C-0017)
Bibliography : p. 93.
A case history of the hydraulics and sedimentation of the Corpus Christi Water Exchange Pass, Texas, from 1973-75 is presented. Qualitative data are given on longshore sediment transport, tidal differentials, flood and ebb tidal discharge, wind waves, and local winds to explain bathymetric changes in the Pass.
1. Corpus Christi Pass, Texas. 2. Tidal inlets. 3. Tidal hydraulics. I. Title. II. Behrens, E. William, joint author. III. Texas. University. Marine Science Institute. IV. U.S. Army. Corps of Engineers. GITI report no. 9. V. U.S. Coastal Engineering Research Center. Contract DACW72-74-C-0017.

GB454 .I5 U581r no. 9 551.4